ACTIVE INSECT FIBRILLAR FLIGHT MUSCLE, ITS MECHANICAL PERFORMANCE AND CROSS-BRIDGE KINETICS

Submitted for the degree of
Doctor of Philosophy

JUSTIN EDWARD MOLLOY

Department of Biology,
University of York.

June 1988

TABLE OF CONTENTS

ACKNOWLEDGEMENTS

I am extremely grateful to David White for his wisdom, encouragement and good humour throughout the course of my studies. I am also very grateful to John Sparrow for his help, numerous suggestions and innovations; particularly in mounting the very small muscle fibres used in this work.

Special thanks are also due to Liz Ball, Vas Kyrtatas and John Lund for projects in which we collaborated and also for their ideas, suggestions, practical assistance and friendship.

I would like to thank Martin Webb for collaborating with the oxygen-exchange experiments and for many helpful discussions. Thanks also to John Wray for several discussions and particularly in pointing out the shortcomings of an early draft of chapter 4.

Special thanks are due to my family and friends who have put up with my many shortcomings whilst I have been writing the tome that was almost completely finished for so long !.

DECLARATION

Except where it is acknowledged in the text the work presented in this thesis is my own. None of this work has been accepted in any previous application for a degree.

Much of Chapter 3 has been published (Molloy et al., 1987) and the results of one experiment, performed in collaboration with Dr. Kyrtatas has been published in Kyrtatas, 1987; this is acknowledged in the text of Chapter 3.

Justin Molloy,
June 1988

ABSTRACT

The kinetics and mechanical performance of glycerol-skinned muscle fibres from the wing muscle of a variety of different insects were examined.

Under forced sinusoidal length oscillation insect fibrillar muscle performs mechanical work on the driving apparatus. In response to a sudden, step, length change muscle fibres generate a large amplitude, delayed tension, transient. The rate constant for this transient determines the frequency of length oscillation at which the maximum power output is obtained. The rate constant was measured in a wide variety of insects and correlated with the wingbeat frequency. The slowest step in the biochemical cycle determines the rate of ATP hydrolysis. This rate constant was measured in different insects but was found to be independent of the wingbeat frequency. These findings are incorporated in a minimal cross-bridge scheme for insect flight muscle.

The ATPase cycle in the common wasp (Vespa vulgaris) was investigated further by measuring the pattern of phosphate water oxygen-exchange by fibres incubated in ^{18}O water. In this insect, as found for the giant waterbug (Lethocerus indicus), the rate constants controlling phosphate release are slow enough to contribute to rate-limitation of the biochemical cycle. The pattern of oxygen-exchange is compared and contrasted to findings from other workers for vertebrate skeletal and Lethocerus muscle.

The maximum power output obtainable from insect flight muscle depends not only upon the intrinsic properties of the muscle but also the operating temperature. The difference in surface area to volume ratio for small and large insects means that alternative strategies

have been adopted to cope with a variable environmental temperature. Strategies to optimise the insect flight motor are discussed.

The genetics of Drosophila melanogaster are the best understood of any eukaryote. Mutations in the flight muscle proteins can be independent of other muscles and lead to viable, flightless individuals. The mechanical properties of the flight muscles of these, very small, insects has been measured in wild type and suitable flightless mutants. The findings are discussed in terms of the likely structural significance in regions of the amino acid sequence.

LIST OF ABBREVIATIONS

A	actin
A_x	absorbance at x nm
Ap_5A	P^1,P^5-di(adenosine-5'-)pentaphosphate
APS	ammonium persulphate
ADP	adenosine-5'-diphosphate
ATP	adenosine-5'-triphosphate
ATPase	adenosine-5'-triphosphatase
bisacrylamide	N,N'-methylene-bis-scrylamide
D.A.	digital to analogue converter
D.C.	direct current
DLM	dorsal longitudinal muscle
DTT	dithiothreitol
EGTA	ethylene glycol bis-(β-aminoethyl ether)N,N,N',N'-tetraacetic acid
EM	electron microscopy or micrograph
f	Huxley (1957) rate constant for cross bridge attachment
f_{PMAX}	frequency of oscillation at which maximum power is obtained
f_{WMAX}	frequency of oscillation at which maximum work is obtained
f_{WB}	wingbeat frequency
g	Huxley (1957) rate constant for cross bridge detachment
GPIB	general purpose interface bus
HMM	heavy meromyosin
HPLC	high performance liquid chromatography
IFM	indirect flight muscle
kg	kilogramme
LMM	light meromyosin
L_s	sarcomere length
LLD	laser light diffraction
LM	light microscopy or micrograph
M	myosin
N.I.M.R.	National Institute for Medical Research
r_3	rate constant for delayed tension generation
^{18}O	oxygen isotope ^{18}O
Pi	phosphate
PST	phosphate starvation transient
S1	myosin subfragment 1
SDS	sodium dodecyl sulphate
TEMED	N,N,N,N',N'-tetramethylethylenediamine
Tris	tris(hydroxymethyl)aminomethane
v	volume
w	weight
WBF	wingbeat frequency

CHAPTER 1 :

INTRODUCTION

INTRODUCTION

This thesis is concerned with the muscles that drive an insect's wings in flight. The mechanical performance, biochemical and mechanical kinetics of muscle fibres, from a variety of different insects are examined. The study addresses three rather different questions :

1) What can a comparative study of the kinetics of muscle contraction, in insects with different wingbeat frequencies, tell us about the cross-bridge cycle in muscle ? (Chapters 3 & 4)

2) How is the performance of the flight muscle in different insects optimised ? (Chapter 5)

3) What changes in muscle function occur, following subtle modifications to the contractile proteins in Drosophila melanogaster ? (Chapter 6)

1.1 THE STRUCTURE OF INSECT FLIGHT MUSCLE :

Upon dissection, the flight muscles are discernible from the other thoracic muscles by their distinct yellow colouration. This is caused by the high concentration of respiratory pigments, present in the plentiful mitochondria (Keilin, 1925). The muscle consists of separate *fibres* (just visible to the naked eye, usually about 50-200μm in diameter, (Tiegs, 1955 and Cullen, 1974)). Upon teasing, the fibres yield very fine *myofibrils*, a few micrometers across. Viewed by phase-contrast microscopy the muscle has a striated appearance. Each striation unit is about 2.5μm long and is called a *sarcomere*. The appearance of insect flight muscle sarcomeres is slightly

different from those of vertebrate skeletal muscle. At rest length, the dark, anisotropic band, occupies about half the length of the sarcomere in vertebrate muscle, but spans nearly the whole length in insect.

The sarcomere striations are apparent because of the varying refractive index of bands of protein. Figure 1.1 summarises the position and properties of some of the proteins in insect flight muscle.

H.E. Huxley (1953), produced 'thin section' electron micrographs of vertebrate muscle, showing thin filaments extending from the Z line and interdigitating with the thick filaments. Hanson & H.E. Huxley (1955) showed that upon extraction of protein, myosin from vertebrate muscle the 'thick' filaments disappeared and following the extraction of actin all that now remained were the 'Z'lines. The thick and thin filaments consist, mainly, of the proteins myosin and actin.

The structure of actin filaments is highly conserved amongst the muscles of different organisms. The globular protein G-actin forms into a double stranded helical filament, F-actin. The repeat distance of each strand is 13.5 monomers (77nm). However, the filament, being a two start helix, repeats every 38.5 nm. In both vertebrate and insect muscle there are other, regulatory, proteins bound to the thin filament. The filamentous protein tropomyosin lies in the groove of the actin helix. A group of globular proteins called troponins (termed TnI, TnT and TnC) are grouped at the cross-over point of the actin helix (every 38.5 nm). Thin- and actin-filament are used synonymously in this thesis.

Myosin filament structure is more variable amongst different organisms. The α-helical myosin tails form the filament backbone and the globular myosin heads project out from the surface. Both the

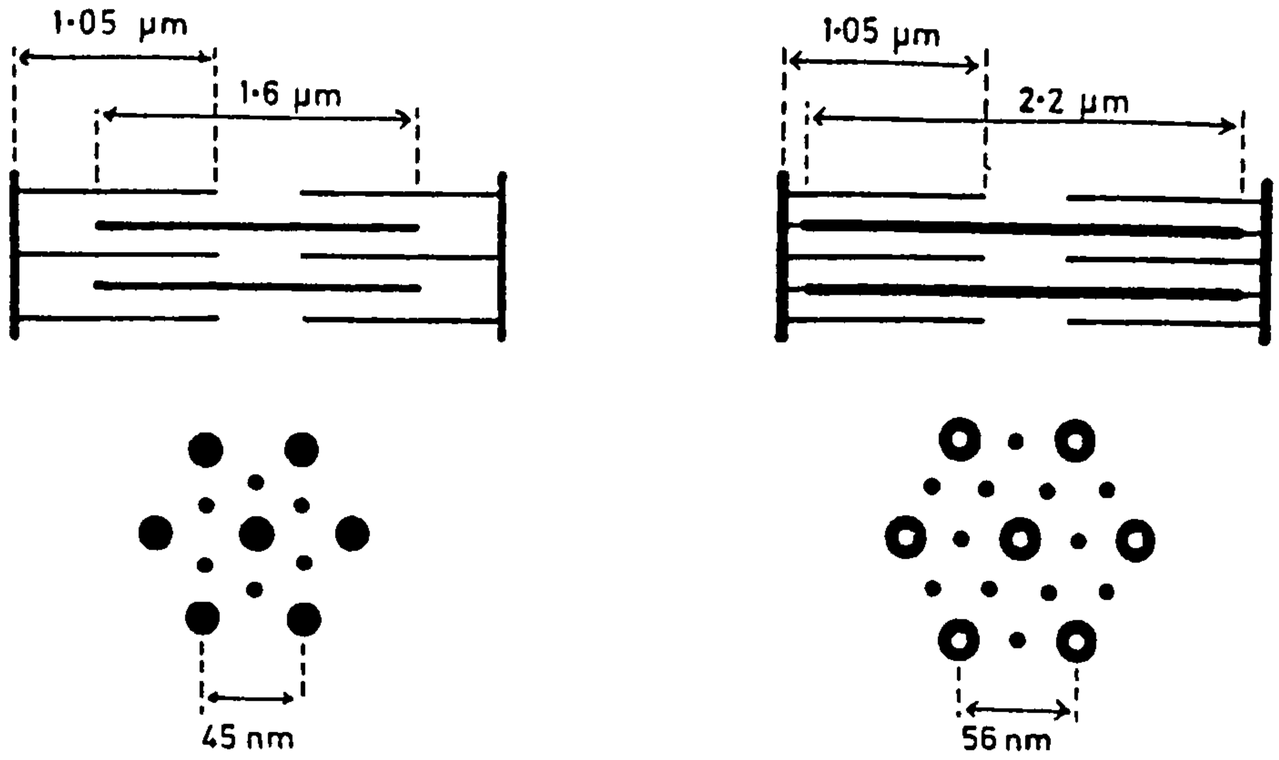

FIGURE 1.1

(a) Structure of vertebrate and insect flight muscle sarcomeres. The central, thick filaments are made predominantly of the protein myosin; the thin filaments consist mainly of actin. The myosin molecule consists of an ∝-helical "tail" (LMM and S2 in b, above) and a globular head (S1, above). The actin filament is made up from a double helix of actin monomers. The protein tropomyosin lies in the groove of the actin filament (the troponin complex is not shown). The ability of myosin to bind to actin and hydrolyse ATP resides in the globular, S1 head.

Myosin mol. wt. : 520,000 daltons

Actin mol wt. : 45,000 daltons

(This figure is discussed further in the text)

From White and Thorson, 1974

ATPase activity and actin binding ability reside in the globular heads or S1 units (Mueller & Perry 1962) of myosin. Thick filaments have an intrinsic polarity, growing out in opposite directions from a central 'bare zone' (a tail-only region where no heads project). Both vertebrate and insect thick filaments have an axial repeat distance of 14.5 nm but the pitch of the helices and the number of myosin heads per crown (the 'start' of the helix) is different. Initial calculations (Chaplain & Tregear, 1966) indicated that there were 6 myosin molecules per 14.5 nm repeat in insects. However, more recent studies (Reedy et al., 1981) conclude that there are 4 molecules per 14.5 nm repeat (i.e. four 'cross-bridges', consisting of two S1 heads each). This compares to the three myosins per crown in vertebrate muscle. One of the pitches of the four start helix in insect muscle is 38.5 nm, this is coincident with the actin repeat distance (Wray, 1979), the importance of this is discussed later. The greater number of myosin heads per crown in insect muscle is complemented by a higher proportion of actin filaments. The actin to myosin filament ratio in insect flight muscle is 3:1 compared to 2:1 in vertebrate muscle. The thick filaments of insect flight muscle have a hollow core which contains an additional protein, of unknown function, called *paramyosin* (Bullard, 1983). The ends of the thick filaments are linked to the Z-line by *connecting* or *C*- filaments (the evidence has been summarised by Ashurst, 1977). Thick- and myosin- filament are used synonymously.

1.2 MODELS OF MUSCLE CONTRACTION :

1.2.1 Sliding Filaments and Cross-bridges :

Noticing that the thick and thin filaments interdigitated, H.E. Huxley (1953) concluded that :

> "....stretching of the muscle takes place, not by an extension of the filaments, but by a process in which the two sets of filaments slide past each other; extensibility will then be inhibited if the myosin and actin are linked together."

A.F. Huxley and Niedergerke (1954) observed that the length of the A-band did not change whereas the I-bands shortened in contracting muscles, viewed by interference light microscopy. They too concluded that muscle shortened by the relative sliding of the thick and thin filaments.

Aubert (1951), showed that the force produced by a muscle depended in a characteristic fashion upon the length at which the muscle was held. More recent data obtained for single frog fibres is shown in Figure 1.2 (Gordon et al., 1966). The significance of this is that the degree of thick and thin filament overlap determines the amount of force that is generated.

In 1957 A.F. Huxley advanced an hypothesis for the mechanism of muscle contraction. The basis of the model was that :

> "A relative force between adjacent filaments of the two kinds is generated at each of a series of points within the zone in which they overlap."

It was the first cross-bridge model for muscle function and many of its basic ideas persist in all such models.

1.2.2 The Cross-bridge states :

In the model, side pieces (now referred to as cross-bridges), projecting from the thick filament, interacted cyclically, with the thin filament. At any time a given cross-bridge could be in either of two states; attached or detached to the thin filament. Equilibrium between the two states depended upon two rate constants; f for the attachment process, and g for detachment.

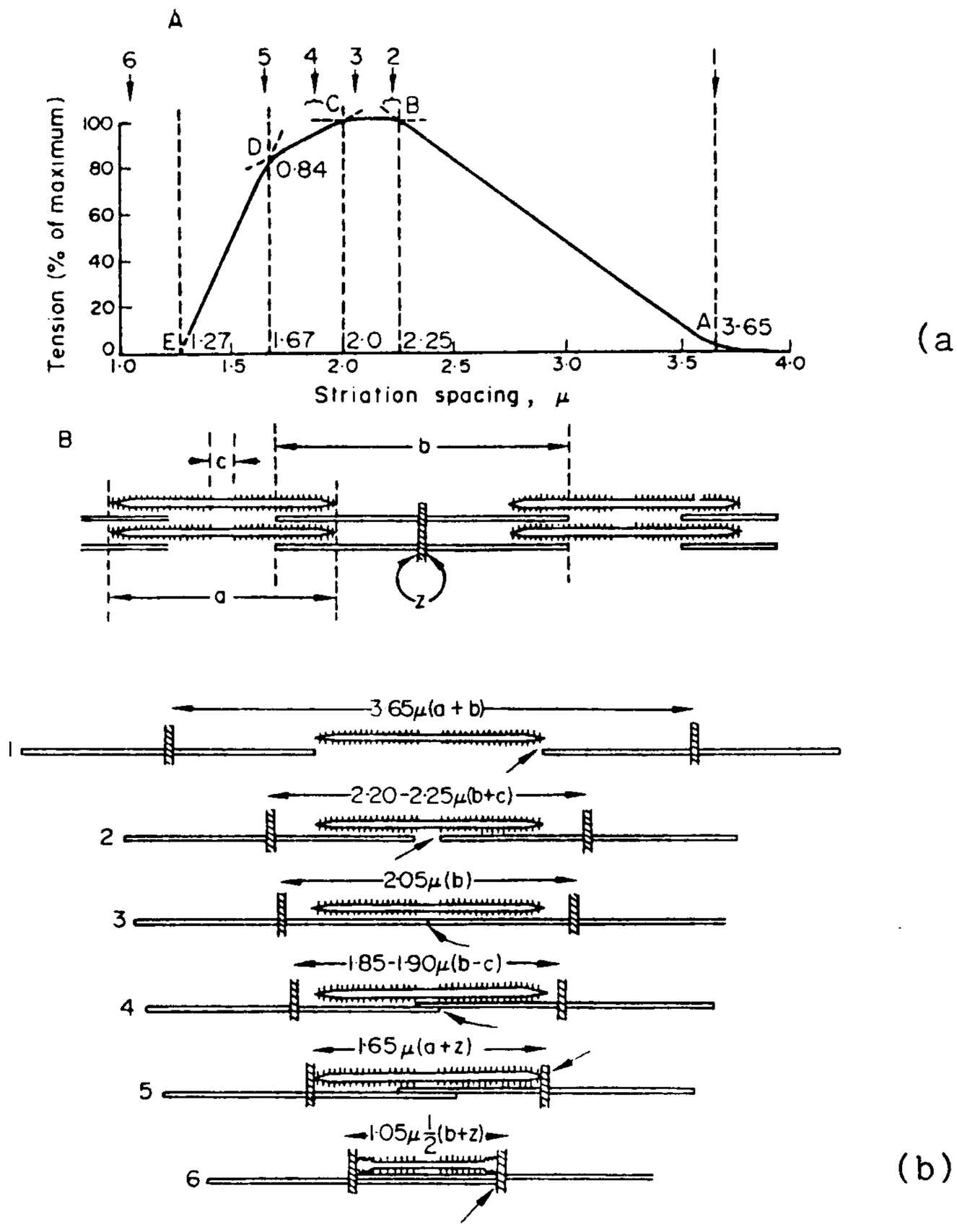

(a)

(b)

FIGURE 1.2

Part (a) shows how the isometric tension developed in frog semiteninosus muscle depends upon the sarcomere length.

Part (b) shows the appearance of the sarcomere at the different sarcomere lengths. The numbers 1-6 refer to the regions of the graph above (also labelled 1-6)

(from Gordon et al., 1966)

1.2.3 How Forces were Generated :

Within the hypothesised cross-bridge there was a compliant structure. Because of this, random thermal motion forced the cross-bridge to oscillate about an equilibrium position. Attachment could therefore occur with the elastic element distorted. For single values of f and g no net tension would be generated by a group of cross-bridges. At any moment in time there would, on average, be equal numbers of stretched and compressed ("pulling" and "pushing") compliant links. The way that the model worked was to have the values of f and g dependent upon cross-bridge distortion. Figure 1.3 shows how the rate constants were made to depend upon distortion.

Cross-bridges were unable to attach at negative disortions (ie. f=0 for "pushing" bridges), and detachment was rapid (g is large). For positive distortions, f and g increased linearly with distortion, with f being about 8 times larger than g (ie. 80% of bridges attached over the whole range). The limit of positive distortion at which attachment could occur by random thermal motion was termed *h*. At distortions greater than h, attachment became impossible (f=0) and detachment became the only option again.

To prevent the model from being that of a "perpetual motion machine" the detachment of cross-bridges was coupled with the hydrolysis of a high energy phosphate compound (ATP).

Muscle held at a constant length (isometric) maintains a constant tension because the attached bridges all have positive distortions. In an actively shortening muscle the velocity of inter-filament sliding is fast in comparison to the rate constant for detachment. Cross-bridges are "carried" to regions of lower, and negative, distortions before they have time to detach. They perform mechanical work, by exerting a force through a distance. At the maximum velocity

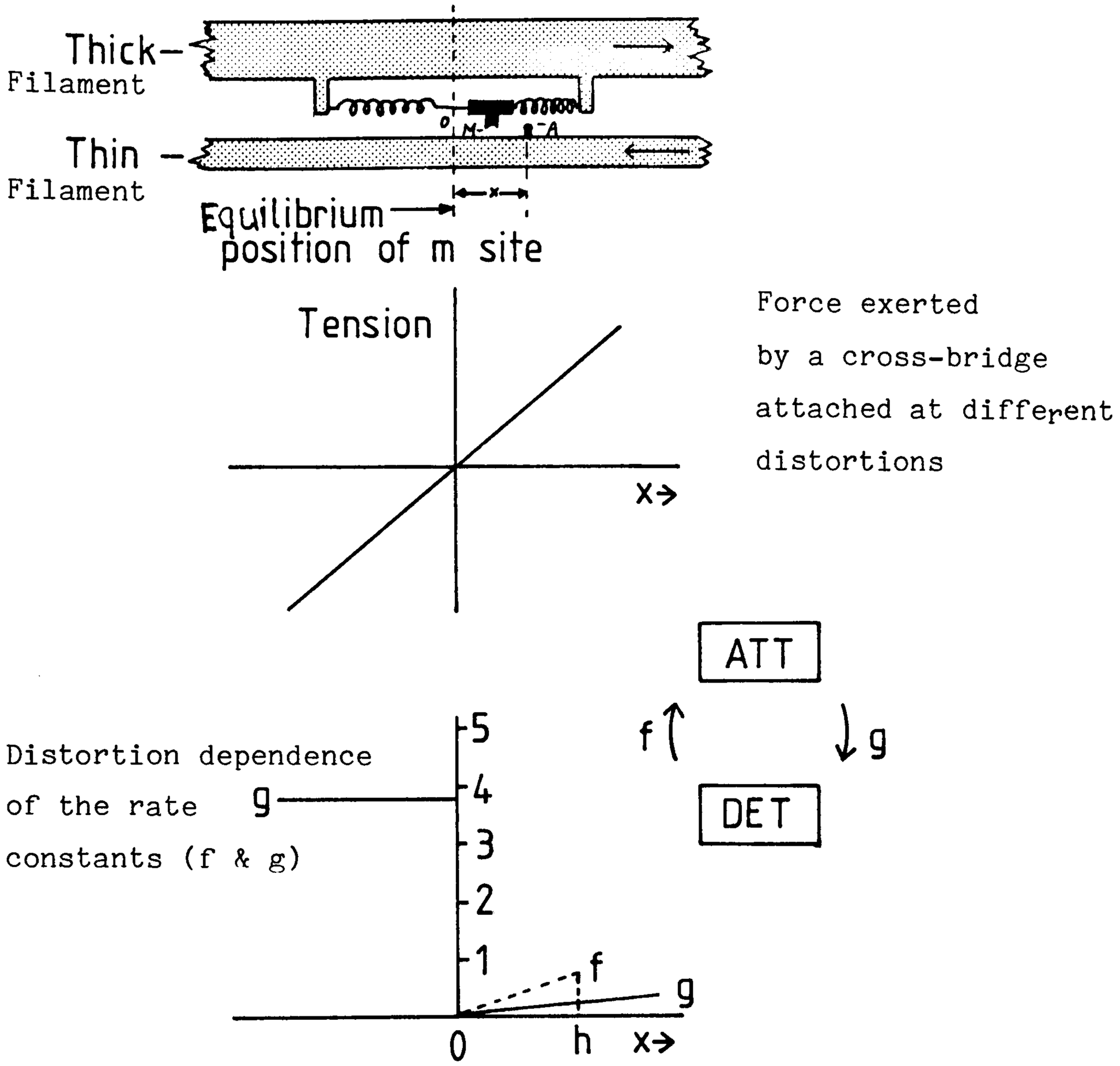

FIGURE 1.3

The cross-bridge model of Huxley (1957). The myosin (M) "site" is suspended on a Hookean elastic element and may be in either of two states; attached (ATT) or detached (DET) to an actin site (A)
The rate constants for attachment (f) and detachment (g) depend in a characteristic way upon distortion (x).
The lower part of the figure shows how f and g were made to depend upon distortion. The model accounted closely for all of the steady state properties of muscle described by Hill (1938).
From Huxley (1957).
The model is described more fully in the text.

of shortening, force from pulling bridges is counteracted by that from pushing bridges, resulting in zero net force. The force and work produced by the muscle depends in a characteristic way upon the shortening velocity. Huxley solved the differential equations governing the behaviour of the cross-bridges during steady shortening. The chosen values for f and g, and their distortion dependencies, were such that the model accounted closely for all of the steady-state phenomena, described by Hill (1938), for the behaviour of live frog muscle.

In 1969 H.E. Huxley proposed that the myosin heads (or Sls) produced forces in a slightly different manner :

> "..the contraction mechanism may be a rigid attachment of the globular head of the myosin molecule to the actin filament and an active change in the angle of attachment associated with the splitting of adenosine triphosphate."

The strongest, direct evidence in support of this hypothesis was from work using insect flight muscle. Reedy et al. (1965) showed that the angle of cross-bridges attached in rigor was approximately 45° whereas muscle that was fixed in relaxed conditions had cross-bridges angled at near to 90°. To date there are no conclusive structural data to show that cross-bridges change angle during the cross-bridge cycle in active muscle. Attempts to demonstrate changes in cross-bridge angle include the use of time-resolved X-ray diffraction and electron paramagnetic resonance (E.P.R.) (reviewed by Huxley & Kress, 1985). The most convincing argument supporting H.E. Huxley's proposition is described in the next section.

1.3 RAPID MECHANICAL EXPERIMENTS :

A.F. Huxley (1957) tried only to explain steady-state phenomena i.e. where, for given conditions, the attached and detached cross-

bridge populations did not change with time. Following a perturbation to the steady-state a relaxation occurs either to a new steady-state or back to the original. A 'complete model' should also account for this transient kinetic behaviour of muscle.

In order to make kinetic measurements, the rate at which the steady-state is perturbed must be very much faster than the most rapid step in the relaxation process. If this is not the case then part of the relaxation will occur during the course of the perturbation, making the results more difficult to interpret. For the same reasons, the assay system used to follow the relaxation process must be rapid.

Podolsky (1960), using a "fast" mechanical test apparatus, performed experiments in which the tension generated by a muscle fibre was suddenly altered and the resulting length changes monitored. They found that rapid fluctuations in the velocity of shortening occured immediately after the step change in tension and before the new steady speed of muscle shortening was achieved. By modifying the distortion dependencies of Huxley's (1957) attachment (f) and detachment (g) rate constants, Podolsky et al. (1969) were able to account for their findings. Testable predictions of these modifications were; (1) that rapid cross-bridge detachment should occur immediately following a step change in tension, and (2) during steady shortening the number of attached cross-bridges should increase with the velocity. Subsequent experiments have refuted these predictions (Ford et al., 1985, 1986).

Huxley and Simmons (1971) presented a more cogent explanation for the transient mechanical behaviour of muscle fibres. They performed experiments in which the length of a muscle fibre was held constant and the tension was free to change. They designed a tension transducer with a resonant frequency of over 4 kHz (Huxley & Simmons,

1968) and using an electrical feedback circuit (Gordon et al., 1966) sudden length changes were made in less than one millisecond. They performed length step experiments of varying step size on single live frog muscle fibres. The characteristics of the resulting tension transients are summarised below and in Figure 1.4 :

1) An initial tension change occured simultaneously with the length change (the tension level reached being referred to as T1). The size of this tension change was proportional to the size of the length step and can be attributed to an elastic element. The amount of elasticity (stiffness) was directly proportional to the sarcomere length (degree of overlap) (Huxley & Simmons 1971b)

2) An early tension recovery, which was very nearly monotonic in its time course reached a transient tension plateau (referred to as T2). The amplitude of the recovery was not directly proportional to the length step size, as would be expected of a simple viscous element. The amplitude of these recoveries was again directly proportional to the sarcomere length. The rate constant for the early tension recovery was very much greater for large releases than for small releases or stretches, being an exponential function of the size of the length step.

3) There was, occasionally, a transient reversal of tension recovery (a delayed tension change) which in all cases was followed by a slow monotonic tension recovery to the original steady tension (called T0).

Because the early tension events scaled with the degree of filament overlap they were attributed to the cross-bridges themselves.

FIGURE 1.4

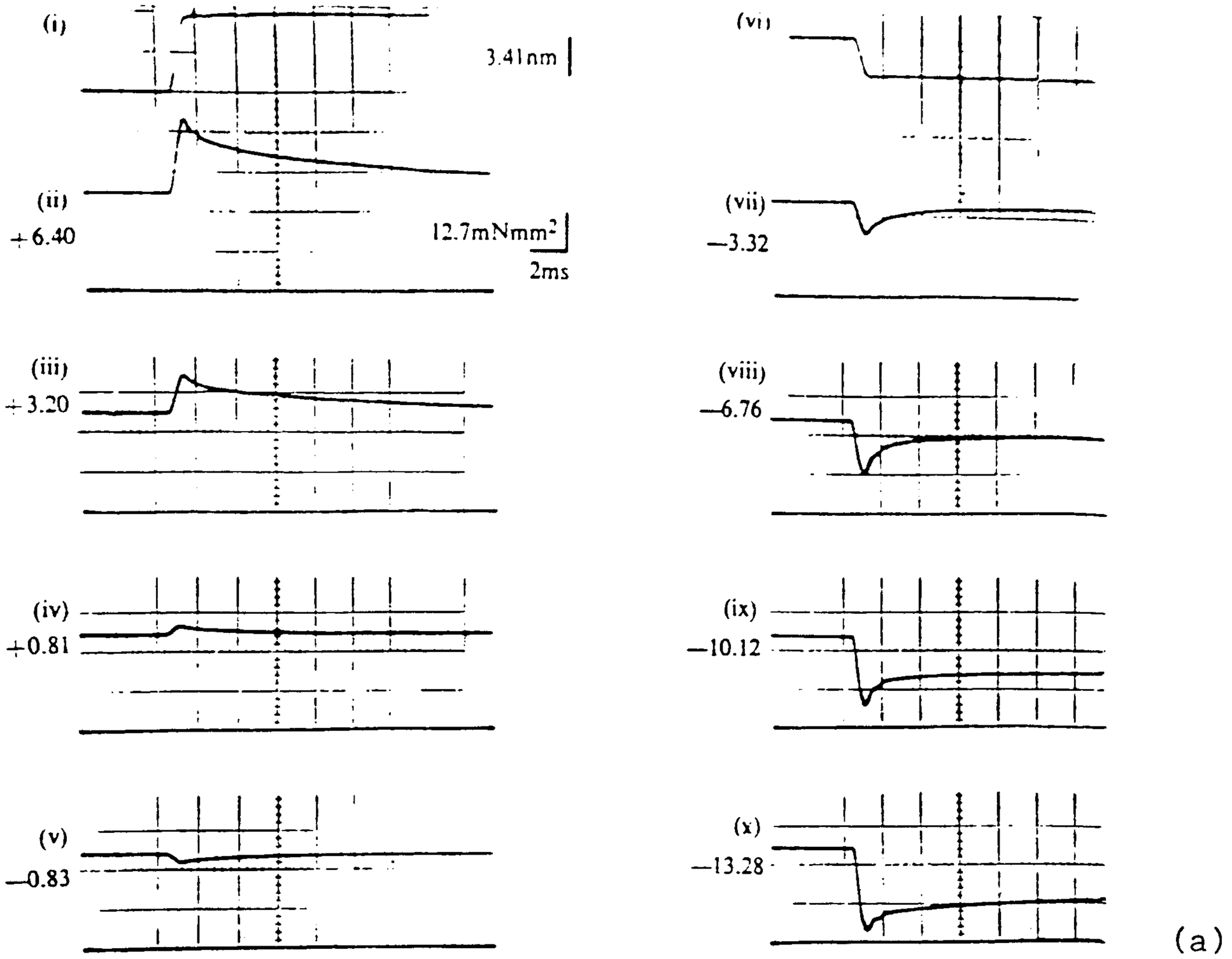
(i)
3.41nm
(ii)
+6.40
12.7mNmm⁻²
2ms
(iii)
+3.20
(iv)
+0.81
(v)
−0.83
(vi)
(vii)
−3.32
(viii)
−6.76
(ix)
−10.12
(x)
−13.28

(a)

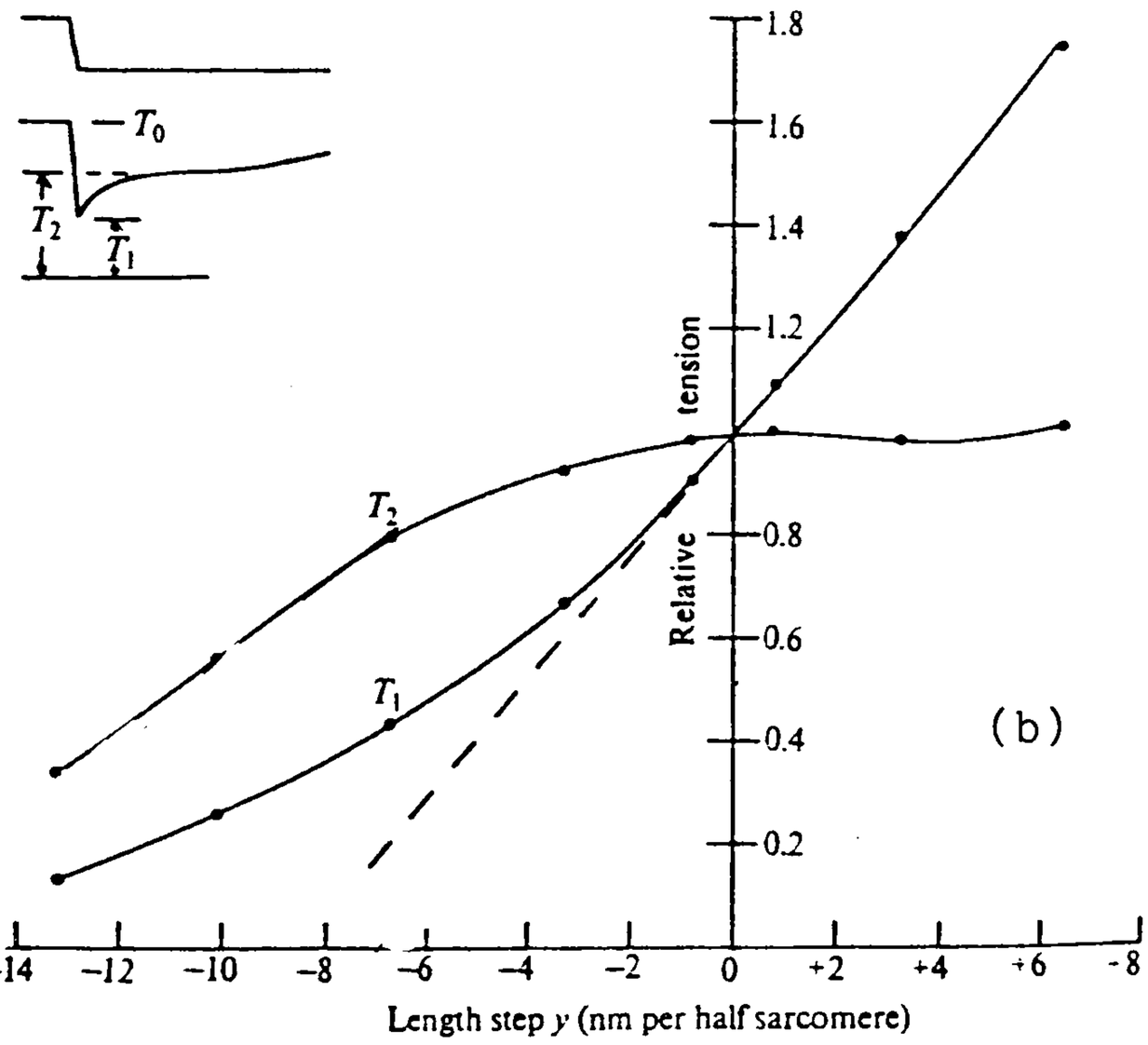
T_0
T_2
T_1
1.8
1.6
1.4
1.2
1.0
0.8
0.6
0.4
0.2
Relative tension
T_2
T_1
−14 −12 −10 −8 −6 −4 −2 0 +2 +4 +6 −8
Length step y (nm per half sarcomere)

(b)

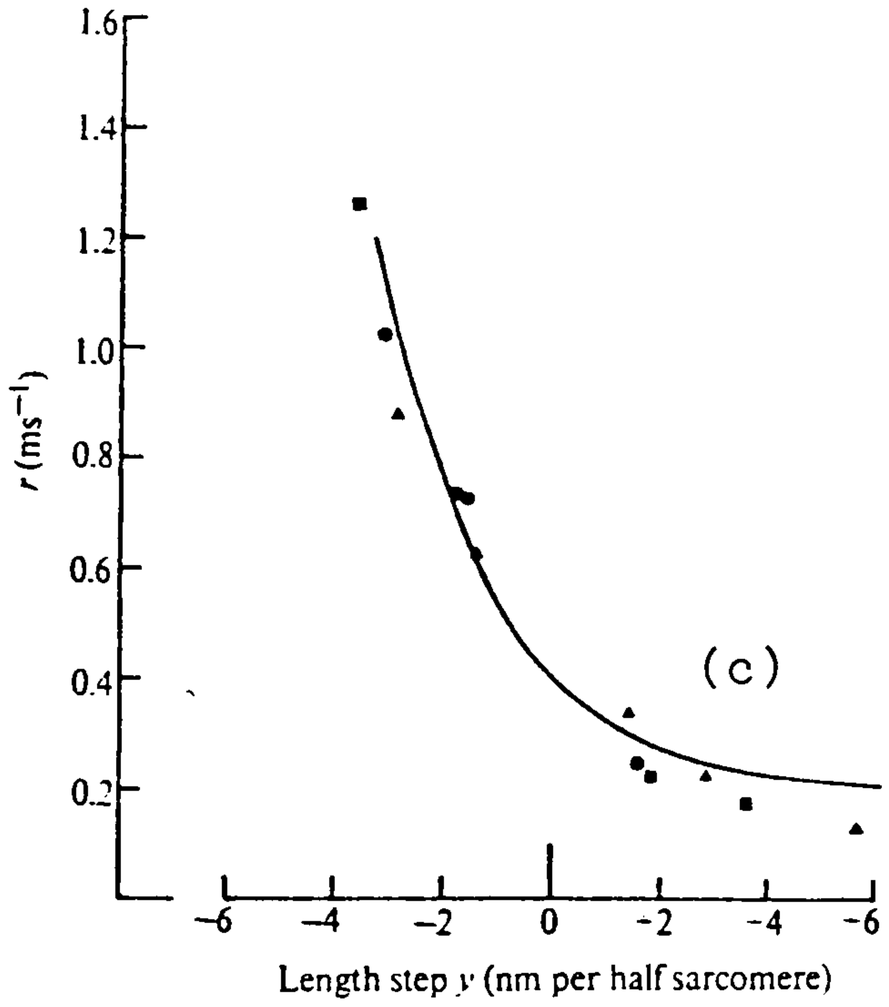
1.6
1.4
1.2
1.0
0.8
0.6
0.4
0.2
r (ms⁻¹)
−6 −4 −2 0 −2 −4 −6
Length step y (nm per half sarcomere)

(c)

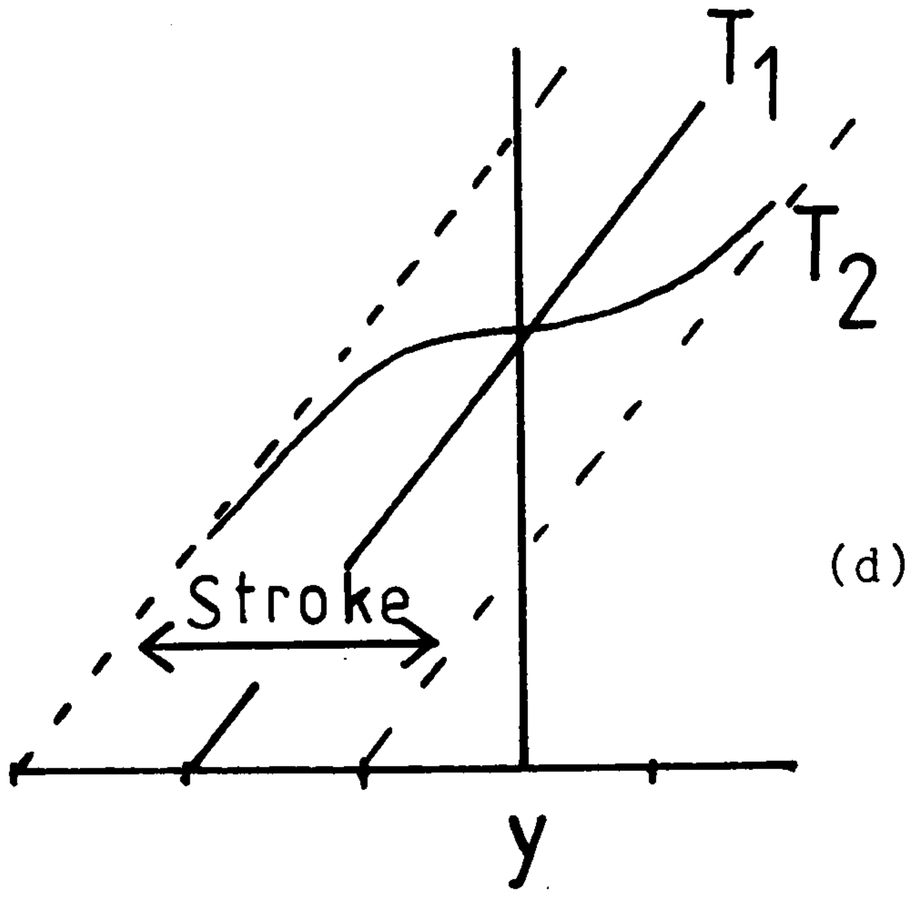
T_1
T_2
Stroke
y

(d)

The explanation for the early recovery phase was based on H.E. Huxley's proposal that forces were generated by a change in angle of attached cross-bridges. The size of the cross-bridge *stroke* could be determined directly from a graph of T2 versus length step size (see Figure 1.4). The finding that some part of the cross-bridge contained a Hookean elastic element meant that individual cross-bridges could generate forces "in their own time". Energy being stored in the elastic component as a cross-bridge changed angle from one conformation to another (only two states were considered). The stored energy could be discharged as work only when the filaments moved past one another, allowing a high chemo-mechanical efficiency.

A tacit assumption of their formulation was that the attached cross-bridges were symmetrically distributed about a mean value of distortion. This greatly simplified the model since equations relating to a cross-bridge with the mean distortion were sufficient to describe the sum of the whole population. Another simplifying factor was that cross-bridges were allowed only two stable conformations which in an isometric muscle fibre were equally populated.

The change in cross-bridge angle was used to couple directly the biochemical energy change to a mechanical energy change. They drew an energy diagram with the two stable conformations as energy wells. The reaction coordinate represented the angular position of the cross-bridge between the two stable states. The energy required to stretch the elastic component was superimposed upon this reaction coordinate. The choice of shape for the original energy diagram affects the way in which the forward and reverse rate constants are affected by the mechanical energy contribution. This is shown in Figure 1.5.

Using Boltzman statistics they calculated the rate and

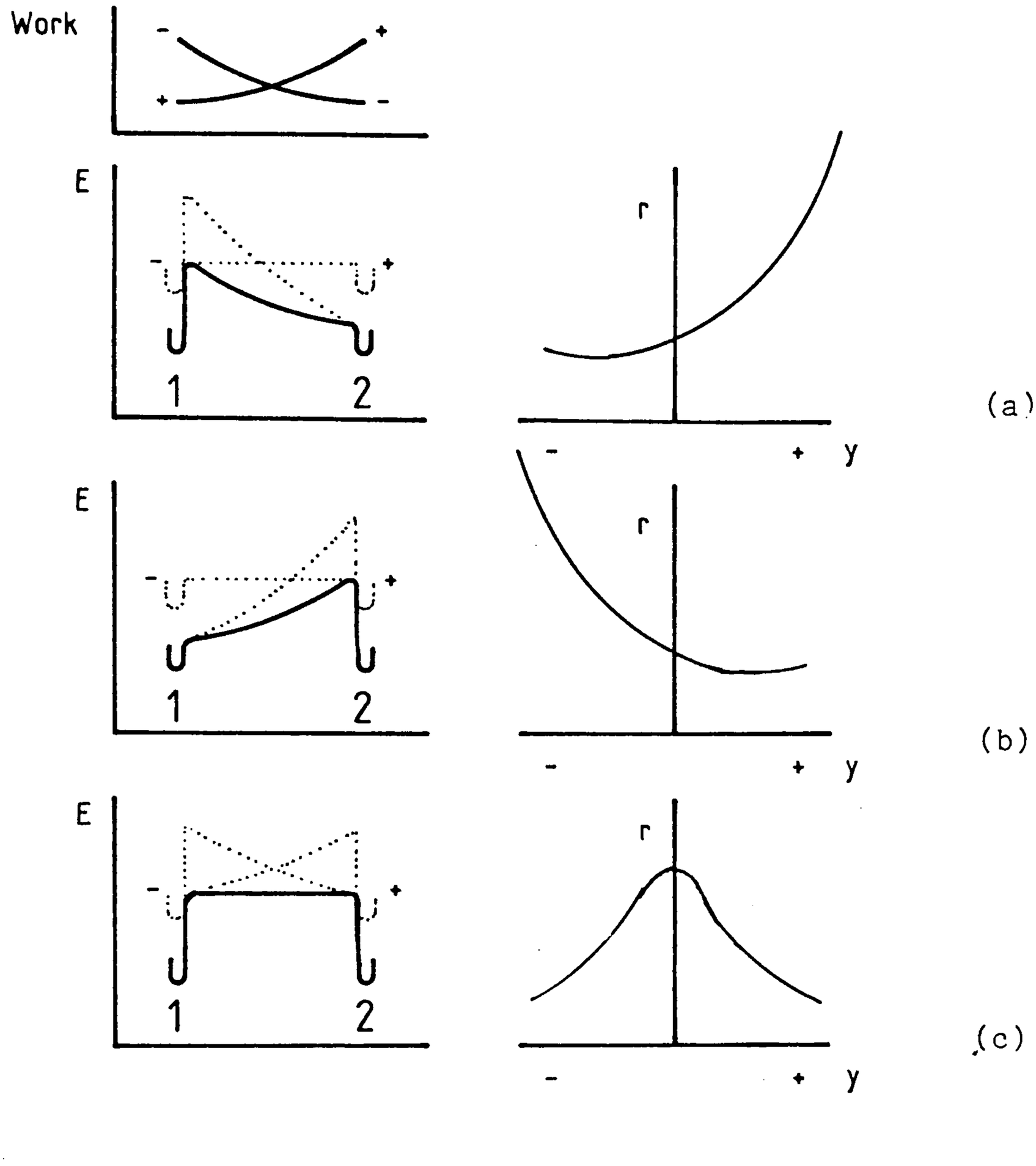

FIGURE 1.5

The diagrams on the left are the energy profiles for the transition between two attached cross-bridge states. State (1) is the pre-working stroke state and state (2) is a post-work stroke state. The mechanical work performed by the working stroke is shown at the top left hand side; this "work" term is added into the energy diagrams below.

Depending upon the shape of the original energy diagram either the forward, reverse or both rate constants governing the transition between the two states is affected by distortion.

The dependence of the rate constant for the early tension recovery (in the Huxley & Simmons type experiments) is shown in the diagrams on the right. The shape of energy diagram chosen by Huxley and Simmons (1971) to model their data is like that of row (b) above.

equilibrium constants governing the cross-bridge behaviour for different length step sizes. The main dilemma was that the cross-bridge stiffness and stroke size required to model the transient tension response to step length changes was smaller (by a factor of about 2) than that required energetically and in order to generate the observed steady-state tensions found for activated muscle fibres. By making the cross-bridge angle change occur in more than one step (multiple attached states) both the transient kinetic characteristics and the kinetic and steady state tensions could be accounted for.

Hill (1974) produced a "Theoretical Formalism for the Sliding Filament Model" which extends and brings together the ideas of Huxley and Simmons (1971) and Huxley (1957). He gives due consideration to the shape of the energy diagrams describing transitions between attached states and to the probability functions governing attachment and detachment.

1.4 MAPPING THE BIOCHEMICAL STATES TO THE MECHANICAL STATES :

One problem with purely mechanical studies is that the interpretation of the assay (the measured length or tension changes) is model specific. The type of model presented by Huxley and Simmons (1971) is inherently testable because it combines events in the biochemical pathway with mechanical energy transduction.

In recent years the challenge has been to link the biochemical and mechanical events. Biochemical kinetics in whole fibres have been difficult to measure because the rate of diffusion of chemicals is very slow compared to the biochemical rate constants. It has not been possible to mimic the forces present in intact muscle fibres in kinetic measurements made on isolated muscle proteins in solution.

1.4.1 Solution Biochemistry :

The "Lymn-Taylor Scheme" (Lymn & Taylor, 1971) provided the initial basis of the biochemical pathway for ATP hydrolysis by actomyosin in solution. It is likely that the intermediaries will be similar in intact muscle fibres but that the rate constants of some steps will be different (see Scheme 1.1). Eisenberg and Hill (1985) reviewing the solution biochemistry work, conclude that myosin might not completely detach during the cross-bridge cycle, but that there is a rapid equilibrium between attached and detached states referred to as "weakly bound states" (see also Geeves et al., 1984). Tension generation can occur only when cross-bridges are "strongly bound" (being associated with the release of product phosphate) and the recovery stroke when they are weakly bound to actin (with either ATP or ADP+Pi bound to the myosin head). A cartoon of this idea is shown at the bottom of Scheme 1.1.

Sheetz and Spudich (1983) developed a technique which allows the relative movement of myosin molecules and actin filaments to be visualised in solution. The velocity of fluorescent beads coated with myosin (HMM) moving over actin filaments in the prescence of ATP can be measured directly by microscopy. The exciting aspect of this work is that the problems of chemical diffusion are minimised and that in the future it might be possible to impose forces on small numbers of isolated cross-bridges.

Several techniques have been developed to study the biochemical kinetics in whole muscle fibres. They fall into two categories, transient kinetic techniques and steady-state kinetic techniques. These techniques make use of *skinned* muscle fibre preparations.

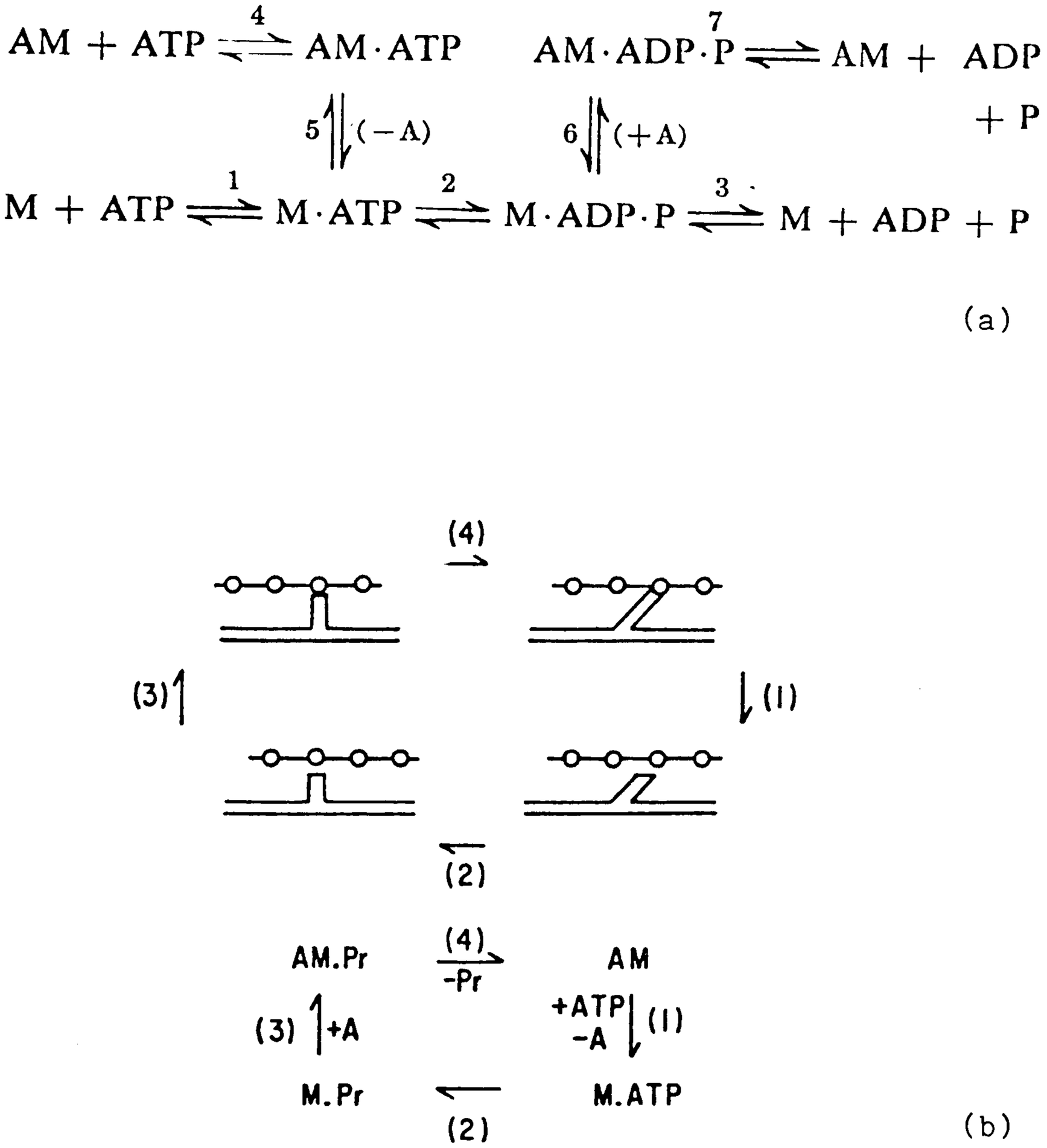

SCHEME 1.1

Part (a) shows the Lymn-Taylor scheme (Lymn & Taylor, 1971). (A = actin; M = myosin). Part (b) shows how the biochemical scheme could be mapped onto a structural, mechanical model.

1.4.2 Skinned Muscle Fibres :

One disadvantage of live muscle fibre experiments is that the chemical environment of the contractile proteins is not under direct control. The muscle membrane can be either mechanically removed or chemically disrupted to allow bathing solutions to enter the myofibrillar space. Chemical skinning with a concentrated glycerol solution (50% v/v) (Szent-Gyorgyi, 1949) has the advantage of replacing the cytoplasm with a solution of low freezing point. Fibres can then be stored for several months at low temperature.

There are two main problems with skinned muscle fibres. Firstly, the preparation is less "physiological" and proteins may be lost or damaged (Poole 1984). Secondly, the supply and removal of metabolites (ATP and ADP + Pi) can occur only by passive diffusion with the bathing solution and may be a rate-limiting factor.

1.4.3 Transient Biochemical Techniques :

Inert, photolabile ("caged") compounds can be diffused into skinned muscle fibres and the active component released on a millisecond time scale by a flash of laser light (Goldman et al., 1982). In this way transient tension changes following the sudden release of ATP into a fibre in rigor can be monitored. Caged compounds provide the necessary link between biochemical perturbations and mechanical transients. Hibberd and Trentham (1986) and White (1987) have reviewed the results of these experiments. The main conclusions are listed below :

1) Following the rapid photolysis of caged-ATP within a fibre in the rigor state (in the absence of calcium ions) the tension falls with a complicated time course to the relaxed level. There is a brief tension "hump" followed by an approximately monotonic

tension fall. The rate constant of the tension fall depends upon the concentration of ATP released within the fibre (Goldman et al., 1982).

2) The same experiment performed in the presence of calcium ions shows a brief tension dip followed by a rapid tension rise to the active tension level appropriate to the concentration of free calcium. The addition of phosphate ions to the incubation solution increases the rate constant for the tension recovery and reduces its amplitude (Hibberd et al., 1985b)

In point 1 (above) the tension fall is attributed to rapid, ATP dependent, dissociation of strongly bound cross-bridges (AM) to form weak binding M.ATP and M.ADP.PI states. The tension hump is explained by cooperativity of tightly bound, rigor, cross-bridges allowing neighbouring bridges to cycle actively and generate tension. Point 2 indicates that the tension generating step must precede the rate-limiting step (being faster than the overall ATPase rate). The effects of added phosphate are most easily explained if the AM.ADP.Pi state generates less tension than the AM.ADP state. Added phosphate shifts the equilibrium of the reaction AM.ADP.Pi $\rightleftharpoons$ AM.ADP + Pi to the left reducing the final tension level. Additionally, the rate constant for tension generation, being the sum of the forward and reverse rate constants for this step, will be increased by the presence of phosphate.

1.4.4 Steady-state Biochemical Experiments :

Oxygen-exchange provides a means of studying the biochemical kinetics in skinned muscle fibres without perturbing steady-state. When ATP is hydrolysed by actomyosin, an oxygen from the solvent water

becomes incorporated into the product phosphate. However, the phosphate is not released immediately but remains in the catalytic site for some time. During this time reversal of the hydrolysis step may occur. The bound phosphate is free to rotate in the catalytic site, and there is an equal probability of any one of the four oxygen atoms being displaced upon reversal (Sleep et al., 1980).

When a skinned muscle fibre is incubated in labelled ^{18}O water, phosphate produced from ATP hydrolysis can contain from 1-4 labelled oxygen atoms. When the product phosphates are analysed by mass spectrometry a distribution of incorporation is found. The distribution is a statistical function of the ratio of the reverse hyrolysis rate constant and rate constants controlling phosphate release. A difference is found in the ATPase kinetics of insect and vertebrate muscle fibres when probed by oxygen exchange. The steps controlling phosphate release are rate-limiting for all cross-bridges in insect fibres (Lund et al., 1987, 1988), but only for bridges with large positive distortions in vertebrate fibres (Webb et al., 1986). Oxygen-exchange experiments were performed in collaboration with Dr. J.N. Lund (University of York) and Dr. M.R. Webb (N.I.M.R., Mill Hill) and are discussed at greater length in chapter 4.

1.5 INSECT FIBRILLAR FLIGHT MUSCLE :

Insect flight muscle performs cyclical contractions, the frequency of which is determined by the wingbeat frequency. Every time an insect uses its flight muscles, the degree of muscle shortening and the velocity of shortening are very nearly the same. The uniformity of function has led to the evolution of a specialised muscle tissue with uniform structure.

The flight muscle of the giant waterbug (genus Lethocerus) has

been used extensively as a model system for the study of muscle contraction (see Tregear, (ed) 1977). There are a number of reasons why insect flight muscle is an ideal experimental material :

1) The uniform structure within the filament lattice means that X-ray diffraction patterns and E.M.s are the most distinct of any muscle tissue.

2) The uniformity of the individual fibres means that mechanical and biochemical experiments on single fibres are very repeatable.

3) The phenomenon known as *stretch activation* means that skinned muscle fibres can be activated extremely rapidly, simply by suddenly changing the length of the muscle. Under forced sinusoidal length oscillation skinned muscle fibres perform mechanical work which can be maintained for several hours.

4) Although giant waterbugs are sometimes difficult to obtain this is made up for by the very stable glycerol skinned material.

5) The wingbeat frequency of different insects varies over a very wide range. A comparative study of the mechanical and biochemical kinetics in different insects gives valuable information about how the cross-bridge cycle can produce tension at very different rates.

1.5.1 A Scaling Problem for Small Insects :

Viscous forces exerted by a fluid are relatively much greater for small bodies than large ones. Paradoxically, the phenomenon that keeps small dust particles airborne presents a problem for small flying insects. Small insects need to beat their wings very rapidly inorder

to move the comparatively viscous air over their wings to generate aerodynamic forces. Conventional excitation-contraction coupling systems are simply not fast enough to control the flight muscles of these animals. Instead, they have evolved a muscle type with a novel activation mechanism.

1.5.2 Excitation-Contraction Coupling :

In most muscles, contraction is brought about by a change in the electrical potential of the cell membrane, the *sarcolemma*. The electrical changes cause a membrane system, the *sarcoplasmic reticulum*, to release calcium ions into the muscle cell. The calcium ions bind to regulatory proteins which, in turn, "switch on" the contractile proteins to produce a contraction. In muscles that require frequent contractions, a rapid on-off switching is necessary. Using this conventional control system, the song muscle of the cicadá Okangana attains a contraction frequency of 550Hz (Josephson, 1985). Much of this muscle consists of an extensive sarcoplasmic reticulum, required for the rapid calcium pumping. Consequently, the power-to-weight ratio is very low and also a lot of energy is wasted on pumping calcium ions across the muscle membrane.

Sotavalta (1947), found that by shortening the wings of certain insects (thereby reducing the inertia) the frequency of the wingbeat rose. Clearly there was a feedback system operating to match the muscle contraction frequency to the resonant frequency of the wings. Pringle (1949) measured the electrical activity in flight muscles of the blowfly Calliphora. In this animal, the muscle action potentials were not coincident with the wing movements. He recorded about 40 wingbeats for each depolarisation of the muscle, and termed the muscle type *asynchronous*. The mechanical "feedback" resided within the

muscle fibres and the stimulus for each contraction was myogenic.

1.5.3 Evolution of Indirect Fibrillar Flight Muscle :

The wings of all insects are driven by muscles situated in the thorax. There are two different ways in which the muscles are linked to the wings. In large primitive insects the muscles are connected directly, by tendons, to the wing base (ie. dragonflies, Odonata; Locusts, Orthoptera; Cockroaches, Dictyoptera; Moths and butterflies, Lepidoptera.). The muscles of insects, whose ancestors evolved more recently, insert onto the thoracic cuticle. They move the wings indirectly by distorting the shape of the thorax (Pringle, 1957) (ie. Flies, diptera; Wasps and bees, Hymenoptera; Beetles, Coleoptera; Bugs, Hemiptera.). The importance here is that long tendons connecting muscles directly to the wings cause a backlash, or hysteresis, limiting the upper frequency at which the muscles can drive the wings. The stiffer connection of indirect flight muscles results in less backlash, allowing higher wingbeat frequencies.

The flight muscles of some insects tease into single fibres very much more easily than others. On the basis of this difference flight muscles are termed either *fibrillar* or *non-fibrillar*. Cullen (1974) investigated the distribution of these muscle types amongst different insects (see Table 1.1).

1) Flies (Diptera)
2) Bees and Wasps (Hymenoptera)
3) Beetles (Coleoptera)
4) Some Bugs (Heteroptera)
5) Booklice (Psocoptera)
6) Thrips (Thysanoptera)

Table 1.1
Insects with fibrillar flight muscle (from Cullen, 1974).

It is the reduced membrane system in insects with asynchronous

muscle, which makes the fibres easy to separate (Smith, 1966). The terms asynchronous, fibrillar are therefore synonymous.

The high power to weight ratio of fibrillar muscle means that once evolved in an insect order it is retained, even when larger species, with very low wingbeat frequencies, evolve later (for instance "giant", belostomatid bugs, genus Lethocerus (Cullen 1974)).

Herein, the term "insect flight muscle" refers only to indirect, fibrillar flight muscle type.

1.6 THE MECHANICAL PROPERTIES OF INSECT FLIGHT MUSCLE :

Initial mechanical experiments were performed on flight muscles of the bumble bee, Bombus (Boettiger, 1957) and the lamellicorn beetle, Oryctes (Machin & Pringle, 1959). Live muscle, still attached to the thoracic cuticle, was mounted on a mechanical test apparatus. The length and tension of the muscle were monitored simultaneously, and the muscle could be activated with suitably implanted electrodes. The findings of these experiments are summarised below :

1) The stiffness of the relaxed muscle was very much higher than that of relaxed vertebrate muscle.

2) When the activated muscle acted against a suitable inertial load, undamped, maintained oscillations in length occured. Using a length motor with an electronic feedback circuit which allowed the mechanical damping to be controlled, the power output of the muscle could be measured directly (Machin & Pringle, 1959)

3) In response to sudden, step length changes, a large amplitude delayed rise in tension occurred, similar to a tetanic contraction in vertebrate muscle (Boettiger, 1957)

Later, experiments with glycerol-extracted muscle fibres from the giant waterbug (genus Lethocerus) were performed. Jewell and Ruegg (1966) demonstrated that the mechanical activation is an inherent property of the contractile proteins themselves. Skinned muscle fibres bathed in a salt solution containing ATP and a small amount of "free" calcium performed mechanical work under forced sinusoidal length oscillation. Further, both the mechanical work and usage of ATP depended upon the frequency of oscillation (Steiger and Ruegg, 1969).

Pringle (1978) discussed the activation of muscle by stretch and noted that it is a property of all muscle types but that it is especially developed in insect flight muscle. The rate constant of the delayed tension transient, observed in length step experiments determines the sinusoidal oscillation frequency at which the maximum work is obtained. There is a simple formula relating the two types of experiment :

$$r = 2\pi f \qquad .....(1.1)$$

r = rate constant for delayed tension
f = oscillation frequency to produce the maximum work

1.6.1 Models for Stretch Activation :

Early ideas about how the delayed rise in tension following a step change in length arose depended upon an exponential change in the amount of calcium bound to the regulatory proteins (Jewell & Ruegg, 1966 and Julian, 1969). Cross-bridges that were previously "inactive" were recruited with an exponential time delay. Julian (1969) produced a mathematical model which was based on Huxley's (1957) "two state" model. The attachment rate constant now contained a factor with an exponential time dependence (refered to as the activation function γ).

Thorson and White (1969) realised that the delayed activation of insect muscle need not involve a time-dependent calcium binding. The exponential delay in tension could be produced by the straightforward relaxation kinetics of Huxley's two state model. All that was required was for the length change to act as a forcing function upon either one of the rate constants (f or g) or by modulating the number of available cycling bridges. The time course of the tension relaxation is then determined by the sum of the attachment and detachment rate constants (f+g).

White and Thorson (1972) showed that the mechanical kinetics of insect muscle fibres were strongly affected by the presence of millimolar concentrations of phosphate. In the absence of phosphate the tension response to a large amplitude length change (>0.5%) became non-linear. This corresponded with the appearance of an additional, slow relaxation tension transient (the so called phosphate starvation transient or PST). In the presence of phosphate ions the tension transient remained very much more linear and the delayed tension transient was faster and of a smaller amplitude. White (1973) was able to model the PST only with a "three-state" model in which one attached state maintained less tension than a previous one. The PST arose because upon stretch activation the tension generating state became temporarily overpopulated, and decayed on a slow time scale. The effect of added phosphate ions was to accelerate this decay. The importance here is that the main tension generating state is one in which phosphate is still bound to actomyosin. This is not easily compatible with the conclusions from caged ATP studies with vertebrate muscle.

It is important to note that the main rationale behind the argument for a three state model is that the PST is due to some extra

state in the cross-bridge cycle. An alternative argument is that it is due to the build up of phosphate ions within the muscle fibre and is a diffusion artefact.

1.6.2 Structural Correlates for Stretch-Activation:

Any meaningful model must have a biochemical and structural correlate. The strongest arguments for how stretch activation arises in insect muscle are drawn from comparisons with vertebrate muscle, which does not show the effect to the same extent. There are three major structural differences between the two muscle types:

1) Connecting filaments, which contribute significantly to the muscle stiffness (White, 1983).

2) Hollow thick filaments with their paramyosin filling.

3) A coincidence of the actin and myosin helical repeat distance (38.5nm) (Wray, 1979).

Wray (1979) showed that point 3 provides a very neat explanation for how stretch activation might arise. He showed that the register of cross-bridges and actin "sites" changes as a thick filament moves relative to its neighbouring thin filaments. The sites change from mismatch to match following a length change of about 3% (thought to be the degree of muscle shortening in vivo, (Boettiger & Furshpan, 1954)) see Figure 1.6. Abbott and Cage (1979) performed careful mechanical experiments and were able to demonstrate that muscle stiffness had a peak at strains of 3% and then again at 6% above rest length. White et al. (1988) explain why the expected 3% periodicity of activation is not observed more often by other workers. They state that half sarcomeres which are "out-of-register" will be unstable. These half

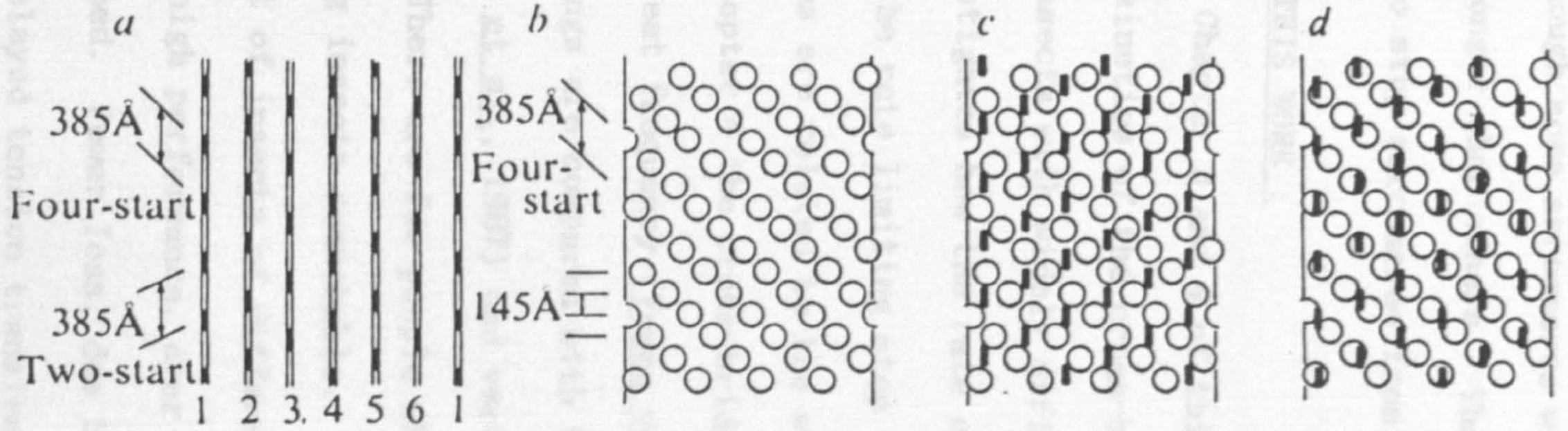

Filament geometry in insect fibrillar flight muscle (Wray, 1979)

FIGURE 1.6

The six stripped lines in (a) represent the 6 actin filaments which surround a thick filament. They have been "unwrapped" so that they can be drawn in 2-dimensions, the dark regions are potential myosin binding sites. (b) shows a thick filament which again is drawn as if it has been sliced down one side and opened out, the open circles represent the"reach" of each cross-bridge. In (c) the diagrams have been superimposed, because of the identity of one of the helical repeats (at 38.5nm) none of the myosin sites are aligned with actin sites. However, by moving the filaments relative to one another (changing the sarcomere length) actin sites now come into reach of the cross-bridges. The more effective interaction of cross-bridges with actin sites following a length change (c→ d) could explain how stretch activation in insect flight muscle arises.

Unlike insect flight muscle vertebrate muscle has a vernier relationship between the actin sites and cross-bridge projections, length changes therefore do not change the degree of match..between cross-bridges and actin sites.

sarcomeres generate little tension, and will be stretched by neighbouring sarcomeres. Any half sarcomere with cross-bridges and actin sites in poor register will therefore "jump" to a length where better match is obtained. The system described means that the degree of activation will be uniform along the entire length of the myofibril although some sarcomeres will have "jumped" and be 3, 6 or maybe even 9% longer than others. The function of the connecting filaments may be to stop sarcomeres from being greatly overextended.

1.7 THIS WORK :

Chapter 3 and 4 of this thesis forms a comparative study of how the kinetics of the cross-bridge cycle are adapted to suit the needs of insects with widely differing wingbeat frequencies. Chapter 3 investigates how the rate constant for delayed tension generation and the rate limiting step in the cross-bridge cycle in skinned muscle fibres are related to the wingbeat frequency of the intact insect. In Chapter 4 the cross-bridge kinetics of an insect with a high wingbeat frequency (Vespa vulgaris) is probed by oxygen exchange. The findings are compared with the pattern of exchange found in Lethocerus (Lund et al., 1987) and vertebrate muscle (Webb et al., 1985).

There are few people who do not find the speed and agility of flying insects remarkable. In Chapter 5 the efficiency and power output of insects of different sizes and the adaptations which permit this high performance, over a range of environmental temperatures, is examined. Power loss, due to the strong temperature coefficient of the delayed tension transient, is circumvented by large insects, which regulate their thoracic temperature, and is ameliorated by small insects, which tune their wingbeat frequency to suit the kinetics of their muscles.

The genetics of the fruitfly, Drosophila melanogaster are the best understood of any eukaryote. The development of techniques used to mount very small muscle fibres (only 0.5mm long) have allowed the mechanical kinetics of the flight muscles to be studied. Chapter 6 forms part of a collaborative study; the properties of muscle fibres from wild type flies are compared to fibres from flies with mutant muscle proteins. The precise nature of the genetic lesions were determined (by Drs. Ball and Sparrow, University of York and the laboratory of E. A. Fyrberg, Baltimore, U.S.A.) and so a structure-function relationship in the contractile proteins could be established.

CHAPTER 2 :

MATERIALS AND METHODS

MATERIALS AND METHODS

2.1 EXPERIMENTS ON WHOLE INSECTS :

2.1.1 Collection of Experimental Insects :

Some of the insects were obtained from cultures; all the Drosophila species (fruit-flies) were obtained from the laboratory of Dr. J.C. Sparrow (University of York) and Calliphora erythrocephala and Calliphora vomitoria were hatched from fishing maggots. These insects were available throughout the year. Other insects were collected locally by netting (Chinery, 1986), and were available only at certain times of the year. Finally, insects of the genus Lethocerus (giant waterbugs) were imported; Lethocerus griseus from Mr. G. Scott (Florida, U.S.A), L. collosicus, Dr. M.K. Reedy (Trinidad) and L. indicus, Dr. R. Sanit (Thailand). The insects were kept in fish tanks at York University, being fed on live goldfish. Giant waterbugs were available for much of the year.

2.1.2 Identification of Collected Insect Species :

Locally collected insects were identified to genus and occasionally to species with a general field guide (Chinery, 1986). All the hoverflies were identified to species using Stubbs and Falk (1983).

2.1.3 Wingbeat Frequency Determination :

The sound produced by the beat of an insects wings has a period the same as that of the wingbeat. This principle was used by Sotavalta (1947), who had 'perfect pitch' and was able to determine the wingbeat frequency by listening to the insect. One of the methods used here relies on the same principle; the sound of an insect in

free-flight was recorded with a microphone and the electrical signal was displayed on a storage oscilloscope (Tektronix 5223) set at an appropriate sweep speed. The wingbeat frequency was calculated knowing the time taken for the waveform to repeat. Occasionally an apparent frequency doubling occurred, this could be due to the wings 'clapping' at the top and bottom of a wing stroke or by the wings getting out of phase with one another (particularly in the non-dipteran insects). Because of the difficulty of inducing flight in the Lethocerus species, the sound of the insect flying in the laboratory was recorded on a cassette tape recorder and the sound was later played into the oscilloscope (via the headphone output socket). One possible source of error with acoustic methods of wingbeat frequency determination is the 'Doppler effect'. The observed frequency becomes distorted if the sound emitter moves either away from or towards the observer (in the same way that a police car siren changes tone as the car passes). However, for an insect moving at 6 ms^{-1} the maximum error would be only ±2%.

The wingbeat frequency of the very small flies (Drosophila species) was measured by glueing the fly to a crystal gramophone 'pick-up'. The vibrations produced by the flying insect induce a small voltage in the 'pick-up'. The voltage was displayed on the oscilloscope and the frequency determined as before. This method is not as reliable as the first method for two reasons; 1) The wingbeat frequency is measured while the insect is tethered, 2) It is not certain that the recorded vibrations are of the same time period as the wingbeat. However, the values recorded for Drosophila agree well with other published values (Greenewalt, 1962 and Laurie-Ahlberg, et al., 1985).

The third method was to tether insects in front of a stroboscope

and to adjust the frequency of the light flashes to the highest frequency at which a motionless, single image of the wings was obtained. The advantage of this method is that it is certain that the true wingbeat frequency is being measured, the disadvantage is that the insects are again tethered, which may alter the 'normal' frequency.

2.1.4 Measurement of Thoracic Temperature in Flight :

A small, bead-thermistor was mounted on the end of a drawn-out pasteur pipette, of 1mm tip diameter. A Wheatstone-bridge amplifier was built with chosen values of resistors in the other arms of the bridge to give a linear output in voltage with change in temperature of the thermistor (see Figure 2.1a). The output of the amplifier was connected to a galvanometer for an instant readout of temperature and an external socket provided output to a chart recorder. The thermistor was always calibrated before use against a mercury thermometer in the range 0-50°C. (see Figure 2.1b). The thoracic temperature of the medium sized insects (larger flies, bees and wasps) was measured either by impaling the thorax of the flying insect on the thermistor probe or by inserting the thermistor into the insect thorax just after flight termination. The larger insects (giant waterbugs) were allowed to fly free in the laboratory and were recaptured as soon as possible after flight termination. The thoracic temperature was measured for several minutes so that a cooling curve could be plotted and extrapolated back to the time when the waterbug was airborne.

2.1.5 Determination of *in vivo* Muscle Shortening :

The thoracic movement of an insect in tethered flight was measured. The insect was mounted below a travelling microscope,

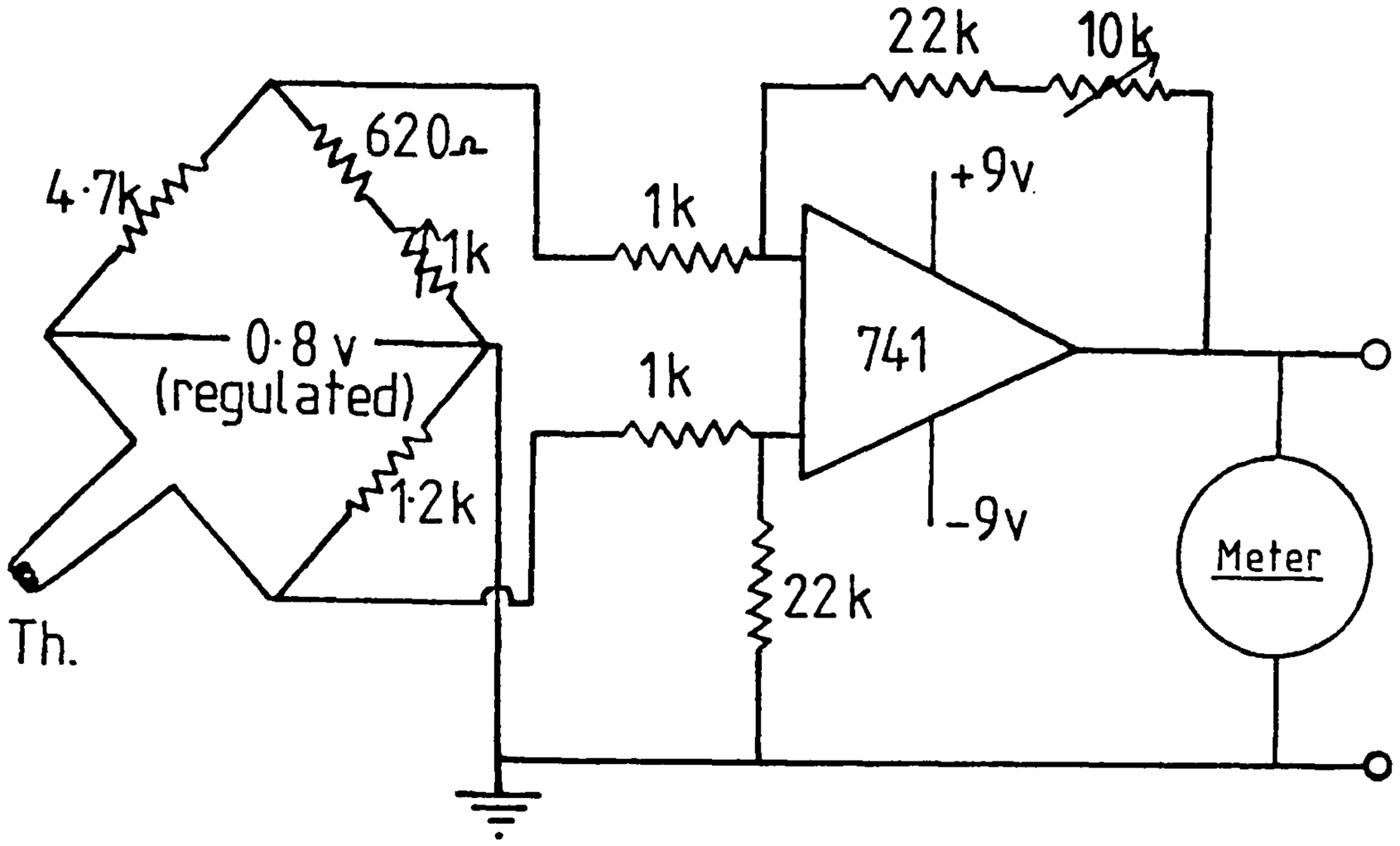

(a)

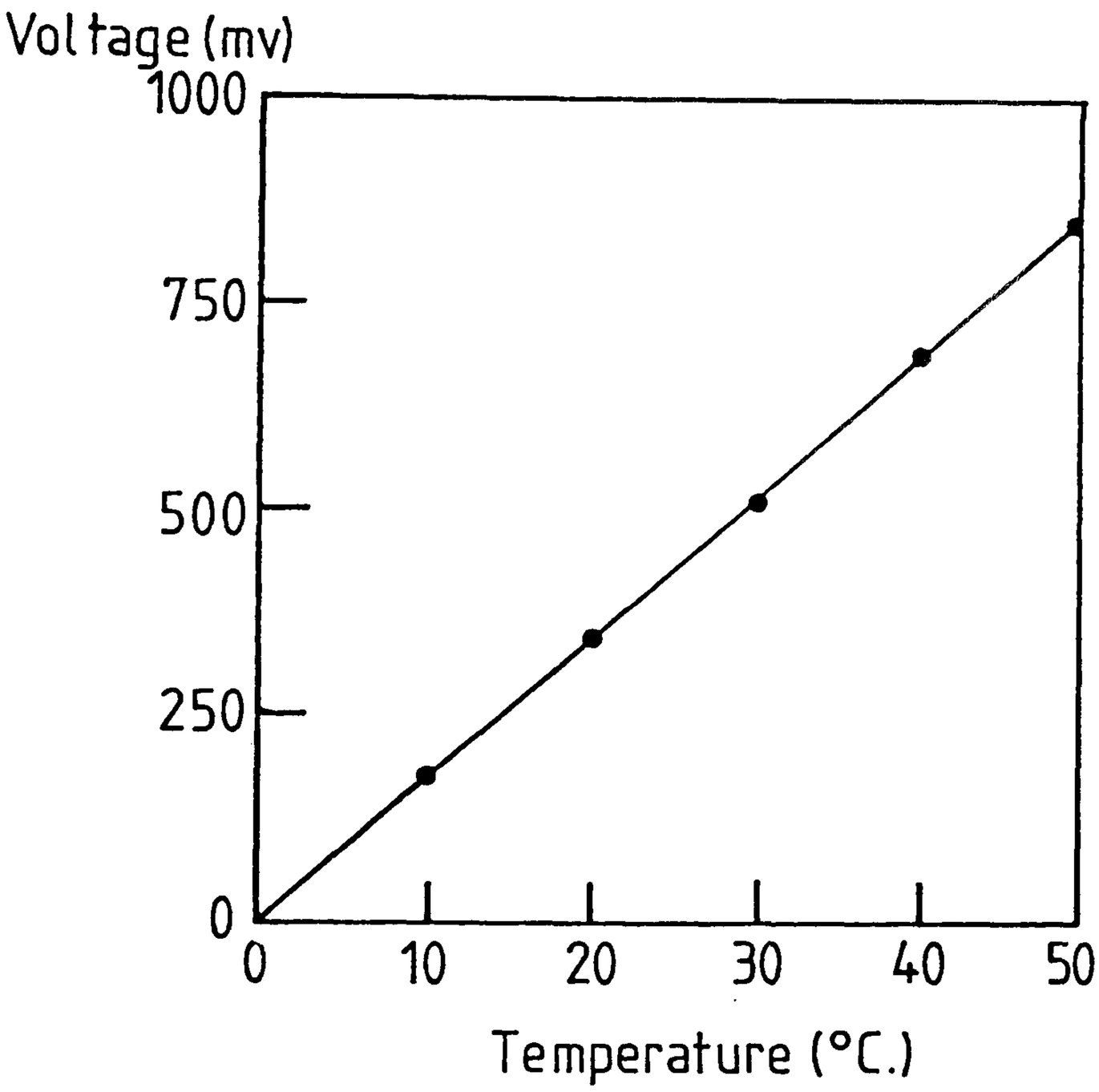

(b)

Thermistor Calibration.

FIGURE 2.1

Figure 2.1a shows the circuit used to measure changes in the electrical resistance of the thermistor (Th.). The output was monitored both on a meter and via external leads to a chart recorder. A calibration graph, of output voltage vs. temperature is shown in figure 2.1b.

fitted with a 4X objective lens and an eye-piece graticule. The insect was illuminated with a stroboscope. The flash frequency was adjusted so that the length of the thorax could be measured while the wings were 'frozen' at the extremes of the up and down stroke.

2.2 MUSCLE DISSECTION :

2.2.1 Very Large Insects (Giant waterbugs) :

Dissection of the indirect flight muscle of giant waterbugs has been described previously (Barber & Pringle, 1966). Two longitudinal cuts made either side of the thorax allow the dorsal and ventral halves to be separated. The dorsal-longitudinal (DLM) indirect flight muscles (IFM) remain attached to the dorsal half of the thorax. In order to determine the mass of the indirect flight muscles all of the fibrillar muscle was scraped from the thorax and weighed on an electronic balance (Mettler H20). This muscle was then used either for myofibrillar preparations (used by other workers in the laboratory), or for cytochrome c determinations (see below). Skinned fibres, used for mechanical experiments, were prepared by glycerol extraction of the DLMs while still attached to the thorax (see below).

2.2.2 Medium Sized Insects (Large flies, bees and wasps) :

The head and abdomen of the insect were removed and the gut was pulled out of the thorax. The tip of a micro-dissection scissor was inserted into the head-end of the thorax and with the thorax held firmly, a cut was made all the way around to leave the thorax sagittally bisected. Smaller insects were cut in half under a dissection microscope, held in place with a pair of watchmakers forceps. Flight muscle mass determinations were made by removing all the thoracic muscle with a small spatula and weighing the muscle on the electronic balance. Muscle mass determinations in small insects

were made on the contents of several thoraces.

2.2.3 Very Small Insects (Fruit flies) :

The smallest fly used was *Drosophila melanogaster*, weighing less than 1mg with a length of about 1.6mm. The other species *D. hydeii* and *D. funebris* are about 1.5 and 2.5 times this length (resp.). Specially prepared dissection instruments were required for the dissection. Watchmakers forceps were sharpened on carborundum paper (C600 grade) under a dissection microscope. Tungsten-wire dissection needles were sharpened electrolytically, by passing an alternating electric current through the needle while it was slowly withdrawn from a saturated sodium nitrite solution. The dissection method for these insects was devised by Dr. J.C. Sparrow, University of York.

A piece of plasticene was pushed into a glass embryo-cup and a narrow channel made in the surface with the handle of a scalpel. Flies were anaesthetised with either diethyl-ether or CO_2 and placed in the plasticene channel, with the dorsal thorax exposed. The insect was fixed in place by embedding the wings in the plasticene. A longitudinal cut was made along the length of the dorsal thorax with the point of one of the tungsten needles and the head and abdomen of the insect were removed with a pair of forceps. The thorax was cut free of the wings with a pair of micro-dissection scissors and was transferred to a small dissection dish containing a 50% glycerol solution. The thorax was bisected completely by cutting through the ventral surface of the thorax with the dissection scissors, under a dissection microscope. The DLM's were then glycerol extracted while still attached to the thorax. Just prior to an experiment the DLMs from one half thorax were cut free of the thorax at either end using the micro-dissection scissors.

2.3 WHOLE MUSCLE EXPERIMENTS :

2.3.1 Sarcomere Length Determination :

The IFM sarcomere length was measured in two different ways; by light microscopy and by measurement of a laser light diffraction pattern.

1) Light microscopy :

Glycerol extracted muscle fibres (see below) immersed in a relaxing solution (see below) were viewed under a phase contrast microscope fitted with an eyepiece graticule. The length of about 20 sarcomeres was measured and the average sarcomere length calculated.

2) Laser light diffraction :

Sarcomere striations are clearly visible under phase contrast microscopy because of the variation in refractive index along the sarcomere. At low angles of incident light, 'internal reflection' at refractive index interfaces occurs (ie the Z-line). The reflected light from the muscle sarcomeres undergoes interference and a diffraction pattern is produced (Rudel and Zite-Ferenczy 1979). The spacing of the diffraction pattern maxima is related to the sarcomere length (see Figure 2.2).

$$L_s \sin \theta = n \lambda \qquad \text{.....(2.1)}$$

L_s = Sarcomere length
n = 1,2,3...
θ = Angle of n^{th} interference maximum
(Equation 2.1 is derived in Figure 2.2)

If all the sarcomeres were aligned precisely along the fibre axis and the incident light was normal to the fibre, no diffraction pattern would be observed. However, there is a population of orientations, centred about the fibre axis, and diffraction maxima are observed on

$$d = L_S \cos\alpha$$

$$d = \frac{\lambda}{2 \sin\alpha}$$

$$2 L_S \sin\alpha \cos\alpha = \lambda$$

$$* \; L_S \sin 2\alpha = \lambda$$

$$\underline{L_S \sin\theta = \lambda}$$

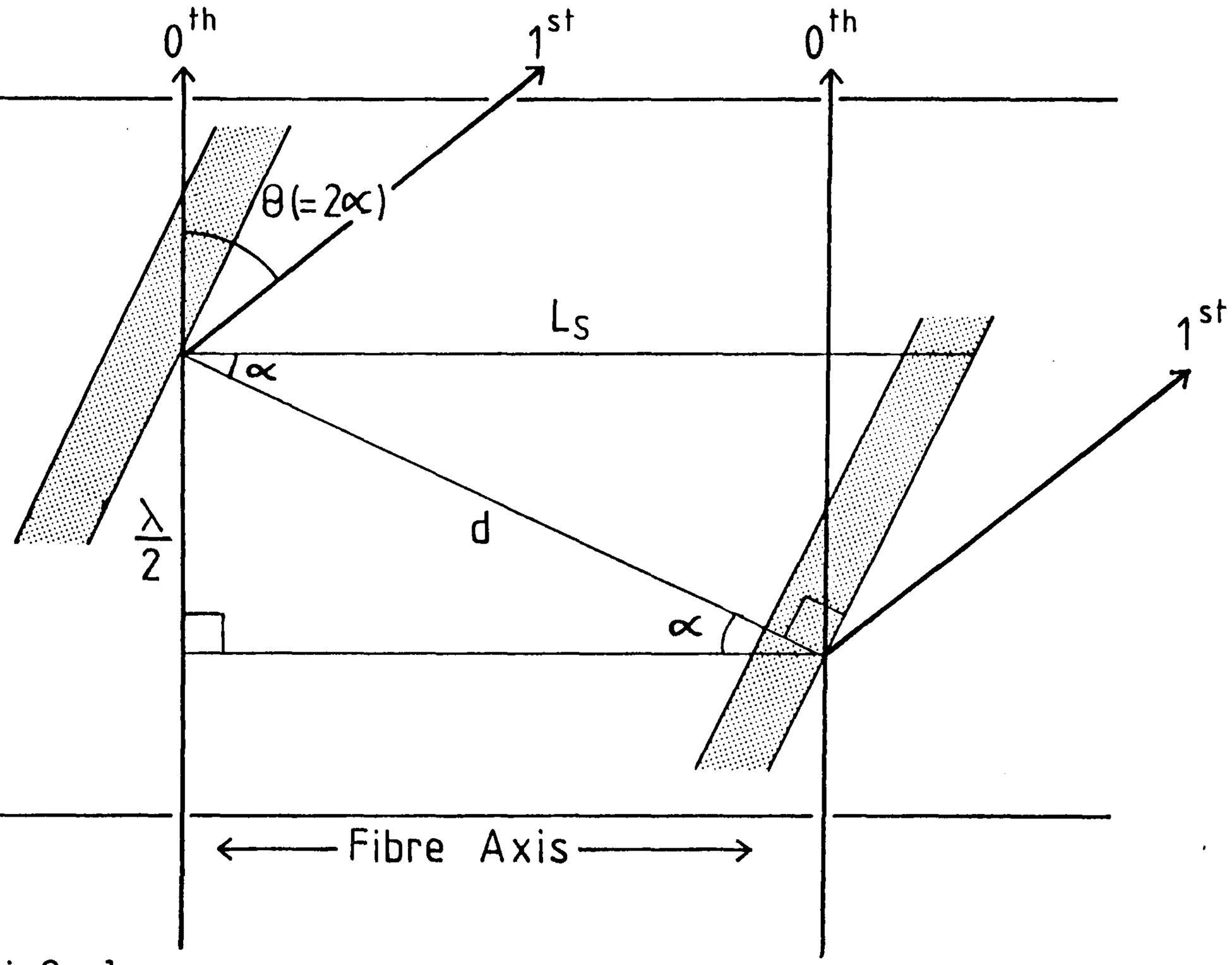

[* $\sin\alpha \cos\alpha = \frac{1}{2} \sin 2\alpha$]

FIGURE 2.2

Diagram to show how interference maxima are produced from light diffraction by muscle. Solid lines show the light path and the shaded regions represent part of the sarcomere with a low refractive index, light is reflected at the interface. The maxima are labelled 0^{th} and 1^{st}.

either side of a central maximum. Figure 2.2 shows how a first order maximum is produced on one side of the central maximum by a, non-axially orientated, sarcomere (exaggerated in the Figure). A fine beam of Helium-neon laser light (0.95mW, 633nm, He-Ne laser, Spectra-Physics 155A) was used to create the diffraction pattern. Muscle fibres were placed in a droplet of relaxing solution on a microscope slide. The diffraction pattern was measured at a known distance from the fibre (10-20cm). The angle of the first maximum from the central maximum (θ in Equation 2.1) was then calculated.

2.3.2 Cytochrome c Determination :

The respiratory pigment cytochrome c was extracted and assayed from the IFMs. The yellowish colour of the IFMs is caused by the very high concentration of cytochrome c in this muscle.

1) Extraction :

Cytochrome c is loosley bound to the mitochondrial membrane and is unique amongst the respiratory pigments in that it is easily extracted with a hypertonic solution (Estabrook & Pullman, 1967).

A known mass of muscle (usually about 20mg) was homogenised in an Eppendorf tube in 1ml of extraction buffer (see Table 2.1). The tube was left to stand at 4°C. for 4 hours. The suspended matter was removed by spinning in a bench centrifuge (Eppendorf, Bench centrifuge, Anderman 5414) for 5 minutes. The solution was pipetted into a spectrophotometer cuvette and the optical absorbance was measured over the range 600-350nm (Shimadzu, UV-240). The cytochrome c was fully reduced by addition of a known volume of ascorbate (ascorbic acid, 100mg/ml + potassium carbonate to pH 7.00).

KCl	0.5 M
Triton-X100	0.5% V/V
Phosphate buffer	20 mM
pH	7.00

Table 2.1
Cytochrome c extraction buffer.

2) Estimation :

Cytochrome c has three characteristic absorbance maxima; 550nm, 520nm, and 410nm (α, β and γ peaks resp.). The peak at 550nm is the sharpest and also shows a characteristic rise in absorbance upon reduction. The absorbance coefficient of cytochrome c at 550nm is 27.7 (cm^2/mol) (Lehninger 1975), the molecular weight = 12,384 (Chan & Margoliash, 1965).

Standard solutions of cytochrome c (Sigma Chemicals) were prepared. The optical absorbance of cytochrome c in the extraction buffer was the same as the absorbance in water and agreed well with the published value (see Figures 2.3 (a & b)).

2.4 GLYCEROL-EXTRACTION OF THE INDIRECT FLIGHT MUSCLES :

As described in chapter 1, the purpose of glycerol-extraction is to disrupt the muscle membrane systems, leaving the bare muscle proteins bathed in a buffered solution of low freezing point. The process is otherwise known as chemical 'skinning'.

2.4.1 Extraction Solution :

The constitution of the glycerol-extraction solution is given in Table 2.1. The solution is similar to that used by White & Thorson (1972). The solution was made up in advance and stored at -20°C. for up to 2 months.

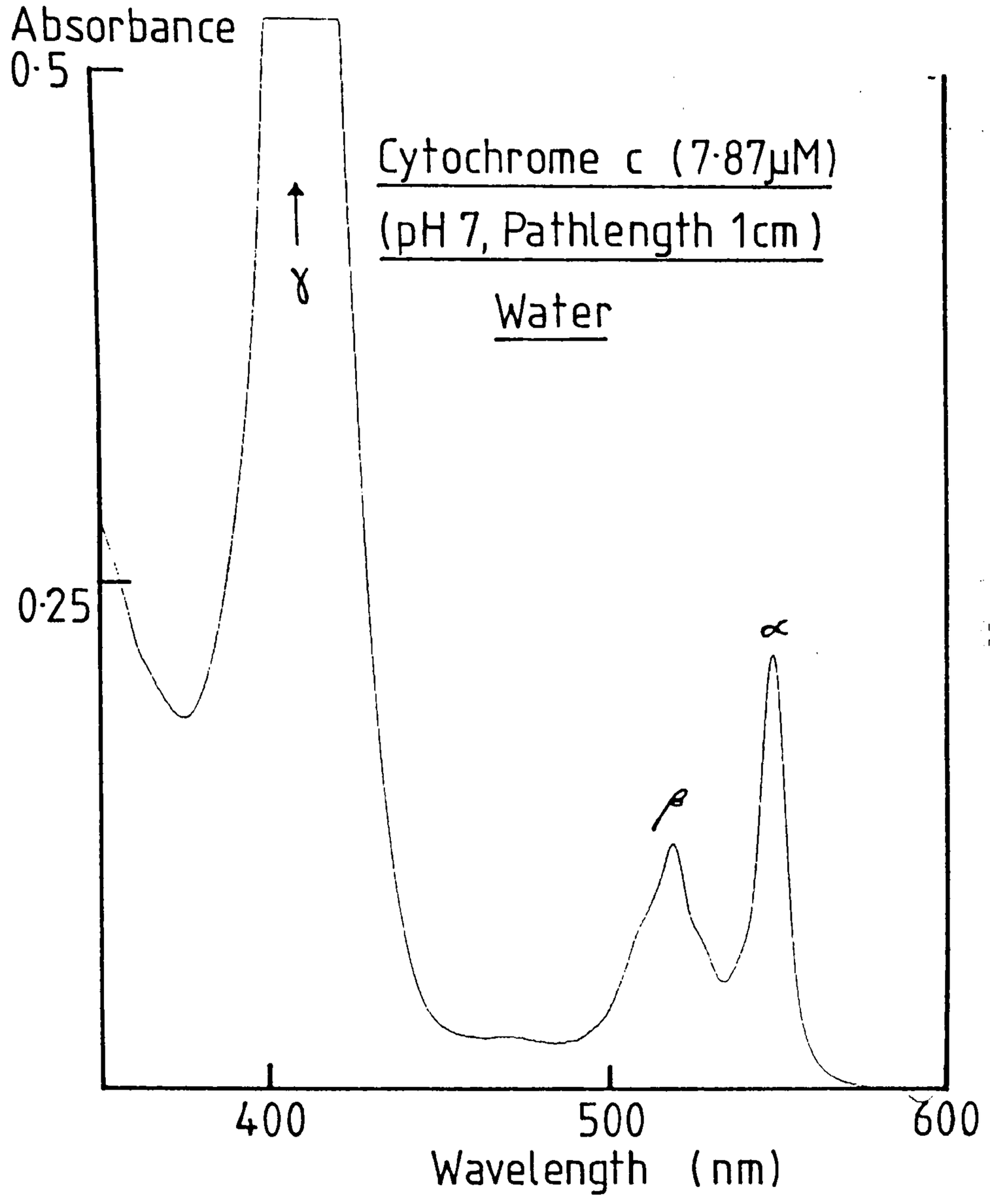

(a)

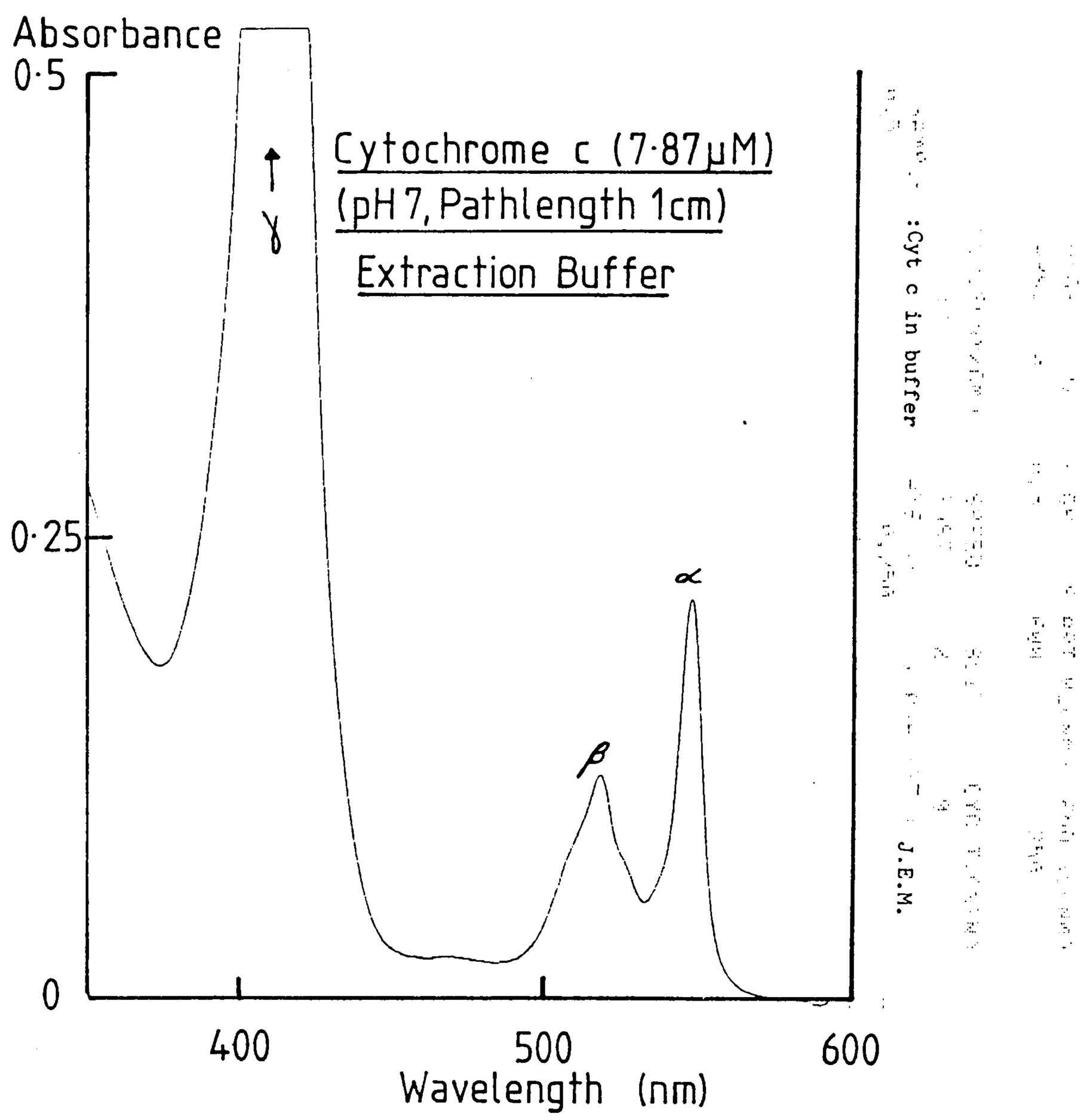

(b)

FIGURE 2.3

Absorption spectra of cytochrome c dissolved in (a) distilled water and (b) extraction buffer (described in Table 2.1). The ∝ absoption peak was used to estimate the amount of cytochrome c present in the flight muscles.

Glycerol	50% (V/V)
Potassium Phosphate buffer	20mM
(K_2HPO_4 + KH_2PO_4 (1 : 2))	
Sodium Azide	1mM
DTT	1mM
$MgCl_2$	2mM
Adjusted to	pH 7.0

Table 2.1.
Constitution of the glycerol-extraction solution.

The solution is *p*H buffered with potassium phosphate. The reducing agent dithiothreitol was added to slow the breakdown of the muscle proteins by oxidation of the sulfhydryl groups. Magnesium ions were added to reduce the enzymatic degradation of the myosin light chains (Weeds & Pope, 1977) and sodium azide to reduce bacterial contamination.

2.4.2 Glycerol-Extraction Procedure :

Prior to the extraction procedure the stored glycerol solution was allowed to warm up to 0°C. The dissected thoraces were immersed in the solution and placed on a stirrer in a cold-room (4°C.). The solution was stirred by a small magnetic 'flea'. The extraction solution was changed after 1 and 6 hours. After 24 hours the thoraces were transferred to fresh solution and stored at -20°C. Muscle fibres were used after two days and within 2 weeks of extraction, except for giant waterbug fibres which were used for up to 2 months.

2.5 SKINNED FIBRE EXPERIMENTS :

2.5.1 Experimental Solutions :

The constitution of the experimental solutions was based on those used by White and Thorson (1972). A computer analysis of the solutions was made (Perrin, 1967, modified by Dr. D.C.S. White to run on the IBM PC) to determine the concentrations of free metal ions and

complex species present (see Tables 2.2a-e and Table 2.3). The association constants were obtained from Martell and Smith (1974-76, 1983). Solutions were stored at -20 °C where little or no degradation of ATP occurred with time (checked with high performance liquid chromatography (HPLC), see below).

Immediately before each experiment, creatine kinase (Boehringer, Mannheim) was added to the solutions (2mg/ml) which contained creatine phosphate, to provide an 'ATP backup' system (see Scheme 2.1). This reduced the problem of rate-limiting ATP and ADP diffusion in and out of the muscle during mechanical experiments.

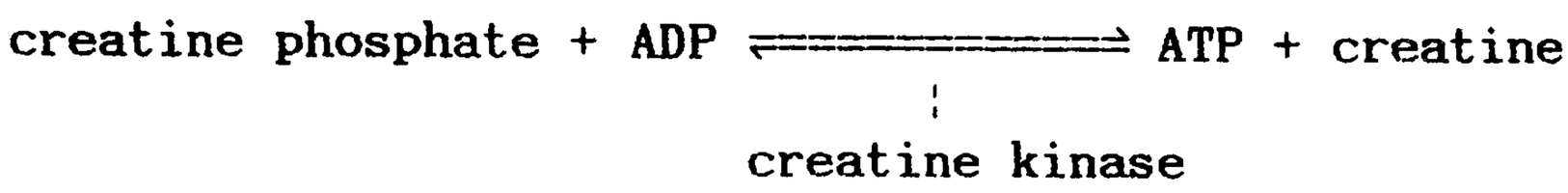

Scheme 2.1
The creatine phosphate/creatine kinase ATP back-up system.

2.5.2 Fibre Preparation :

After glycerol-extraction, bundles of muscle fibres were removed under binocular microscope at low power. Under high power, single fibres were removed from the bundle. In species where single fibres are difficult to isolate the muscle was pared down to a diameter of about 80 μm. Either end of the fibre was then carefully crimped in aluminium 'T' clips (see Figure 2.4a) (Goldman & Simmons, 1984b). The 'T' clips made it possible to mount very short fibres on the mechanical test apparatus (eg. fibres from Drosophila melanogaster, only 0.5mm long).

The aluminium 'T' clips were manufactured from aluminium kitchen foil. Two different techniques were used to make the 'T' clips. The first 'T' clips to be used were produced by a photo-etching process.

	(a)		(b)		(c)		(d)
Solution name	Ko	Lo	Kcp	Lcp	Kox	Lox	Ao
ATP(Na_2)	18.5	18.5	15.0	15.0	15.0	15.0	-
$MgCl_2$	15.5	15.5	15.0	15.0	14.0	14.0	12.0
CP(Na_2)	-	-	8.0	8.0	-	-	-
KCl	-	-	-	-	18.0	18.0	50.0
Histidine	20.0	20.0	20.0	20.0	20.0	20.0	20.0
EGTA	6.0		6.0		5.0		5.0
Ca(EGTA)	-	6.0	-	6.0	-	5.0	-
*p*H	7.0	7.0	7.0	7.0	7.0	7.0	7.0
Mg^{++}	0.7	0.8	1.0	1.1	1.1	1.1	10.7
*p*Ca	-	4.8	-	4.7	-	4.7	-
Ionic strength	123	122	128	128	117	117	98

	(e)
Inhibitors:	
NaN_3	1.0
Ap5A	10.0 μM
Quercitin	0.5
Oligomycin	1.0 μg/ml

Ap5A = P^1,P^5-Di(adenosine-5'-)pentaphosphate

Table 2.2

Constitution of the experimental solutions (all concentrations in mM (except where stated); K_n = relaxing, L_n = activating, Ao = rigor.

Solution name	Lo 10	Lo 12	Lo 15	Lo 18.5	Lo 29
ATP(Na_2)	10.0	12.0	15.0	18.5	29.0
$MgCl_2$	10.0	11.5	14.0	15.5	-
MgO	-	-	-	-	25.0
KCl	55.0	41.0	22.0	-	-
Histidine	20.0	20.0	20.0	20.0	20.0
Ca(EGTA)	5.0	5.0	5.0	6.0	5.0
CaCl2	-	-	-	-	0.2
*p*H	7.0	7.0	7.0	7.0	7.0
Mg^{++}	1.3	1.1	1.2	0.8	0.9
*p*Ca	4.7	4.7	4.7	4.7	4.7
Ionic strength	127	124	121	122	125

Table 2.3

Constitution of the experimental solutions used in experiments in which the concentration of ATP was to be varied (all concentrations in mM)

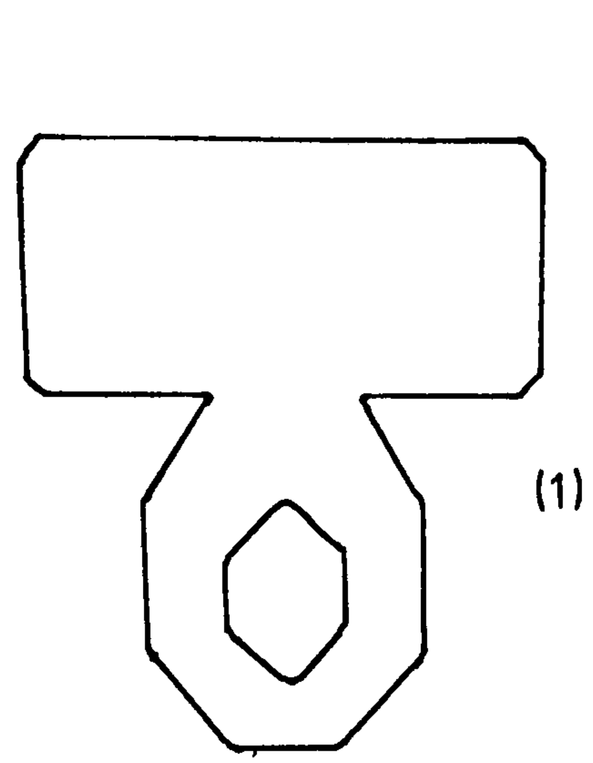

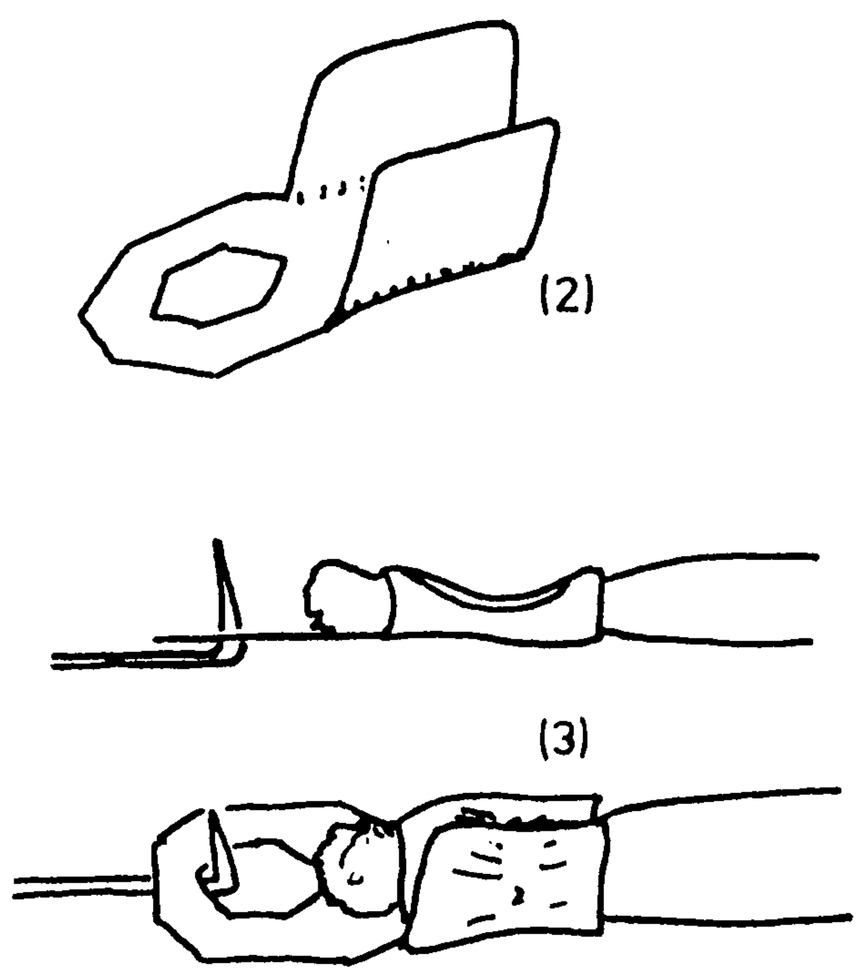

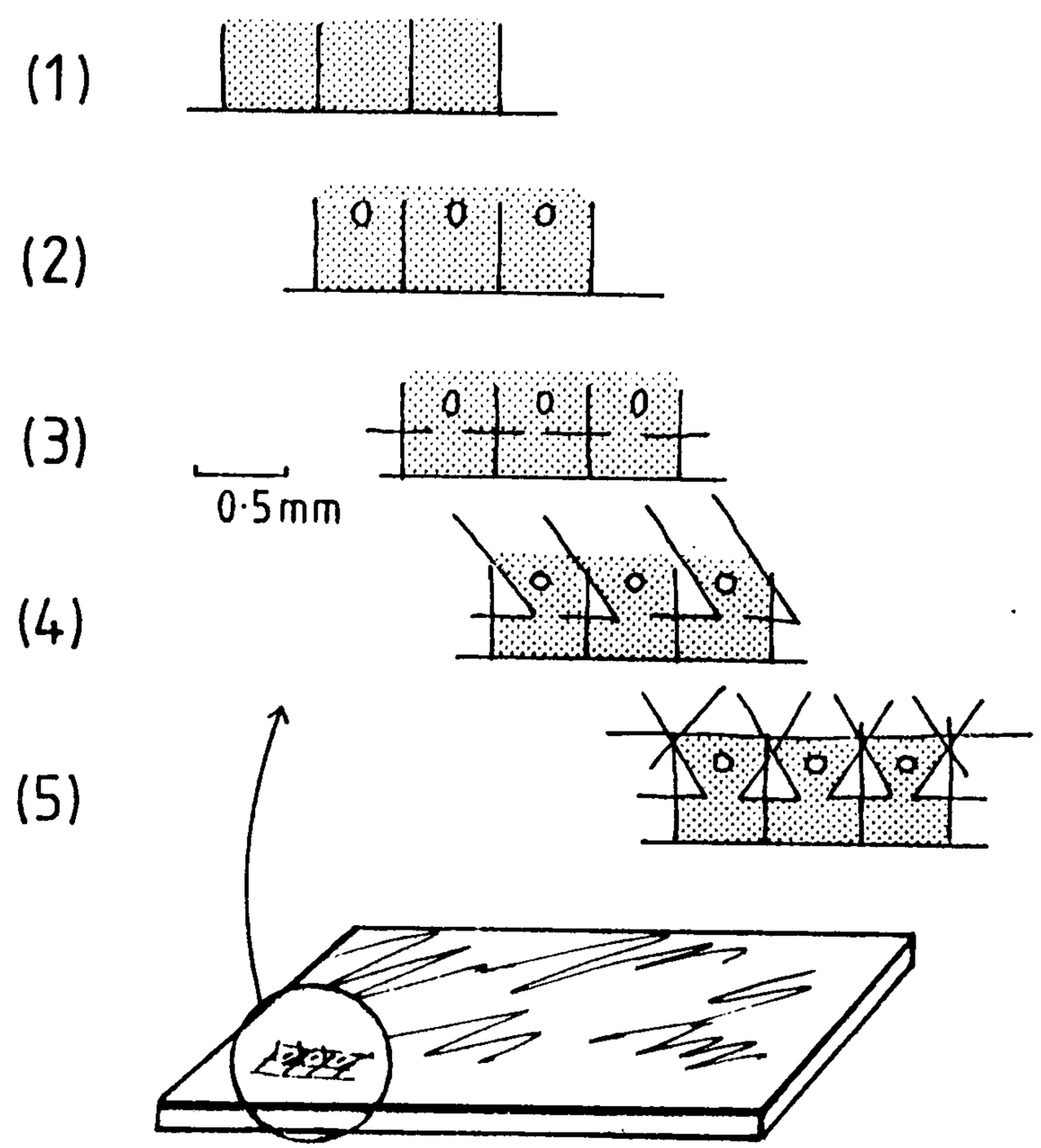

(a) (b)

FIGURE 2.4

Figure 2.4a shows how single muscle fibres were "crimped" in the aluminium foil "T" clips. Muscle fibres were crimped under a dissection microscope. Figure 2.4b shows the sequence of cuts used to manufacture the "T" clips. Aluminium cooking foil was glued to a microscope slide with cellulose nitrate glue to prevent the foil from tearing while it was cut with a sharp scalpel blade.

However, the process reduced the foil thickness, and so reduced the stiffness of the foil. Also the etching process left a sharp leading edge on the 'T' clip which tended to cut into the fibre. Better 'T' clips were produced by cutting the foil 'by hand'.

Aluminium kitchen foil was stuck to a microscope slide with cellulose nitrate glue. The glue was made by dissolving cellulose nitrate centrifuge tubes (Beckman, U.S.A) in acetone. The foil could then be cut, without tearing, with a sharp scalpel blade. Figure 2.4b shows the sequence of cuts used to produce the 'T' clips rapidly. Although more laborious to manufacture than the photo-etched 'T' clips, the hand-made 'T' clips were a significant improvement.

2.6 THE MECHANICAL TESTING APPARATUS :

The test bed consisted of a mild steel plate which rested on top of a motor-cycle inner tube. The inner tube was retained in a rectangular former made from 90° aluminium angle. The mass of the steel plate provided damping at low frequencies and the inflated inner tube damped the high frequency background vibrations present in the building. The mild steel plate was drilled and threaded to accept mountings for a tension transducer, bath assembly and length changer. The tension transducer and length motor had hooks, which extended into the incubation bath, to which the muscle fibres were attached. Electrical signals, proportional to the length and tension were simultaneously recorded on a digital, storage oscilloscope. The storage oscilloscope was connected to an IBM Personal Computer so that data could be stored and later analysed by the computer. The general layout of the apparatus is shown in Figure 2.5.

Two sets of mechanical test apparatus were constructed; one set-up was used for measuring the mechanical kinetics of skinned fibres

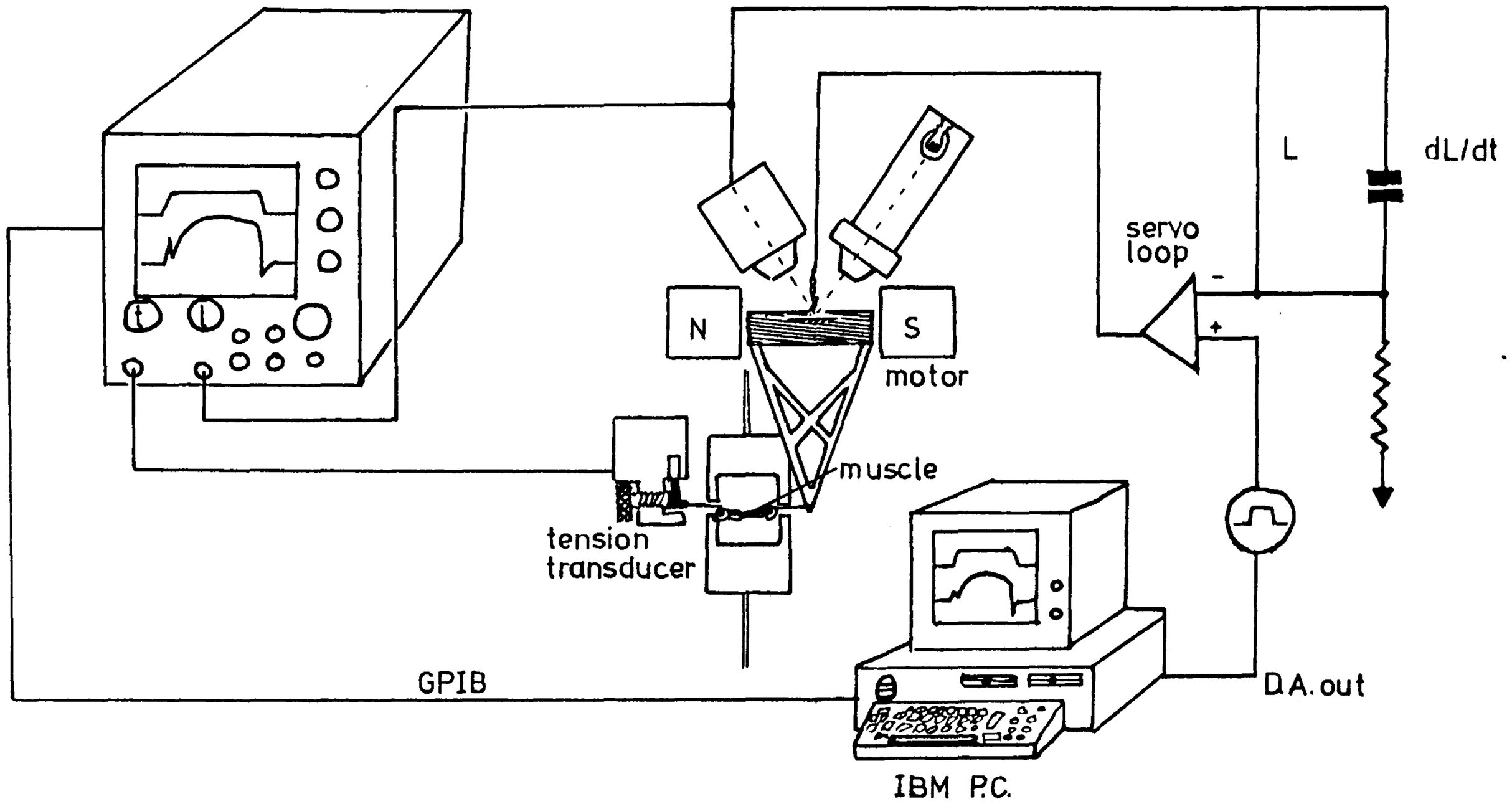

FIGURE 2.5

General lay-out of the mechanical test apparatus and devices used to monitor and record the length and tension signals. GPIB, General purpose Interface Bus; D.A. out, length input signal produced by the IBM Personal Computer.

the other was used for ATPase determinations.

2.7 THE TENSION TRANSDUCER :

The same basic design of tension transducer was used in both mechanical set-ups :

The tension transducer (Akers AE801, SensoNor a.s., Knutsrodveien 7, P.O. Box 196, 3191 Horten, Norway) consisted of a silicon beam (0.5mm X 5mm X 2mm) with two piezoresistive components bonded on opposite sides at the base. The silicon beam was critically damped by an oil meniscus lying between the transducer and a movable vane (Figure 2.6a). Small deflections at the tip of the beam affect the resistance of the two resistive components at the base. The two resistors were included in adjacent arms of a Wheatstone bridge and the change in voltage across the bridge was amplified by a low noise amplifier (Burr-Brown 3500E) (Figure 2.7). The circuit cancels out noise affecting both transducers equally. A hook, attached to the tip of the beam, passed through a slot in the side of the incubation bath. Surface tension prevented the solutions from running out. The requirement of the hook was that it should be light-weight, stiff and thin enough to fit through the slot. A short length of grass stem was bonded to the tip of the transducer with araldite, onto which was attached a length of fine glass capillary tubing having a fine tungsten-wire hook fixed into the far end (Figure 2.6b) with acrylate glue. Because of its high density, the length of tungsten wire was kept to a minimum. The joint between the capillary tube and the grass stem was made with shellac, which was softened with a hot soldering iron to facilitate fine angular adjustment of the hook.

The tension transducer assembly was mounted on a micro-manipulator, bolted to the metal base plate, which had a coarse and

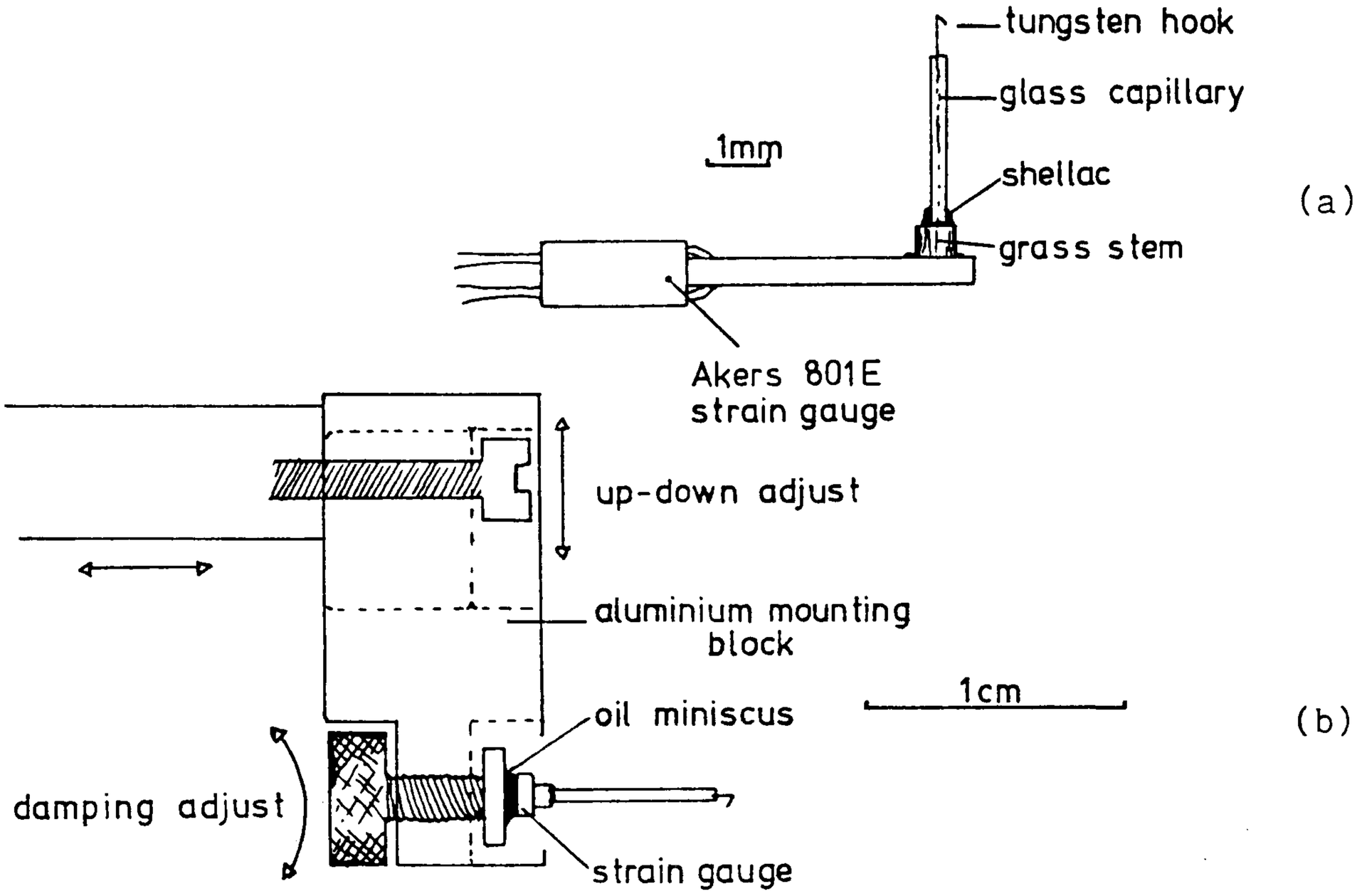

FIGURE 2.6

The tension transducer; 2.6a shows how the hook, used to mount the muscle fibres, was constructed. 2.6b shows how the transducer was fixed to the micromanipulator.

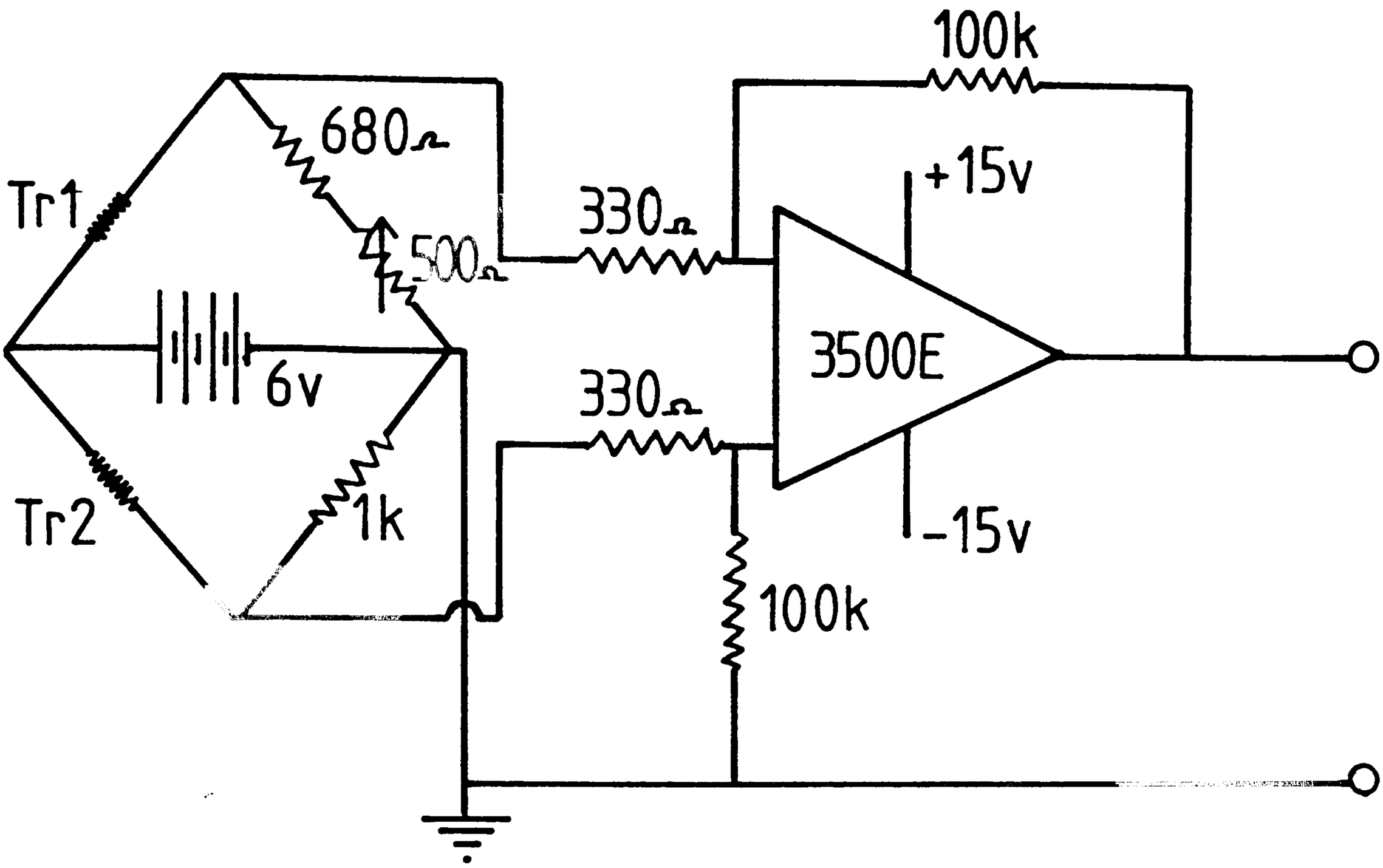

Tension Transducer Amplifier

FIGURE 2.7

Electrical circuit used to measure the change in electrical resistance of the tension transducer caused by forces exerted by an attached muscle fibre. The circuit was designed by Dr. D.C.S. White.

fine adjustment. The tension hook position could be adjusted over a large distance with great accuracy.

The tension transducer was calibrated by hanging known weights on the hook to produce a calibration graph (see Figure 2.8). The sensitivity of the transducers used was near to 9μN/mV with a noise level of 3.5μN. The resonant frequency of the undamped transducer was tested both unloaded and loaded with a fibre. In the first instance the transducer housing was tapped and the resulting oscillations recorded. In the second instance the tension oscillations following a sudden step length change made on a fibre were recorded. The undamped resonant frequency in both cases was about 8.3kHz (see Figure 2.9a,b).

The mechanical apparatus used for ATPase determinations had a bath system (see Figure 2.10b) which did not allow the tension hook to enter the side of the bath. An 'L' shaped piece of capillary tube was used so that the hook could enter the top of the bath. This modification greatly reduced the resonant frequency but increased the sensitivity of the tension transducer. The sensitivity and resonant frequency were measured as before; the resonant frequency was 1.1kHz.

The frequency response of the tension transducer is limited by its resonant frequency. The resonant frequency should be at least 10 times higher than any measured tension oscillation.

2.8 THE MUSCLE BATHS :

The bath system for both set-ups was mounted on an X-Y micropostioner. This allowed accurate positioning of the baths under the mounted muscle fibre.

2.8.1 Set-up Used for Measurement of Mechanical Kinetics :

A small temperature-regulated perspex bath was constructed (see Figure 2.10a). The central muscle bath (volume 80μl) had a slot cut

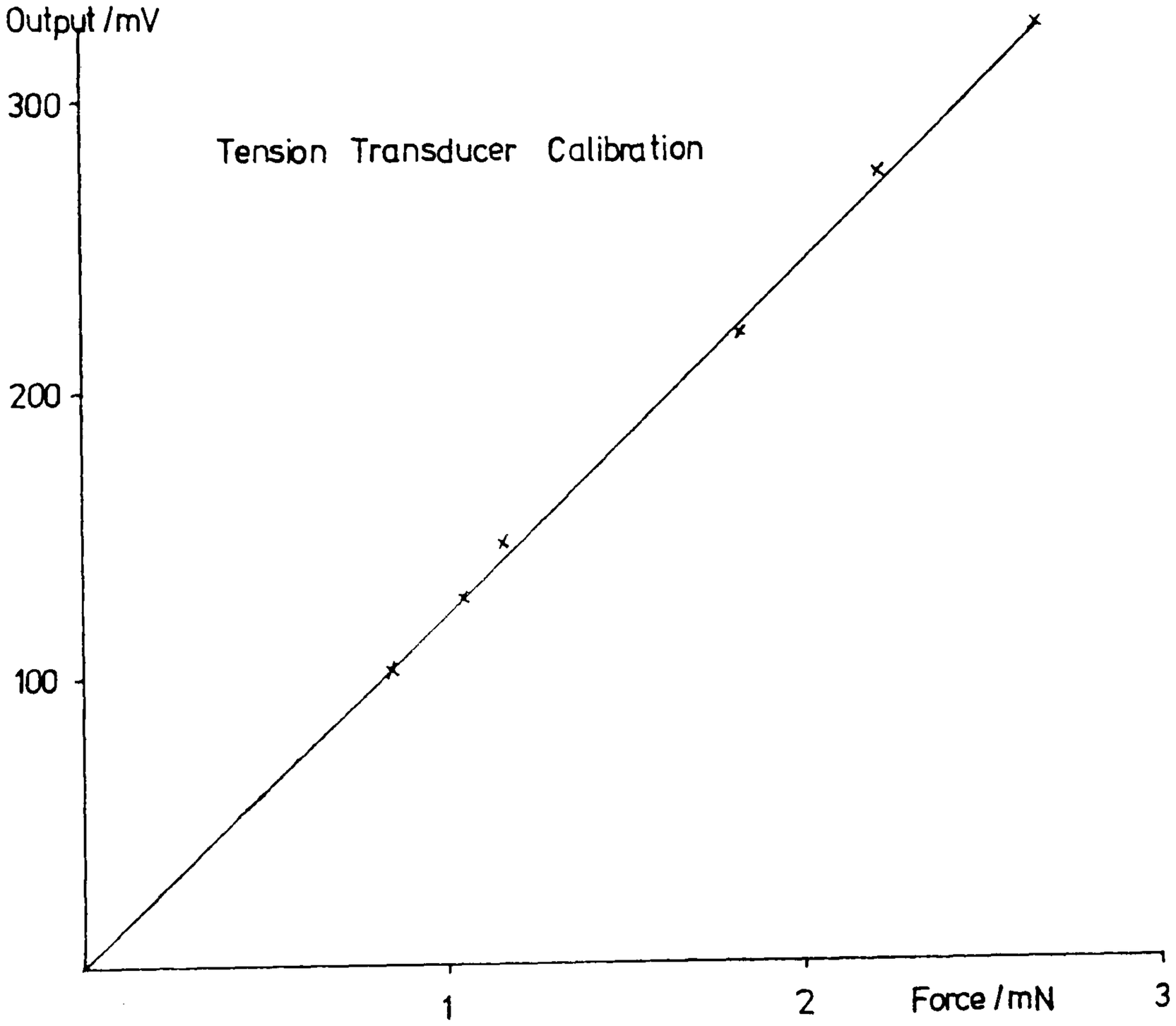

FIGURE 2.8

Calibration graph for the tension transducer; the calibration here is about 8 μN/mV.

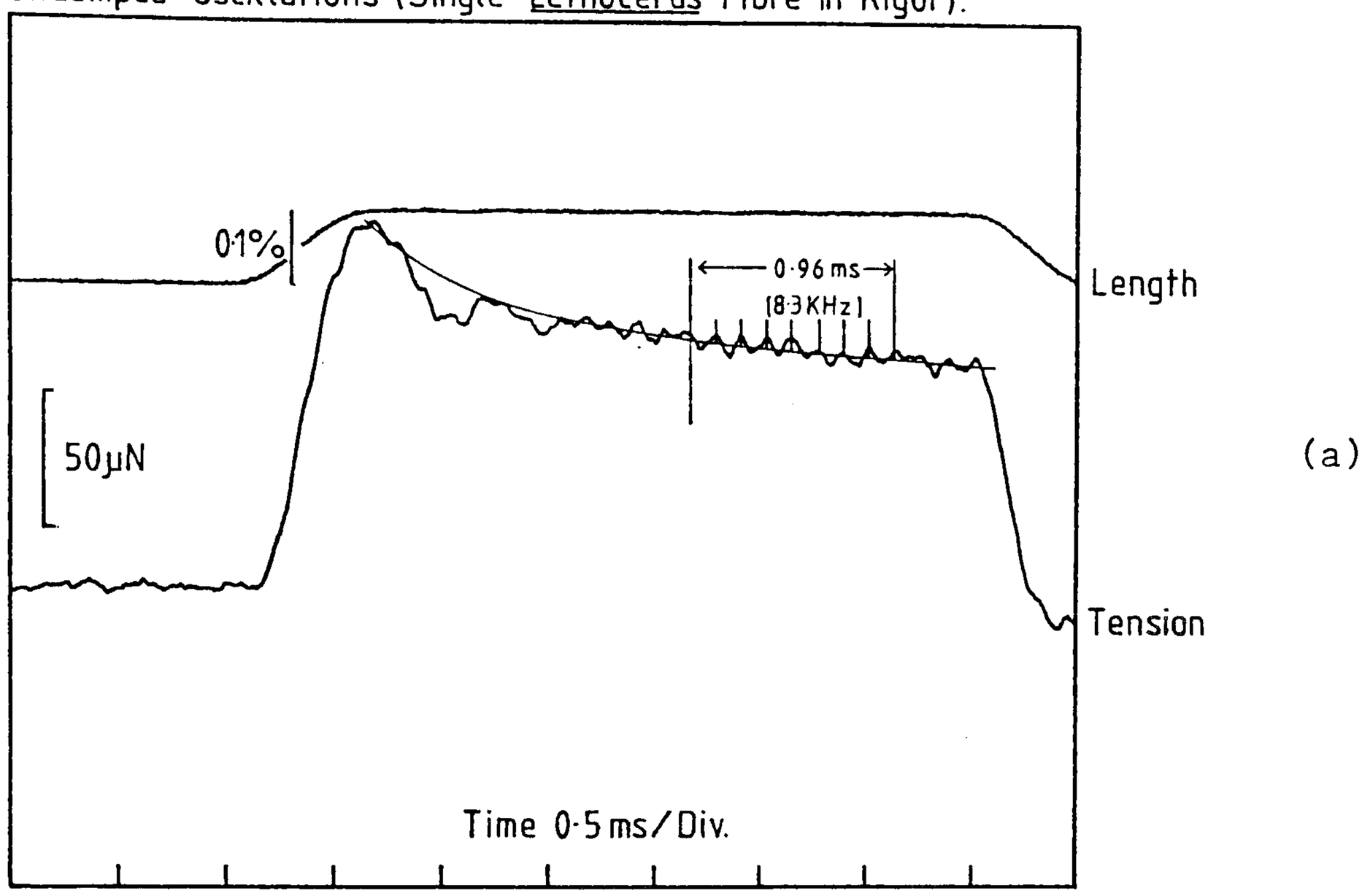

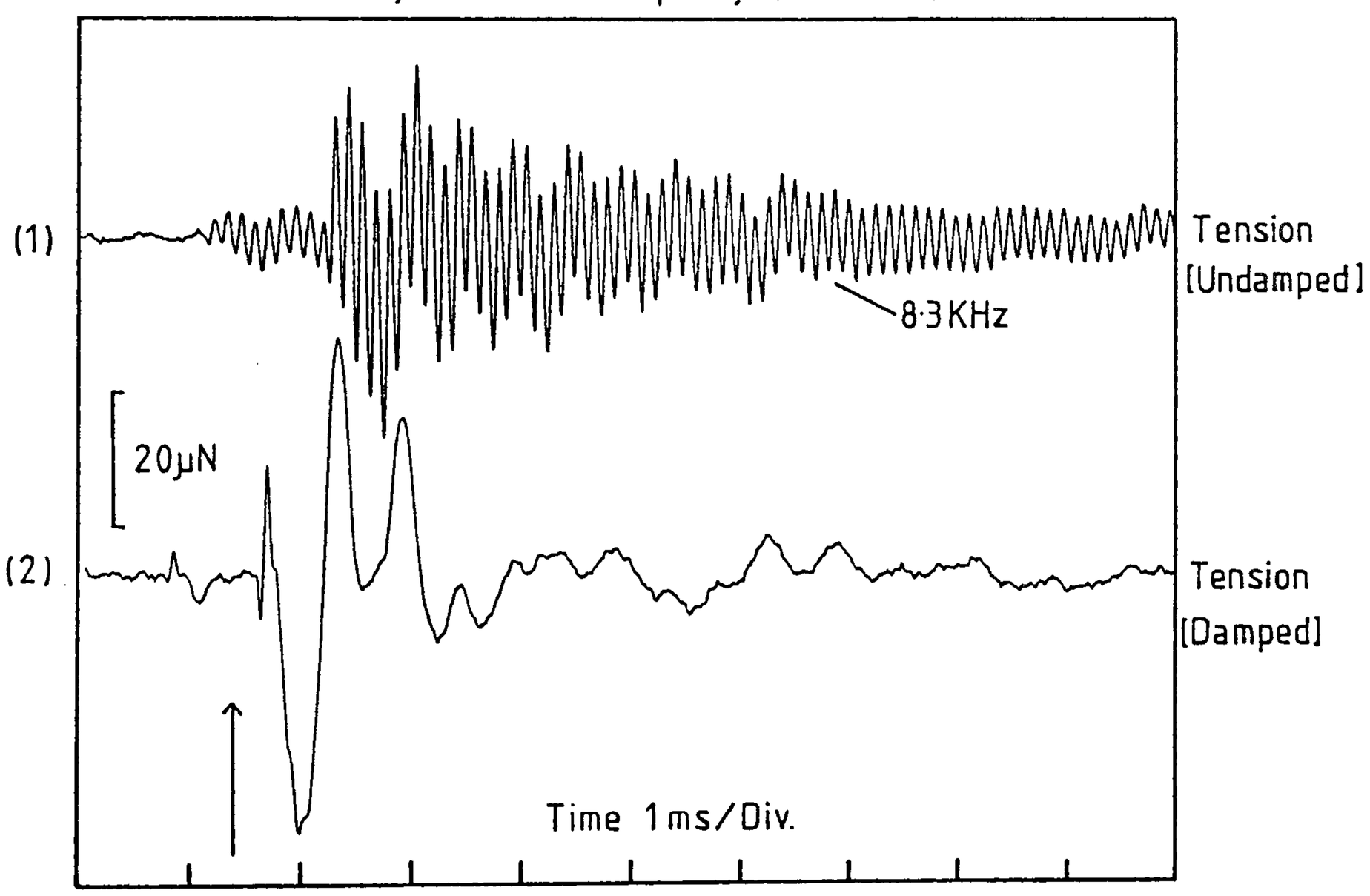

FIGURE 2.9

Determination of the resonant frequency of the tension transducer. In (a) the tension oscillations following a rapid length change made on a muscle fibre in rigor were monitored. In (b) the transducer housing was tapped; 1 when the transducer was undamped, 2 when it was damped by an oil miniscus (see Figure 2.6b).

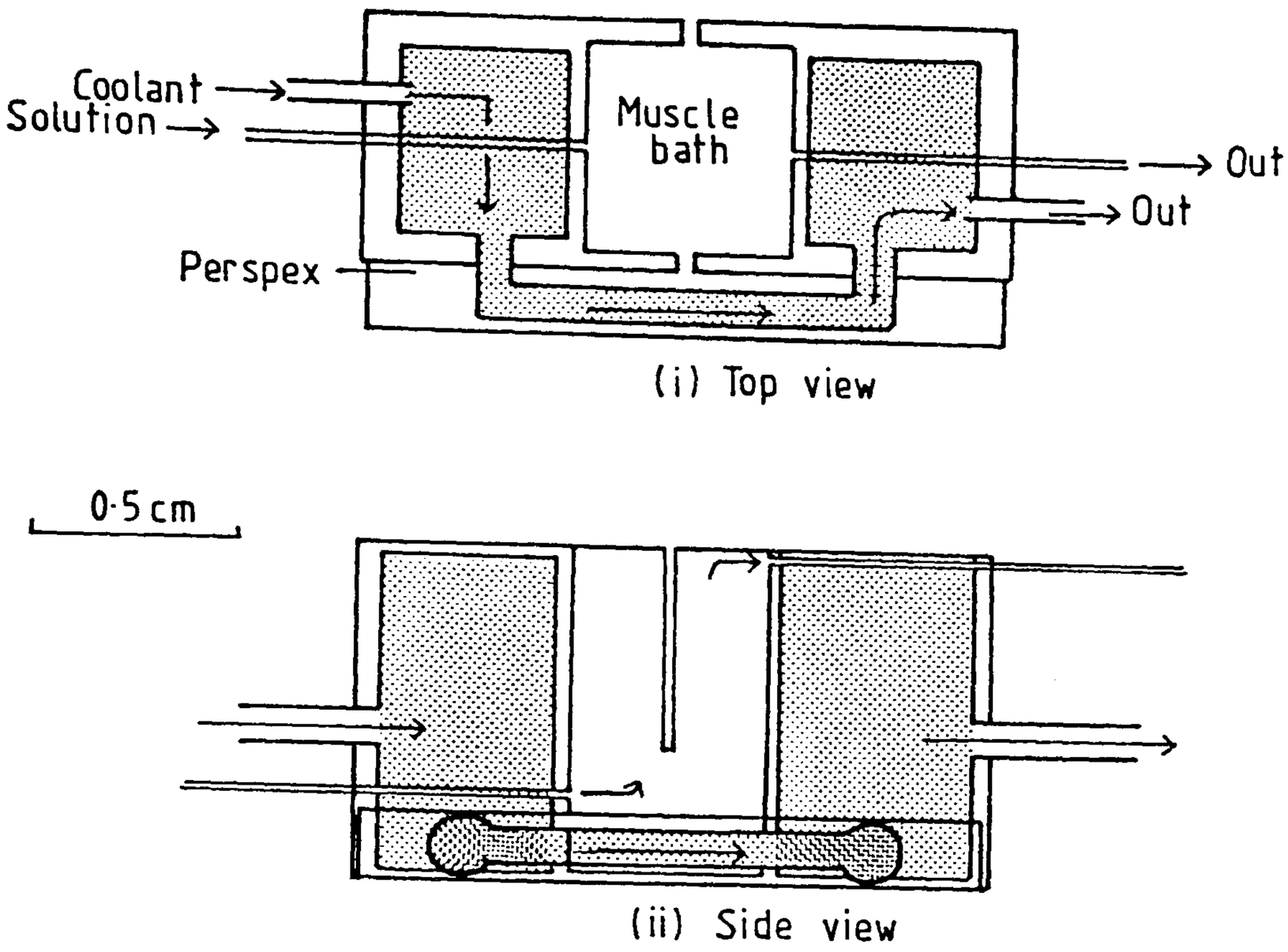

FIGURE 2.10

Muscle incubation baths used in (a) mechanical experiments (b) experiments where the ATPase activity was measured. In (a) the hooks from the test apparatus entered the side of the bath (via the slots) in (b) the hooks entered from above. The recess in (b) retained a layer of silicone oil. Both bath systems were mounted on an X-Y micropositioner.

in each side to allow hooks from the tension transducer and motor to enter the bath. The central muscle bath was temperature regulated by two side chambers which were circulated with temperature controlled water from a water bath (Thermomix, 1442D, B.Braun, Melsungen). Incubation solutions could be exchanged by means of two tubes, connected to glass syringes (Hamilton, Bonaduz.). One of the tubes entered the base of the muscle bath (supply) the other was connected to the top of the bath (drain).

2.8.2 Set-up Used for ATPase Determinations :

A row of seven, small (30µl), temperature controlled baths was constructed. The baths were milled into a recess in the top of a perspex block (see Figure 2.10b). After the baths had been filled with the incubation solutions a layer of dry silicone oil was run into the top recess. The layer of oil prevented evaporation of the incubation solutions. During 'oxygen-exchange' experiments (Chapter 4) the layer of silicone oil prevented contamination of the ^{18}O water incubation solutions with atmospheric ^{16}O water. These baths did not have slots cut in the sides to accept the tension and length transducer hooks because the low viscosity oil would run out. The length and tension transducer hooks were 'L' shaped and entered the top of the incubation baths.

2.9 THE LENGTH MOTOR :

The purpose of the length motor is to change the length of the muscle fibre in response to an input length signal. The input signal is a voltage provided either by a waveform generator (TWG300, Feedback Ltd.) or more complicated waveforms produced by the IBM Personal Computer. The motor should be able to follow the input waveform as

accurately as possible, in order to do this it must have a high resonant frequency.

The motor performance is most conveniently tested by measuring the rise time in response to a square wave input.

The set-up used for the ATPase measurements consisted of a commercially available mechanical vibrator (Ling Dynamics, model 101). The resonant frequency of this length motor was greatly improved by having a driving current controlled by an electrical servo-loop (White 1983). The fastest measured rise time was just under 1ms.

A new, faster, motor of the same design as that used by Ford et al. (1977) was built. This motor was used for experiments to measure the mechanical kinetics of skinned muscle fibres.

The motor consists of coil of aluminium wire suspended on a stiff mounting in a magnetic field. The magnetic field is provided by a horseshoe magnet attached to two pole pieces combined with an iron core. A pyramid of grass stems, glued to the coil, communicates any movement of the coil to the work area. Movement is monitored by two photodiodes which detect the change in position of a light beam being reflected by a mirror attached to the motor coil.

The motor was constructed in four stages;

2.9.1 The Coil :

To minimise weight, the coil was 'formerless' and made of varnished aluminium wire (127μm dia', 3.5m long). The central core of the motor was used as the former for winding the coil. In order to produce an even spacing between the coil and the core, insulating tape was wound around the core, three layers on the sides and five layers on the top and bottom. Two pieces of perspex were screwed onto the front and back of the core to prevent the windings from slipping off. Two layers of windings were made, approximately 50 turns in all,

leaving about 3.5 cm trailing for later connection to the driving electronics. Araldite, diluted in benzene was spread over the winding making sure that it flowed between the two layers. The pole pieces were coated in two layers of insulating tape and the motor was assembled. The motor and coil were then baked at 60°C for four hours. When the glue was heated it flowed into the coil and any air bubbles were displaced. The motor was disassembled while still hot so that the insulating tape remained soft and easy to remove.

2.9.2 Motor Position Detector :

The lamp and photodiode housings were made of aluminium and contained the optics required to direct a beam of light onto a mirror attached to the motor coil and back onto a pair of photodiodes. The filament of a 6 volt, 0.3 amp bulb in the lamp housing was brought to a focus at the level of an objective lens after passing through a square aperture (2.11a). The aperture was focused on the photodiodes after being reflected by a mirror attached to the motor coil. The image of the aperture on the pair of photodiodes (PIN spot 2D, United Detector Technology, California, U.S.A.) was the same size as one of the photodiodes. The lamp housing was adjusted so that, when the motor was switched off, the image of the aperture covered half of each of the two photodiodes. Movement of the coil altered the angle of the mirror and caused the aperture image to move more onto one or other of the two photodiodes. The electrical output from the photodiodes was amplified and used to measure the position of the coil.

FIGURE 2.11

FIGURE 2.11 :

a) Arrangement of the photo-detector for the length position signal

b) Construction of the coil, pyramid and pole pieces.

[(a) and (b) redrawn from Ford et al., 1977]

c) The servo-loop electronic circuit; amplifiers 1, 2 & 3 are low noise operational amplifiers (LF356BN); amplifier 4 is a D.C.-coupled audio amplifier (CE 1004, Crimson Elektrik). The photodiodes were PIN Spot 2D (United Detector Technology).

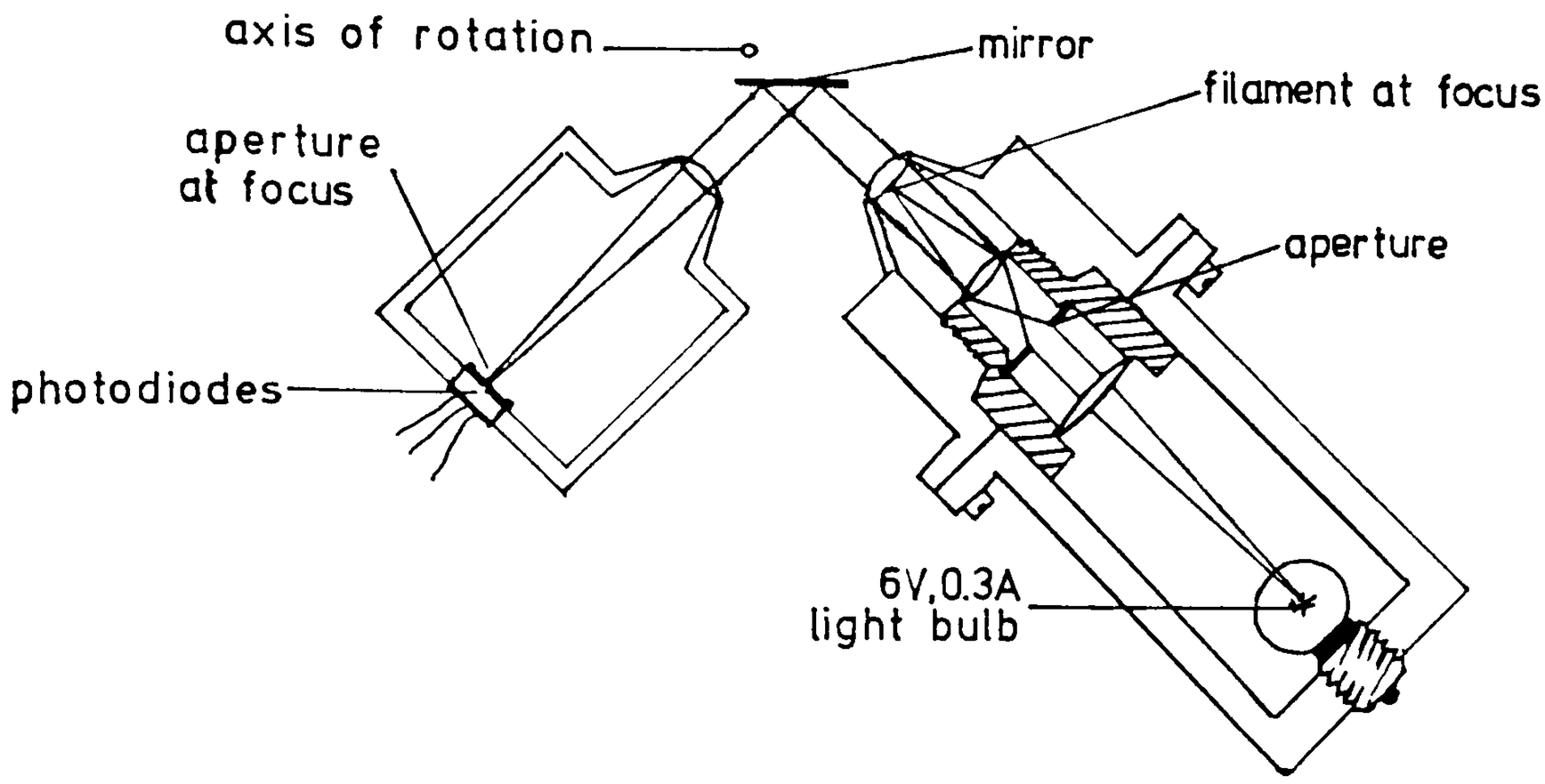

(a)

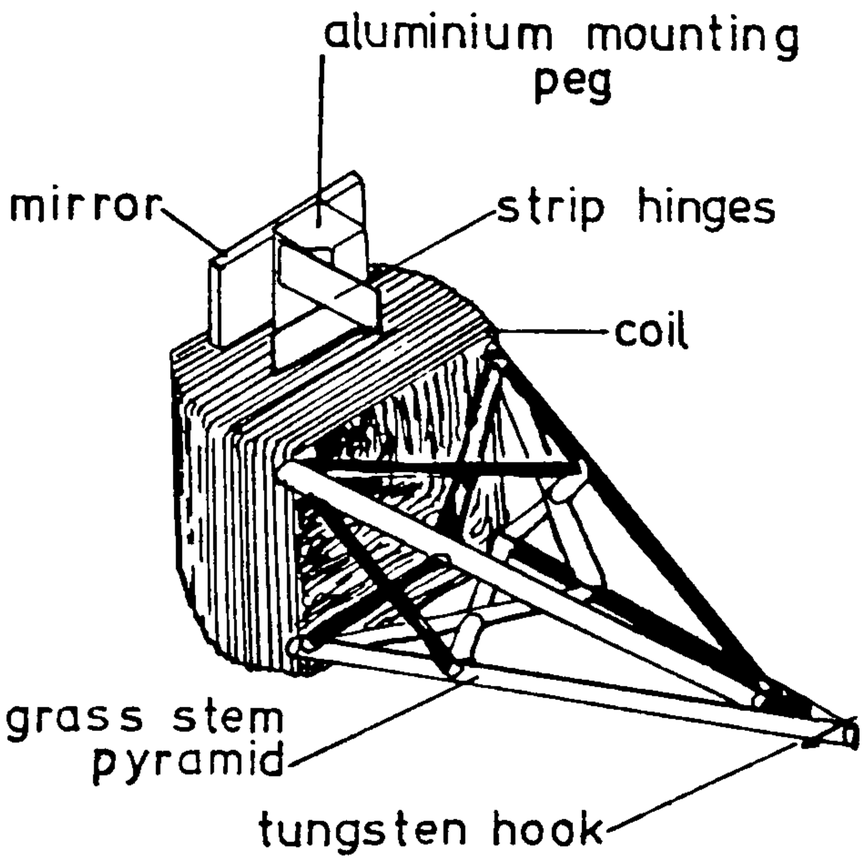

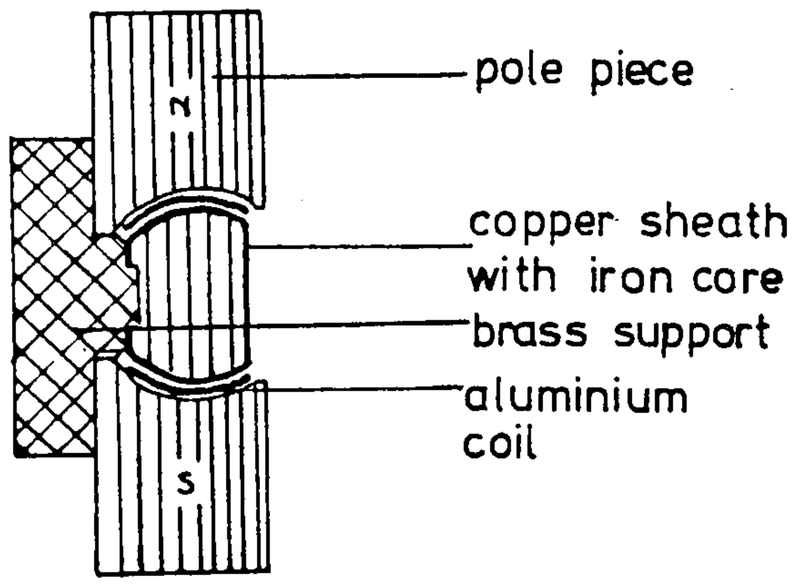

(b)

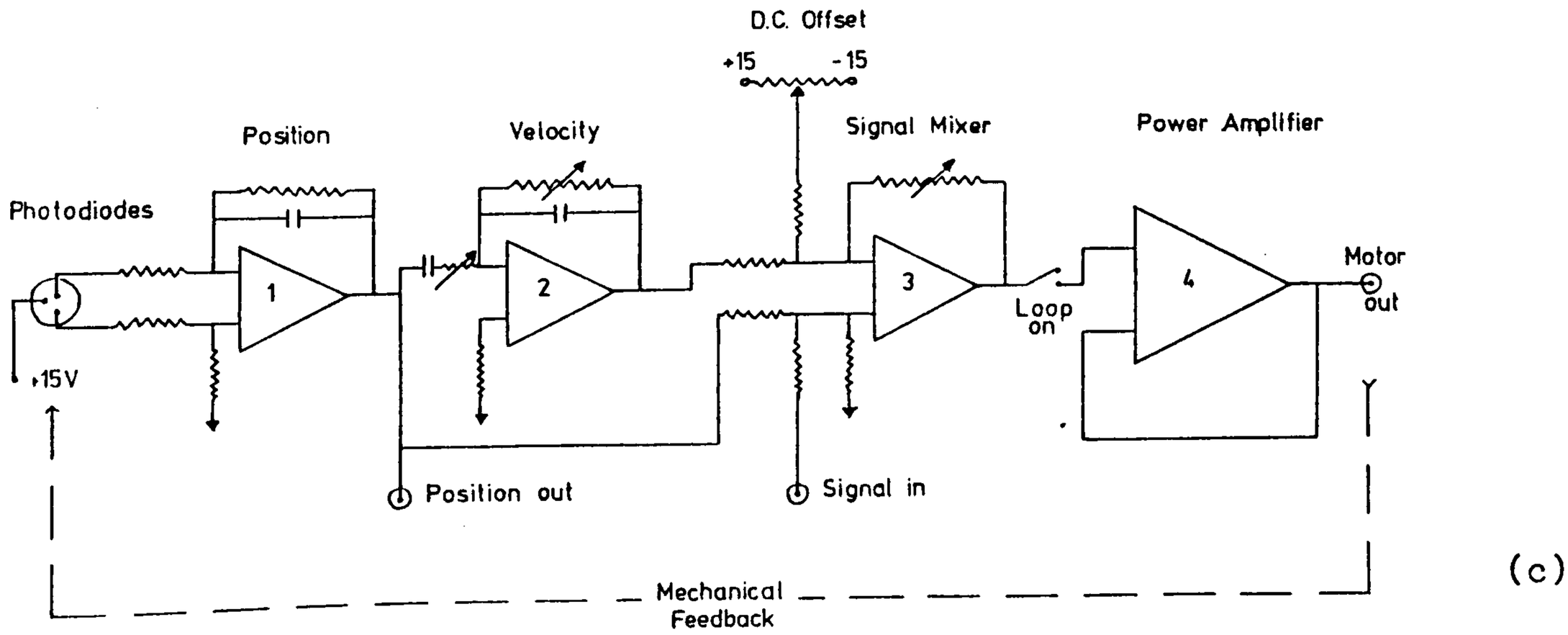

(c)

FIGURE 2.11

2.9.3 Coil and Pyramid Assembly :

The coil was mounted between the pole pieces of a powerful horseshoe magnet. The mounting was made from crossed strip-hinges glued to aluminium pegs that were fixed to the top and bottom of the coil, with araldite (see Figure 2.11b). The strip hinges were bolted to the motor housing. The coil, suspended on the mounting hinges was able to move freely between the pole pieces. A 6mm square of mirrored cover-slip (mirrored by Brashear's process) was glued to the lower mounting peg and deliberately off-centered to avoid distortion of the reflected image on the photodiodes (Figure 2.11a).

Dried grass stems coated in araldite were glued together on a plasticene former in the shape of a pyramid. The base of the pyramid was glued to the aluminium coil.

Finally, a sharpened tungsten wire hook was glued to the tip of the pyramid with acrylate glue.

2.9.4 The Electronics to Drive the Motor :

An electronic servo-loop was built which accurately controlled the position of the length motor. The position signal from the photodiodes, and a signal proportional to the velocity of the motor movement was compared with the input signal. The difference was amplified and fed to a D.C.-coupled audio amplifier (CE1004, Crimson Elektrik, Leicester, U.K.) which had a power output of up to 100 W. The output of this amplifier was used to drive the motor (see Figure 2.11c).

A 'position out' or 'length signal' from the photodiode amplifier gave a measure of the length hook position.

2.9.5 Motor Performance :

The rise time of the motor was improved by using a square-wave length signal input with a 200μs ramp at the start and end. Using such an input signal the fastest measured rise time was 350μs. The electrical components of the servo loop were carefully adjusted to obtain a fast rise time and ensure that the length signal did not have spurious oscillations. The length signal recorded the movement of the mirror attached to the motor coil. An experiment was performed to check that the movement of the hook attached to the tip of the pyramid was not different from this signal. A light beam was directed from above so that the tip of the pyramid cast a shadow on a pair of photodiodes below. The pyramid was displaced using a micromanipulator and the signal from the photodiodes was found to be linear over a narrow range of movement. The signal from these photodiodes was compared with the length signal (see Figure 2.12a) using a storage oscilloscope. The length position signal gave a reliable measure of the position of the tip of the pyramid.

The length motor was calibrated by changing the D.C. offset (see Figure 2.11c) voltage to the servo-loop and measuring the hook movement with a travelling microscope. The length position output voltage was plotted against the hook movement, measured with an eyepiece graticule (Figure 2.12b). The sensitivity was usually about 150μm/V, with a noise level of 0.14μm

2.10 DATA ACQUISITION :

An IBM Personal Computer (PC) was used both to generate length signals to drive the motor and to collect, store and analyse data that was captured by the digital storage oscilloscope (Tektronix 5223). The oscilloscope had front panel controls to set the amplifier gains

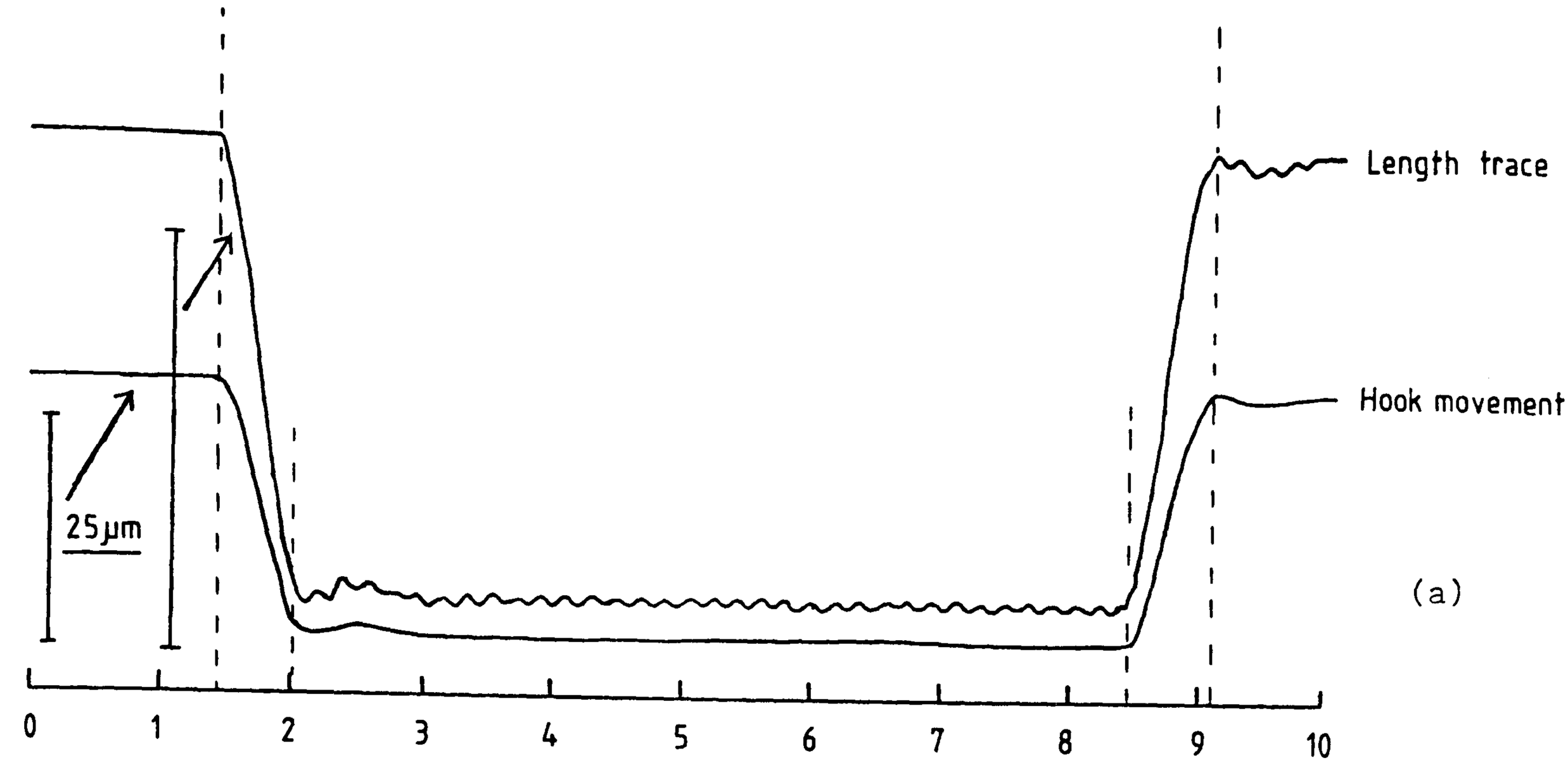

(a)

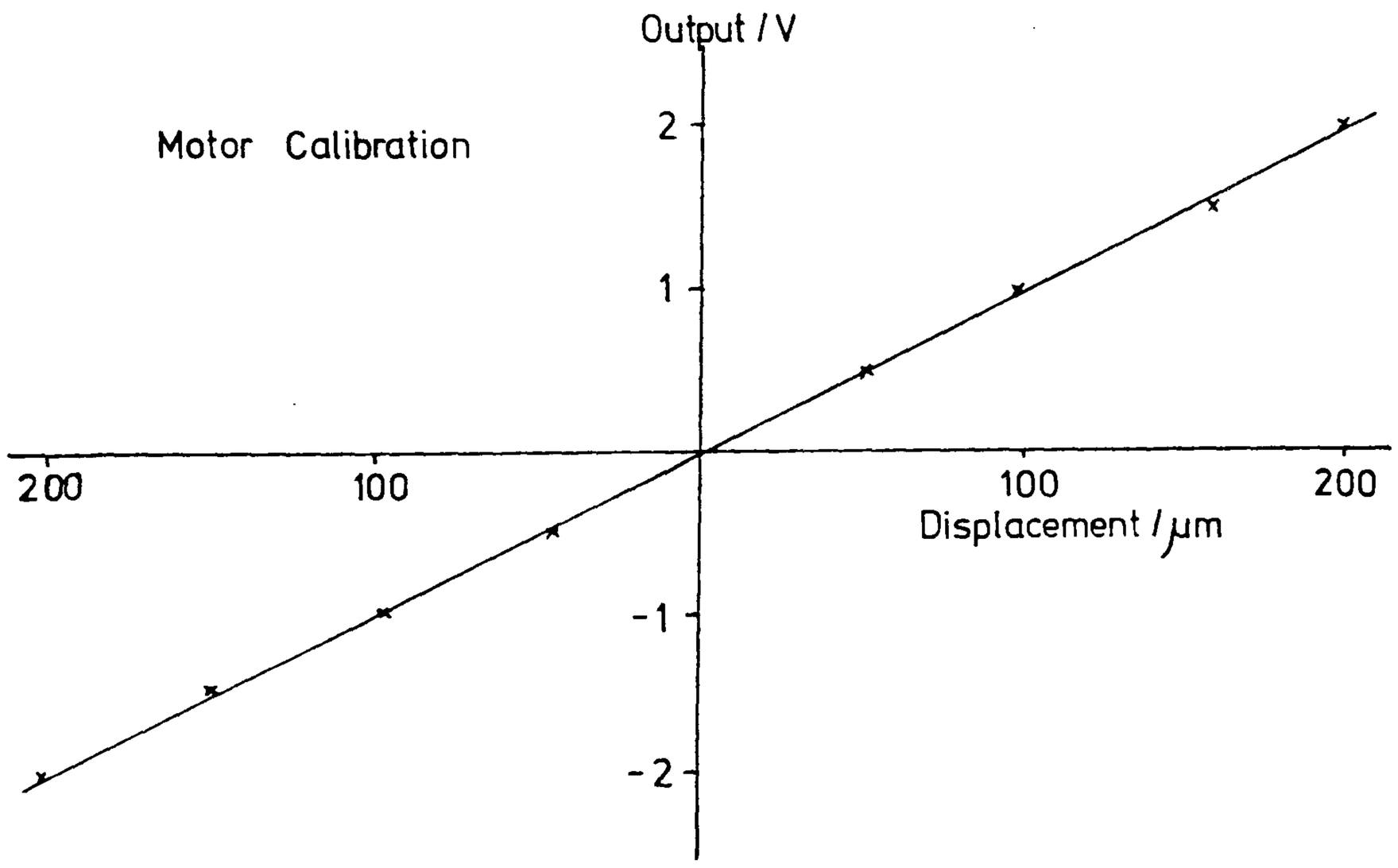

(b)

FIGURE 2.12

The hook movement (monitored by a pair of photodiodes which registered the movement of the shadow cast by the hook)was compared with the length trace (produced by the circuit of Figure 2.11c) in 2.12a. This is discussed in the text.

2.12b shows the length motor calibration (here approximately 100µm/V)

and time base. A General Purpose Interface Bus (GPIB) enabled rapid transfer of parallel data to and from the IBM PC.

The IBM PC was fitted with an interface card (Labmaster, Tecmar) which had the necessary timers and digital to analogue converter to drive the motor and trigger the oscilloscope. There was also a GPIB board (Central Equipment Corporation) linked to the digital oscilloscope.

Muscle experiments were controlled with a BASIC program "MP.BAS" which made calls to various machine code routines to transfer, store and plot data rapidly (based on Drew, 1984).

An additional machine code routine was written to plot work loops and calculate the loop area. Dr D.C.S. White also made numerous modifications to the program. Most importantly a routine was written to convert the tension data into a form suitable as input to an exponential curve fitting program (Provencher 1976). The length and tension data received from the oscilloscope were in binary numbers (proportional to the voltage) sampled at regular time intervals (see Section 2.11.1, below).

Every stored data trace (the result of a single sweep of the oscilloscope screen) was accompanied by an initial data set and the experimental parameters referring to that particular trace.

Prior to any new set of experiments a test program "SETUP.BAS" was run to test the motor performance and make necessary adjustments to the servo-loop controls.

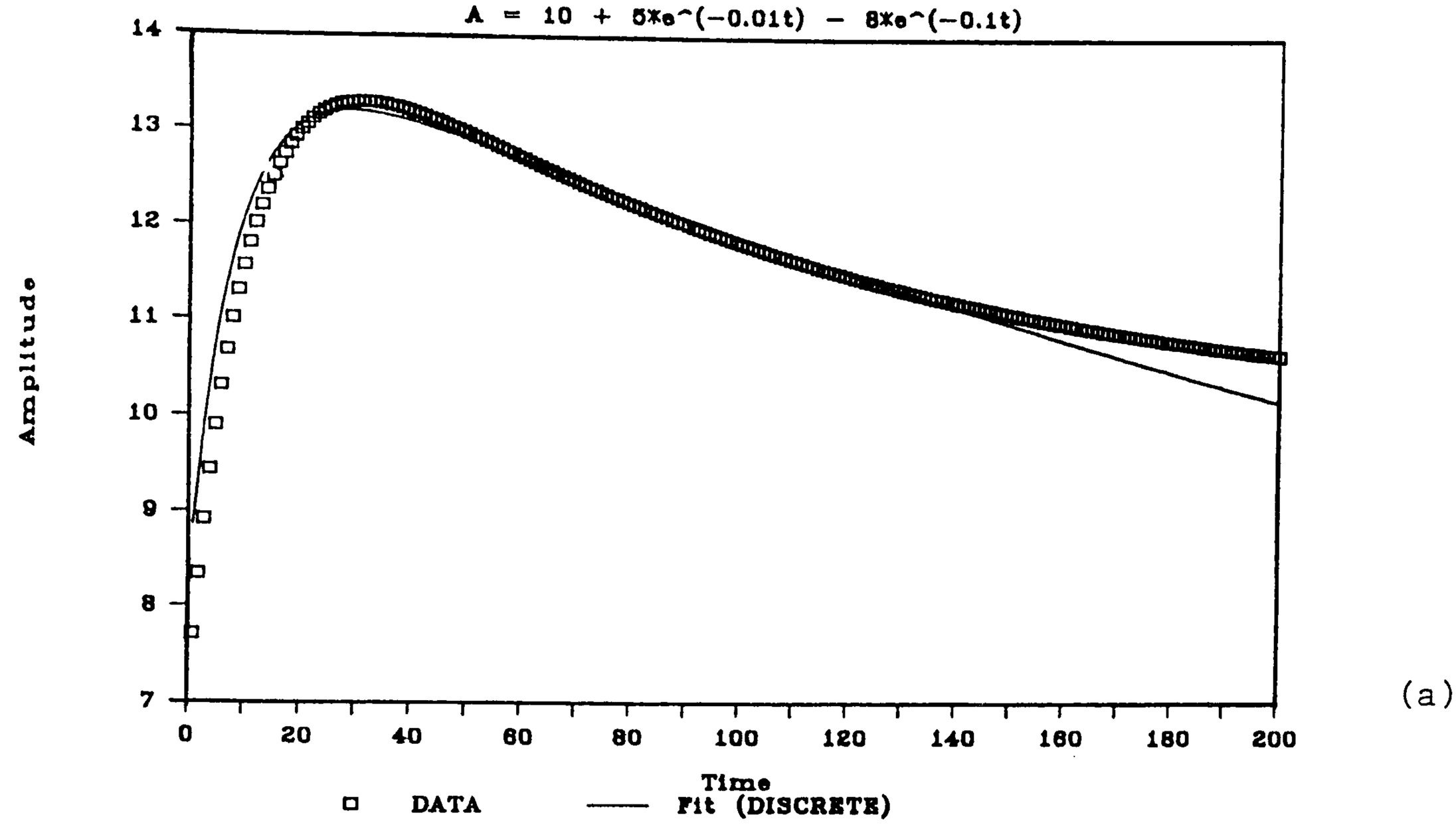

(a)

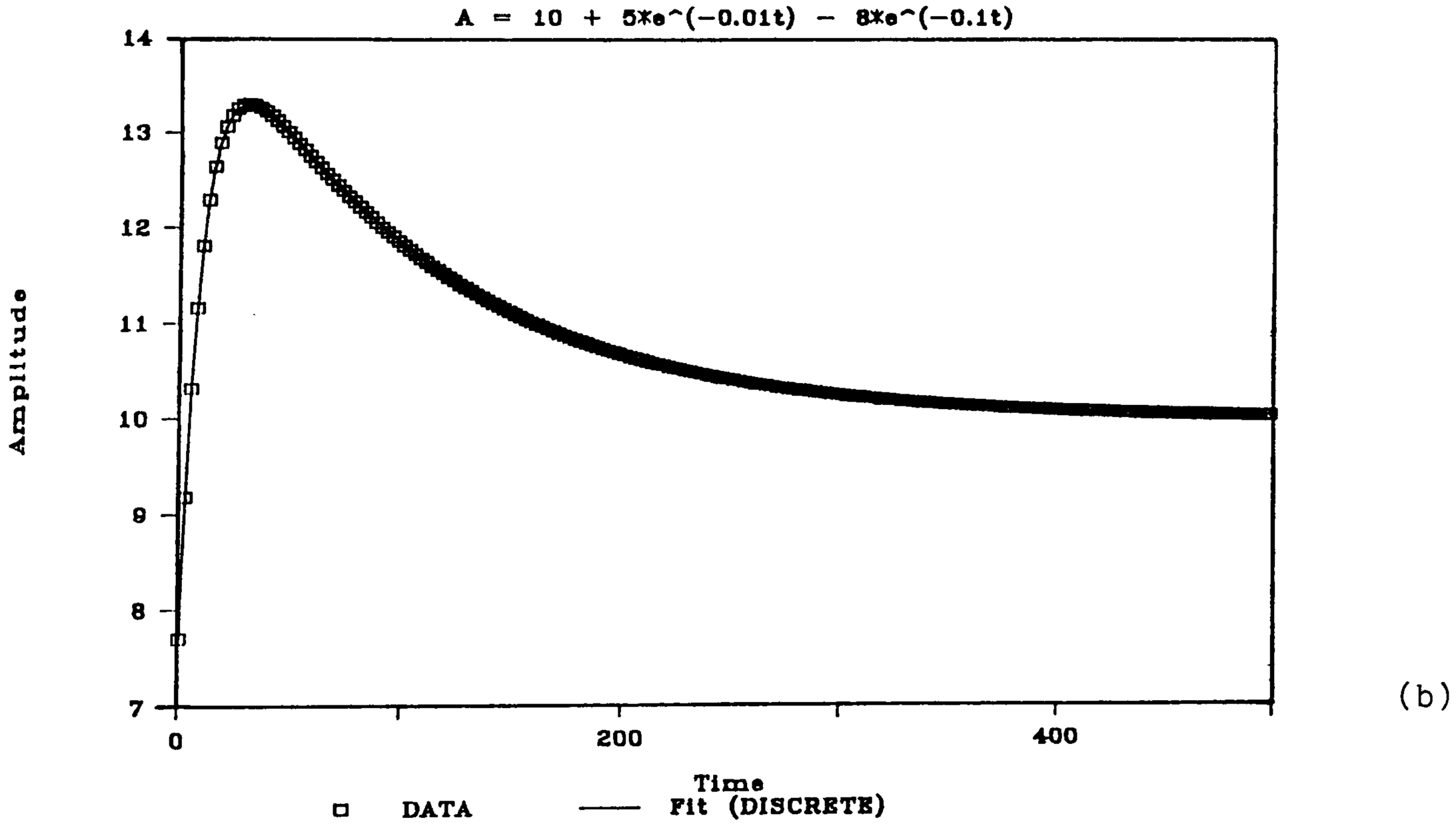

(b)

FIGURE 2.13

Simulated data sets were used to test the effect of "windowing" on the quality of fit produced by the program DISCRETE (Provencher, 1977). (a) shows that a poor fit to the data is obtained when the end point of the slowest transient is not represented in the data set. (b) shows a much better fit to the same data set but on a slower time scale.

2.11 DATA ANALYSIS :

2.11.1 Mechanical Kinetics :

Stored data traces were retrieved and displayed on the computer screen. The tension transient data were 'windowed' between two time points and analysed by a curve fitting program DISCRETE (Provencher, 1976), on the university mainframe computer (VAX). The program fits data as the sum of upto 5 exponential processes (either rising or falling). The windowing of the transient tension data was important in determining how good the 'best fits' to the data were. Simulated data sets were used as test input files. The most important feature was that the data set should include points near to the end-point of the slowest exponential process. Results from test runs of the program DISCRETE made on a simulated data set are shown in Figure 2.13.

2.11.2 Oxygen-Exchange :

Analysis of the fractional distribution of ^{18}O labelled phosphate from oxygen-exchange experiments was made with a program written by Dr. M.R. Webb (N.I.M.R., Mill Hill). This program was converted to VAX BASIC so that data could be analysed at the University of York. The program provides a least squares 'best fit' to modelled distributions.

2.12 MEASUREMENT OF WHOLE FIBRE ATPase ACTIVITY :

The specific ATPase activity of skinned fibre preparations was determined in terms of ATP molecules hydrolysed per myosin head per second by measuring two parameters; 1) the amount of myosin S1 in the fibre; 2) its rate of ATP hydrolysis.

2.12.1 Estimation of the Fibre Myosin Content :

Calibrated gel densitometry, was used to estimate the total myosin content of the fibre. Fibre samples were electrophoresed on SDS polyacrylamide gels together with 5 rabbit myosin standards. The integral absorbance of the stained myosin heavy chain bands was used to estimate the amount of myosin in the fibre samples. Details of the procedure are given below.

2.12.2 Sample Preparation:

Rabbit myosin standards were prepared from a rabbit myosin preparation kindly donated by Drs. White and Kyrtatas. The myosin was estimated by measuring the intrinsic protein absorbance at 280nm. An aliquot of the myosin was optically scanned against a deionised water blank in quartz cuvettes over the range 340-200nm (Shimadzu UV-240). The extinction coefficient of a 1% myosin solution is 5.3 (eg. lmg/ml has an A_{280} of 0.53 A.U.). The molecular weight of myosin = 520 kDa (Margossian & Lowey, 1982). Because the ATPase activity of myosin resides in the S1 heads of the molecule one mole of myosin contains two moles of active sites. Therefore one microgram of myosin contains 3.85 pmoles of active sites.

Fibre mass was calculated by assuming that the concentration of S1 was the same as found in Lethocerus (0.2mM, Chaplain & Tregear 1966) and that the density was approximately the same as water i.e. 2×10^8 pmole S1 $\equiv$ 1 kg wet weight. This conversion factor was used to normalise the measured power outputs to W/kg wet weight.

Skinned muscle fibres and rabbit myosin standards were dissolved in 20µl of sample buffer (see Table 2.2 below) and boiled for 5 minutes.

DTT	1.5% W/V
SDS	2.0% W/V
Tris	25mM
Glycerol	10% V/V
Bromophenol blue (Sigma)	30µg/ml
pH	6.8

Table 2.2
Constitution of the SDS sample buffer.

The samples were loaded onto a polyacrylamide gel together with a range of myosin standards to provide an internal calibration. The range of fibre sizes used here was from 0.5-3.5pmoles (Sl/fibre preparation). The myosin standards loaded onto the gel were also in this size range.

2.12.3 Polyacrylamide Gel Electrophoresis :

A two phase gel system was used, consisting of a stacking gel and below it a separating gel. The stacking gel had 15 wells into which the samples were loaded. The gel was run at a constant 200 Volts, for about 4 hours, on a slab gel electrophoresis apparatus (LKB 2001). The buffer system used was the same as Laemmli (1970). The gel was stained with Coomassie Brilliant Blue R (Sigma) and destained with 10% acetic acid. The constitution of the solutions is given in Table 2.3.

Stacking gel :

Acrylamide*	5% (W/V)
Tris	125mM
SDS	0.1% (W/V)
Ammonium persulphate	2.3mM
TEMED	6.4mM
pH	6.8

Separating gel :

Acrylamide*	12.5% (W/V)
Tris	375mM
SDS	0.1% (W/V)
Ammonium persulphate	1.5mM
TEMED	4.0mM
pH	8.65

(*Acrylamide = acrylamide + bisacrylamide (39:1))

Running buffer :	
Glycine (A.R. grade, Fisons)	400mM
SDS	20% (W/V)
Tris	50mM
Gel staining solution :	
Acetic acid	10% (V/V)
Isopropanol	25% (V/V)
Coomassie Brilliant Blue	0.05% (W/V)
Gel destaining solution :	
Acetic acid	10% (V/V)

Table 2.3

The integral absorbance of the myosin heavy chain bands was determined by either a linear or raster scan. The gel scanning apparatus (Chromoscan 3, Joyce-Loebl) was used in transmission mode with a wavelength filter of 546nm. The raster scans were rather unreliable, the chief cause of this was gel movement during the course of a scan. The glass plate on which the wet gel rests is moved very rapidly under the light beam and by the end of a scan the gel had often moved from its original position. Much more reproducible results were obtained by making a linear scan of all the myosin bands. The integral absorbance of the linear scan peaks was estimated by cutting out and weighing the peaks.

Figure 2.14 shows that the integral absorbance of the stained myosin heavy chain bands is linearly related to the myosin content of the sample. Calibration lines were most accurate for total active site contents greater than 0.5 pmoles (eg. more than 0.13 μg myosin).

2.12.4 Estimation of Skinned-Fibre ATPase Rate :

Using HPLC it is possible to separate and assay the nucleotide species in a solution. There are three aspects of the HPLC method that make it very useful as an assay system; 1) it is very sensitive, being able to detect picomolar quantities of nucleotide, 2) it is possible

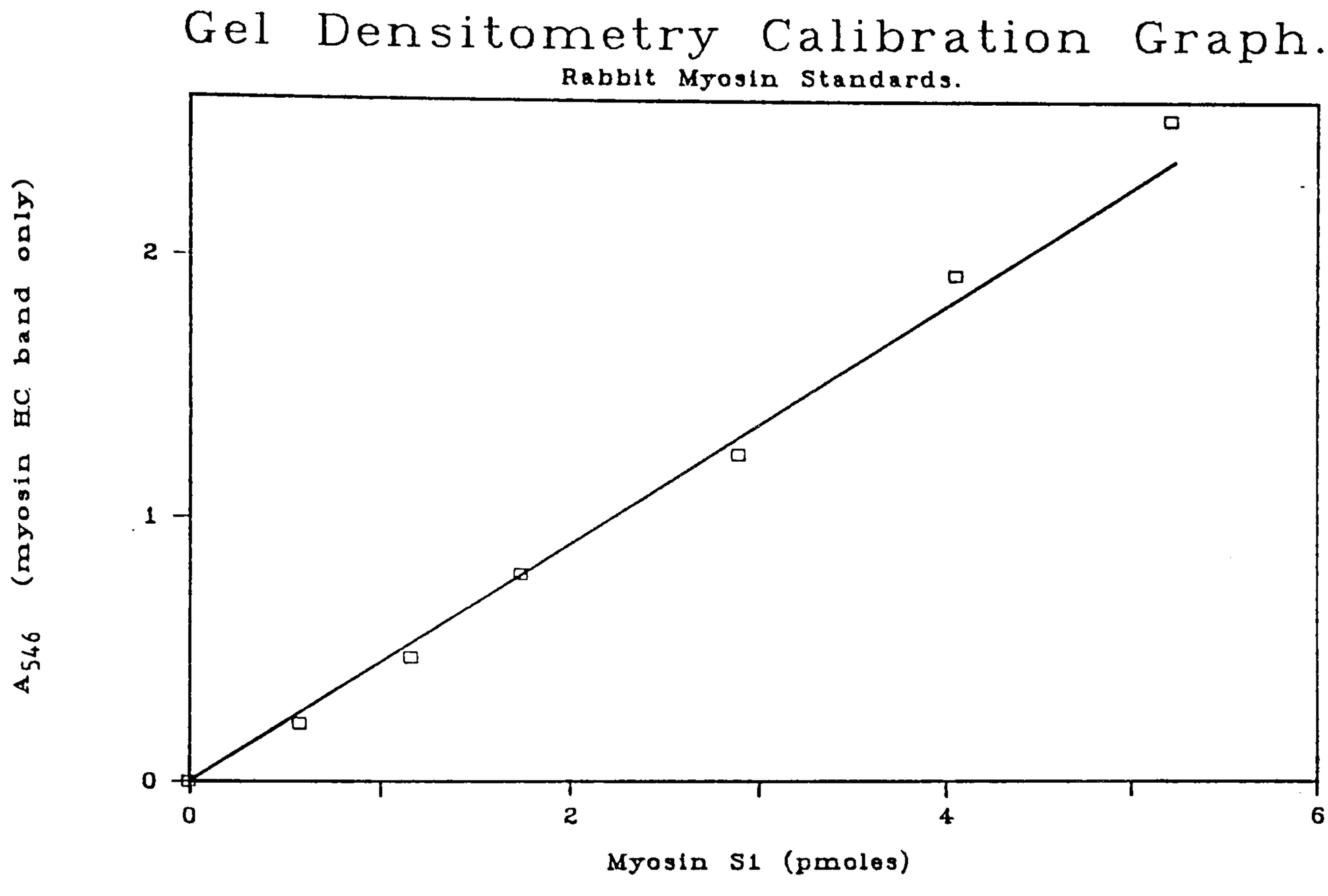

FIGURE 2.14

Gel densitometry calibration graph; the integral absorbance of the myosin heavy chain band on the poly-acrylamide gel was estimated by performing a linear scan with a gel scanning apparatus (Joyce-Loebel, Chromoscan 3). The myosin standards were prepared from a rabbit myosin preparation kindly donated by Dr. Kyrtatas and Dr. White (university of York). The gel system and staining procedure is described in the text.

to assay both ADP and ATP accurately in the same sample, 3) estimations can be made in about 5 minutes. The importance of point 2) is that this allows the ATP:ADP ratio to be determined. The calculation of the amount of ATP hydrolysed by the fibre in the incubation solution is independent of the sample size injected into the HPLC. Very small aliquots (1-5µl) could be removed (without worrying about pipetting errors) to estimate the rate of ATP hydrolysis. Sample "blanks", which had not been used for a fibre incubation, were estimated for background ATP hydrolysis at the start and end of every experiment.

A schematic diagram of the HPLC apparatus is shown in Figure 2.15.

2.12.5 Experimental Protocol :

Incubations were performed on the mechanical test apparatus designed specifically for this purpose (see above). The seven incubation baths were filled with known volumes of solution (see above) and covered with silicone oil to prevent evaporation. The incubation solutions for these experiments did not contain the creatine phosphate/creatine kinase ATP backup system. The muscle bath was raised so that a skinned muscle fibre, mounted between the length and tension hooks, was immersed in one of the baths. After a known period of time (usually about 5-10 minutes) the bath was lowered and the muscle removed to the next incubation solution. In this way further hydrolysis of ATP by the fibre was immediately stopped and a small aliquot of incubation solution could be removed, at will, and assayed by HPLC. Aliquots from a control bath (with no muscle fibre present) were also assayed to assess the background rate of ATP hydrolysis.

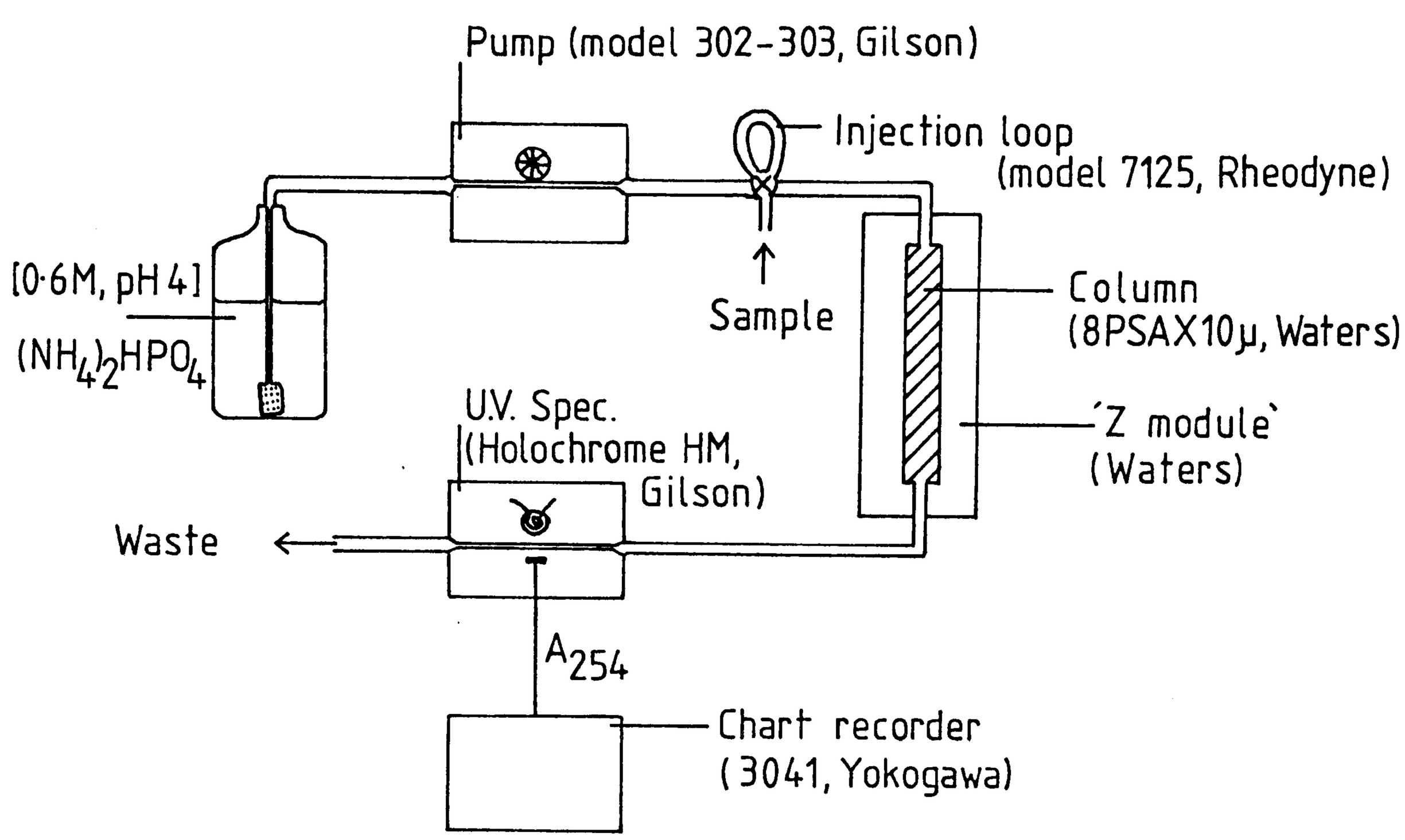

High Performance Liquid Chromatography

FIGURE 2.15

Schematic diagram of the HPLC apparatus, The pump was operated in a constant flow mode (at the fastest speed, to produce sharp absorption peaks). The sample consisted of 1ul of incubation solution and 19ul of running buffer, $(NH_4)_2HPO_4$. This was injected into a 20μl injection loop. The sensitivity of the UV spec. could be adjusted to produce desired peak sizes on the chart recorder.

By filling the baths with different incubation solutions the effect of different chemical environments on the ATPase rate could be measured. Also the mechanical state of the fibre could be altered. By having brief incubation times a single fibre could be used for a series of different experiments which negated the problem of fibre-to-fibre variation.

The method by which the rate of ATP hydrolysis was calculated is detailed below. The catalytic site activity was determined by assaying the amount of myosin active sites in the fibre preparation (as above).

2.12.6 Calculation of the Rate of ATP Hydrolysis :

The optical absorbance of ATP and ADP (A_{254}) as they were eluted from the HPLC column (strong anion exchange, 8PSAX10μ, Waters) was monitored on a paper chart recorder. Because the absorbance coefficient of ADP and ATP is similar, the amounts can be estimated from the integral area of the absorbance peaks. The appearance of the peaks was similar and the relative peak areas proportional to the peak height x half height width. Because the ADP retention time is less than ATP the half height width was smaller and a 'peak height adjustment' was made. The peak height adjustment was determined by injecting known amounts of ADP and ATP and recording at a fast chart speed (Figure 2.16). Knowing the peak height adjustment for ADP (usually a factor of about 1.4) the integral areas could be calculated from the ATP and ADP peak heights.

The rate of ATP hydrolysis in an incubation bath was calculated as below (Scheme 2.2) :

$$\text{ATP hydrolysis (\%)} = \frac{\text{ADP peak height} / 1.4}{(\text{ADP peak height} / 1.4) + \text{ATP peak height}}$$

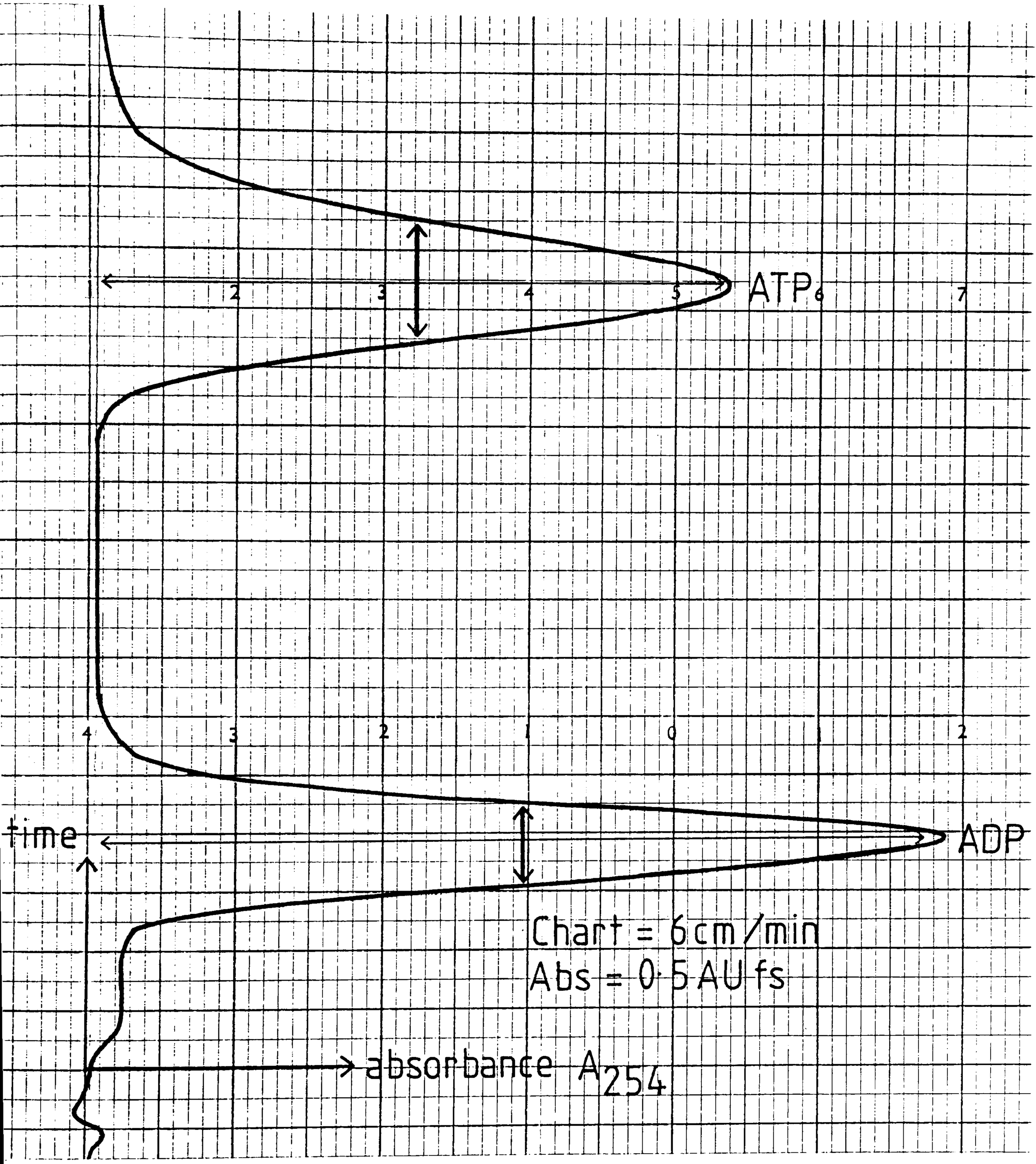

FIGURE 2.16

A peak height adjustment was made by measuring the half height width of the ADP and ATP peaks from the HPLC chart recorder ouput. This meant that the integral peak areas could then be calculated from the measured peak heights.

$$\text{ATP hydrolysis (moles/fibre/second)} = \frac{[\text{ATP}] * \text{bath volume} * (\text{ATP hydrolysis (\%)})}{\text{Time}}$$

$$\text{ATP hydrolysis } s^{-1} = \frac{\text{ATP hydrolysis (moles/fibre/second)}}{\text{fibre size (moles active sites)}}$$

Scheme 2.2
Calculation of the skinned fibre ATPase activity.

CHAPTER 3 :

KINETICS OF FLIGHT MUSCLE FROM INSECTS WITH DIFFERENT WINGBEAT FREQUENCIES

KINETICS OF FLIGHT MUSCLES FROM INSECTS WITH DIFFERENT WINGBEAT FREQUENCIES*

3.1 INTRODUCTION :

Small insects usually beat their wings at a higher frequency than large insects. For energetic reasons, the wingbeat frequency is close to the natural resonant frequency of the wing movement, determined by the inertia of the wings and the stiffness of the wing mounting. This chapter examines how the kinetics of the cross-bridge cycle are tailored to the needs of insects with different wingbeat frequencies.

The tension response to a sudden length change shows a large delayed tension component (phase 3, Figure 3.1), whose rate constant (r_3) determines the frequency at which the muscle can deliver maximum power to the wings (Equation 1.1).

1) The rate constant for the delayed tension transient was determined in fibres from insects with a wide range of wingbeat frequencies. It was found to be roughly proportional to the wingbeat frequency in the flying insect.

2) The measured ATPase rate is related neither to the rate constant for tension production nor to the wingbeat frequency of the insect.

3) The ATPase rate was controlled by the rate-limiting step in the cross-bridge cycle. This step was always slower than the rate constant for the delayed tension transient.

4) Insects with widely different wingbeat frequencies have muscles with similar mechanical power output.

* See declaration on Page viii.

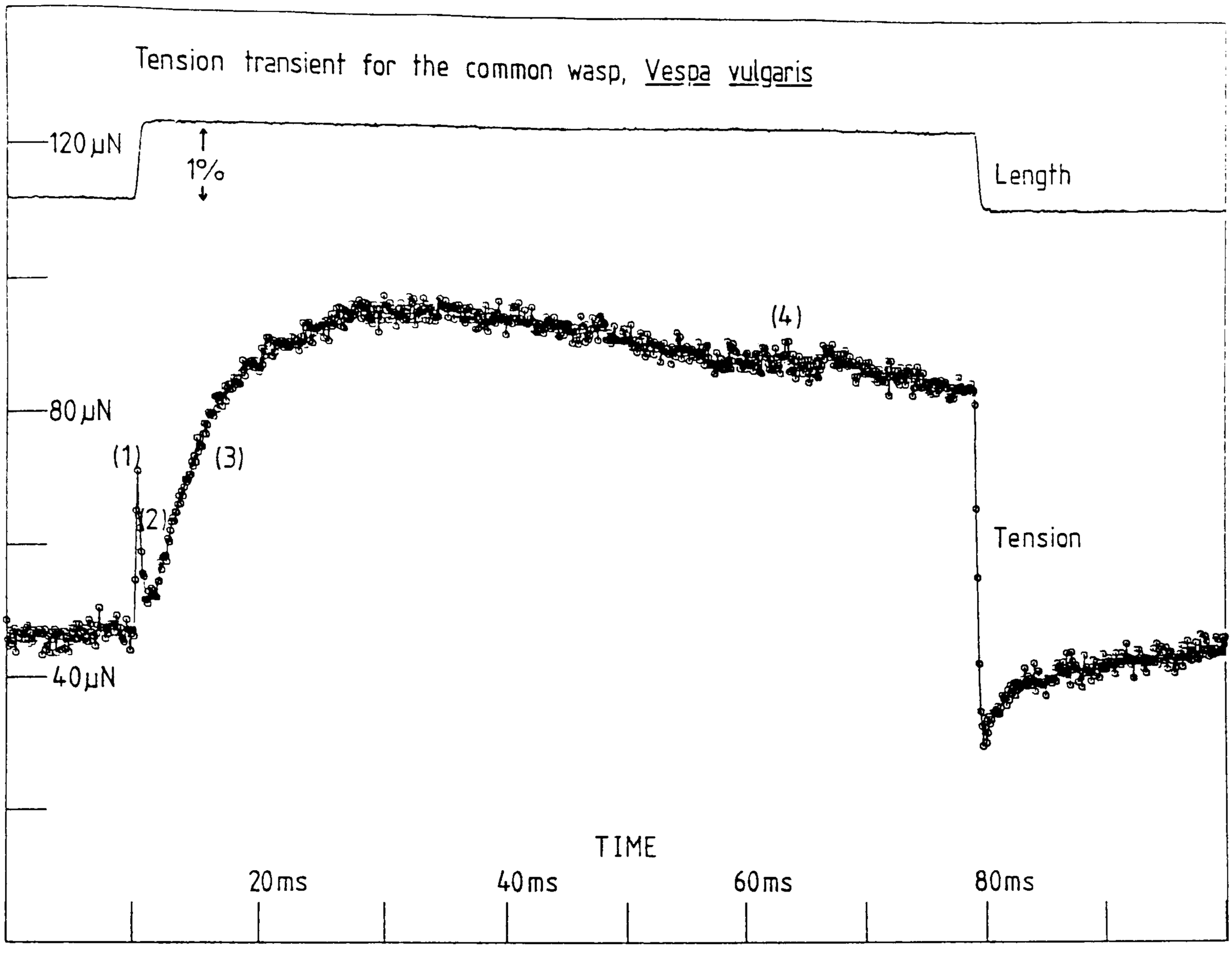

FIGURE 3.1

Tension transient from the common wasp, Vespa vulgaris in response to a sudden 1% length change.

There is a rapid tension change (phase 1) that occurs simultaneously with the length change followed by a rapid tension fall (phase 2). The large amplitude delayed tension (phase 3) is then followed by a slow tension relaxation to a new (higher) steady state tension (phase 4).

Experiment was performed at 20°C. as described in Section 3.2 and 3.2.1.

The conclusion is that the rate-limiting step in the cross-bridge cycle, which limits the ATPase activity, follows the state in which maximum active tension is produced, and that a preceding step is faster in smaller insects, correlating with the wingbeat frequency.

3.2 MATERIALS AND METHODS :

A large variety of insects were obtained, they were either captured locally, imported or reared from culture. The range of size of insects was from a 12g giant waterbug to a 1mg fruitfly. The wingbeat frequencies of the different insect species were determined at an ambient temperature of 25°C. I was not able to induce flight in one species of giant waterbug, Lethocerus colossicus, the wingbeat frequency of a similar sized species (L. indicus) was assumed to be similar.

Mechanical and biochemical experiments were performed on single demembranated muscle fibres, or fibres which had been pared down to a diameter of less than 80μm. The initial procedure for all of these experiments was the same :

1) The fibres were mounted on the mechanical test apparatus and were immersed in a relaxing solution. Rest length was established by adjusting the micromanipulator, which holds the tension transducer, until the muscle fibre was just taut (when the measured tension was just zero).

2) The relaxing solution was washed out of the bath with activating solution. The tension rise was measured by giving a series of brief pulse releases to find the zero tension baseline and/or from measurements made on a slow-speed paper chart record.

3.2.1 Transient Tension Response to a Step Length Change :

These experiments were performed at two temperatures 15°C. and 20°C.. The solutions used are shown in Table 2.2b. The problems of neucloetide diffusion were reduced by the CP/CPK back-up system.

The active transient tension responses to a 1% length step were recorded for each species. A suitable oscilloscope timebase was selected so that the response could be satisfactorily analysed by a curve fitting program.

3.2.2 Frequency of Maximum Power Output :

The frequency of maximum power output was determined by length oscillating the muscle over a range of frequencies (at a 3% p-p amplitude). The power output was determined from the area of length-tension diagrams. The same fibre was subjected to a step length change and the transient tension response was analysed as above.

3.3 ATPase DETERMINATIONS :

3.3.1 Diffusion-Limitation Control Experiments :

In the absence of a backup-system (i.e. CP/CPK), skinned fibre experiments rely on diffusion for the transport of ATP, ADP and Pi. In some instances diffusion becomes rate-limiting and controls the activity of the preparation. Under these circumstances the core of the fibre is starved of ATP and goes into rigor. The effects of this problem are modelled and discussed later. Control experiments were performed to test for diffusion-limitation.

The most obvious sign of diffusion-limitation occurs when the fibre enters the 'high-tension state' (Jewell and Ruegg, 1966). Muscle tension rises to an unusually high level and the mechanical work is reduced or abolished. Experiments in which the high-tension

state was observed were abandoned.

Diffusion limitation will be reduced by :

1) raising the ATP concentration in the bathing solution,

2) stirring the solution in the muscle bath,

3) reducing the fibre diameter (increasing the surface area to volume ratio).

Each of these factors were changed to test for diffusion-limitation of the measured ATPase. By using fibres pared down to different diameters it was possible to test if fibres from a particular species of insect were liable to diffusion limitation. Also internal controls on individual fibre preparations were made by :

1) Monitoring the mechanical performance of the fibre, noting the fibre tension and mechanical power output.

2) Incubating the fibre in solutions with a range of different ATP concentrations.

3) Incubating the fibre in an unstirred and then a stirred bath.

Control experiments were made under conditions where the fibre was maximally activated. Results of experiments to test specifically if fibres, of each species of insect tested, were diffusion-limited are described later.

3.3.2 Relaxed and Fully-activated ATPase Measurements :

The ATPase activity of demembranated muscle fibres under a variety of chemical and mechanical conditions was determined using HPLC. The solutions used for these experiments contained inhibitors for non-myosin ATPase activity (Table 2.2a&e) and did not contain a

CP/CPK back-up system. The myosin content of the fibre preparation was determined by gel densitometry.

The row of seven temperature controlled baths were filled with a known volume of the incubating solutions. The first bath always contained relaxing solution and served as a wash bath to remove the skinning solution from the fibre. Zero length was set in this bath, as for the mechanical experiments (above). By moving the baths the muscle fibre was incubated in sucessive solutions. Fibres were incubated for a period of time which allowed approximately 3-5% hydrolysis of the total ATP. The mechanical power output of fibres which were length oscillated (under optimum conditions) was determined as above.

The calcium activation of fibres oscillated (3% peak-peak amplitude) at the frequency of maximum power output was also measured. The concentration of free calcium in the incubating solution was varied in the range *p*Ca 4.8 to *p*Ca 8.0. Solutions were made by mixing activating and relaxing solutions in the ratios below (Table 3.1).

Ko (mls)		Lo (mls)	[Ca]mM	[EGTA]mM	*p*Ca
0	+	1	6.0	6.0	4.8
0.03	+	0.97	5.8	6.0	5.1
0.12	+	0.88	5.3	6.0	5.53
0.3	+	0.7	4.2	6.0	6.00
0.6	+	0.4	2.4	6.0	6.51
0.8	+	0.2	1.2	6.0	7.00
1	+	0	-	6.0	~ 8.00*

Table 3.1

**p*Ca in the absence of added calcium ~ 8.00 (Portzehl et al, 1964)

3.4 RESULTS FROM MECHANICAL EXPERIMENTS :

The species of insect used in this study, their measured wingbeat frequencies, and rate constants for the delayed tension are given in Table 3.2.

Species	Wingbeat frequency (Hz)	r_3 (s^{-1}) 15°C.	r_3 (s^{-1}) 20°C.
1) *Lethocerus*			
colossicus	38_*	6.2	20.4± 1.8
indicus	38_a	12.9± 1.1	-
griseus	44_a	7.7± 1.5	25.0± 1.7
2) *Tipula* spp.	47_{ab}	49.3±17.0	65.5± 6.7
	63_{ab}	44.2± 2.6	-
3) *Melolontha* *melolontha*	48_a	-	46.0
4) *Vespa* *vulgaris*	97_{ab}	111.8±20.3	145.2± 7.4
5) *Calliphora* *vomitoria*	120_{ac}	188.3±13.0	216.0
6) *Lucilia* *ceasar*	140_a	-	121.5± 6.1
7) *Bombus* *terrestris*	150_{ab}	135.0±49.0	202.0
8) *Apis* *mellifera*	154_{ab}	138.0	186.0± 9.8
9) *Episyrphus* *balteatus*	165_{bc}	201.0± 3.0	443.5±48.5
10) *Drosophila*			
funebris	180_c	-	386.0±35.2
hydeii	180_c	241.8±20.0	-
melanogaster	200_c	232.4±15.4	385.5±40.5

1) Giant waterbugs 2) Craneflies 3) Cockchafer
4) Common wasp 5) Bluebottle 6) Greenbottle
7) Bumblebee 8) Honeybee 9) Hoverfly
10) Fruitflies

Method of WBF determination (See Chapter 2 for details) :

$_a$) Sound in free-flight
$_b$) Stroboscopic
$_c$) Glued to gramophone pick-up
$_*$) Value for L. indicus assumed.

Table 3.2

Wingbeat frequencies and mechanical rate constants for the delayed tension active transient (phase 3, Figure 3.1) measured at two temperatures, solutions as Table 2.2a&b. Values for r_3 are quoted ± SEM, except when less than 3 determinations were made where only the mean is quoted.

3.4.1 Transient Tension Response to a Step Change in Length :

Figure 3.2 shows the transient tension response for four different species of insect. Notice that the timebase in the four figures is different. The timecourse of the transient tension response was analysed as a sum of exponentials, and the rate constant of the 'delayed tension' phase (r_3) plotted against wingbeat frequency (f_{WB}) (Figures 3.3 and 3.4). The central data point represents the mean and the vertical bar the range of results. The fitted lines are the least squares linear regressions. A possible reason for the negative intercept is discussed later. Relationships between the rate constant for tension production (r_3) and wingbeat frequency (f_{WB}) are given by:

$$r_3^{15\ deg.C} = 1.4 \cdot f_{WB}^{Thoracic\ Temp.} + constant \quad \ldots\ldots 3.1$$

$$r_3^{20\ deg.C} = 2.2 \cdot f_{WB}^{Thoracic\ Temp.} + constant \quad \ldots\ldots 3.2$$

3.4.2 Frequency of Maximum Power Output :

Length-tension loops and the calculated work per cycle and power output are shown for five species of insect in Figure 3.5. The length-tension plots cycle anticlockwise when the muscle is delivering work into the driving apparatus. The frequency of maximum power, f_{PMAX}, occurs at a higher frequency than the frequency of maximum work per cycle, f_{WMAX} (given by Equation 1.1).

Figure 3.6 shows the relationship between r_3 and f_{PMAX} for a variety of insects measured over a range of temperatures. The least squares regression line (which was not constrained to pass the origin)

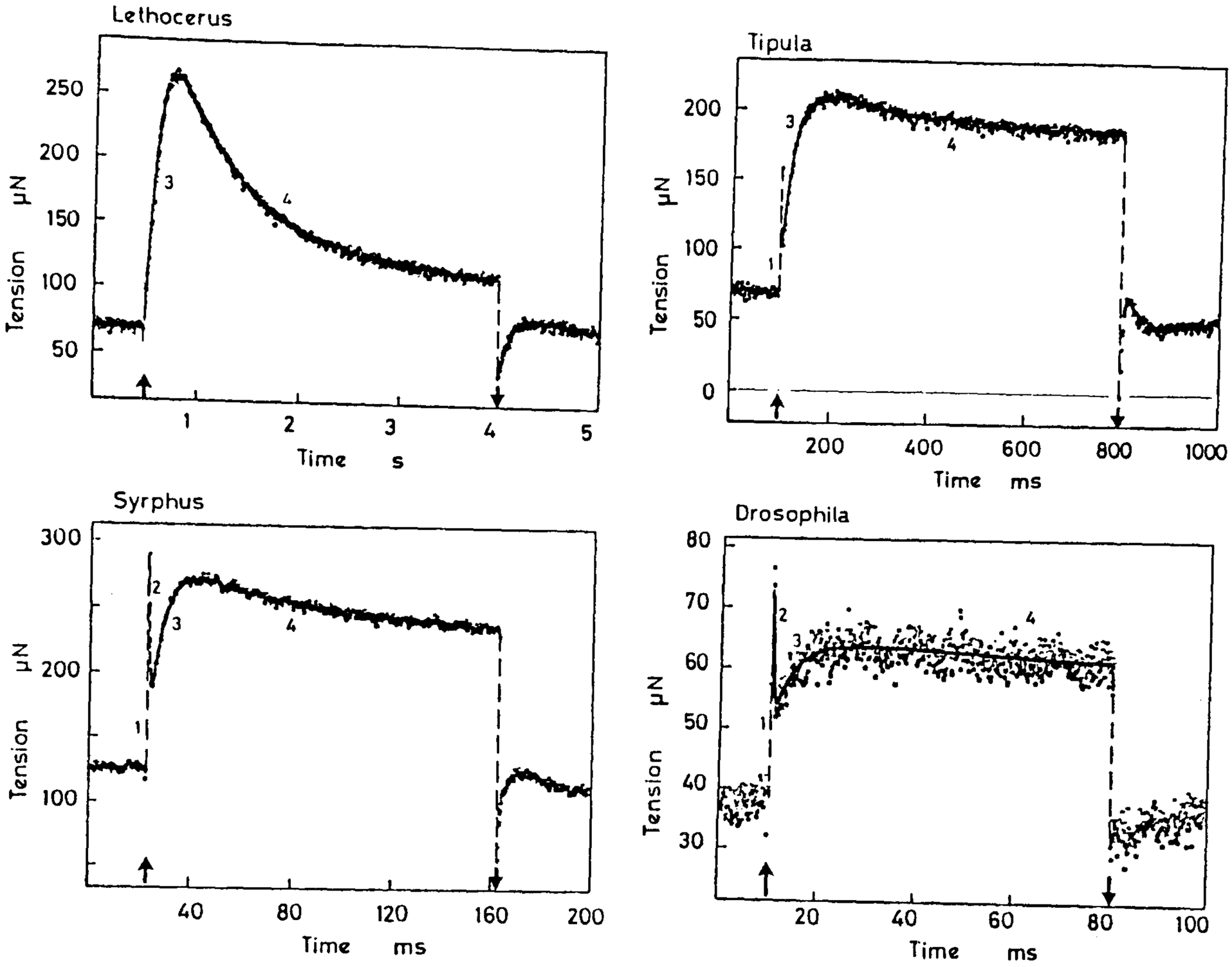

FIGURE 3.2

Transient tension response to a sudden step length change. The experiments were performed at 15°C. according to Section 3.2 and 3.2.1. The numbered phases are the same as those in Figure 3.1 (because of the slow time base used in traces for Lethocerus and Tipula phases 1 and 2 are not clearly visible). The important point to notice is that the time base of the four records is different; the rate constant for the delayed tension transient is faster for the smaller insects (with higher wingbeat frequencies).

The dots represent sampling by the digital oscilloscope and the solid lines (most clearly visible in the record for Drosophila) is the fitted line produced by the curve fitting program DISCRETE (Provencher, 1977).

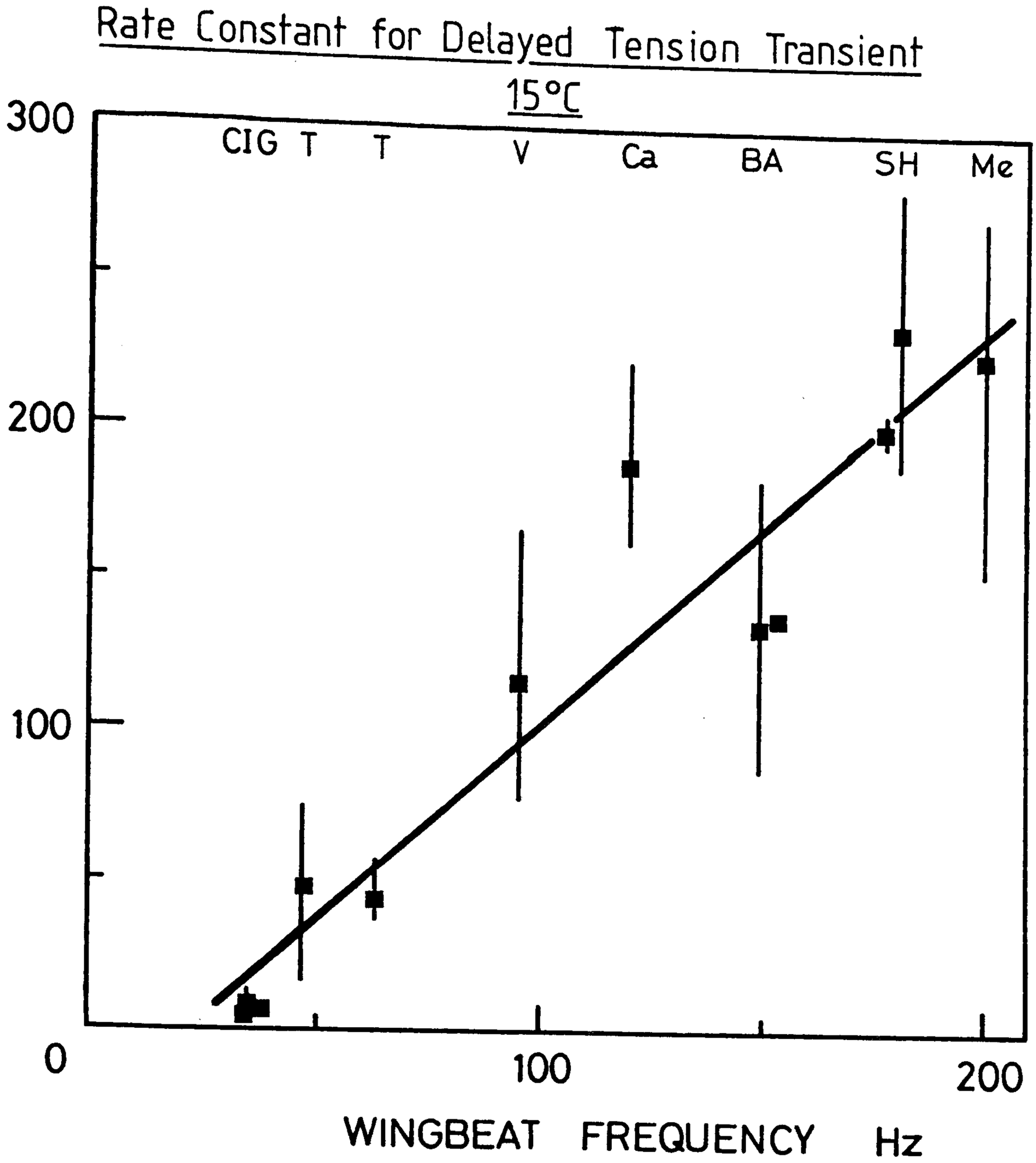

FIGURE 3.3

Relationship between the rate constant for the delayed tension transient (phase 3, Figure 3.1) and the wingbeat frequency of the insect from which the muscle fibre came.

Experiments were performed at 15°C., according to Section 3.2 and 3.2.1. The filled squares represent the mean result and the extent of the lines the spread of the data. The fitted line is the best fit to the means.

The species used were :

C,I,G: Lethocerus collosicus, indicus and griseus.

T : Tipula Spp.

V : Vespa vulgaris

Ca : Calliphora vomitoria

B : Bombus terrestris

A : Apis mellifera

S : Syrphus ribesii

H,Me : Drosophila hydeii and melanogaster

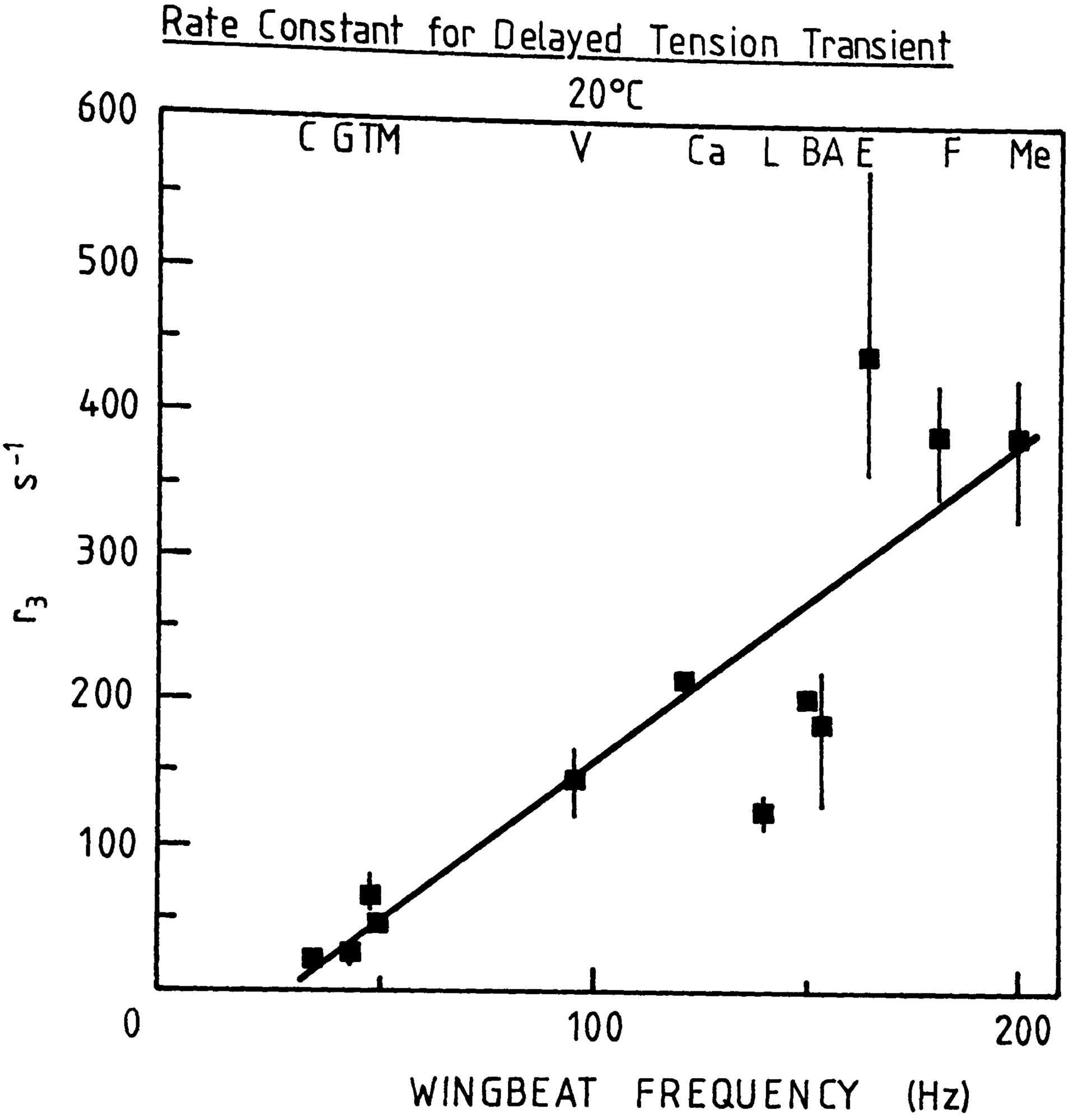

FIGURE 3.4

Relationship between the rate constant for the delayed tension transient (phase 3, Figure 3.1) and the wingbeat frequency of the insect from which the muscle fibre came.

Experiments were performed at 20°C., according to Sections 3.2 and 3.2.1. The data is presented as for Figure 3.3.

The species of insect used were labelled as Figure 3.3, with the additional insects ..

M : Melolontha melolontha

L : Lucilia ceasar

E : Episyrphus balteatus

F : Drosophila funebris

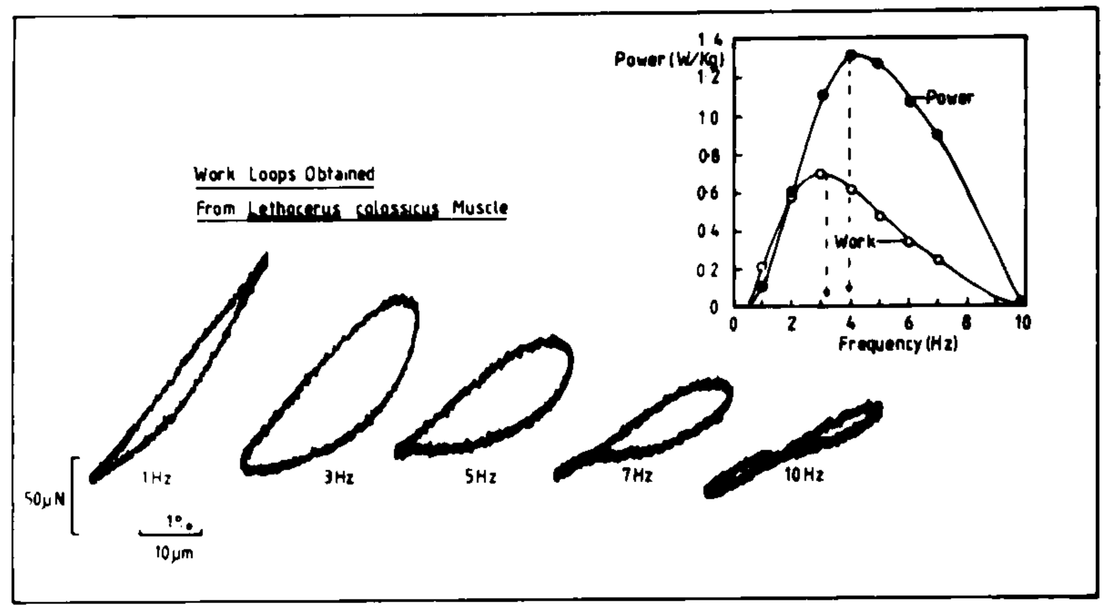

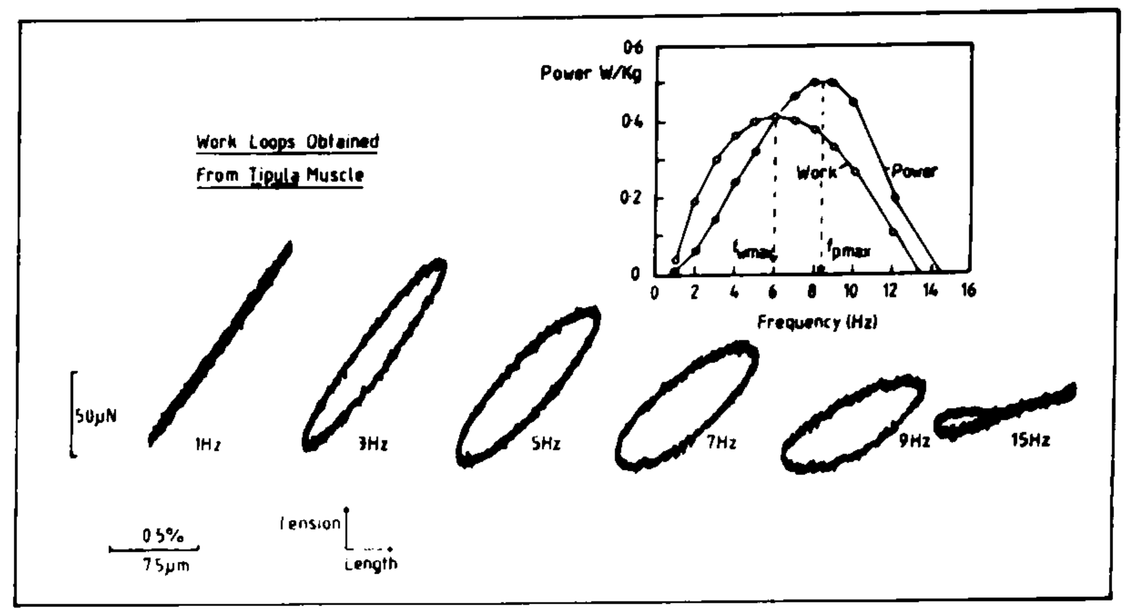

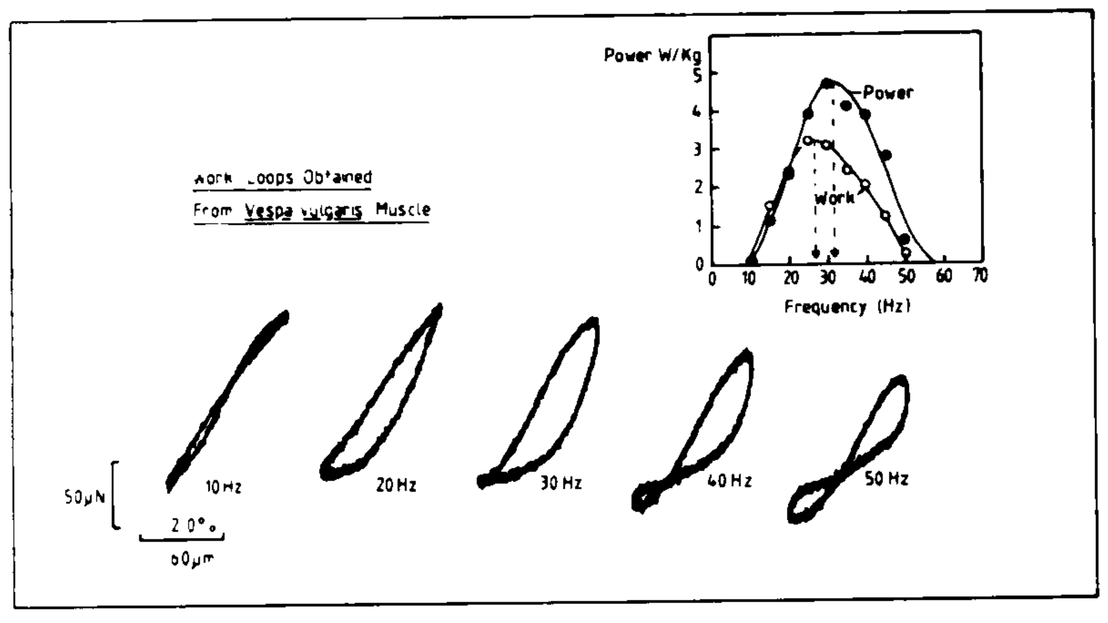

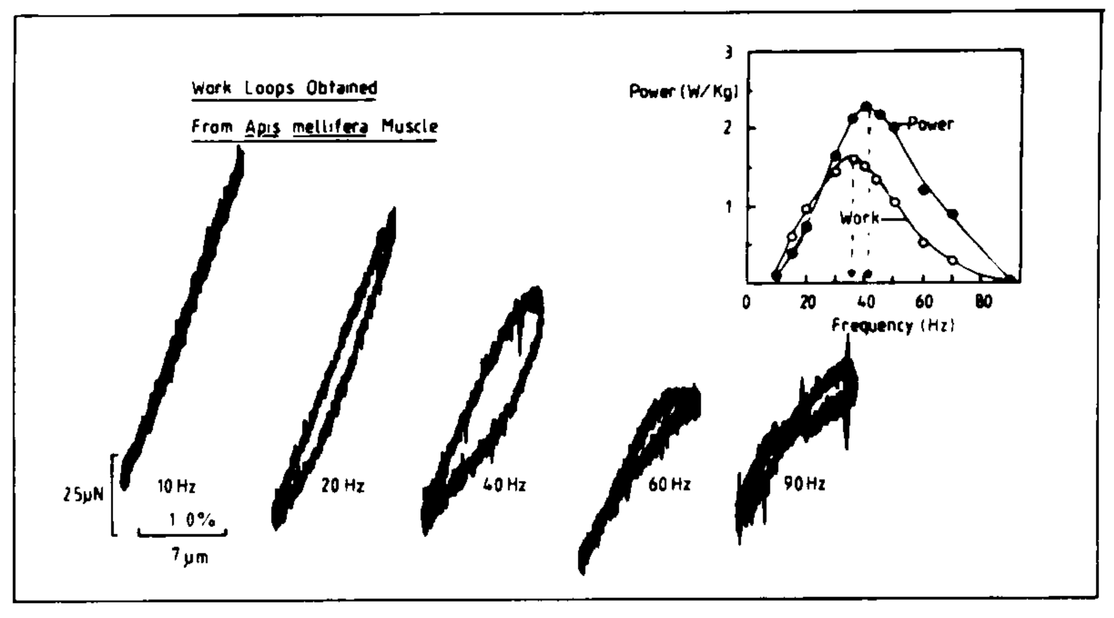

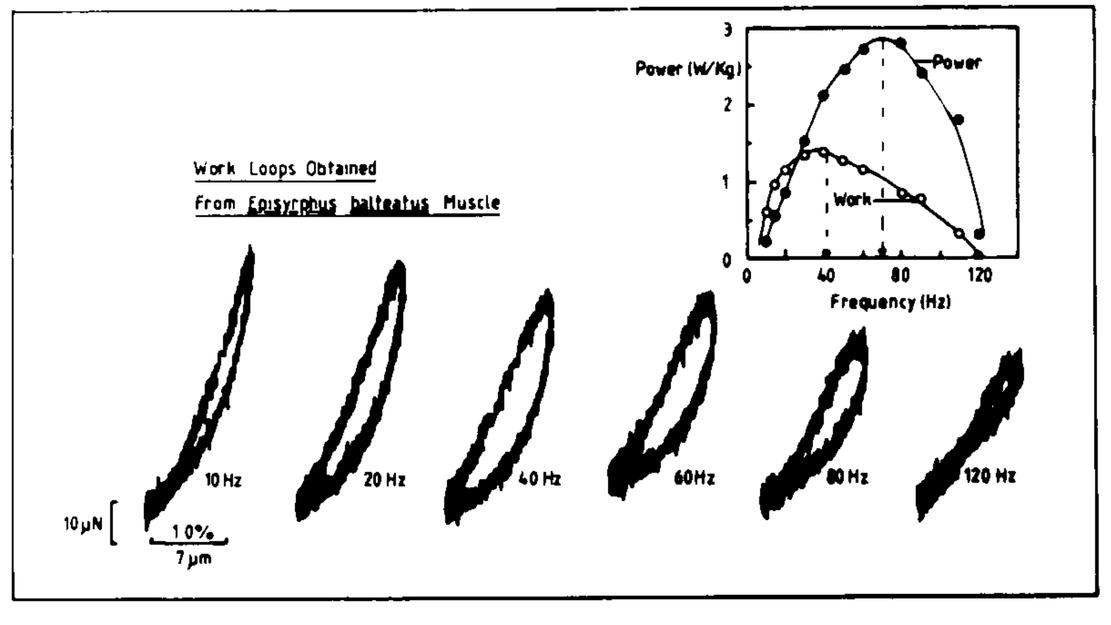

FIGURE 3.5

Length-tension diagrams and calculated work and power outputs for five species of insect. Measured at 20°c. conditions as described in the text.

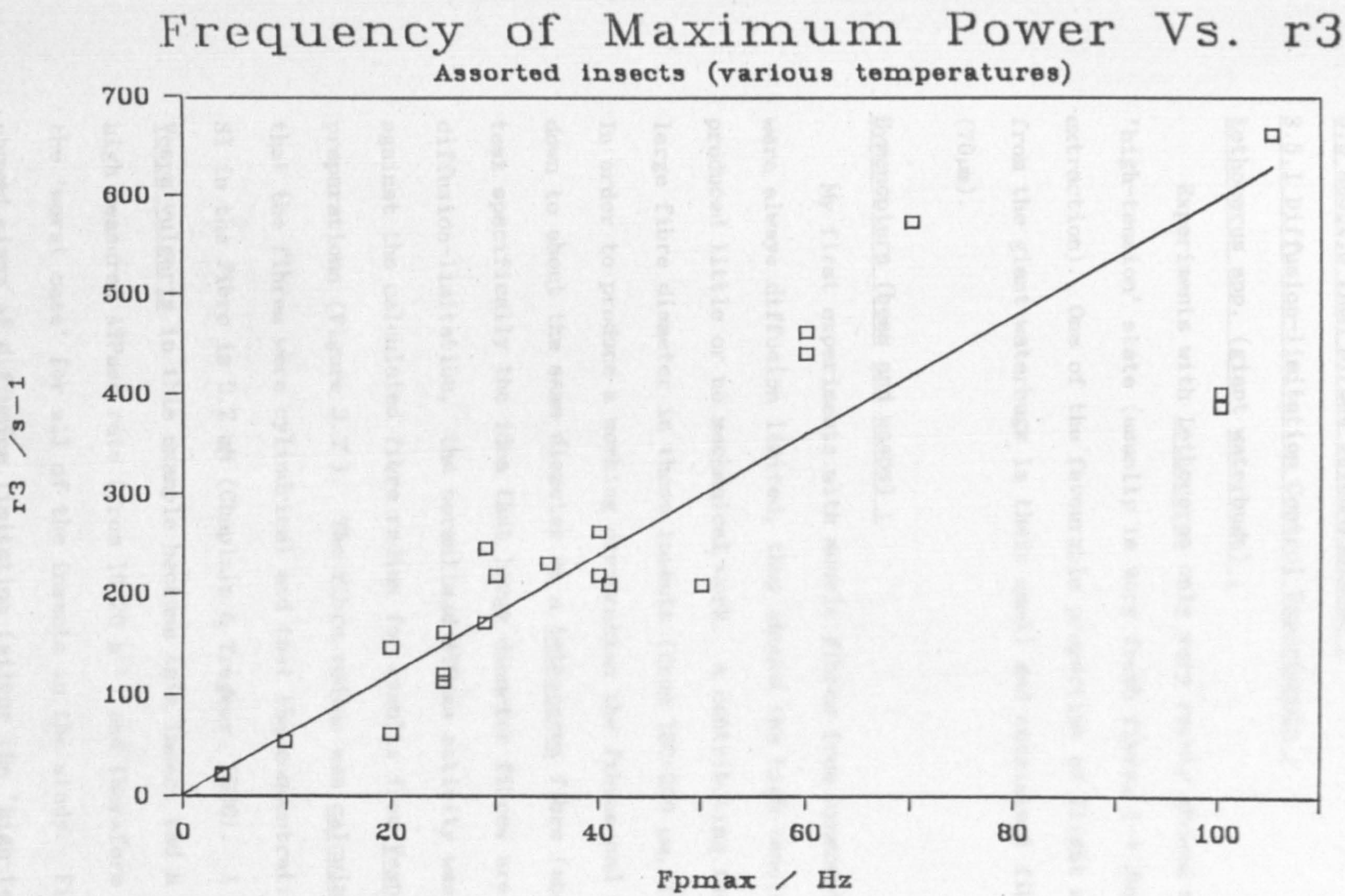

FIGURE 3.6

The rate constant for the delayed tension transient was recorded shortly after the frequency of maximum power had been measured (Section 3.2.1 and 3.2.2). The experiments were performed on a variety of insects at different temperatures to give a wide spread of results.

gives:

$$r_3 = 6.0 \cdot f_{PMAX} \quad \ldots\ldots 3.3$$

3.5 RESULTS FROM ATPase DETERMINATIONS :

3.5.1 Diffusion-limitation Control Experiments :

Lethocerus spp. (giant waterbugs) :

Experiments with Lethocerus only very rarely showed signs of the 'high-tension' state (usually in very fresh fibres 1-4 days after extraction). One of the favourable properties of flight muscle fibres from the giant waterbugs is their small and consistent fibre diameter (70μm).

Hymenoptera (bees and wasps) :

My first experiments with muscle fibres from hymenopteran insects were always diffusion limited, they showed the high-tension state and produced little or no mechanical work. A contributing factor is the large fibre diameter in these insects (from 100-200 μm, Tiegs 1955). In order to produce a working preparation the fibres had to be pared-down to about the same diameter as a Lethocerus fibre (about 70μm). To test specifically the idea that large diameter fibres are prone to diffusion-limitation, the normalised ATPase activity was plotted against the calculated fibre radius for results from Vespa vulgaris preparations (Figure 3.7). The fibre radius was calculated assuming that the fibres were cylindrical and that the concentration of myosin Sl in the fibre is 0.2 mM (Chaplain & Tregear, 1966). I used Vespa vulgaris in this example because this insect had a consistently high measured ATPase rate (from 10-20 s^{-1}) and therefore demonstrates the 'worst case' for all of the insects in the study. Fibres which showed signs of diffusion limitation (either the 'high-tension state'

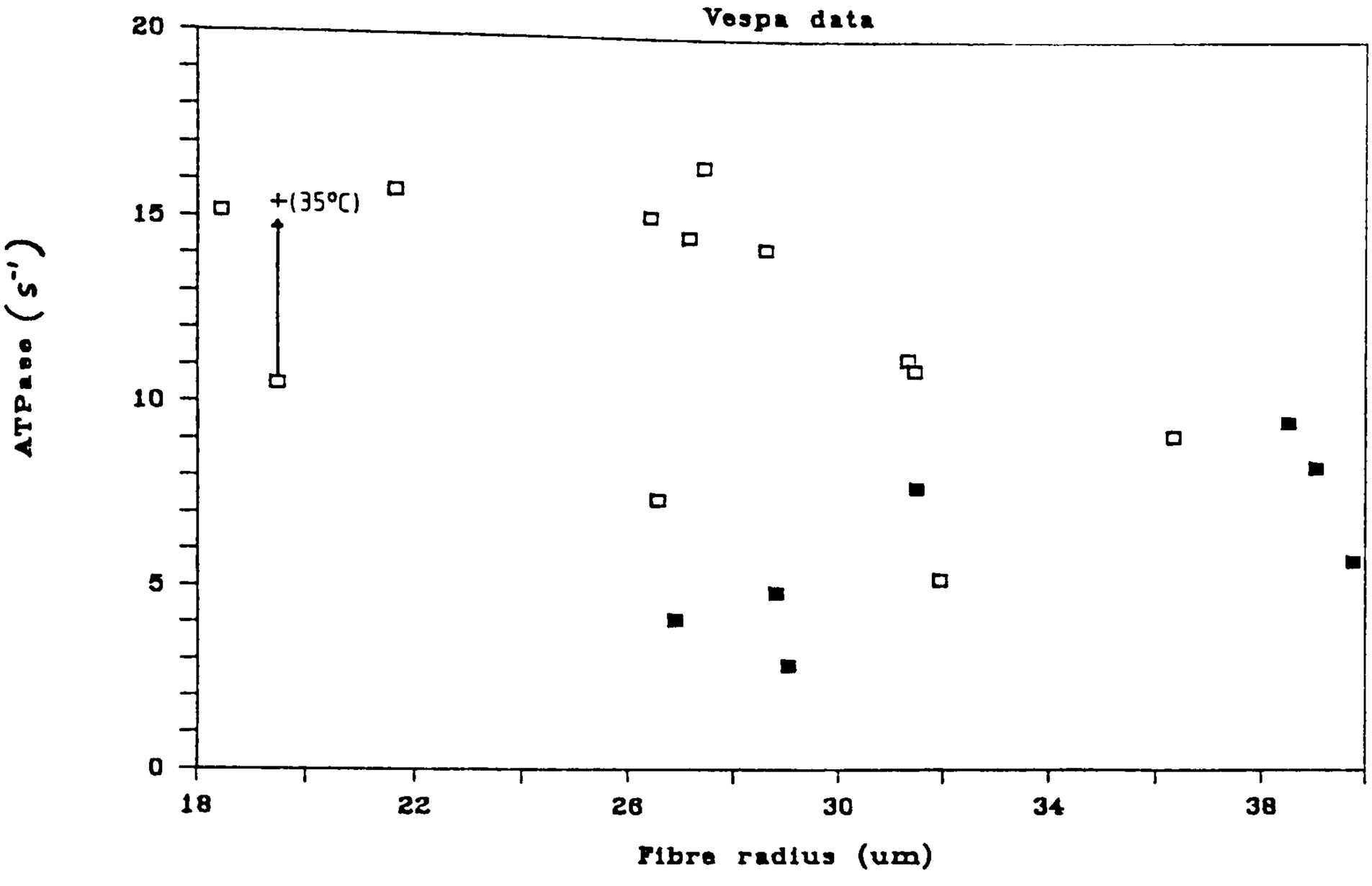

FIGURE 3.7

Maximum measured fibre ATPase activity plotted against the calculated fibre radius (assuming that the fibres were cylindrical and that the concentration of myosin S1 = 0.2mM) The filled symbols are from experiments in which the fibre showed signs of diffusion limitation (low power output or the high-tension state). These fibres generally had lower measured ATPase activities. The calculated fibre radius was not always a reliable indicator that the fibre was subject to diffusion limitation (i.e. fibres in the size range 26-32 μm radius). One experiment was performed at two different temperatures (20° and 35°C.) the large increase in the measured ATPase activity at the higher temperature implies that the fibre was <u>not</u> diffusion limited at the lower temperature.

or an increased ATPase activity when the incubation bath was stirred) are shown as the filled symbols. Fibre preparations viewed by light microscopy were far from cylindrical the calculated fibre radius cannot be used as an *a priori* indicator of diffusion-limitation.

An additional diffusion-limitation control experiment was performed in which a small diameter fibre was incubated at two temperatures, 20°C and 35°C. The measured ATPase rate was much higher at the higher temperature. This finding is discussed later.

Diptera (flies) :

The fibre structure in dipteran insects is not as clearly defined as in hymenoptera or hemiptera (Tiegs, 1955). In all cases the muscle preparations consisted of pieces of muscle tissue pared down to an approximate diameter of 70μm. Like the hymenopteran experiments the fibre preparations were of a variable diameter. I only observed the 'high-tension' state once in dipteran muscle (a particularly large diameter Tipula preparation). In a series of experiments on the hoverfly, Episyrphus balteatus (which I performed in collaboration with Dr. V. Kyrtatas) we measured the ATPase activity under conditions where the concentration of Mg.ATP was varied in the range 10mM to 29mM (Table 2.3). The results are shown in Table 3.3. There is no correlation between the concentration of Mg.ATP and either the measured power output or the ATPase activity. This implies that the experiments are not diffusion limited at the lowest concentration of ATP used (10mM).

Summary of Diffusion-limitation Control Experiments :

Monitoring the mechanical performance of the fibre preparations and incubating in a stirred and a non-stirred bath were the best

	Solution (Table 2.3) (mM ATP)	Oscillation Amplitude (%)	Oscillation Frequency (Hz)	ATPase activity (s^{-1})	Power output (W/kg)
A	29	2.4	82	3.2	3.2
	15	2.4	82	4.0	5.4
	10	2.4	82	3.9	5.9
	29	2.4	82	3.3	4.4
	29	ISOMETRIC		1.6	-
	29	2.4	82	2.9	3.8
B	29	2.2	70	3.7	0.9
	18.5	2.2	70	3.4	1.3
	12	2.2	70	3.3	0.9
	18.5	2.2	70	3.2	0.9
	29	2.2	70	3.5	0.9
C	Ko	ISOMETRIC		0.8	-
	18.5	ISOMETRIC		2.3	-
	18.5	3.0	82	3.1	2.1
	29	3.0	82	2.8	1.0
	18.5	3.0	82	2.8	1.9
	18.5	ISOMETRIC		2.6	-

Table 3.3
The ATPase activity and power output of flight muscle fibres from the hoverfly, Episyrphus balteatus, measured under different concentrations of ATP in the incubation solution. The solutions were described in Table 2.3, except Ko (Experiment C) in Table 2.2a. The ATPase activities were determined from the rate of accumulation of ADP in the incubation solution (measured by HPLC). The power outputs were calculated from tension-length diagrams recorded during the sinusoidal length oscillation. The myosin S1 content of the fibres was measured by calibrated gel densitometry.

These experiments were performed in collaboration with Dr. V. Kyrtatas, the data was also presented in Kyrtatas (1987).

internal controls for diffusion limitation. When any of the internal control experiments indicated that a preparation was diffusion-limited the measured ATPase activity and power output were excluded from the final data set.

The final data set, presented in the next section, consists only of results from experiments which showed no sign of diffusion-limitation.

3.5.2 Fibre ATPase Activities :

Calcium activation measurements :

Because of fibre-to-fibre variation the best results were obtained by performing a series of incubations with a single fibre. It is important to note that the activity of an individual fibre usually falls with time and the order in which the incubations are performed affect the shape of the apparent calcium activation curve. 'Carry-over' of solution from one bath to the next can also alter the free-calcium ion level.

Calcium activation of the fibre ATPase was measured for four species of insect. ATPase activity is shown as a function of free calcium ion concentration in Figure 3.8. In all the species tested the free-calcium level that produced half maximum activation was between pCa 6.0 and 6.4 (about 0.5μM free calcium).

Relaxed and fully-activated ATPase measurements :

The measured ATPase activity at pCa 8 (relaxed) and while producing the maximum mechanical power output at pCa 4.8 (fully activated) is shown for a variety of insects in Figure 3.9. The data points represent the mean results and the vertical bars show the range of values obtained. There is no correlation between the wingbeat frequency of the intact insect and either power output or fully

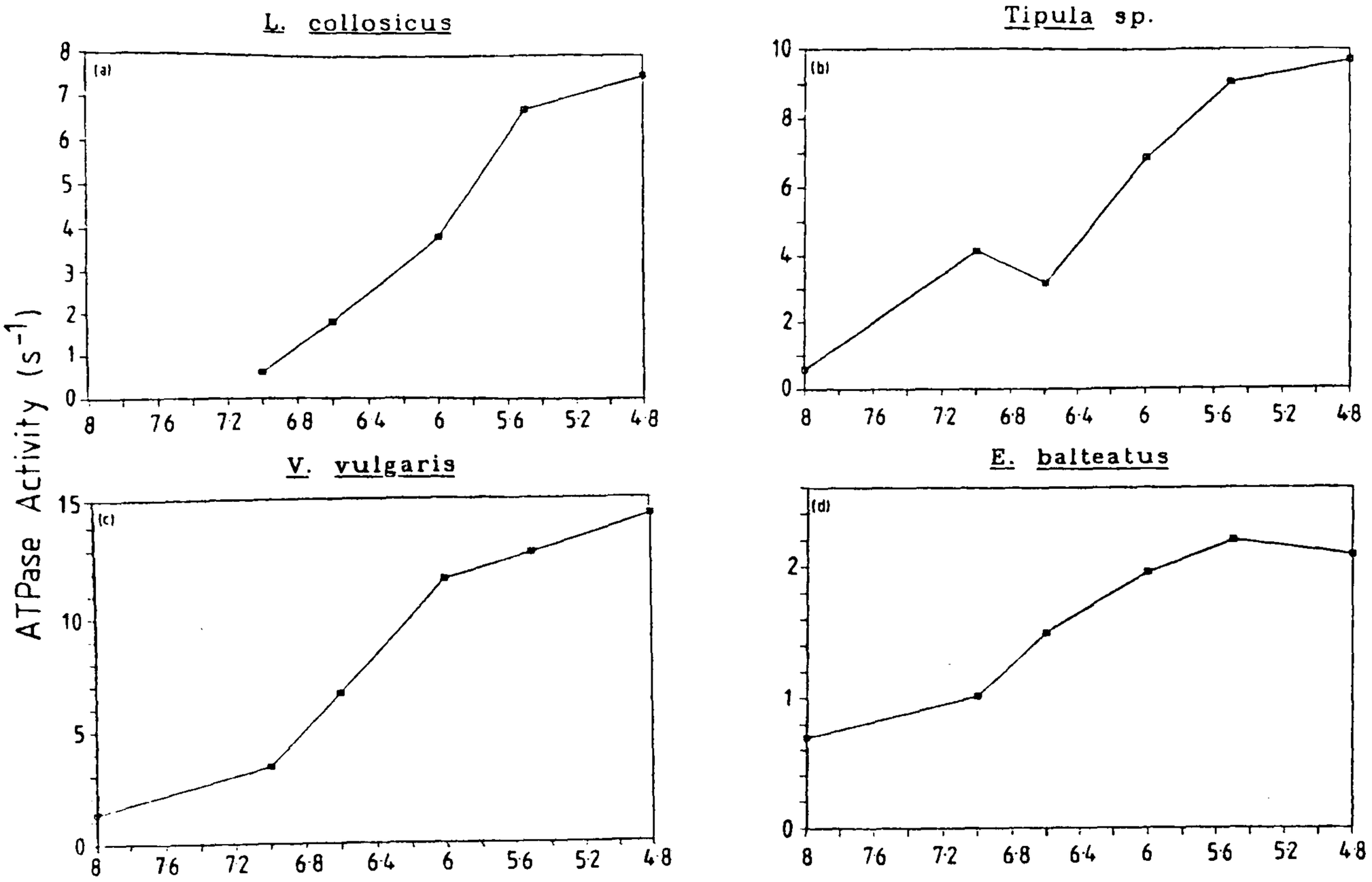

FIGURE 3.8

Calcium activation of the fibre ATPase (during mechanical oscillation, 3% peak-peak) for 4 species of insect. In all cases the pCa for half, full activation was between 6 and 6.4. Experimental details are described in the text (Section 3.3.2). The experiments were performed at 20°C.

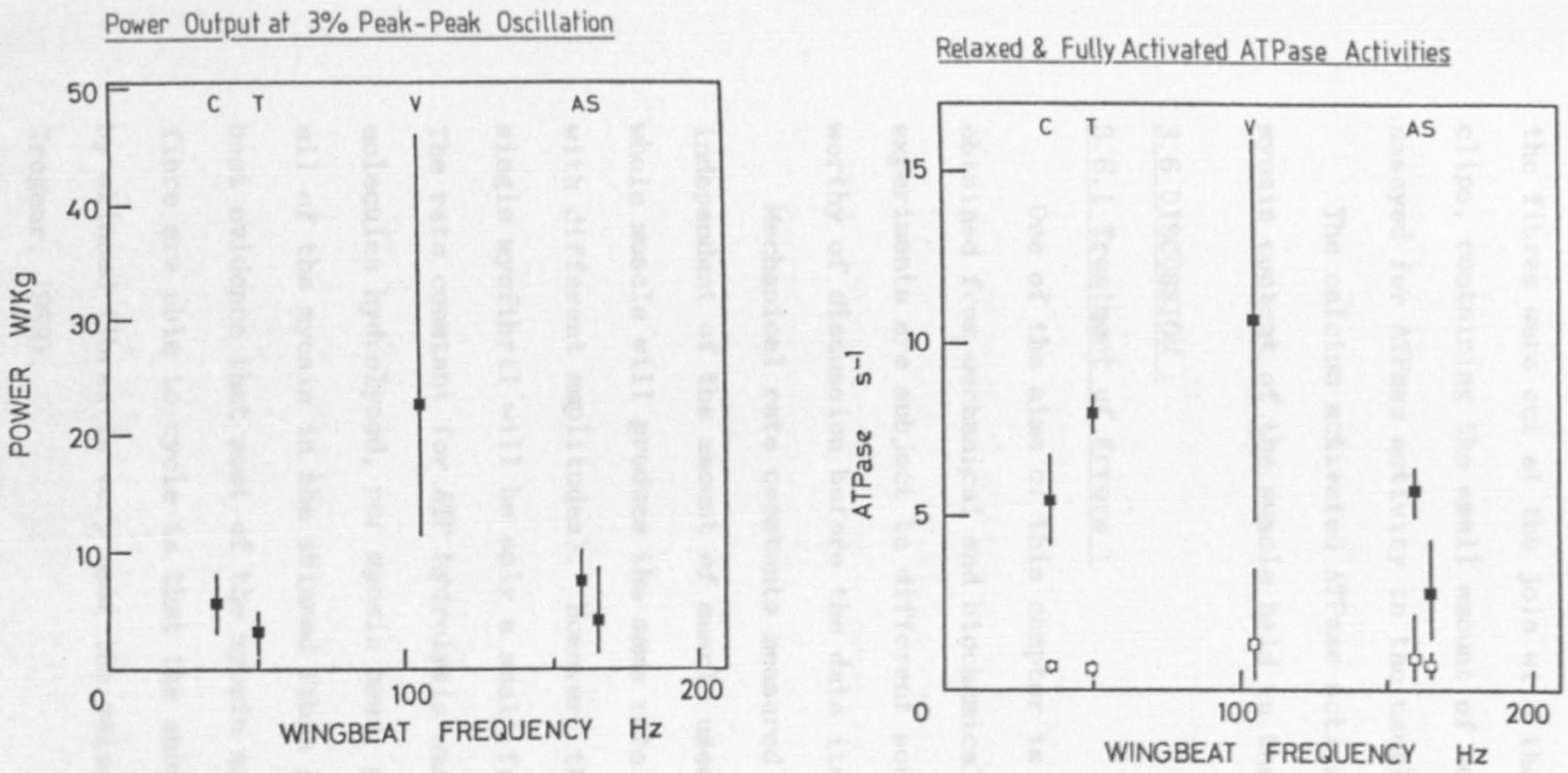

FIGURE 3.9

Relationship between the maximum measured mechanical power output and wingbeat frequency and the relaxed (□) and fully oscillation activated (■) ATPase activities. In both graphs the symbols represent the mean result and the lines the extent of the data. The power ouputs were measured from the area of length-tension diagrams and the ATPase activities by the rate of accumulation of ADP in the incubation solution (determined by HPLC). The fibre size was determined by calibrated gel densitometry.

activated ATPase activity, and no regression line is given.

3.5.3 Fibre 'End-Effect' Control Experiment :

The ATPase activity of the portion of muscle held in the aluminium 'T' clips was measured. Five Vespa fibres were crimped and the fibres were cut at the join with the 'T' clips. The Ten 'T' clips, containing the small amount of muscle held in the clip were assayed for ATPase activity in the usual way.

The calcium activated ATPase activity was 0.9 s^{-1} and the total myosin content of the muscle held in the clips was 2.63 pmoles of S1.

3.6 DISCUSSION :

3.6.1 Treatment of Errors :

One of the aims of this chapter is to compare rate constants obtained from mechanical and biochemical experiments. These experiments are subject to different sources of error, which are worthy of discussion before the data itself is discussed.

Mechanical rate constants measured from tension transients are independent of the amount of muscle used, a single myofibril or the whole muscle will produce the same rate constants when tested (but with different amplitudes). However, the rate of ATP hydrolysis of a single myofibril will be only a small fraction of the whole muscle. The rate constant for ATP hydrolysis was stated as the number of ATP molecules hydrolysed, per myosin head, per second. This assumes that all of the myosin in the skinned fibre preparation is active. The best evidence that most of the myosin molecules in a skinned muscle fibre are able to cycle is that the amount of active tension produced by skinned fibres is very near the values for live fibres (Pringle and Tregear, 1969).

3.6.2 Errors in the Myosin Estimations :

If the gel densitometry is subject to a constant 'noise' (e.g. some constant loss of protein or uneven staining/destaining of the gels) then myosin determinations on very small fibres will have a large percentage error. For this reason I excluded data from fibres with a myosin content estimated below 0.5 pmoles Sl. Fibres below this size gave extremely variable data which I attributed to the large errors in the myosin estimations.

3.6.3 Errors Caused by Diffusion-Limitation :

I have modelled the passive diffusion of nucleotide in a manner similar to Cooke and Pate (1985) but with the important additional effect of bath stirring. The differential equations governing the rate of diffusion of a chemical into an infinitely long cylinder have been solved (see e.g. Carslaw & Jaegar, 1959). For a muscle fibre in steady-state there will be a concentration gradient through the fibre.

The concentration at a given radius is given by :

$$C(r) = C(o) - \frac{B\ (a^2 - r^2)}{4D} \qquad \ldots\ldots\ 3.4$$

Where :

C(o) = concentration of chemical outside fibre (M/m^3).
C(r) = concentration at radius r (M/m^3).
a and r = radius of fibre, given radius (m).
B = rate of use of chemical ($M/m^3/s$).
D = rate of diffusion of chemical (m^2/s).

For a fibre incubated in an unstirred bath the concentration of ATP at a given distance from the fibre is given by :

$$C(r_2) = C(r_1) - \frac{B\ a^2}{2D}.\ln(r_1/r_2) \qquad \ldots\ldots\ 3.5$$

$C(r_1)$ = concentration at a distant point, r_1 (equal to that of the bathing solution)
$C(r_2)$ = concentration at a given innner radius r_2, eg. fibre radius.

Glyn and Sleep (1985) found that ATP binds very tightly to myosin in skinned rabbit muscle fibres. The Km for ATP binding was found to be about 17μM. The following model makes the approximation that the ATPase rate is unaffected until the concentration is zero.

Figure 3.10 shows the concentration gradient through two fibres, one with a low ATPase rate and one with a high ATPase rate, both bathed in an unstirred solution. We can see that the ATP concentration has fallen to zero in the centre of the second fibre (the 'rigor core' described in Section 3.3.1); the second fibre is diffusion-limited and its maximum measurable ATPase rate (B_{max}) is given below under conditions when the bath is perfectly stirred and when it is not stirred :

Stirred :

$$B_{max} = \frac{4D.C(o)}{a^2} \qquad \ldots\ldots 3.6$$

Unstirred :

$$B_{max} = \frac{4D.C(o)}{a^2 + 2a^2.\ln(r_1/a)} \qquad \ldots\ldots 3.7$$

Notice that the measured ATPase activity (B_{max}) is independent of the intrinsic activity (B) in a diffusion-limited fibre. Another point to notice from Equations 3.6 and 3.7 is that the measured ATPase activity (B_{max}), of a diffusion-limited fibre, is increased by stirring the bath, changing the concentration of ATP in the bathing solution or reducing the fibre diameter.

The diffusion coefficient (D) is directly proportional to the absolute temperature. The finding that the ATPase activity of a fibre measured at two temperatures (Section 3.5.1 - Hymenoptera) showed a

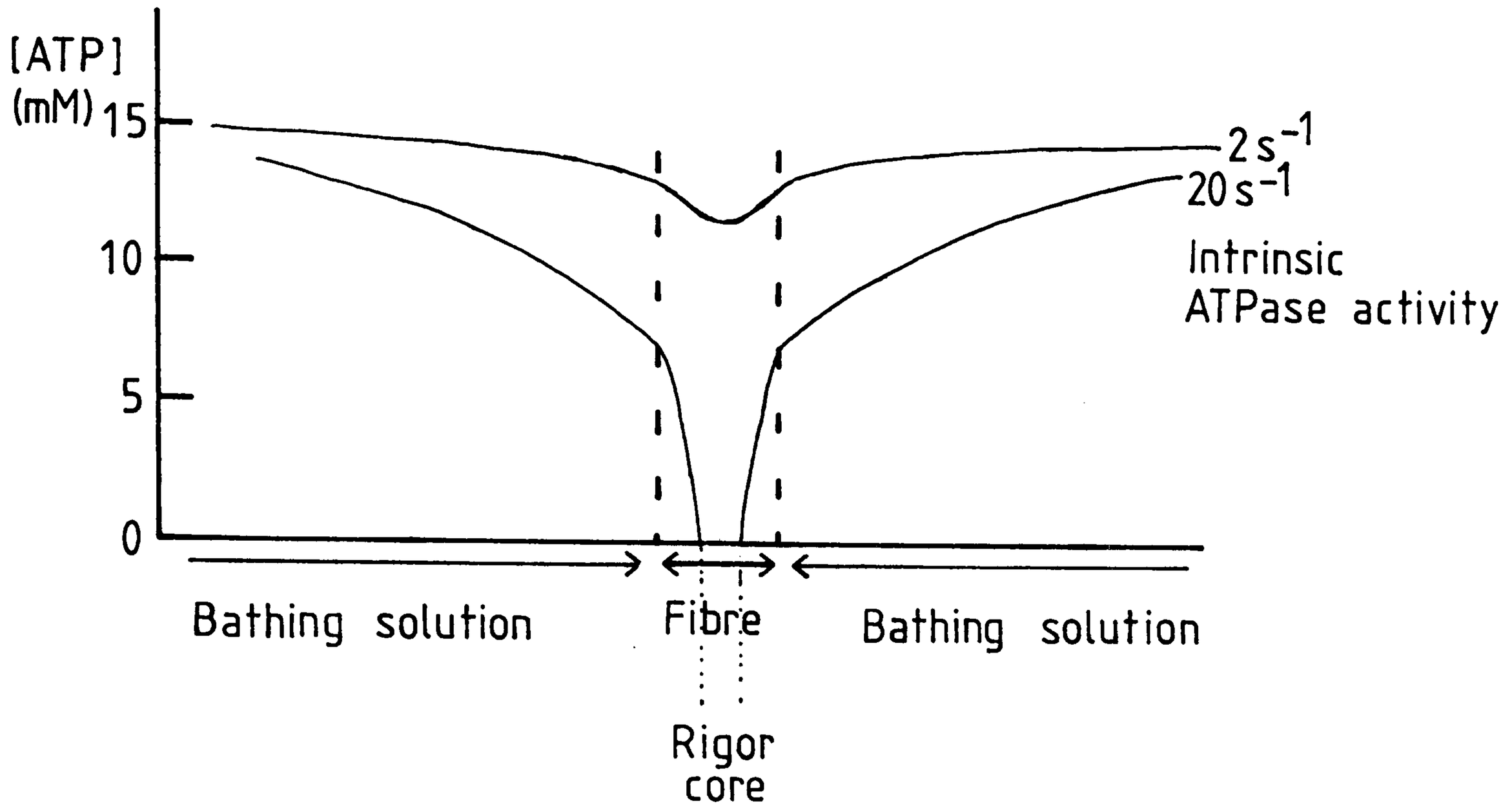

FIGURE 3.10

The concentration gradient of ATP through the bathing solution and muscle fibre in an unstirred muscle bath. Two different intrinsic ATPase activities have been assumed. The centre of the fibre with an intrinsic activity of $20s^{-1}$ is starved of ATP and is therefore in rigor. The degree of bath stirring will affect the shape of the concentration gradient in the incubation solution. Increased stirring will raise the concentration of ATP at the fibre surface.

The fibre radius was assumed to be 40μm in this example and the diffusion coefficient was taken as $1.2 \times 10^{-10} (m^2 s^{-1})$ and the concentration of myosin active sites within the fibre as 0.2mM.

marked increase with temperature, is good evidence that the measured activity at the lower temperature was not diffusion-limited.

3.6.4 End-Effect Errors :

The part of the muscle fibre held in the 'T' clip contributes little to the ATPase activity (being enclosed in the foil it will almost certainly be diffusion-limited, and not accessable to mechanical activation). The results from Section 3.5.3 indicate that the 'T' clips contain about 0.5 pmoles of S1, and that this protein has only one tenth of the maximum activity. The average fibre size in all experiments was about 1.5 pmoles S1. The muscle in the 'T' clips, with low activity, causes a maximum underestimate of the ATPase activity of 50%. No correction was made for this source of error in the data presented, because of the difficulty in assessing the error in any individual experiment.

3.6.5 Temperature and Phosphate Concentration Fluctuations :

The temperature in the muscle bath used for mechanical experiments (measured with the thermistor probe used for thoracic temperature measurement) showed brief fluctuations of up to 1°C. although the mean value was well regulated. This is probably due to air currents causing sudden, evaporative cooling. The rate constant of the delayed tension transient is very temperature sensitive (Q_{10} = 2.9, Chapter 6). Because the mechanical measurements are made over a brief time scale they could be subject to a maximum error of ≃10% (caused by a 1°C. temperature fluctuation).

The rate constant of the delayed tension transient is dependent upon the concentration of phosphate (White and Thorson, 1972). The amount of product phosphate accumulating in the skinned fibres will alter the rate constant. Effects of this unpredictable variation

in phosphate concentration could have been ameliorated by including 5-10mM phosphate in the incubation solution (further accumulation of phosphate then has little effect; White & Thorson, 1972). However, the delayed tension transient amplitude is dramatically reduced by phosphate (White and Thorson, 1972). Inclusion of millimolar phosphate in the incubation solution would have reduced the signal to noise ratio in the delayed tension transient records from small insects.

The ATPase measurements were made in an incubation bath that was covered with silicone oil. The layer of oil prevents evaporative heat loss and confers temperature stability. Also ATPase measurements are made over a period of several minutes and are representative of the mean bath temperature.

3.7 THE MECHANICAL PERFORMANCE OF FLIGHT MUSCLE FROM DIFFERENT INSECTS :

For all the species tested the maximum power output occurred at a lower frequency than the wingbeat frequency in the intact insect (see Table 3.4, below).

Species	f_{PMAX}	f_{WB}
Lethocerus griseus	8	44
Tipula spp.	17	50
Vespa vulgaris	30	100
Apis mellifera	40	160
Episyrphus balteatus	75	165

Table 3.4

Table of measured frequency of maximum power output (f_{PMAX}), at 20°C. and measured wingbeat frequency (f_{WB}), at an ambient temperature of 25°C.

The major explanation for this is temperature. The mechanical measurements on the single, skinned fibres were made at low temperatures (15°C. and 20°C.) to minimise problems of nucleotide

diffusion across the fibres. However, the wingbeat frequencies were measured at an ambient temperature of 25°C. Further, the thoracic temperature in many insects is known to be raised during flight; this is true particularly for the larger insects. The thoracic temperature of flying water bugs is 40°C (L. indicus, and L. griseus see Chapter 6), of the bees Apis and Bombus is 39°C and 40°C respectively (Heinrich, 1974 and 1979) whereas for the small glabrous insects I found values of 27°C in Tipula and 29°C in Vespa. If the rate constant r_3 were measured at the flight temperature the effect would be to reduce the intercept of Figures 3.3 and 3.4 by raising the points for larger insects with lower wingbeat frequencies more than for the smaller insects with higher wingbeat frequencies.

If the flight muscle is to develop its maximum, specific power output (maximum power weight for weight) in the living insect then f_{PMAX} should coincide with the wingbeat frequency. From Equations 1 and 3 we find :

$$f_{PMAX}^{15\ deg.C} = 0.23 \cdot f_{WB}^{Thoracic\ Temp.} + constant \quad ..... (8)$$

and from Equations 2 and 3 we find :

$$f_{PMAX}^{20\ deg.C} = 0.37 \cdot f_{WB}^{Thoracic\ Temp.} + constant \quad ..... (9)$$

The constant of proportionality in Equations 8 and 9 will approach unity if the temperature difference between the mechanical experiments and flight is taken into account. However, there remains a discrepancy in the performance of the flight muscle from the small dipteran insects whose thoracic temperature in flight is close to ambient (25°C.). Another factor which may affect the frequency of maximum power output is the waveform of the length changes. The

factors determining the form of the wingbeat are not clearly understood but, the motion at the wingtip is often not sinusoidal (Miyan and Ewing, 1985), the waveform used to measure power output in these experiments. Non-linearities in the transient tension response (asymmetry in the response to stretch and release) may limit the work produced at high frequencies. The more complex length change waveform *in vivo* might extend the frequency range over which the muscle can do work.

The relatively constant power output and ATPase activity measured in species of insect with widely differing wingbeat frequency requires that the work per oscillatory cycle in the flying insect be smaller in insects with higher wingbeat frequencies. A theoretical study (Pennycuick & Rezende, 1984), based on the energy available from mitochondria, suggests that insects with fibrillar muscle should have higher mass specific power output with higher wingbeat frequencies, requiring the work per cycle to be independent of size. This is contrary to the findings here except for Vespa.

Previous estimates of power output have frequently measured the oxygen consumption by the flying insect. The rate of oxygen consumption by unrelated species of insect has been measured many times (Figure 3.11, from Kammer & Heinrich 1978); no clear relationship between power input and insect size is apparent from these studies. It is probably not correct that mass specific oxygen consumption scales with either mass or wingbeat frequency for insects in general. A systematic study of insects of different size, a study of the oxygen consumption in hovering euglossine bees, which have fibrillar flight muscles, (Casey et al., 1985) showed that the mass specific rate of oxygen consumption is much greater in smaller bees.

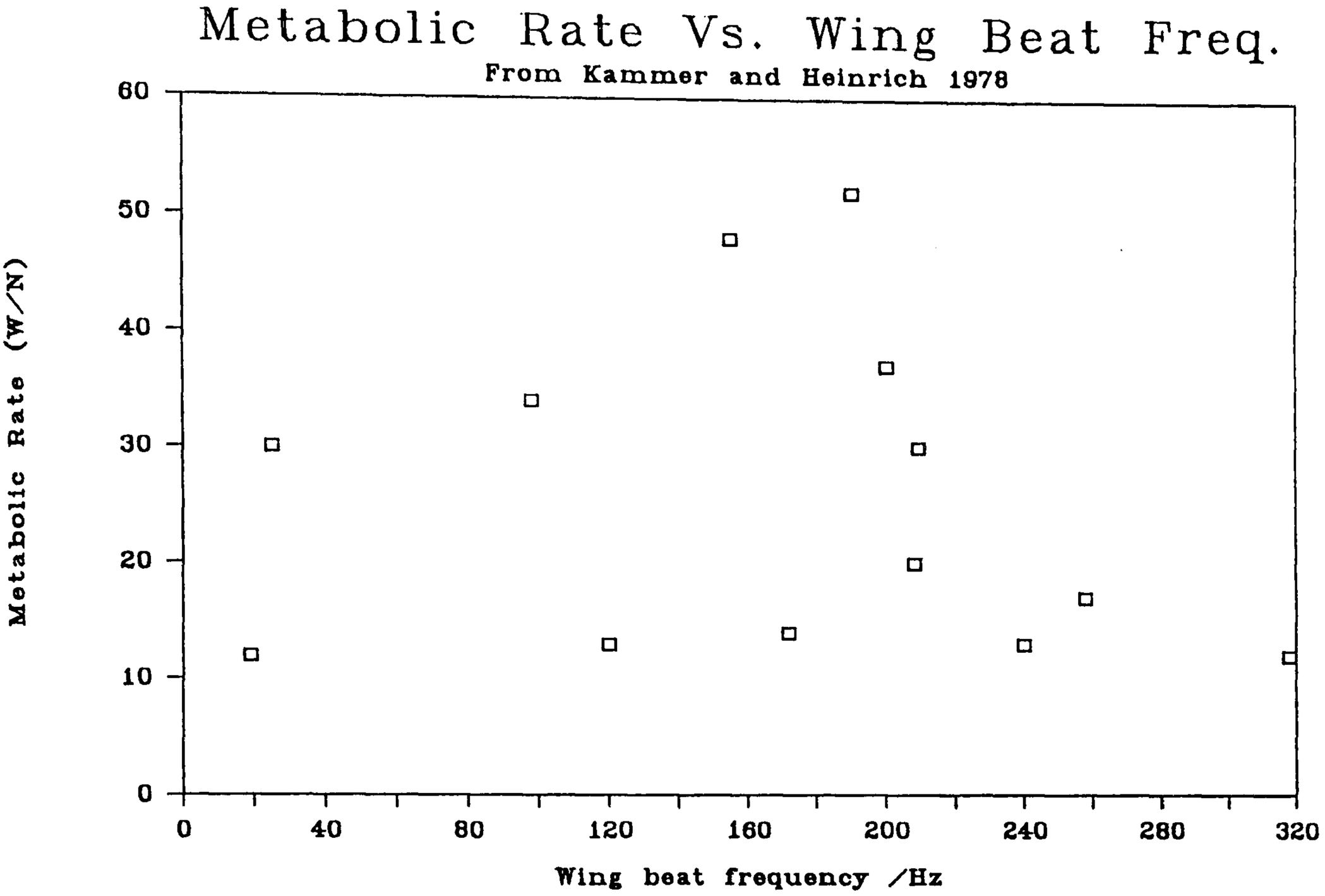

FIGURE 3.11

Previous studies show that there is no correlation between the wingbeat frequency and the rate of oxygen consumption by a wide variety of flying insects. (data collected by Kammer and Heinrich, 1978). Symbols represent the measured oxygen consumption (converted to equivalent mechanical power output assuming 20J/ml of O_2 and 20% efficiency) plotted against the wingbeat frequency of the insect.

Perhaps in a restricted group of closely related insects it is possible that the specific power output does vary with wingbeat frequency. Some of these ideas are discussed in more detail later (see Chapter 6).

3.8 A MINIMAL CROSS-BRIDGE SCHEME :

When an activated fibrillar muscle fibre is held at a fixed length the cross-bridge cycle settles to a steady-state. The concentrations of the intermediaries in the biochemical pathway are fixed and there is constant a flux through the pathway. The flux through the pathway is controlled by the rate-limiting step which determines the ATPase activity of the muscle. The tension that the muscle developes depends upon two factors; the number of attached cross-bridges and their distortion. If the muscle fibre is stretched suddenly, the steady-state is perturbed and a relaxation to the new steady-state occurs. The transient tension response reflects changes in cross-bridge attachment and/or conformation. The best explanation of the tension transient phases (shown in Figure 3.1) is given by Thorson and White (1983).

Phase 1 : The elasticity of the attached cross-bridges produce a tension change that is roughly proportional to the length change and occurs simultaneously with the length change. The tension change for a given length change (or stiffness) is dependent upon the number of attached cross-bridges at the moment before the stretch.

Phase 2 : The increased tension in the attached cross-bridges places a constraint upon the bridges. The cross-bridges shift so as to relieve the constraint, leading to a transient fall in tension. The 'shift' could be either cross-bridge detachment (Podolsky et al.,

1969) or a conformational change in an attached state (Huxley & Simmons, 1971). Thorson and White (1983) provide experimental evidence which supports the latter of these two possibilities.

Phase 3 : Insect muscle is activated by stretch; both the cycling rate (ATPase) and the tension are increased by stretch. The rate constant for the delayed tension transient will be the sum of the forward and reverse rate constants leading to the tension generating state. If the tension generating state is to be significantly populated at steady-state the forward rate constant must be large compared to the reverse step.

The measured maximum ATPase rate, in this study, was always 10 to 100 times slower than the rate constant for the delayed tension transient. With the exception of Vespa there is no significant change in the fibre ATPase activity with wingbeat frequency. The rate constant leading to the tension-generating state in the cross-bridge cycle must be relatively fast and correlate with the wingbeat frequency of the insect. The rate-limiting step is slower and must (if the tension generating state is to be sufficiently populated) come after the first tension-generating state and is not correlated to the wingbeat frequency of the insect. The findings presented in this chapter lead directly to the minimal model of the cross-bridge cycle shown in Scheme 3.1.

Experiments performed in the following chapter (Chapter 4) provide information about which states in the biochemical pathway may be tension generating and which step is likely to be rate-limiting for the cycle. The point in the cross-bridge cycle at which stretch activation may act is also discussed.

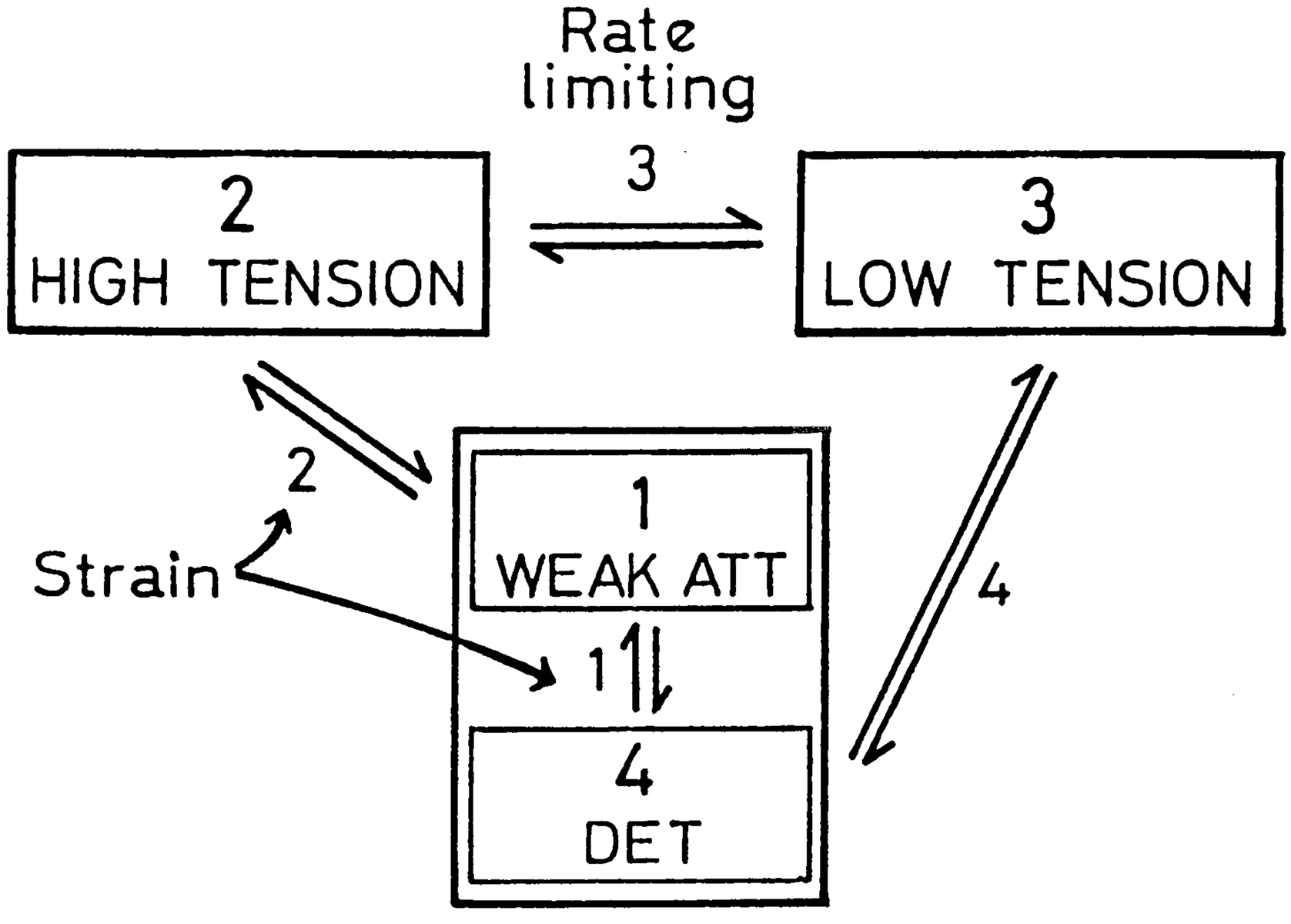

SCHEME 3.1

A minimal cross-bridge model; States 1 (weakly attached) and 4 (detached) are myosin states with low affinity for actin; states 2 and 3 are tension generating myosin states with high affinity for actin. The rate constants between the weak binding states are assumed to be rapid compared to the other rate constants in the cycle. The equilibrium constants are such that the cycle is traversed clockwise. The two strong-binding states are designated "high tension" and "low tension" to denote the tension exerted by a cross-bridge in those states in the isometric muscle. Stretch activation acts to change the rate constants of step 1 or 2; the rate constants of step 2 must correlate with the wing-beat frequency of the insect. Step 3 is rate-limiting and does not correlate with the wingbeat frequency of the insect.

CHAPTER 4 :

THE ATPase ACTIVITY OF FIBRILLAR FLIGHT MUSCLE FROM THE COMMON WASP *VESPA VULGARIS* PROBED BY PHOSPHATE WATER OXYGEN EXCHANGE

THE ATPase ACTIVITY OF FIBRILLAR MUSCLE FROM THE COMMON WASP, *VESPA VULGARIS* PROBED BY PHOSPHATE-WATER OXYGEN EXCHANGE.

[The experiments described in this chapter were carried out in close collaboration with the following people : Dr. John N. Lund and Dr. Martin R. Webb* (University of York, and *N.I.M.R. Mill Hill, London)]

4.1 INTRODUCTION :

When ATP is hydrolysed by muscle, an oxygen atom from the solvent water becomes bound to the product phosphate. The hydrolysis step in the cross-bridge cycle is freely reversible, and the phosphate is free to rotate in the catalytic site. From one to all four oxygen atoms can be exchanged between the phosphate and the solvent water before the phosphate is finally released. This chapter describes experiments in which skinned muscle fibres hydrolyse ATP in the presence of water whose oxygens are labelled (^{18}O). By measuring the distribution of labelled oxygen atoms on the product phosphate, information is obtained about the rate constant for the reverse hydrolysis step and rate constants controlling phosphate release. This method is called "oxygen exchange". In a series of experiments I have examined the pattern of oxygen exchange in muscle fibres from the common wasp, Vespa vulgaris, under a variety of different conditions. These results are compared to other published results from oxygen exchange experiments on flight muscle from the giant waterbug Lethocerus and vertebrate skeletal muscle (Lund et al., 1987, 1988, Hibberd et al., 1985 and Webb et al., 1986).

1) When the muscle is relaxed or only partially activated, a minimum of two hydrolysis pathways are required to model the distribution of labelled oxygens on the released phosphates.

2) The pattern of exchange in fully activated muscle fibres is typical of a single pathway for ATP hydrolysis. This means that the myosin molecules are behaving in a uniform fashion with respect to oxygen exchange.

3) Results from Vespa show a great similarity to those of Lethocerus but the pattern of exchange is consistent with the release of phosphate being ten times faster in Vespa.

4) The ATPase rate in Vespa is about ten times faster than in Lethocerus.

5) The oxygen exchange results can most easily be explained if the steps controlling phosphate release are limiting for the ATPase rate, being about ten times faster in Vespa than Lethocerus.

The conclusion is that the steps controlling phosphate release are rate-limiting for the cross-bridge cycle. Therefore, the state preceding phosphate release is the first tension-generating step in the cross-bridge cycle. In vertebrate muscle the first attached state following ATP hydrolysis is a weak-binding actomyosin.ADP.Pi (AM.ADP.Pi) state, in which no tension is developed, and which is in rapid equilibrium with the corresponding detached (M.ADP.Pi) state. If this is also the case for insect flight muscle then the first tension-generating process must be an isomerisation between two AM.ADP.Pi states.

4.1.1 Oxygen Exchange :

Exchange of oxygen atoms between the solvent water and terminal phosphate of ATP during hydrolysis provides a method for studying the

reaction kinetics by a steady-state technique. Product release (ADP + Pi) does not occur instantaneously following hydrolysis and for a moment there is a chance for the products either to reform in the catalytic site (reversal of the hydrolysis step) or to be released. The degree of oxygen exchange is a statistical function of probabilities for phosphate release and reverse hydrolysis.

There are three reasons why oxygen exchange can be measured in intact muscle fibres.

1) Oxygen from the solvent water always binds to the terminal (ejected) phosphate of ATP.

2) The products remain in the catalytic site for some time, and reversal of the hydrolysis step may occur. Meanwhile, the phosphate is free to rotate and there is an equal probability of any of the four oxygens being displaced when a reversal occurs.

3) The pattern of oxygen exchange can be measured by incubating a muscle fibre in ^{18}O water and by analysing the pattern of ^{18}O incorporation in the product phosphates by mass spectrometry.

Scheme 4.1 shows how the exchange of labelled (^{18}O) for unlabelled oxygens on the terminal phosphate of ATP comes about. The proportion of phosphate with 1,2,3 and 4 labelled oxygens is given in terms of probabilities for the phosphate release and hydrolysis reversal steps (p and q, resp.) below :

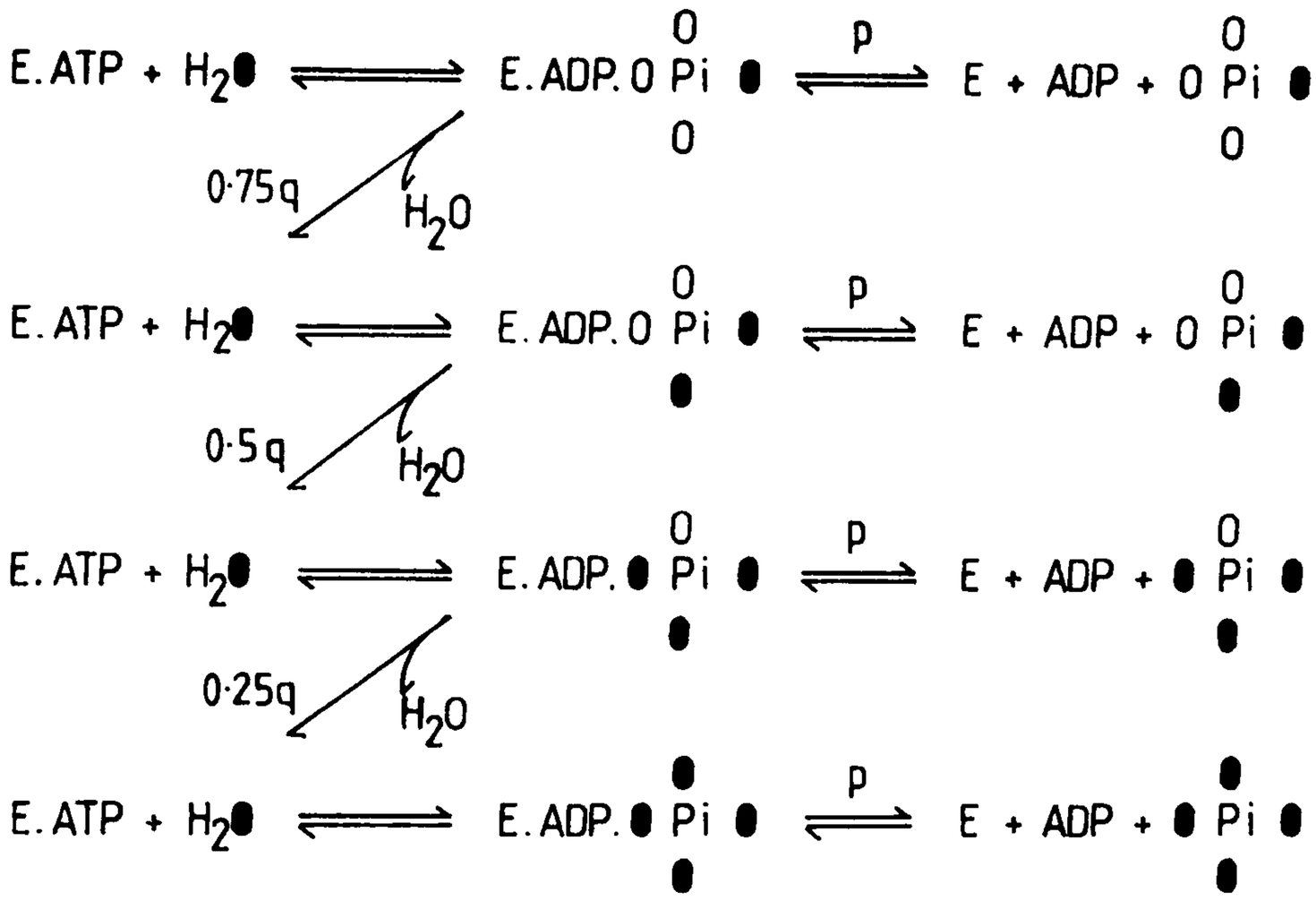

SCHEME 4.1

Scheme to describe how oxygen-exchange between solvent water and the terminal phosphate of ATP arises during its hydrolysis by muscle fibres. p represents the probability of phosphate being released, q is the probability of reversal of the hydrolysis step.
Filled ●'s are ^{18}O, open are ^{16}O ; E represents the catalytic site (this is strictly either myosin alone or actomyosin in muscle fibres).
From Hibberd and Trentham 1986.

Proportion

o o Pi * o	F_1 =	$\frac{p}{(0.75*q + p)}$
o o Pi * *	F_2 =	$\frac{p}{(0.5*q + p)} * \frac{(0.75*q)}{(0.75*q + p)}$
o * Pi * *	F_3 =	$\frac{p}{(0.25*q + p)} * \frac{(0.5*q)}{(0.5*q + p)} * \frac{(0.75*q)}{(0.75*q + p)}$
* * Pi * *	F_4 =	$\frac{p}{p} * \frac{(0.25*q)}{(0.25*q + p)} * \frac{(0.5*q)}{(0.5*q + p)} * \frac{(0.75*q)}{(0.75*q + p)}$

..... 4.1

The previous equations are simplified by expressing the proportions (F_1 - F_4) in terms of the ratio p/q, denoted by the letter 'R' (Webb & Trentham, 1981) :

F_1 = R/(0.75+R)

F_2 = R/(0.5+R) * 0.75/(0.75+R)

F_3 = R/(0.25+R) * 0.5/(0.5+R) * 0.75/(0.75+R)

F_4 = R/R * 0.25/(0.25+R) * 0.5/(0.5+R) * 0.75/(0.75+R)

..... 4.2

The theoretical distributions of oxygen label in released phosphate, for various values of R, are plotted in Figure 4.1. For values of R > 1.5 and R < 0.05 there is rather little change in the expected distribution of label with change in R. This means that the method of monitoring oxygen exchange is most sensitive when the phosphate release step is faster than 0.05 times, and slower than 1.5 times, the rate constant for the reverse hydrolysis step.

The actual proportions of label in the product phosphate is determined by conversion of the product to volatile, triethyl

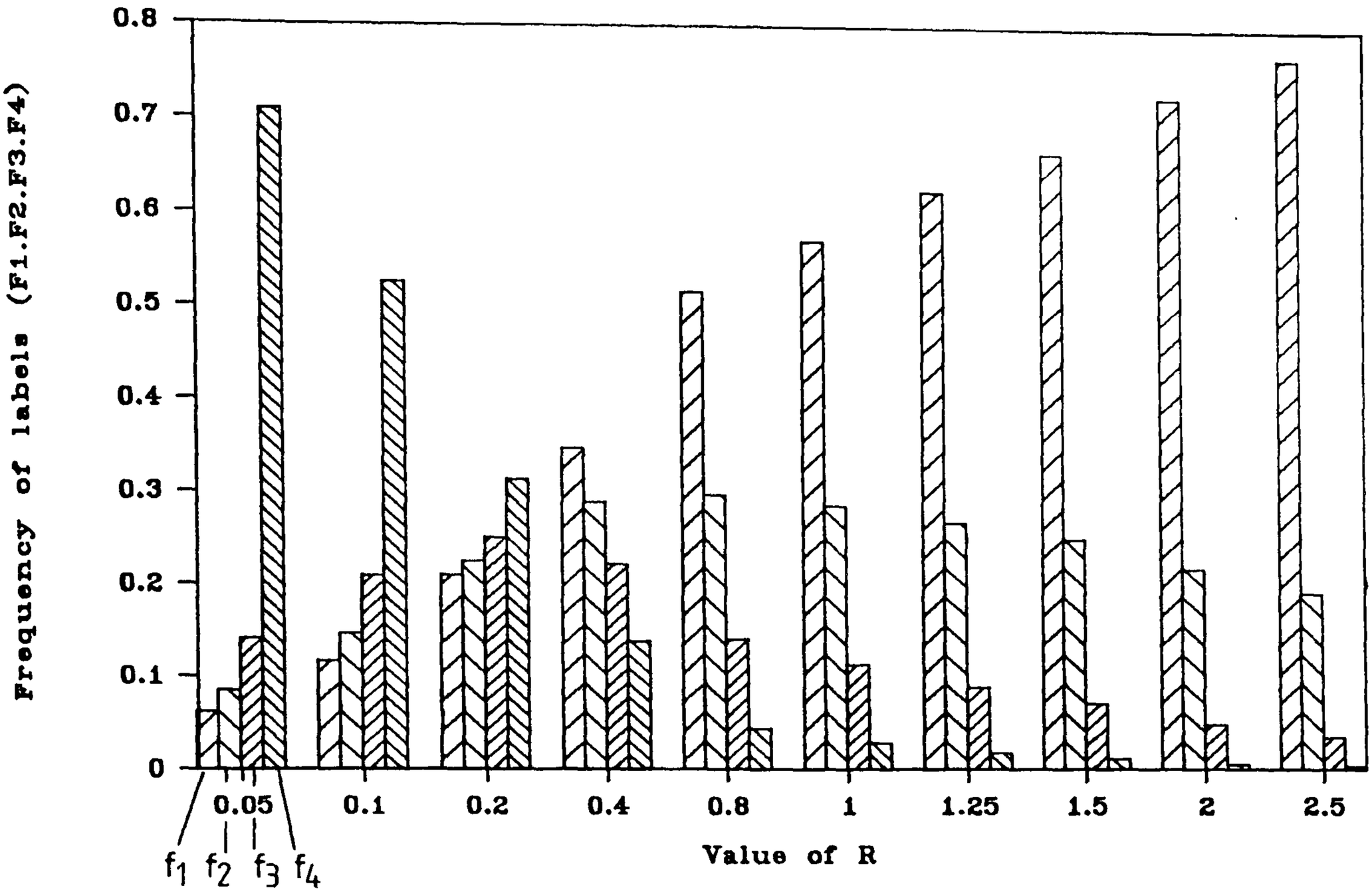

FIGURE 4.1

The theoretical distributions of oxygen label in the released phosphate, for various values of R.

R is the ratio of the probability of phosphate being released against the probability of reverse hydrolysis. (see Equation 4.2)

phosphate and analysis by mass spectrometry.

4.2 MATERIALS AND METHODS :

4.2.1 Choice and Collection of Material :

The common wasp, Vespa vulgaris, was chosen as the most suitable insect for this study for several reasons:

1) The muscle preparations were very stable over long periods of time, producing good work loops for up to two hours.

2) The high wingbeat frequency (100 Hz) of this insect means that the mechanical rate constants are 5-10 times faster than Lethocerus.

3) Relatively long lengths of fibre (2-3mm) could be mounted on the mechanical test apparatus. This means that sufficient phosphate could be collected for analysis by mass spectrometry.

Diffusion-limitation was a major problem with whole fibre preparations from Vespa flight muscle. A contributing factor is the large fibre diameter (175μm). Working preparations were obtained by paring down whole fibres to about 70μm diameter, as described in Chapter 3.

The specimen used in these experiments was a locally captured queen, Vespa vulgaris. The muscles were glycerol extracted and used after 7, and within 14 days after extraction.

4.2.2 Mechanical Experiments and Experiments on The Intact Insect :

These experiments were reported in the previous chapter (Chapter 3); Table 4.1 summarises the findings for both Lethocerus and Vespa.

	L. indicus	V. vulgaris
Experiments on the intact insects :		
f_{WB}	38 Hz	100 Hz
Thoracic temperature	42°C.	31°C.
	(Ambient temperature = 25°C.)	
Experiments on single skinned muscle fibres :		
f_{PMAX}	4 Hz	30 Hz
f_{WMAX}	3 Hz	25 Hz
r_3	$20*s^{-1}$	$160\ s^{-1}$
ATPase (fully activated)	$2*s^{-1}$	$12\ s^{-1}$
Power (max.)	5 W/kg	22 W/kg
	(Experimental temperature = 20°C.)	

* Lund et al., 1987

Table 4.1
Comparison of the operating conditions and mechanical properties of fibrillar flight muscle from Vespa vulgaris and Lethocerus indicus (summary of data presented in Chapter 3.)

The stiffness of both Vespa and Lethocerus muscle was measured in three different test solutions; activating, rigor and gluteraldehyde fixative, and also during the course of a tension transient following a step-length change in activating solution. Two different methods were used; a step length change was performed with the oscilloscope set on a fast time base and tension versus length was plotted over the period of the length change, the gradient of this plot gives the stiffness; a high frequency (550Hz), small amplitude (0.1-0.2%) sinusoidal length oscillation was superimposed on the length signal, the amplitude of the tension oscillations is proportional to the dynamic stiffness.

4.2.3 Oxygen-Exchange Experiments :

The methods for these experiments have been described previously, (Lund et al., 1987 and Hibberd et al., 1985) but are included here

briefly for completeness.

4.2.4 Solutions :

Two solutions were prepared by Dr. John Lund; a 'relaxing' solution and an 'activating' solution. The solutions were the same as Table 2.2c. One ml of each solution was removed and lyophilised (in a freeze drier). In order to displace ^{16}O water present as water of crystallisation, a small amount of ^{18}O water was added to redissolve the dry matter and the solution was lyophilised again. Finally, one ml of ^{18}O water was added to reconstitute the solution. The final concentration of ATP was checked with HPLC.

4.2.5 Experimental Protocol :

The experimental set-up was the same as used in the fibre ATPase determinations. For all incubations the muscle bath temperature was regulated to 20°C.

During the experiments care was taken to avoid contamination of the ^{18}O solutions with ^{16}O water. As soon as the solutions had been laid out in the muscle baths they were covered with a layer of dry silicone oil to prevent condensation of atmospheric ^{16}O water in the baths. Prior to incubating the muscle in an experimental bath, the fibre was washed in two baths of 60µl of ^{18}O relaxing solution, to remove ^{16}O water from the fibre. In the second of these 'wash baths' zero tension was established by stretching the fibre with the tension hook micromanipulator until the fibre was just taut.

Sequential incubations in the row of baths, each containing 30µl of activating solution, were performed under three different mechanical conditions; 1) isometric, 2) oscillated at the frequency for maximum work, 3) released by 15-20% so that no tension was

developed ('slack'). In addition, two separate experiments were performed in relaxing solution. To reduce the incubation time for the relaxed treatment, 7 fibres were crimped in parallel, in a strip of aluminium foil (diffusion limitation was not a problem because of the low ATPase rate in relaxing solution).

In all cases the muscle was incubated for sufficient time to produce 5% hydrolysis of the total ATP (monitored by HPLC). This gave a yield of about 20 nmoles of phosphate in each bath. At the termination of each incubation all the solution was evacuated from the muscle bath and quenched with 1 ml of ^{16}O water so that further breakdown of ATP would yield unlabelled phosphate. Also, 28 nmoles of unlabelled phosphate (known as 'carrier Pi') were added to each sample to reduce losses of the sample during triethylation, before mass spectrometry.

4.2.6 Controls :

Immediately prior to each incubation a small quantity of solution (5µl) was removed from the incubation bath and reacted with dry PCl_5 (35µl of solution were laid out in each bath to start with). The phosphate produced in this way was analysed by mass spectrometry to determine the degree of contamination of the solution by ^{16}O water. This is known as the 'enrichment' control.

A control bath (which was not used for a muscle incubation) was checked at the end of the experiment for spontaneous hydrolysis of ATP.

4.3 RESULTS :

4.3.1 Mechanical Experiments :

The results of experiments to measure the stiffness of Vespa and Lethocerus muscle are shown in Figures 4.2 to 4.5. Both Lethocerus

and Vespa muscle has a rigor stiffness that is comparable to that of gluteraldehyde fixed muscle, being about 3-4 times larger than active isometric muscle (this is summarised in Table 4.2). Figures 4.4 and 4.5 demonstrate stiffness changes during the course of an active tension transient, the amplitude of the tension oscillations give an estimate of the dynamic stiffness during the course of the transient. The stiffness of the active fibres increases during the course of the delayed tension transient. The stiffness of a Lethocerus fibre, measured during a large amplitude sinusoidal length oscillation (Figure 4.6), was in-phase with the muscle tension (unfortunatly no Vespa fibres were available when this technique was used).

Solution :	Rigor	Active
	¦--- Relative stiffness ---¦	
Species:		
Lethocerus	100%	15.5%
Vespa	100%	28.4%

Table 4.2
Relative stiffness measurements in Lethocerus griseus and Vespa vulgaris (normalised to stiffness in Rigor). Values calculated from Figures 4.1 and 4.2.

4.3.2 Mechanical Performance During the Oxygen-Exchange Experiment :

Both the experiments on the activated and the relaxed fibres were repeated and similar patterns of oxygen exchange were obtained in the repeat experiments. It is inappropriate to average the patterns of exchange from different experiments, so data for the best experiment only are presented herein.

Figure 4.7 shows how the power output and work per cycle changes with oscillation frequency in flight muscle from the Vespa specimen used for this set of experiments. The frequency of maximum work was about 25-27 Hz and the maximum power output was obtained at 30-35 Hz.

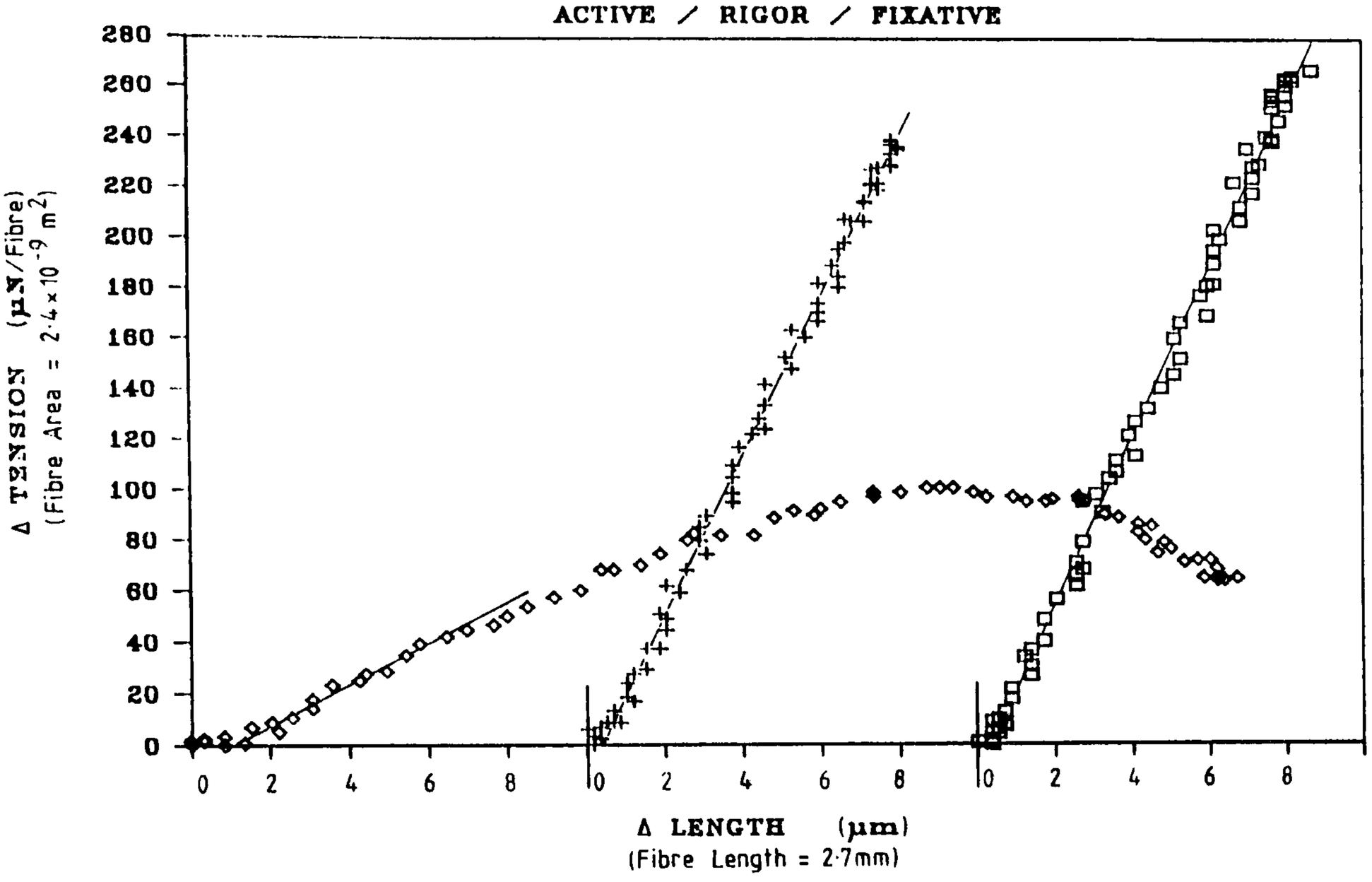

FIGURE 4.2

Instantaneous stiffness plots for L. griseus made in three different test solutions (active, rigor and glutaraldehyde fixative; from left to right, resp.). The stiffness in activating solution is only 15.5% of that in rigor or fixative. The stiffness in rigor is comparable to that in fixative.

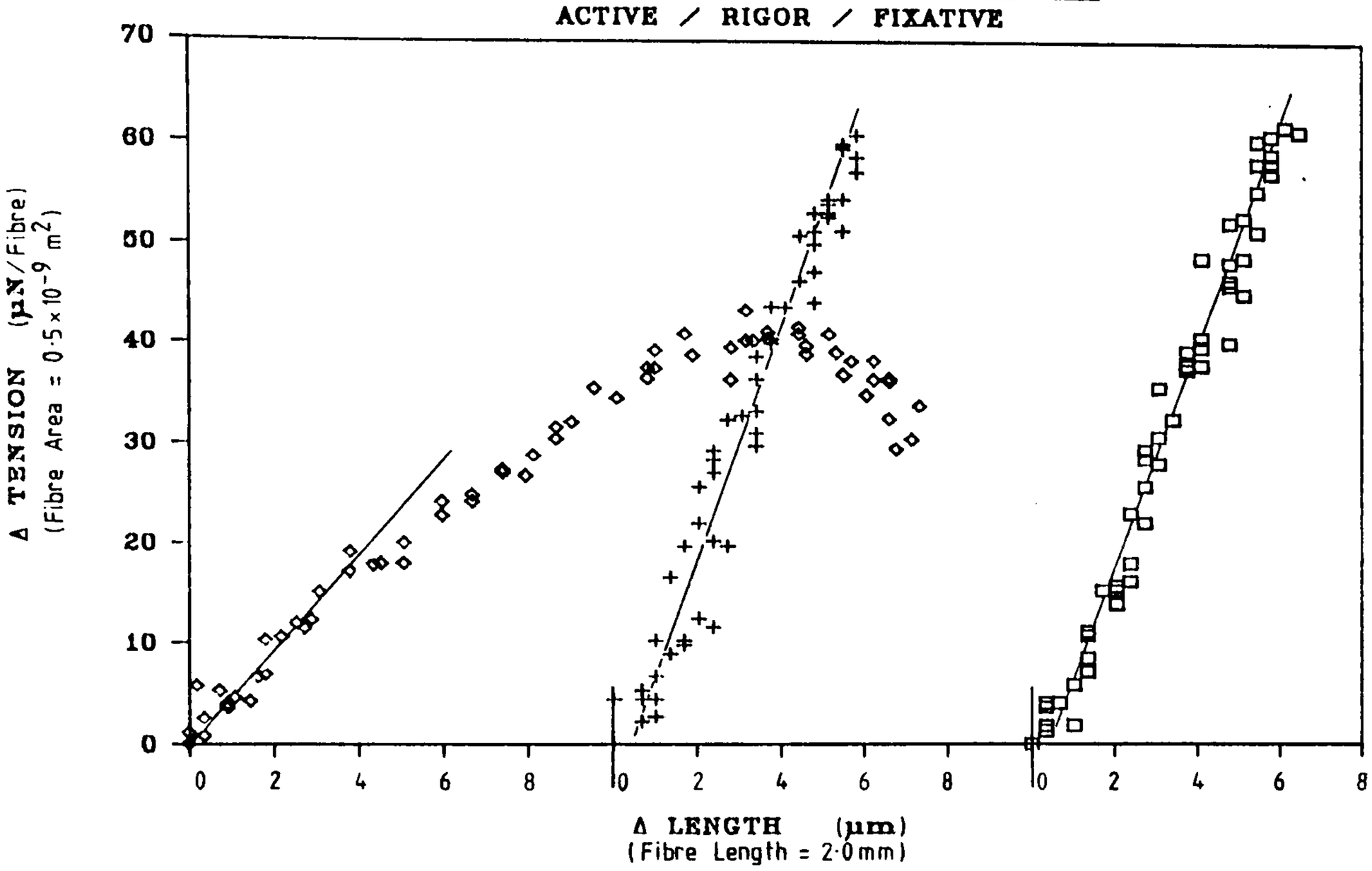

FIGURE 4.3

Instantaneous stiffness plots for V. vulgaris made in three different test solutions (active, rigor and glutaraldehyde fixative; from left to right, resp.) The stiffness in activating solution is 28.4% of that in either rigor or fixative. The stiffness in rigor is comparable to that measured in fixative.

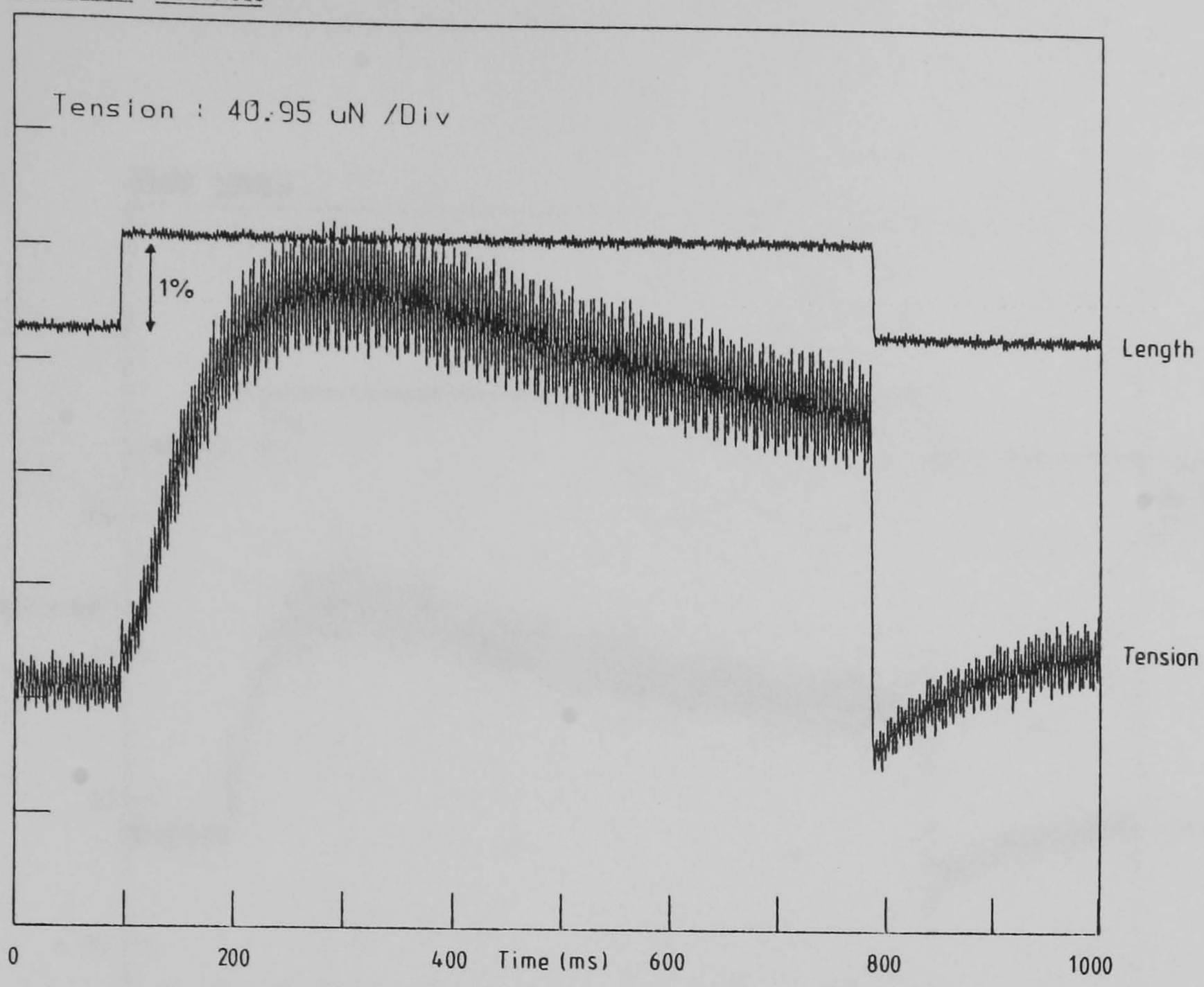

FIGURE 4.4

Dynamic stiffness measured in L.colossicus during the course of an active tension transient. A 0.15% length oscillation was superimposed on the length signal and the resulting tension oscillations are proportional to the dynamic stiffness.

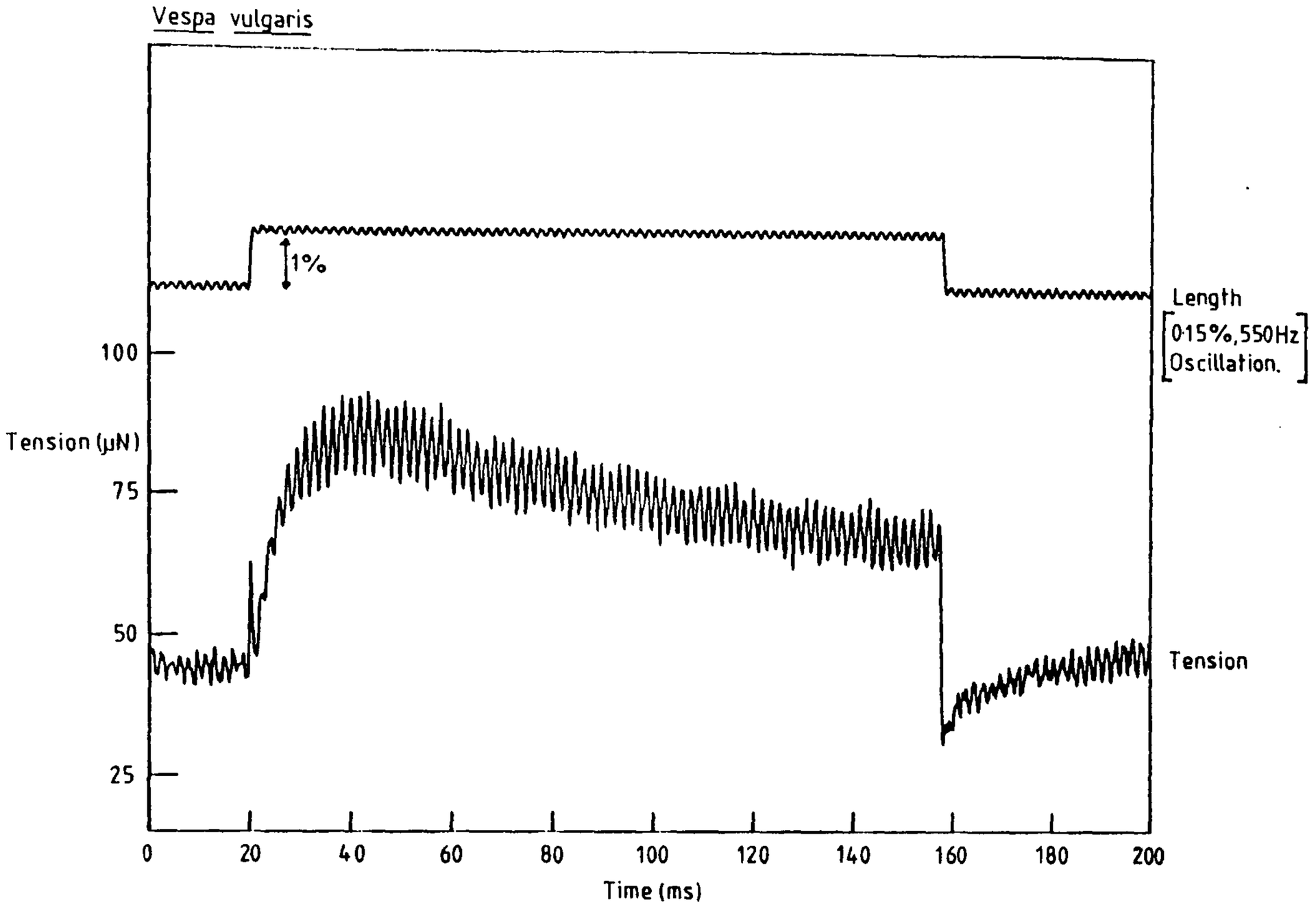

FIGURE 4.5

Dynamic stiffness measured in V. vulgaris during the course of an active tension transient. A 0.15% length oscillation was superimposed on the length signal and the resulting tension oscillations are proportional to the dynamic stiffness.

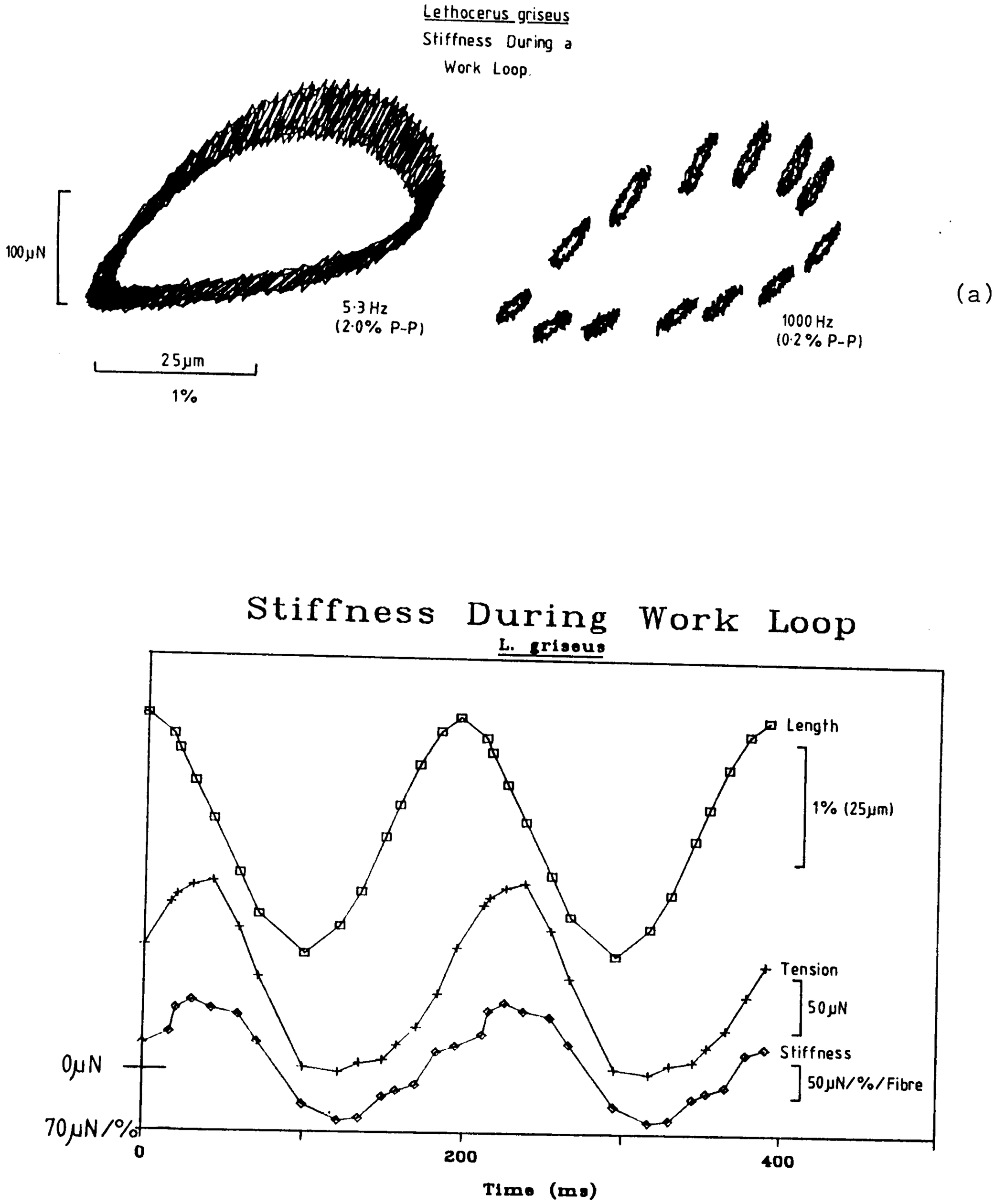

FIGURE 4.6

Changes in the dynamic stiffness of a single L. griseus fibre during the course of a work loop. A low amplitude, high frequency length oscillation was superimposed on the length signal and the high frequency loops were recorded on a fast oscilloscope timebase. The in-phase stiffness component was measured and is plotted in 4.6 b. The stiffness changes are in-phase with the tension changes.

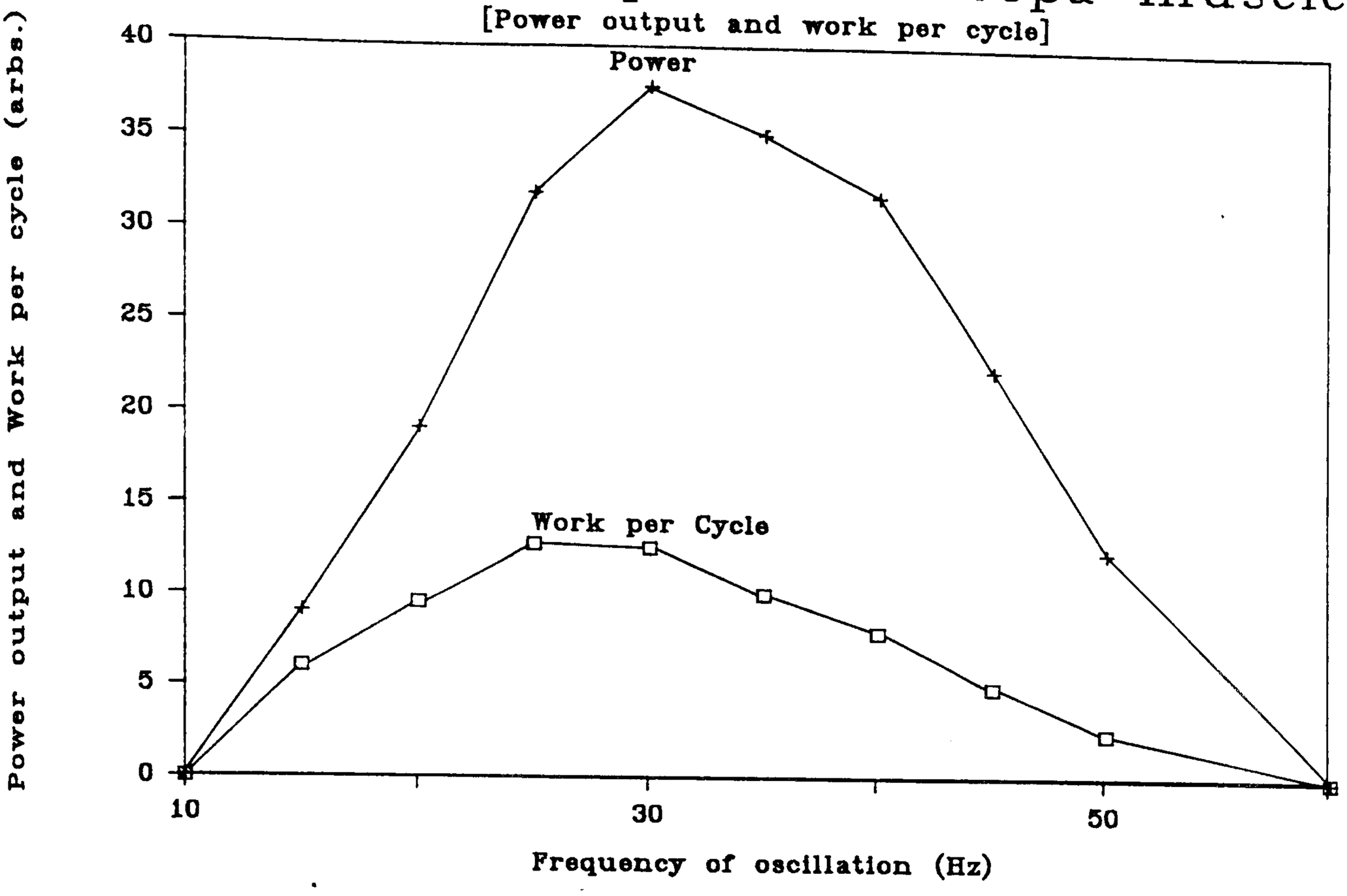

FIGURE 4.7

Work per cycle and power output calculated from length-tension diagrams produced by a single V. vulgaris muscle fibre oscillated at 3% peak-peak amplitude. The frequency at which the maximum work per cycle is obtained is about 27 Hz and the frequency for optimum power production is higher at about 30-35 Hz.

A work loop, recorded during the oxygen-exchange experiment is shown in Figure 4.8; the power output was slightly above average at 26 W/Kg (wet weight).

The response to a step length change is shown in Figure 4.9. The mechanical apparatus used for the ATPase measurements and the oxygen exchange experiment has long 'L' shaped hooks, and the ringing on the tension trace is unavoidable. The fitted rate constant to this trace gave a value of 226 s^{-1} for the delayed tension transient. Experiments performed later (on fibres from the same individual) on the faster mechanical apparatus gave rate constants between 150-170s^{-1} (mean 158s^{-1}).

The measured ATPase activity under the different incubation conditions are given in Table 4.3.

	Relaxed	Active			
		slack	isometric	oscillated	Power
Expt. 1		2.2 s^{-1}	12.4 s^{-1}	15.0 s^{-1}	26.4 W/Kg
Expt. 2	1.5 s^{-1}				

Table 4.3
ATPase activity and power output of Vespa vulgaris muscle fibres during the oxygen-exchange experiment.
ATPase acivities are moles ATP/mole S1/second).

4.3.3 Results of the Mass Spectrometry :

The distribution of 1,2,3 and 4 ^{18}O phosphates were corrected for isotopic impurity (as determined by the PCl_5 'enrichment' controls) and the peak heights were adjusted for contributions from neighbouring peaks. An example of these corrections (for Experiment 1, oscillated) is shown below (Table 4.4).

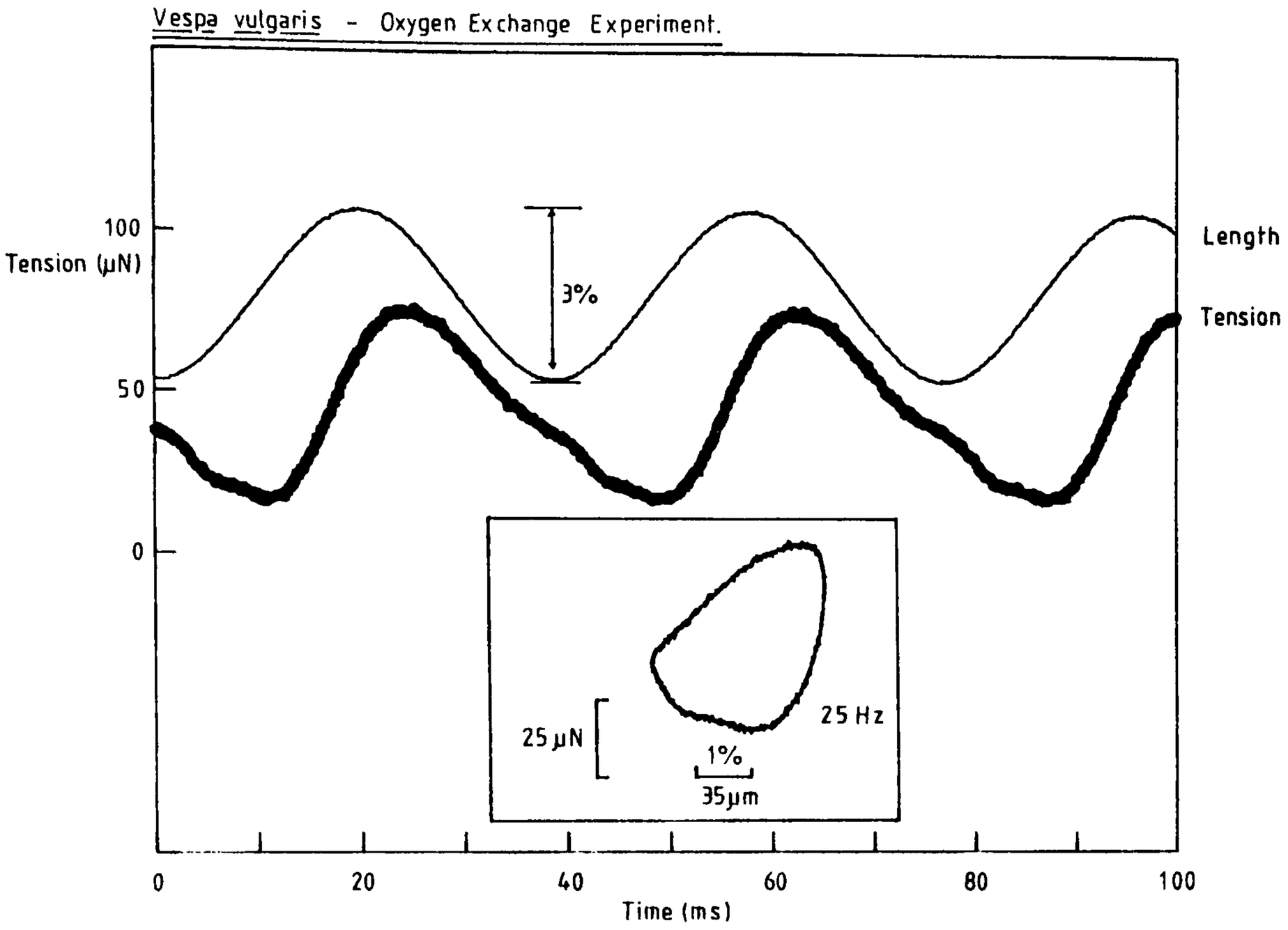

FIGURE 4.8

Power output of the muscle fibre used in the oxygen exchange experiment. The power output was slightly above average at 26 W/kg (compared to the mean result from Chapter 3 of 22W/kg).

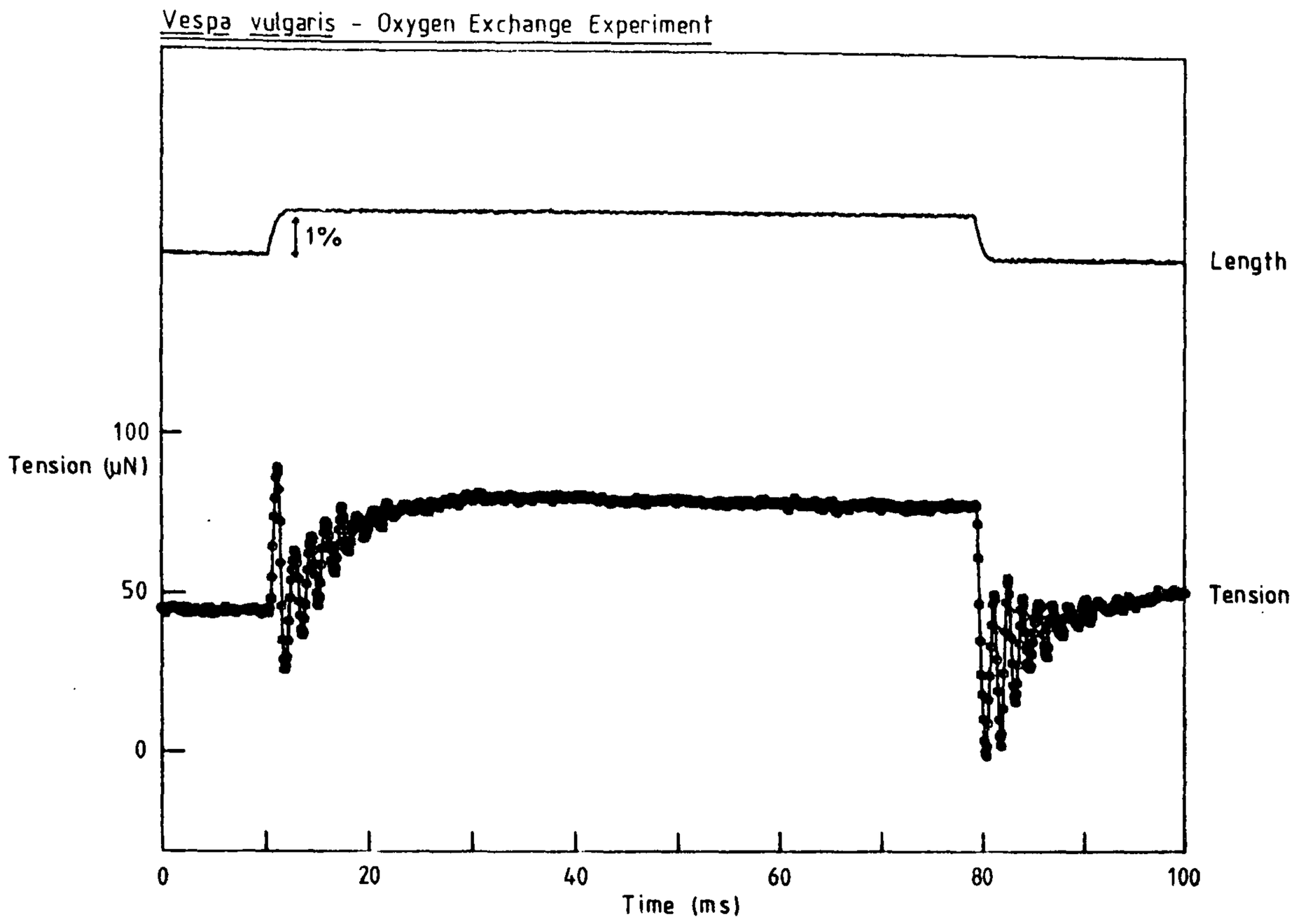

FIGURE 4.9

Transient tension response recorded during the oxygen exchange experiment. The tension oscillations occur because the long "L" shaped hooks used on this mechanical test apparatus were not critically damped. The fitted rate constant to the delayed tension transient was $226s^{-1}$.

TEP (mass spec. peaks)	153	155	F_1 157	F_2 159	F_3 161	F_4 163
Injection 1:	3.55	66.83	21.29	6.34	1.49	0.49
(corrected for)						
a) 153 fragment	0.06	69.21	22.07	6.59	1.54	0.52
b) water enrichment (94.59%)	0.06	67.97	22.55	7.09	1.68	0.64
c) 155 fragment (157 natural abundance)	0.19	0.00	21.93	7.09	1.68	0.64
New percentages	0.19	0.00	69.84	22.56	5.36	2.05
CORRECTED VALUES						
Injection 1:			69.84	22.56	5.36	2.05
Injection 2:			70.60	22.44	5.18	1.61
Injection 3:			70.44	22.64	5.11	1.62
MEAN			70.42	22.59	5.23	1.76
S.E.M.			0.23	0.06	0.07	0.15
4 * (S.E.M.)^2 [157 peak] = 0.21						
Best fit (at R = 1.81)			70.70	22.96	5.57	0.77
When X^2 = 1.32						

Table 4.4
Analysis of mass spectral data for Experiment 1. calcium activated, length oscillated.

Figure 4.10 shows the corrected results of the four different treatments (Oscillated, strained, slack and Relaxed) plotted as histograms. Using the equations of Section 4.2, the 'best fit' to a single value of R was calculated using a computer program to minimise the errors (written by Dr. M.R. Webb). When there was a poor fit to a single value of R (i.e. "relaxed" and "slack, active" data) the best fit produced by two values of R with independent contributions to the total flux were used to model the data. The errors in the fit and probable errors in the experimental data were assessed (see Section 4.3.3). Minimal fits that are compatible with the data are shown in Figure 4.10 ('Relaxed' data from Experiment 2, 'Active' data from Experiment 1). The calculated 'best fits' to the experimental data

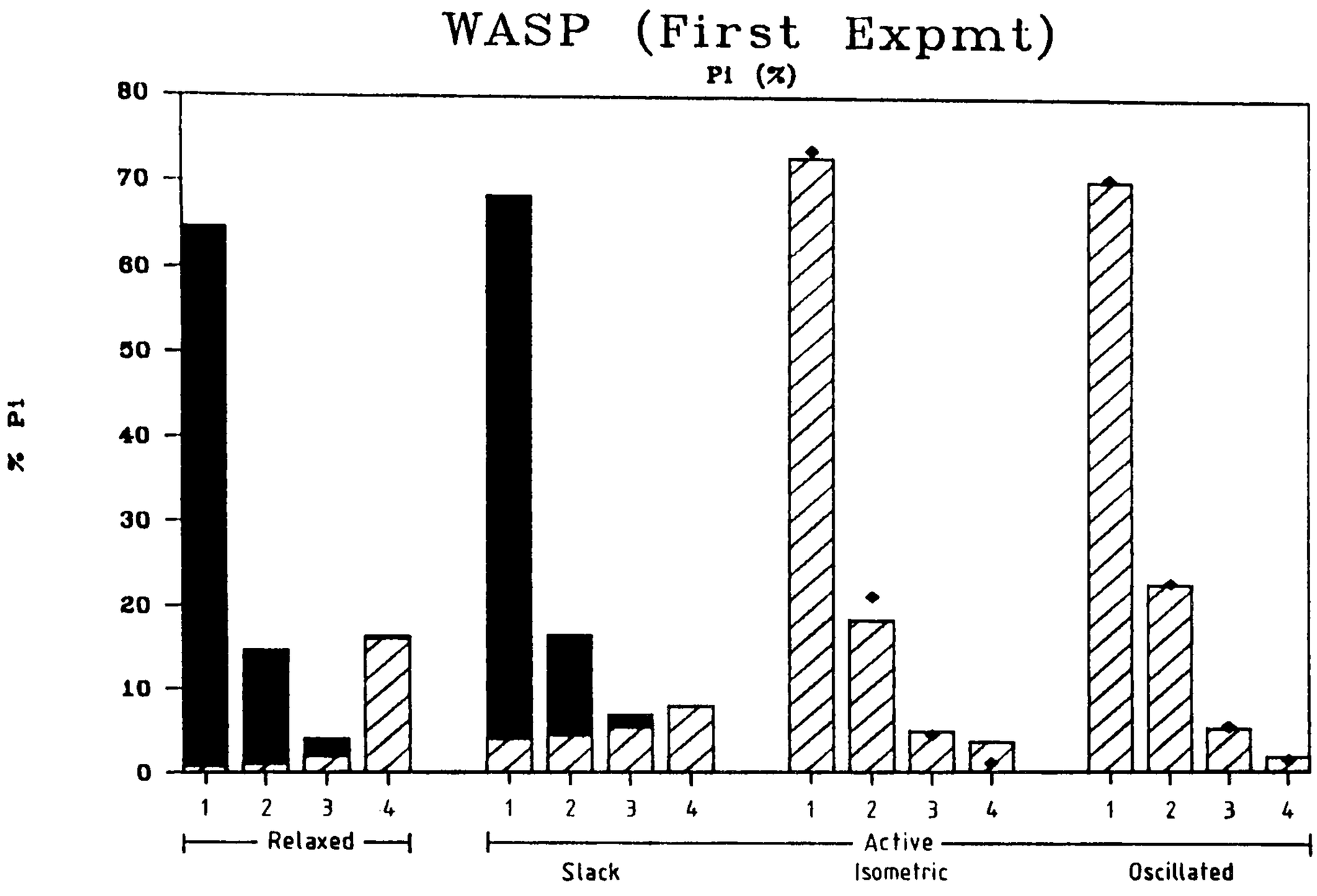

FIGURE 4.10

The pattern of oxygen-exchange obtained from V. vulgaris test when relaxed ($-Ca^{++}$), active ($+Ca^{++}$); slack, isometric, and length oscillated.

The relaxed and slack distributions can only be fitted by assuming two values of R with independent contributions to the total flux, while the distributions obtained from active,isometric and oscillated incubations are compatible with a single pathway for ATP hydrolysis. The fits to a single pathway are shown by the symbols (◆) in the figure.

The values of R and their contributions to the total flux are given below :

	R_1	Flux	R_2	Flux
RELAXED :	3.0	80%	0.03	20%
ACTIVE				
SLACK :	3.56	78%	0.17	22%
ISOMETRIC :	2.11	100%		
OSCILLATED :	1.8	100%		

are shown superimposed on each histogram. The values of R and the contribution to the total flux, for each fit is given in the legends to Figure 4.10.

4.4 DISCUSSION AND CONCLUSIONS :

4.4.1 Definition of 'R' in Terms of Rate Constants :

In the introduction to this chapter the derivation of the parameter R was defined in terms of two probabilites p and q. These probabilities can be mapped onto a full acto-myosin pathway to give R in terms of rate constants in the pathway. Scheme 4.2 gives the best current scheme for the biochemical cycle in intact insect muscle (White et al., 1987).

Scheme 4.2
(From White et al., 1987)

Part of the above scheme, relevent to oxygen exchange, is expanded below. The rapid isomerisation, step 5*, has been omitted for simplicity :

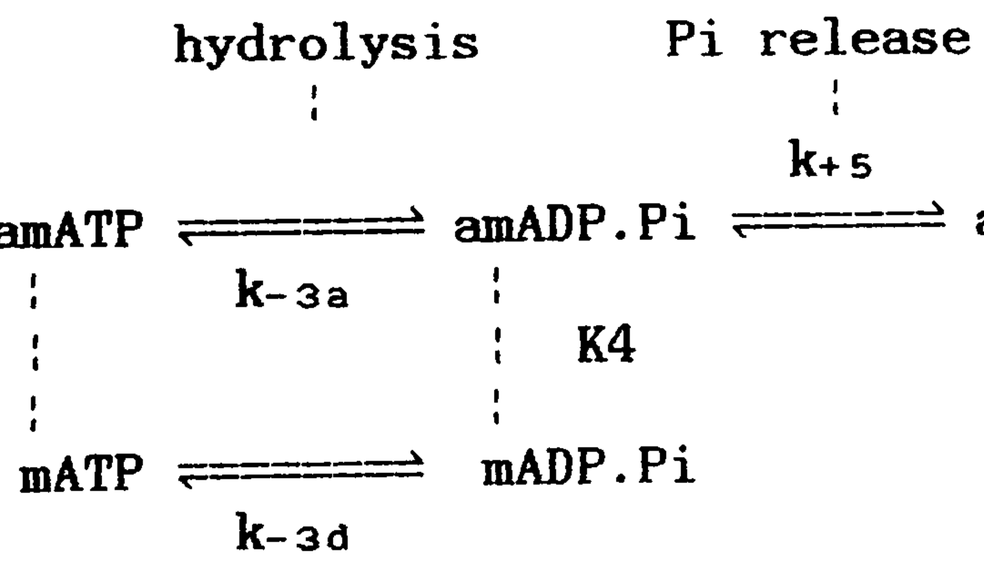

Part of Scheme 4.2

In the equations below, rate constants for step n are designated k_{+n} (forward) and k_{-n} (reverse), with an equilibrium constant K_n. Pseudo first-order rate constants are designated k'_{+n} and k'_{-n}.

Because the actin and myosin molecules are constrained in the filament lattice the concept of protein concentration becomes inappropriate. The rapid equilibrium (step 4) (Hibberd & Trentham, 1986; Schoenberg et al., 1984) can be stated in terms of the fraction of cross-bridges in each state. Here I have termed the proportion in state AM.ADP.Pi, (i) and the proportion in M.ADP.Pi, (j). The equilibrium constant K_4 = i/j, is dimensionless (a ratio).

The probability 'p' of phosphate release is given by the pseudo first order rate constant $k'_{+5} = k_{+5} * i$. The probability 'q' of the reversal of the hydrolysis step may occur via two different routes either with the myosin bound to an actin (subscript 'a' for attached) or on a myosin molecule which is not attached to an actin molecule (subscript 'd' for detached); $k'_{-3a} = k_{-3a} * i$, $k'_{-3d} = k_{-3d} * j$.

The ratio, R, of probabilities for reverse hydrolysis and phosphate release can be stated in terms of rate constants in the biochemical scheme (Scheme 4.2):

$$R = p/q = k'_{+5}/(k'_{-3a} + k'_{-3d}) \quad \text{..... 4.2}$$

or

$$R = k_{+5} * i /((k_{-3a} * i) + (k_{-3d} * j)) \quad \text{..... 4.3}$$

Dividing Equation 4.3 by i we have :

$$R = k_{+5}/(k_{-3a}+(k_{-3d}/K_4)) \quad \text{.....4.4}$$

Rosenfeld and Taylor (1984) found that reversal of the hydrolysis step (k_{-3}) on the myosin head is not altered by the presence of actin. In other words $k_{-3a} \simeq k_{-3d}$, equation 4 is simplified by using a single term k_{-3} to designate reversal of the hydrolysis step :

$$R = k_{+5}/(k_{-3}(1+1/K_4)) \quad \text{..... 4.5}$$

The pseudo first order rate constant k'_{+5} for phosphate release

is given below :

$$k'_{+5} = k_{+5} * K_4/(1+K_4) \quad \text{..... 4.6}$$

Therefore (from Equation 4.5) :

$$k'_{+5} = R * k_{-3} \quad \text{..... 4.7}$$

The value of k_{-3} has been determined in both insect and vertebrate muscle (White et al., 1986; Webb & Trentham, 1981; Rosenfeld & Taylor, 1984). The results for Lethocerus are similar to rabbit; $k_{-3} > 10s^{-1}$ and $15s^{-1}$ (resp.). In the following discussion it is assumed that $k_{-3a} = k_{-3d} = 10\ s^{-1}$ for Vespa.

The number of attached cross-bridges in active insect fibrillar muscle has been estimated at between 10-20% (Abbott, 1972; Pybus & Tregear, 1972; Armitage et al., 1972). The method used in this chapter was to measure the stiffness of skinned muscle fibres. Previous estimates indicate that about 70% of the cross-bridges are attached in rigor (Lovell et al., 1981, Offer & Elliot, 1978 and Kyrtatas, 1987). Using this value the stiffness measurements in Table 4.2 indicate that the proportion attached in activating solution is 19% for Vespa muscle, under isometric conditions. Assuming ~~Given~~ that the equilibrium constant for the hydrolysis step (step 3) in skinned fibres is from 5 to 10 (Webb et al., 1986) the myosin-products state will predominate. This means that K_4 must be < 0.19 for Vespa; I have taken a value of 0.1 for simplicity.

There are two steps in the interpretation of the oxygen exchange data. Firstly, the pattern of exchange is fitted using a value for R that gives the best fit to the distribution. Sometimes a single value of R is not sufficient to model the data and it is necessary to fit the distribution assuming that there are two values for R (two different pathways) with relative contributions to the total flux.

Secondly, modifications to the simple biochemical scheme (Scheme 4.2) may be necessary to explain the existence of more than a single pathway for oxygen exchange.

4.5 FITTING THE DISTRIBUTION OF LABEL :

4.5.1 Simple Pathways :

The best fit to the distribution of label will usually be made by assuming two values of R with different relative contributions to the total phosphate 'pool' (collected product). Theoretical fits are consistent with the data when the error in the fit is less than the errors in the experimental procedure. Errors in estimation of the mass spectrometry peaks were estimated by comparing the results from 3 injections. Hibberd *et al.*, (1985) suggest that the sums of squares of error for the fitted distribution should be less than four times (for each of the 4 peaks) the square of the largest S.E.M. for the injections (see Table 4.4). However, this procedure takes no account of other systematic errors in the experimental procedure (e.g. errors in the 'enrichment' estimate), and is the most rigorous test.

Errors in the 'enrichment' estimate have their largest effect in the 161 and 163 peak adjustments. The estimate of the integral peak area for very small peaks is very dependent upon the baseline estimate for the spectrum. Given these additional sources of error, the data of Table 4.4 can be said to be consistent with a single value for R. In other words, Scheme 4.2 is sufficient to describe the oxygen exchange activity of the maximally activated *Vespa* fibres in Experiment 1.

4.5.2 Complex Pathways :

In order to fit 'U' shaped distributions (eg. the relaxed and

slack activated data presented in Figure 4.10) a minimum of two pathways are required. There are two explanations for why a single value of R is insufficient to describe the data :

1) There are two distinct populations of myosin with different kinetics for oxygen exchange, either :

a) Some myosin may behave in an aberrant fashion due to loss of regulatory proteins (incomplete inactivation at low ca^{++}).

b) Slack activated insect fibrillar muscle may suffer from thick filament end-effects, caused either by thin filaments overlap or by thick filaments penetrating the 'Z' line (Zebe et al., 1968; Lund et al., 1987).

2) There is a Gaussian distribution of rate constants on the attached pathway caused by a range of distortions of attached cross-bridges (Hibberd et al., 1985). The rate constants controlling phosphate release could be distortion dependent, producing a whole range of R values (which are well ~~fit~~ fitted by two theoretical values of R with different contributions to the total flux).

Using the criteria of Section 4.5.1, all of the data from these experiments are compatible with two values of R, with relative contributions to the total flux.

4.6 MODELLING THE 'R' VALUES :

4.6.1 Relaxed Vespa Fibrillar Muscle :

The pattern of exchange showed a "U" shaped distribution which can not be ~~fit~~ fitted by any single value of R (see Figure 4.1). Good fits to the data are achieved by assuming two values of R with independent

contributions to the total phosphate product :

R E L A X E D M U S C L E		
	Low exchange pathway	High exchange pathway
R	3.0	0.03
Flux	80%	20%
Apparent rate constant for phosphate release (if $k_{-3} = 10s^{-1}$)	$30s^{-1}$	$0{\cdot}3s^{-1}$

It seems likely that the low-exchange pathway in relaxed muscle fibres arises from 'damaged' (Ca^{++}, unregulated) myosin heads. The rapid apparent rate constant for phosphate release on the low-exchange pathway is typical of facilitation of product release by myosin binding to actin.

It is thought that steps controlling phosphate release may contribute to rate-limitation in the cross-bridge cycle (Lund et al., 1987, 1988). Because phosphate release is 100 times faster for the low-exchange pathway the number of myosin molecules needed to contribute 80% of the flux is actually rather small, about 4% of the total amount of myosin. The measured ATPase activity of this 'relaxed' preparation is much higher than would be expected from the oxygen consumption of live insects (Kyrtatas, 1987). This observation is reconciled by attributing 80% of this activity to a minority population of aberrant myosin molecules.

4.6.2 Slack Activated Vespa Fibrillar Muscle :

The poor fits to a single pathway for slack activated muscle

fibres are difficult to assess. The experimentally determined, best fit, dual values of R and their relative contributions to the phosphate pool were :

SLACK MUSCLE		
	Low exchange pathway	High exchange pathway
R	3.56	0.17
Flux	78%	22%

The muscle fibres were allowed to shorten until no tension was developed, shortening to 80% of rest length. The structure of the sarcomere in these 'super-contracted' fibres becomes disorganised (Zebe et al., 1968). Any explanations of the observed pattern of oxygen exchange are very speculative, and of little value. I have attempted to model these 'U' shaped distributions in terms of multiple pathways (assuming that there is an even distribution of cross-bridge distortions, similar to the models for active vertebrate muscle (Webb et al., 1986)). Figure 4.11 is a flow diagram showing how the distribution of label in the phosphate pool was determined. Like the model for vertebrate muscle, the rate constants controlling phosphate release are dependent upon distortion. There are two important features of the model presented here; the equilibrium constant K_4 depends upon the distortion of the myosin head from its preferred attachment site (Hill, 1974), and the flux through a given pathway depends upon the rate-limiting step for that pathway. A point to notice is that in both the model used here and that of Webb et al. (1986) the forward rate constant, K_{+5} is made to be distortion independent, while k_{-5} is independent of distortion (this is vital to

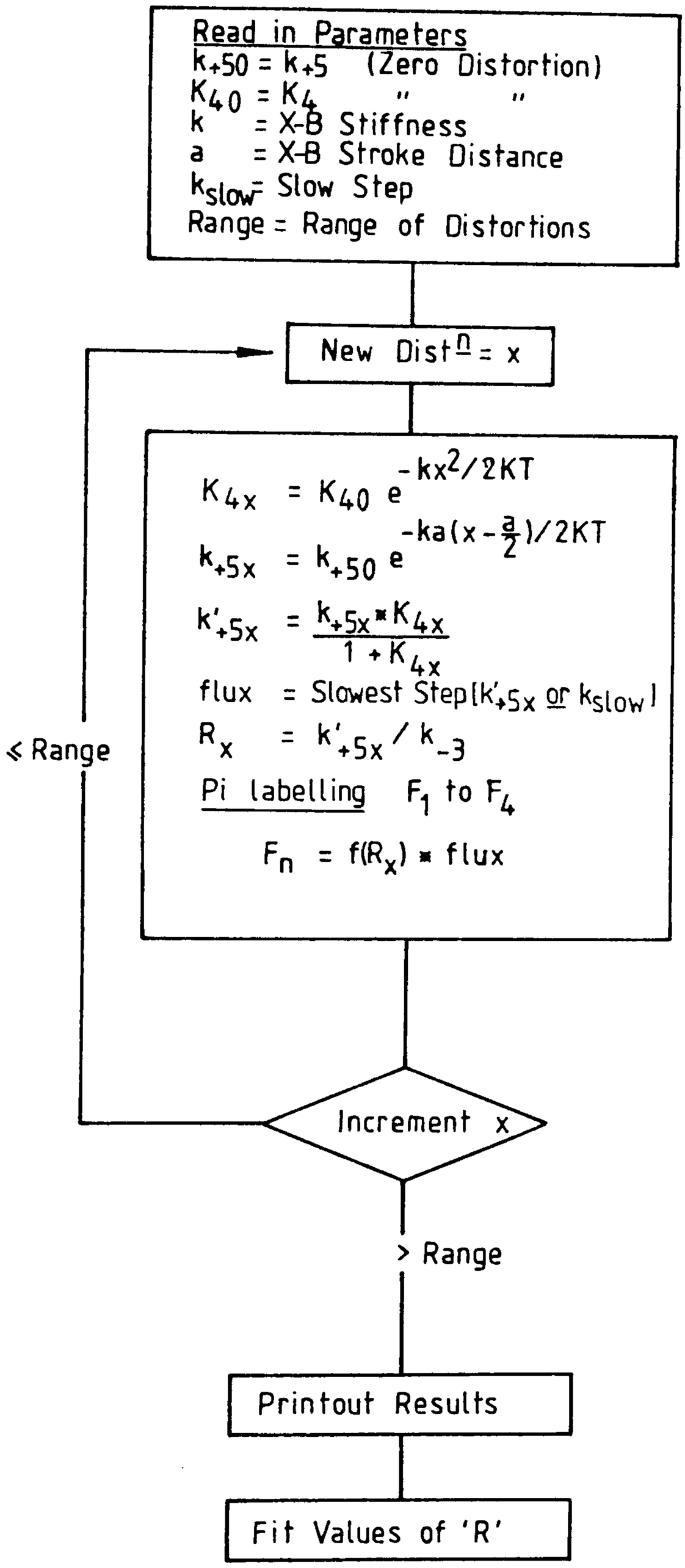

FIGURE 4.11

Flow diagram showing how the computer model worked to calculate the distribution of label in the product phosphate pool. It is assumed that both the rate constant k_{+5} and the equilibrium constant K_4 are distortion dependent. The flux through each pathway (each value of distortion) is determined by the slowest step on that pathway either k_{slow} or k'_{+5}.

produce the range of R values). The model of Huxley and Simmons (1971) contains precisely the opposite assumptions about distortion dependency to account for results from rapid mechanical experiments (Chapter 1, Section 1.3). I have been unable to produce the 'U' shaped distributions, typical of slack muscle fibres, with this type of model. The problem being that the low value for K_4 in insect fibrillar muscle means that there is insufficient flux from bridges with high distortions (with a small value for K_{+5} and high oxygen-exchange). This is perhaps circumstantial evidence that like the relaxed muscle there is a ~~truely~~ bimodal population of myosin molecules with different kinetics for ATP hydrolysis, up to phosphate release.

4.6..3 Isometric Vespa Fibrillar Muscle :

Calcium activation and strain activation of insect fibrillar flight muscle causes a parallel rise in muscle tension and stiffness (Figures 4.1-4.6 and White et al., 1979). The simple explanation is that there is an increase in the number of attached cross-bridges during activation. This could arise because of an increase in the equilibrium constant K_4. The change in value of K_4 will have a direct effect on the oxygen exchange pattern (Equation 4.5). The value of R should increase upon calcium activation. The value of R in well regulated myosin is 0.03 (see above) and upon calcium activation in the isometric state this value rises to about 2.1. The change in ATPase activity (phosphate flux) of these bridges changes from $0.3s^{-1}$ to over $12s^{-1}$.

In relaxed fibres the calculated apparent rate constant for phosphate release = $0.3s^{-1}$ and in calcium activated fibres = $21s^{-1}$ (see Equation 4.7). Values of $R > 1.5$ give rather similar looking distributions of label. So, there is a fair correlation between the

apparent rate constant for phosphate release and the rate-limiting step in the cycle. This implies that for both a 'myosin only' pathway (relaxed muscle) and a full actomyosin pathway (calcium activated muscle, Scheme 4.3) the steps controlling phosphate release are rate-limiting for the cross-bridge cycle.

4.6.4 Fully Oscillation Activated Vespa Fibrillar Muscle :

The pattern of oxygen exchange produced by oscillation activated Vespa fibres is easily compatible with a single value of R. The errors in the fit are within the errors of the experimental techniques. In Experiment 1 the best fit value for R = 1.8, accounts for 100% of the flux eg. $15.8s^{-1}$ (the ATPase activity of the fibre). As before we can estimate the apparent rate constant for phosphate release k'_{+5} (from Equation 4.7). The calculated value for k'_{+5} = $18s^{-1}$ which, like the relaxed and isometric calcium activated fibres, is close to the measured ATPase activity of the fibre.

The observed single value of R implies that the rate constants controlling the release of phosphate from actomyosin (k'_{+5}) must be the same in all cross-bridges. If rate constants on the part of the pathway probed by oxygen exchange are distortion dependent then a single value of R can arise only if the distortion of all the bridges is uniform. At first sight this seems consistent with Wray's (1979) idea that cross-bridges are in good register with potential actin binding sites in fully activated insect muscle fibres. However, closer inspection of Wray's (1979) diagram (Figure 1.6) shows that he has allowed cross-bridges to "reach" about 10nm (the size of the open circles on his diagram). This is approximately the same size as the cross-bridge working stroke (Huxley & Simmons, 1971). Further, a large proportion of the cross-bridges (i.e. about half) are completely

Pagination Error: There is no page 141

out of reach of actin sites. The dilemma here is that a distortion of 10nm must require a large amount of energy (otherwise the cross-bridge working stroke would do no significant amount of mechanical work).

There are two possible solutions :

1) Unlike vertebrate muscle, steps controlling phosphate release are independent of distortion in insect flight muscle i.e. all actomyosin products states are weakly bound.

2) The Wray (1979) diagram must be modified to be consistent with the oxygen-exchange data of both Vespa and Lethocerus.

There is a simple modification that can be made to Wray's diagram: It is reasonable to suppose that force produced by the cross-bridge working stroke acts axially therefore the cross-bridge must be constrained in this direction. If the LMM-HMM "hinge", which allows free azimuthal movement, behaved as a "ball-and-socket" joint (Mendelson et al., 1973) then cross-bridges could swivel, freely, in an arc. This, more restricted, range of movement would be represented as a semi-circle on Wray's diagram. We could take the upper half of the circle on his original diagram to designate this more limited range of movement. Even with this modification, half of the cross-bridges are still out-of-reach of an available actin site. These cross-bridges would be "silent" with respect to oxygen-exchange, but an adjustment should be made to the "active site" estimation.

The rate constant for delayed tension generation in Vespa is about 160 s^{-1}. Since this rate constant is very much faster than the rate-limiting step (and k'_{+5}), the first tension generating step must come before phosphate release (step 5* in Scheme 4.3). The rate constant for tension generation, following a step length change, will be an apparent rate constant given below :

$$k'_{+5*} = \frac{(k_{+5*}+k_{-5*}) * K_4}{(1 + K_4)}$$

If significant tension is to be generated then $k_{+5*} >> k_{-5*}$ and k_{+5*} will be a rapid isomerisation with a rate constant $\simeq$ 700 s^{-1}. In Lethocerus this rate constant will be about 5-10 times slower.

The novel property of insect fibrillar flight muscle is its ability to perform efficient oscillatory work. Assuming-42 KJ/mole ATP (Kushmeric, 1983), the chemo-mechanical efficiency of Experiment 1 was 22%. As stated in Chapter 3 the frequency at which the maximum work is obtained from the muscle depends upon the rate constant for the delayed tension process. In order for efficient work to be performed at this frequency the rate constant for the tension generating step should be similar for all cross-bridges (Tregear, 1967). This prediction is supported by the observed single pathway for oxygen exchange found in both fully activated Lethocerus (Lund et al., 1987, 1988) and Vespa muscle.

In contrast to insect flight muscle, the axial repeat distances of the thick and thin filaments in vertebrate muscle have a vernier relationship. Because of this there is always a range of cross-bridge distortions within the vertebrate sarcomere. Figure 4.12 shows the pattern of oxygen exchange for vertebrate muscle compared to Lethocerus and Vespa. As expected the fully activated vertebrate muscle has a pattern of oxygen exchange typical of complex pathways for ATP hydrolysis. Data from both of the insects is consistent with a single pathway for ATP hydrolysis.

The number of cross-bridges attached in activated vertebrate muscle is close to the number attached in rigor (thought to be near

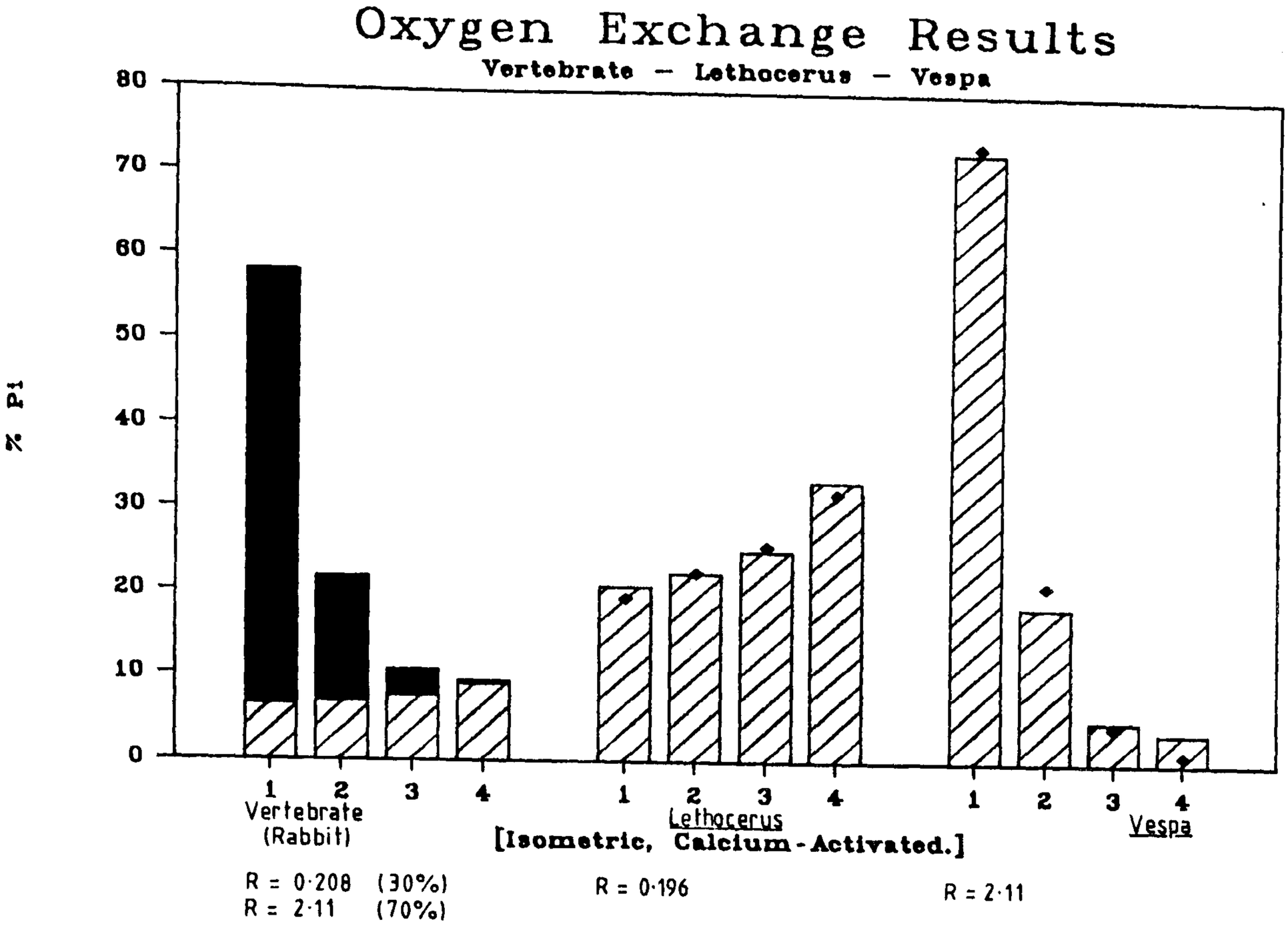

FIGURE 4.12

The pattern of oxygen exchange measured in vertebrate skeletal muscle and flight msucle from two species of insect with fibrillar flight muscle. The pattern of exchange in vertebrate muscle is typical of multiple pathways of exchange while that in insect flight muscle can be modelled assuming a single pathway for ATP hydrolysis.

The rate constant for the reverse hydrolysis steps is similar in all three muscle types. There is a range of values for the apparent rate constant for phosphate release in vertebrate muscle and a single value in insect flight muscle, being about ten times faster in Vespa than Lethocerus.
The symbols (◆) represent the fits to the data whilst the shaded and stripped portions of the distribution for vertebrate muscle are the result of a minimum of two values of R with separate contributions to the total flux.

90%). Figure 4.13 shows the parameters required to model the oxygen exchange data of Webb et al., 1986, using the model of Figure 4.11 (similar to the model proposed by Webb et al., 1986). The cross-bridges that generate the most force in the sarcomere (the most distorted bridges) have the smallest value of R (highest exchange). The flux for these, main tension generating, cross-bridges is limited again by the steps controlling phosphate release (k'_{+5}).

In summary :

1) The matching axial repeat distance in the thick and thin filaments in insect fibrillar flight muscle lead to a homogeneous pattern of oxygen exchange. The vernier relationship in the axial repeat distance in vertebrate muscle produces a complex pattern of oxygen exchange.

2) The small value of K_4 in insect flight muscle, means that the value of the term $K_4/1+K_4$ (Equation 6) will be modulated by the degree of cross-bridge distortion. The effect of negative feedback (White et al., 1986), between sarcomeres within the myofibril is to make cross-bridge distortion proportional to muscle tension.

3) The value of K4 in vertebrate muscle is much larger than insect flight muscle. The effect of distortion upon K4 expresses less effect upon the kinetics of other steps in the cross-bridge cycle.

4) For both insect and vertebrate muscle the steps controlling phosphate release can be rate-limiting for the cross-bridge cycle.

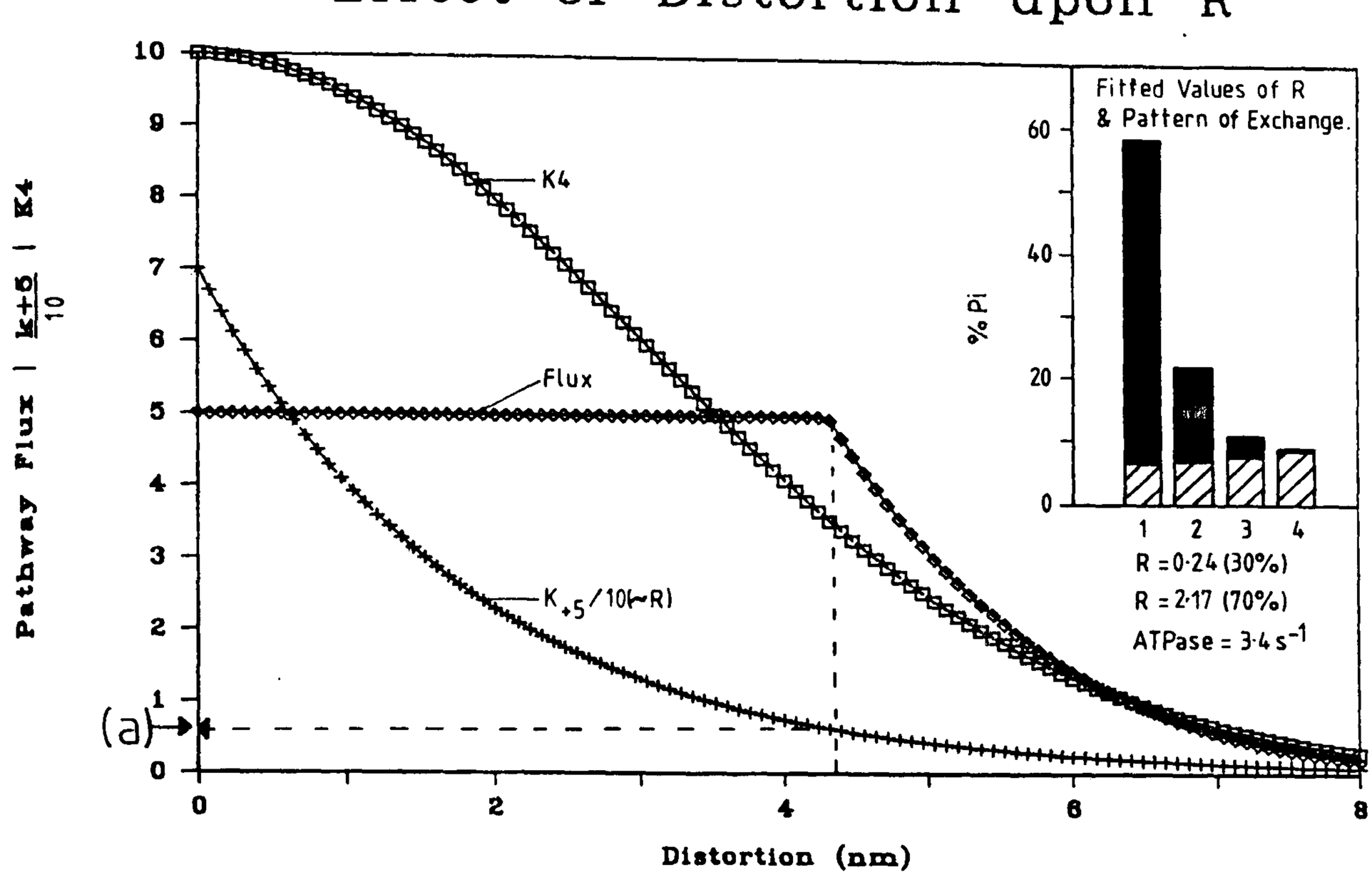

FIGURE 4.13

Graph showing the variation in the values of K_4, k_{+5} and the flux with cross-bridge distortion. The cross-bridge stiffness was assumed to be 2.5×10^{-4} N/m.

At the point (a) on the graph the value $k_{+5} \times K_4/(1+K_4)$ (i.e. k'_{+5}) becomes the slowest step in the cross-bridge cycle (and is therefore rate-limiting).

The pattern of oxygen exchange produced by this model is shown inset and agrees closely with the findings for vertebrate muscle (based on the model of Webb et al., 1986).

The point to notice here is that for the most highly distorted bridges (those that generate the most force) k'_{+5} is rate-limiting for the cross-bridge cycle.

Because the value of K_4 is large in vertebrate muscle the line showing the variation in$(k_{+5}/10)$ is very nearly the same as that for the change in R.

CHAPTER 5 :
STRATEGIES TO OPTIMISE THE FLIGHT MUSCLE PERFORMANCE IN INSECTS OF DIFFERENT SIZES

STRATEGIES TO OPTIMISE THE FLIGHT MUSCLE PERFORMANCE IN INSECTS OF DIFFERENT SIZES.

5.1 INTRODUCTION :

The main constraint on the design of the insect flight 'motor' is that its power output per unit weight (or specific power output) should be as high as possible at the working frequency. Additionally, for an insect to fly for a reasonable length of time, the power output of the contractile proteins must be matched by the supply of ATP from the mitochondria (Weis-Fogh & Alexander, 1977, Pennycuick & Rezende, 1984). In this chapter I have investigated the 'power density' of the mitochondria by measuring the total amount of the respiratory pigment cytochrome c in the muscles of different insects. If the power output of the flight muscle is limited by the supply of ATP then the amount of respiratory pigment should reflect the specific power output of the muscle. Also, if the ATP supply is limiting then the chemo-mechanical efficiency will have a strong effect upon the power output (Ellington, 1985). The chemo-mechanical efficiency was measured directly in several different species of insect.

The power output of the flight muscle depends not only on the intrinsic properties of the contractile proteins and mitochondria, but also the total amount of muscle present and its operating temperature. These two parameters were also investigated.

One conclusion of Chapter 3 was that the rate constant of the tension generating step in the cross-bridge cycle is faster in insects with a high wingbeat frequency. Ruegg (1968) observed that the velocity of muscle shortening, for a given overall length of muscle, will depend upon the sarcomere length. Short sarcomeres, connected in series, have a faster shortening speed than a single sarcomere of the

same length. This chapter investigates whether insects with high wingbeat frequencies exploit this principle as well as having cross-bridges that produce tension more rapidly.

5.2 RESULTS :

5.2.1 The Proportion of Cytochrome c Present in Different Muscles :

Cytochrome c is unusual amongst the respiratory pigments in that it is only loosely bound to the membrane and is extracted easily by hypertonic salt solutions (Estabrook & Pullman, 1967). The amino acid sequence and molecular weight of cytochrome c extracted from moth flight muscle has been determined; both were very similar to that found for vertebrate muscle (Chan & Margoliash, 1965). The simple spectrophotometric assay for cytochrome c used in this study gave reproducible results. The amount of cytochrome c measured in various muscles is shown in Table 5.1. Insect indirect flight muscle (IFM) contains from 3 to 10 times as much cytochrome c as vertebrate heart and skeletal muscle. There is no significant correlation between the amount of cytochrome c and the insect size or wingbeat frequency (see legend to Table 5.1). Levenbook and Williams (1955) found that the amount of cytochrome c in the thoracic muscles of young blowflies was correlated both with age and wingbeat frequency. The blowflies tested here were reared from culture and were 2-3 days old. The age of the other, wild, insects is not known.

5.2.2 Flight Muscle as a Proportion of Body Mass :

Table 5.2 shows the proportion of IFM, per total body mass, measured in a variety of insects. IFM as a proportion of body weight is relatively constant between individuals of the same species but varies over a wide range between species. The proportion of IFM does

<WBF> Species	Cytochrome c g/kg (wet weight muscle)	Reference
Vertebrata:		
Horse heart	0.16	Drabkin 1950
Horse skeletal	0.06	Drabkin 1950
Rat heart	0.45	Drabkin 1950
Rat skeletal	0.1	Drabkin 1950
Insecta:		
Lepidoptera		
Samia cynthia (silk-worm moth)	0.6	Chan & Margoliash 1965 Thorax = 50% muscle
Dictyoptera		
<35>Periplaneta americana (cockroach)	0.86	Baron & Tahmisian 1948 (muscle = 28% dry weight Levenbook & Williams 1956)
Hymenoptera		
<97>Vespa vulgaris (common wasp)	1.34±0.07	This study.
<150>Bombus terrestris	1.04±0.06	This study.
<150>B. pratorum (bumble bees)	0.88	
<154>Apis mellifera (honeybee)	1.31±0.14	This study.
<160>Andrena spp. (mining bee)	1.08±0.08	This study.
Hemiptera		
Lethocerus <44>griseus (giant waterbug)	0.63±0.07	This study.
Diptera		
<47>Tipula spp. (cranefly)	0.93	This study.
<120>Calliphora erythrocephala	0.76±0.03	This study.
<145>Phormia regina (blowflies)	0.76	Levenbook & Williams, 1956 (Value for 2 day old flies)
<165>Episyrphus balteatus (hoverfly)	0.90±0.2	This study.

Table 5.1
Concentration of cytochrome c present in various muscle tissues.

Species		Body mass (mg)	IFM mass (mg)	% muscle
Hemiptera				
L. griseus				
		5870	779.6	13.3
		5150	536.4	10.4
		4670	481.0	10.3
		4386	425.0	9.7
		4470	473.8	10.6
L. colossicus & *L. indicus*	{Yield from myofibril preparations} IFM = 8%-12% of body mass			
		11000 - 13200	-	10
Hymenoptera				
B. terrestris				
	Q	644.1	125.7	19.5
	Q	670.6	129.2	19.3
	Q	580.7	126.4	21.8*
	Q	651.0	126.4	19.4*
B. pratorum				
	Q	276.2	53.5	19.4
	Q	240.4	53.0	22.1
V. vulgaris				
	Q	230.0	24.0	10.4
	Q	221.6	20.4	9.2
	Q	335.2	37.1	11.1
	W	182.1	23.7	13.0
Andrena Spp.				
	F	92.0	14.2	15.4
	F	79.8	11.2	14.1
	F	85.8	11.7	13.6
	F	79.8	11.3	14.2
	F	98.5	14.0	14.2
	F	76.9	11.4	14.8
A. mellifera				
	W	87.1	16.3	18.7
	W	93.2	16.0	17.2
	W	97.5	16.3	16.7
	W	91.6	15.6	17.0
Diptera				
C. erythrocephala				
	{masses are mean of 3 individuals for each estimate}			
		61.6	11.5	18.7
		69.3	15.4	22.3
		44.4	8.2	18.6
		56.7	10.9	19.2

*Same insect before and after 48 hours feeding on 30% sugar/water.

Table 5.2
Whole insect and IFM muscle mass.

not correlate with wingbeat frequency or insect order.

Greenewalt (1962) collected data of the body mass and flight muscle mass for a variety of flying animals. He noted that the scatter in the data for birds was extremely small. The pectoral muscle accounted for close to 15.5% of the body mass in all of the birds tested (with the exception of humming birds; 25%). The scatter in Greenewalt's data for insects was very much greater. The range of values was from 5% to nearly 30%, but again with an average of about 15%. From the data presented by Greenewalt it was not possible to tell if the variation within a given species was as great as that between species. This is because many values were quoted for just a single individual.

5.2.3 The Maximum Power Output of Skinned Muscle Fibres :

The power output of insect flight muscle can be measured directly by attaching either intact muscle (Josephson 1985, Machin & Pringle 1959), or glycerol extracted muscle fibres (Pringle & Tregear 1969), to a mechanical test apparatus. The power output is calculated by measuring the difference in work done by stretching and releasing the activated muscle per unit time. In this study, the lissajous loop (of tension plotted against length) area was calculated and multiplied by the frequency of length oscillation, as described in Chapter 2.

The maximum power output of both skinned and live muscle fibres depends upon several factors: the amplitude and frequency of the length oscillation and the experimental temperature (Josephson 1985, Steiger & Ruegg, 1969, Machin et al., 1959, Pringle & Tregear, 1969).

Figure 5.1 is a family of curves showing how the power output of a single skinned L. indicus muscle fibre changes with the frequency of length oscillation at 3 different temperatures. Changing the

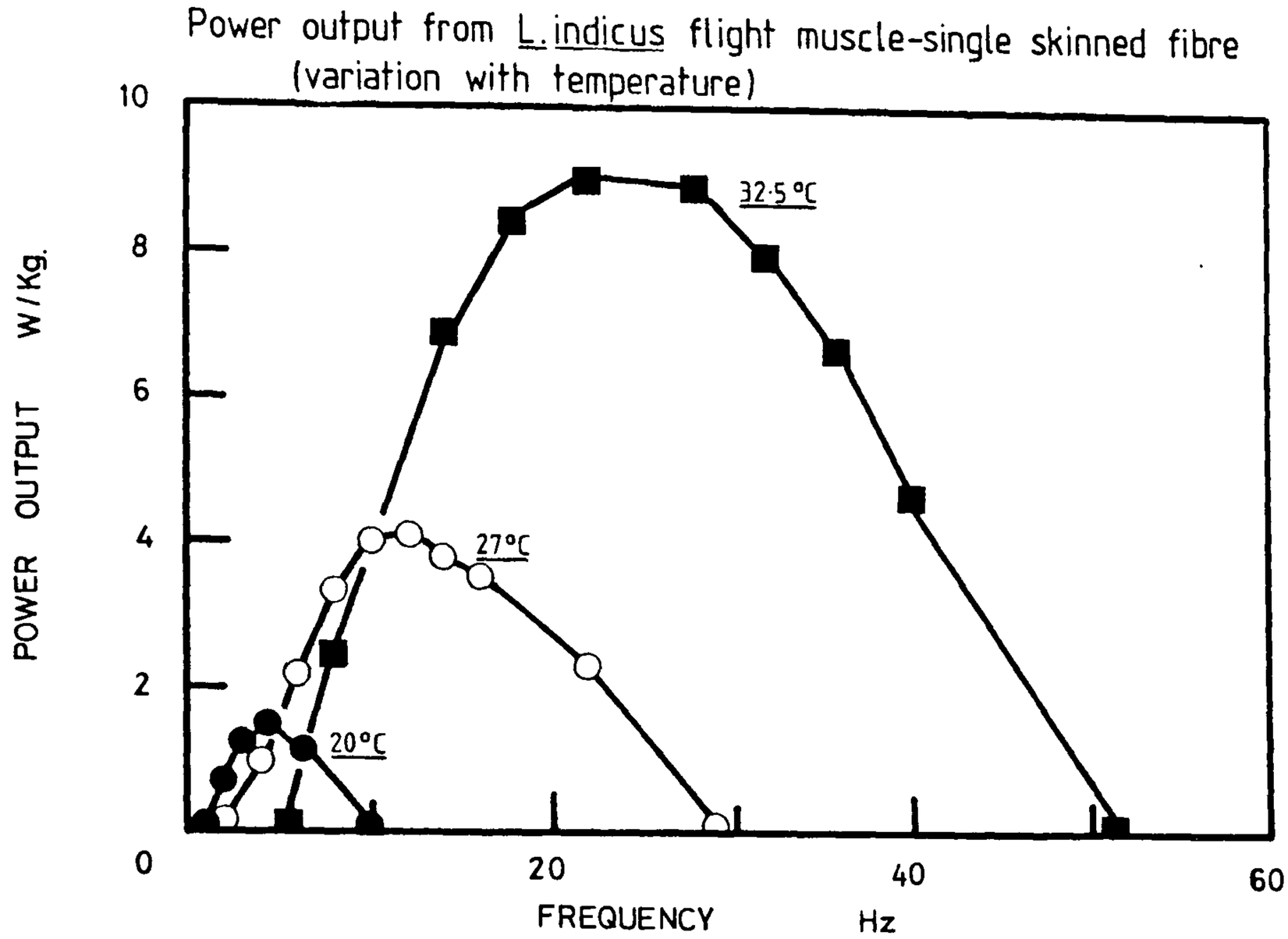

FIGURE 5.1

Family of curves to show how the power output obtained from a single L. indicus fibre is affected by the temperature of the incubation solution. The solutions used were those of Table 2.2b, the experimental protocol is described in section 5.2.3.

temperature of the incubation solution has two important effects:
1) the frequency at which the maximum power output is obtained rises,
2) the magnitude of the maximum power output rises.

A series of experiments was performed on skinned muscle fibres from L. griseus. The change in frequency at which the maximum power output is obtained, and the change in the magnitude of the maximum power output are shown as Arrhenius plots in Figure 5.2. This is the data from the best experiment, the single fibre was tested at 5 different temperatures. Above 30°C, fibres from this particular thorax became diffusion limited and entered the high tension state. Because of fibre-to-fibre variation it is not possible to 'pool' the power output data obtained from different fibres. However, the pooled data, of the 14 fibres tested, for the optimum frequency of oscillation, at different temperatures, had a best fit line very similar to the results shown in Figure 5.2 (see Figure 5.3). The effect of temperature upon the muscle performance is conveniently described by the Q_{10} (the proportional change for each 10 degree rise in temperature). Using the data of Figure 5.2, the Q_{10} of the change in frequency of maximum power (f_{PMAX}) is 2.9 (at 15-25°C.), the Q_{10} of the maximum power output is 6.9 (at 15-25°C.).

Another set of experiments were performed to measure specifically the maximum power output obtainable from skinned muscle fibres. The results of these experiments are shown in Table 5.3. The experiments were performed on fibres from a giant waterbug which had flown, immediately prior to glycerol extraction, in the laboratories at York (this was the same bug that was used in the previous set of experiments).

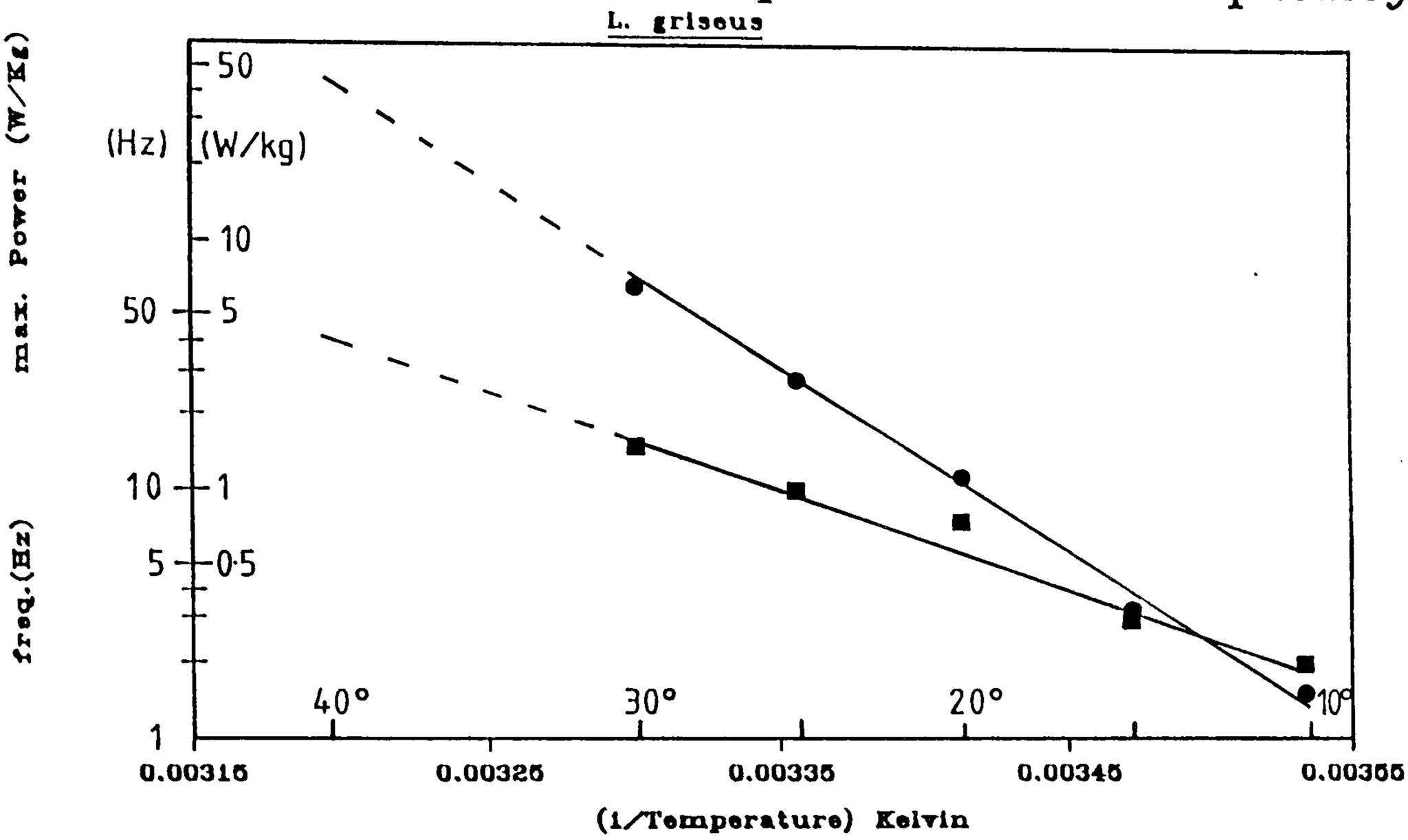

FIGURE 5.2

Arrhenius plots of the power output and frequency of maximum power ouput. The solutions were those of Table 2.2b

(●) = Power output.

(■) = Frequency at which the maximum power is obtained.

Species = L. griseus

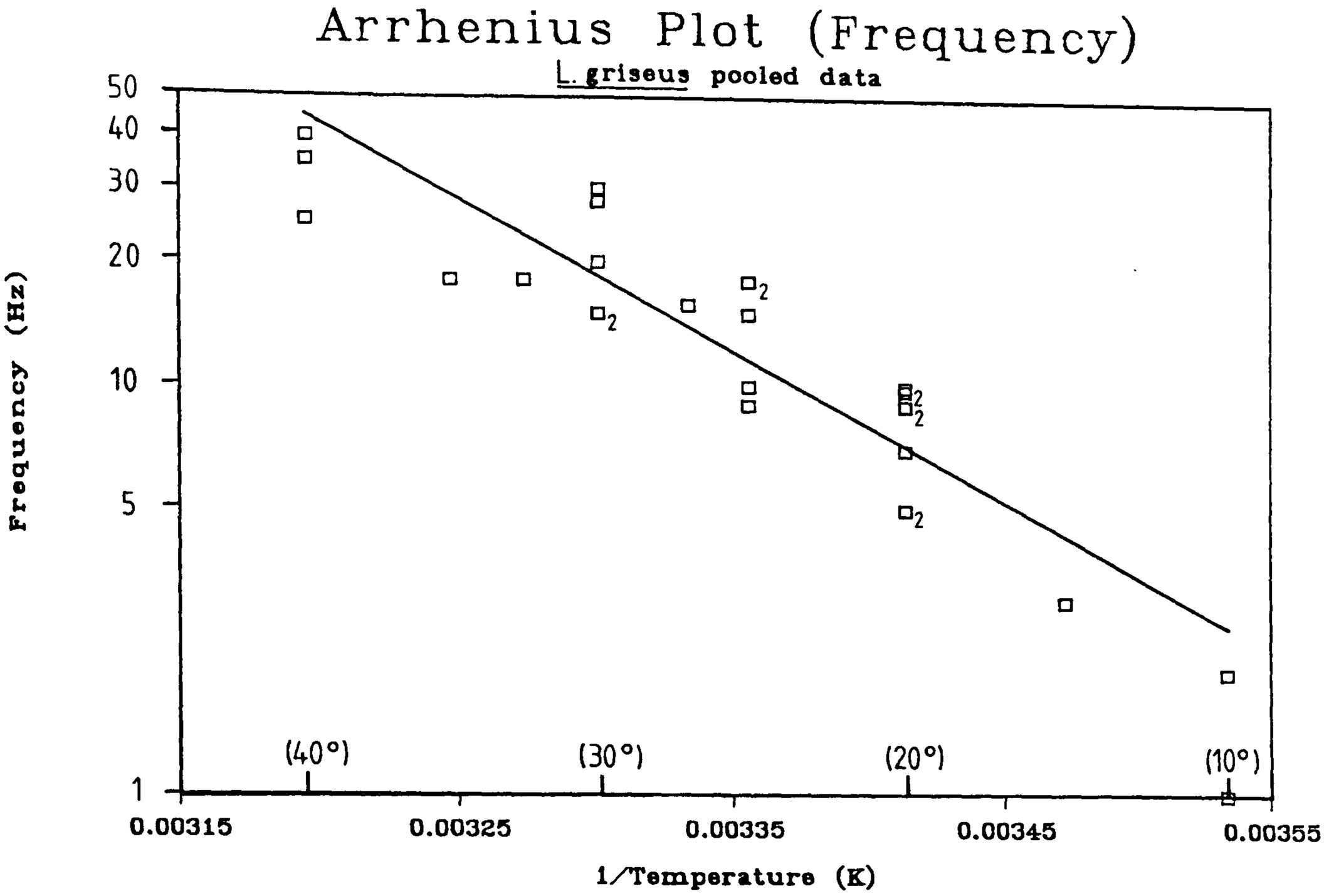

FIGURE 5.3

Arrhenius plot of the frequency of maximum power ouptut.
Data points were obtained form experiments with 14 different fibres.
Solutions were those of Table 2.2b; the number 2 next to a datum point means that two points overlap.
The fitted line is the best fit through all the points.

Temperature (°C.)	Frequency (Hz)	Amplitude (%)	Power output (W/kg)
20	9.0	9.0	17.0
25	9.0	5.5	10.9
25	9.0	10.9	13.5
25	16.0	8.5	30.9
25	16.2	9.1	39.5
30	15.0	6.8	32.8
30	15.4	6.6	43.3
30	25.0	5.5	17.8

Operating conditions in life :
WBF = 44Hz
Thoracic Temp. = 41°C.

Table 5.3

Maximum power output from single, skinned muscle fibres from L. griseus. Each experiment was performed on a different fibre. The amplitude and frequency of length oscillation were adjusted to give the maximum power output possible. The incubation solutions were those of Table 2.2c.

5.2.4 The Chemo-Mechanical Efficiency :

The chemo-mechanical efficiency may be calculated directly by measuring, simultaneously, the power output and ATPase activity of skinned muscle fibres. The free energy of hydrolysis of ATP under the conditions of the experiments performed here is equal to about -42 kJ/mol (Kushmeric & Davis, 1969). The calculated efficiencies of the top 10% of the data (the highest power outputs) presented in Chapter 3 are shown in Table 5.4.

5.2.5 The Thoracic Temperature in Flight :

Many insects have an elevated thoracic temperature when in flight (Heinrich, 1974; 1979; 1987). Some of these insects require a pre-flight warm-up before they are able to take-off (Dorsett, 1962; Leston et al., 1965; Kammer & Heinrich, 1978). The thoracic temperature of some of the insects in this study has not been reported previously.

It is particularly difficult to induce giant waterbugs to fly. Two species, L. indicus and L. griseus flew in the laboratories at York, shortly after importation (from Thailand and Florida, respectively). In preparation for flight the bugs left the water and climbed as high as they were able. They performed a pre-flight 'ritual' consisting of a rapid (1-5 Hz) head movement, presumably caused by repeated contractions of the indirect flight muscles. After about 20 minutes the bugs reared-up on their hind legs, snapped open the elytra and took off. As soon as the bugs landed they were recaptured and the thoracic temperature was recorded.

Figure 5.4 shows three cooling curves which record the change in thoracic temperature after flight for three individual bugs. All three curves extrapolate to over 40°C. at a time when the bugs were still airborne Figure 5.5 shows the sound recording of L. indicus

Species	Power output (nW/pMol Sl)	ATPase (Mol ATP/Mol Sl/s)	Efficiency (%)
L. griseus (25°C)	149.6	9.4	37.9
	87.2	4.3	48.3
V. vulgaris	181.2	15.2	28.4
	135.4	15.8	20.4
	120.3	10.5	27.2
A. mellifera	40.1	5.0	19.3
	14.7	6.2	5.6
	14.1	3.3	10.2
E. balteatus	35.6	4.3	19.7
	13.3	3.9	8.1
Tipula spp.	19.7	7.4	6.3
	29.7	9.7	7.3

Table 5.4

Chemo-mechanical efficiency of IFM from a variety of different insects. The efficiencies were calculated assuming that the free energy of hydrolysis of ATP is -42 kj/Mol under the conditions of the experiments. All experiments were performed at 20°C. except where stated.

Species	Sarcomere length (μm)	Method used
B. terrestris	2.51	L.L.D.
L. indicus	2.83	L.L.D.
	2.77	L.M.
V. vulgaris	2.56	L.L.D.
	2.47	L.M.
D. melanogaster	3.0	E.M.
Tipula spp.	3.6	L.L.D.

L.D. = Laser light diffraction
L.M. = Light microscopy
E.M. = Electron microscopy

Table 5.5

Sarcomere length in different insect species; measured in relaxing solution or fixed in the relaxed state for E.M..

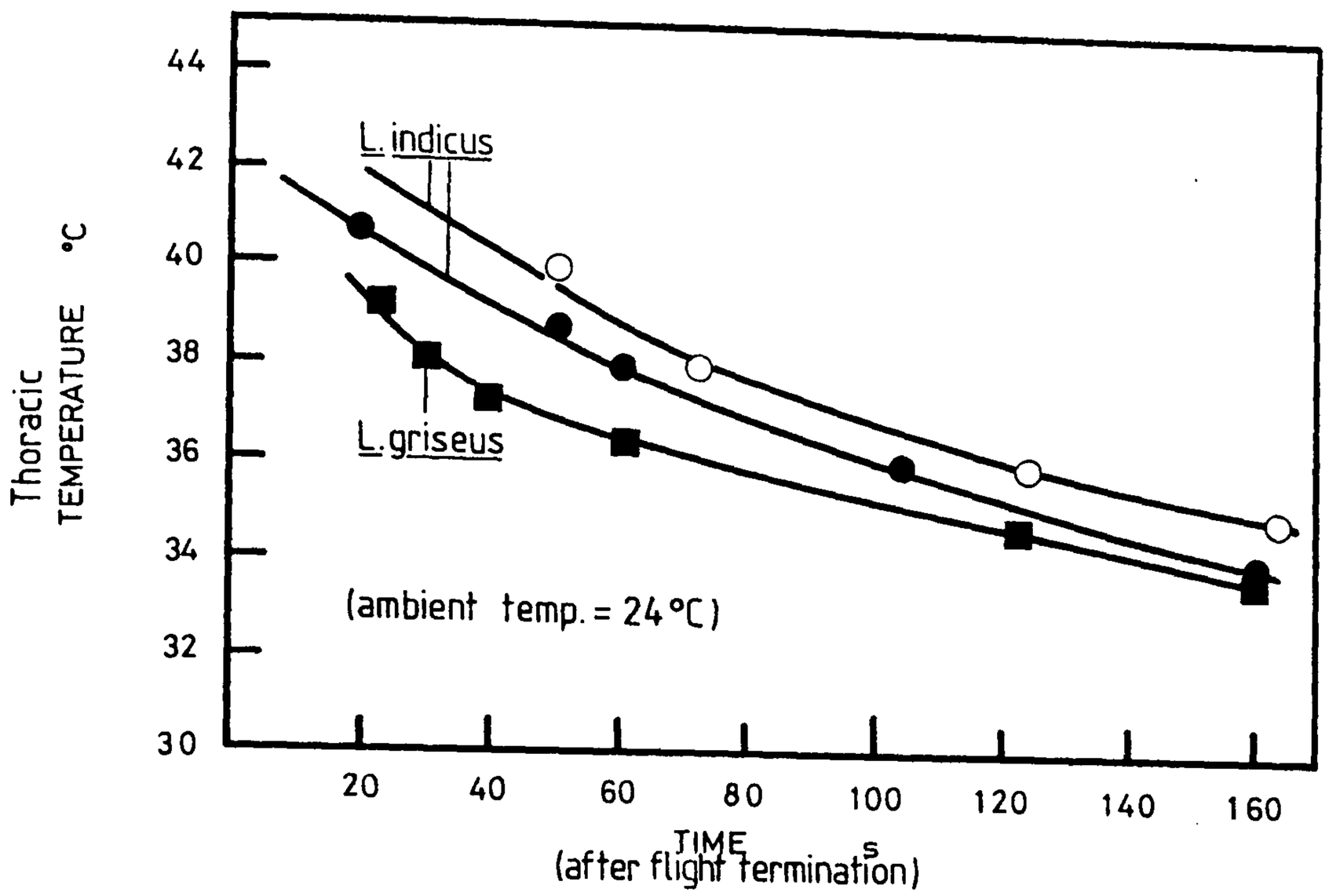

FIGURE 5.4

Thoracic temperature recorded after flight termination in three individual waterbugs. The cooling curves can be extrapolated to a time when the bug was still airborne,to assertain the thoracic temperature in flight.
The ambient temperature in all three cases was 24°C.

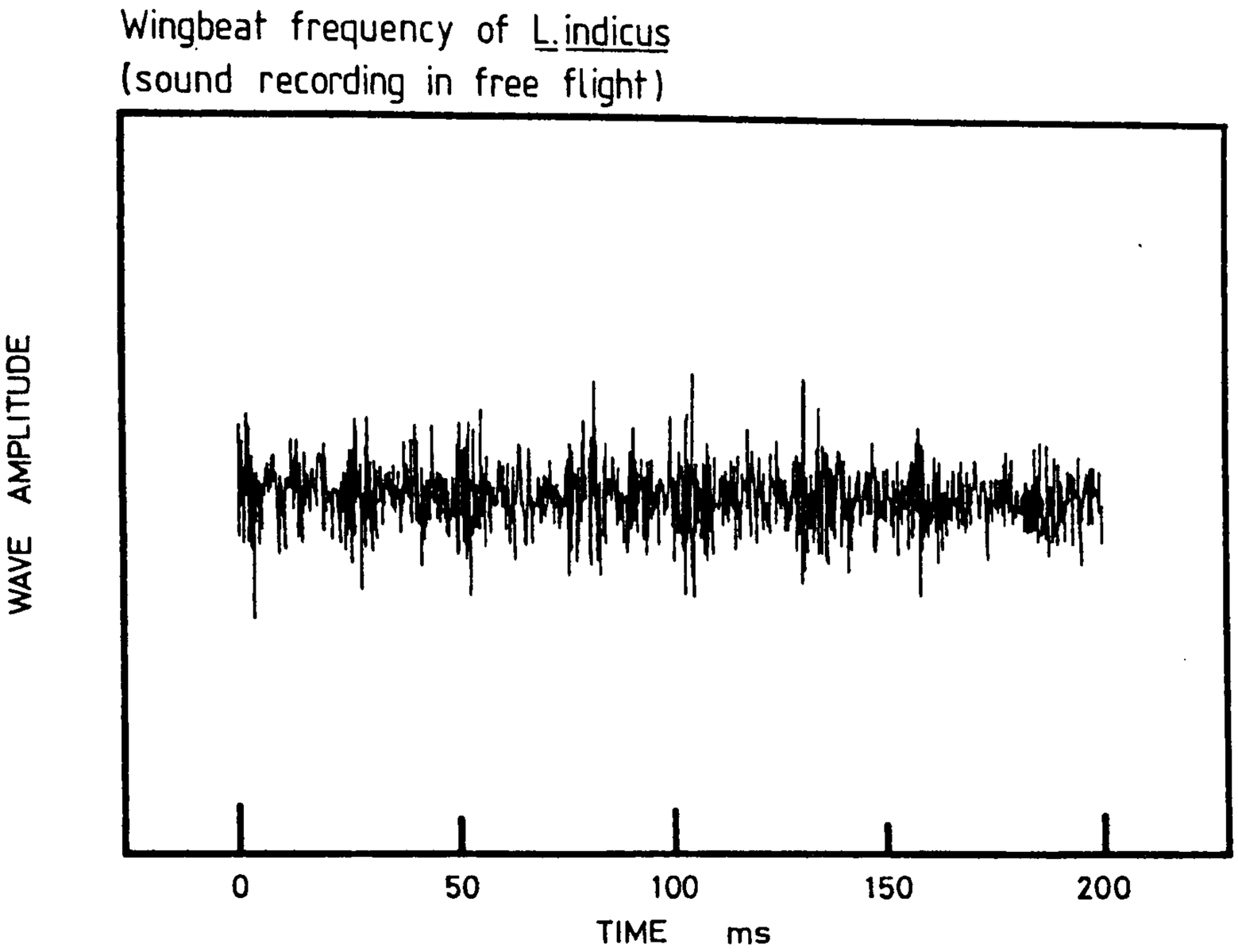

FIGURE 5.5

The sound of L indicus in free flight in the laboratory was recorded on a cassette tape recorder and the signal then replayed into a storage oscilloscope.
The wingbeat frequency, determined from the record above was 38Hz.

in flight. Similar records were obtained for L. griseus; the calculated wingbeat frequencies were; L. indicus, 38Hz and L. griseus, 44Hz.

The measured thoracic temperature in two small, glabrous, diptera, Calliphora erythrocephala and Tipula oleracea, were found to be only 1 or 2 degrees above ambient. The common wasp, which is larger than the honeybee but has rather sparce thoracic hair had a temperature of 29-32°C (ambient 24°C.).

5.2.6 Sarcomere Length and the Degree of Muscle Shortening :

The sarcomere length of skinned IFM fibres, bathed in relaxing solution, was measured either by microscopy or laser light diffraction (as described in Chapter 2). The results are shown in Table 5.5.

The degree of muscle shortening was measured in Tipula oleracea viewed under a travelling microscope with stroboscopic illumination. The length of the thorax was measured when the wings were illuminated in the up and down positions. The difference in length was about 3.5-4% of the mean thoracic length. Unfortunately, it was not possible to induce flight for sufficient time to make the necessary measurements in other insects. Boettiger and Furshpan (1954) found the degree of flight muscle shortening in the bumble bee to be about 2%.

5.3 DISCUSSION :

5.3.1 The Proportion of Cytochrome c Present in Different Muscles :

Keilin (1925) discovered that the highest concentration of cytochrome was to be found in the thoracic muscles of flying insects. He associated the high concentration of cytochrome with the "peculiar activity of these muscles". The high concentration of cytochromes gives the IFMs a distinctive yellow colour.

The amount of cytochrome c found in all the insects tested is much larger than the amounts quoted for vertebrate muscles. The amount of cytochrome c found in the muscles of C. erythrocephala is consistent with the values for young blowflies quoted by Levenbook and Williams (1951). The amount of cytochrome c found in the flight muscle of V. vulgaris and A. mellifera is double that found in Lethocerus and 30% greater than that found in the other insects.

If the amount of cytochrome c in the respiratory chain relative to the other components is optimised then the flux through the respiratory chain will depend upon the amount of cytochrome c present. The conclusion from the data presented here is that the rate of ATP production (per unit weight of muscle) in Vespa and Apis is approximately twice as great as in Lethocerus.

The model of Pennycuick and Rezende (1984) predicts that the mitochondrial partial fraction in muscles from different insects should increase systematically with the wingbeat frequency. The finding here that the proportion of cytochrome c present in different muscles does not change in a systematic fashion is not easily consistent with this model. The comparatively high ATPase rate of fully activated skinned muscle fibres from Vespa (Chapter 3) is consistent with the high level of cytochrome c measured in this particular insect.

5.3.2 The Proportion of Muscle Found in Different insects :

The important finding here is that the proportion of flight muscle in different insects is relatively constant within a given species but varies widely between species. There are two effects of increasing the proportion of flight muscle:

1) The total power output, per unit body weight, will be increased. This may be important for insects that carry a large payload (ie. queen bumble bees carrying eggs or wasps carrying prey) or to provide the necessary power to enable small insects to fly when the environmental temperature is low (the subject of thoracic temperature is discussed further later).

2) The cost of making and maintaining the flight muscle will be increased. The flight muscles account for a very large proportion of the total body protein and resting metabolic rate; thus, to reduce these metabolic loads will be advantageous in all insects.

There is a criticism of studies which estimate the specific power output of insect flight muscle just by measuring the oxygen consumption in the flying insect. Often the proportion of flight muscle is assumed to be 15% in all species. For the insects investigated here this assumption would lead to a 2-fold error in the estimation of the specific power output of the muscle. The high oxygen consumption found in flying euglossine bees (estimation of the specific power output was on the basis of the IFM being 15% of the insect mass; Casey et al., 1985) can be explained, in part, by the more recent finding that these insects contain an unusually high proportion of flight muscle (28%) (Gabriel et al., 1987).

5.3.3 The Power Output and Chemo-mechanical Efficiency :

The Maximum Power Output :

In Chapter 3 the problem of diffusion limitation of skinned muscle fibre experiments was discussed. There is an *in vivo* correlate of diffusion limitation. The maximum sustainable power output of live

muscle may be limited not by the properties of the myofibrils but by the rate at which the surrounding mitochondria can supply ATP (Weis-Fogh & Alexander, 1977).

In order to estimate the maximum attainable power output in Lethocerus, two types of experiment were performed. One was to measure the maximum power output directly. The other was to measure the power output over a range of temperatures and to extrapolate the results to the *in vivo* operating temperature.

The problem with the first approach was that the isolated, skinned, fibres became diffusion-limited at the flight temperature of 40°C. Above 30°C. the fibres entered the 'high tension state', the mechanical power output was then reduced or abolished. The maximum measurable power output in L. griseus at 25-30°C. was around 40W/kg. This value was obtained at very large amplitudes of oscillation (6-9% peak-peak).

In experiments where the fibres were oscillated at lower amplitudes (2% peak-peak) over a wide temperature range the predicted power output at 40°C. was 45W/kg. If the amplitude of length oscillation *in vivo* is 2% then the predicted power output of the muscle in the flying insect would be 45W/kg. However, the *in vivo* muscle shortening is not known and may be nearer to the larger amplitudes (6-9%) used in the second set of experiments. The predicted power output at 40°C. would then be near 250W/kg (assuming that the Q_{10} at the large amplitudes is also 6.3, as measured at 20-30°C. in fibres oscillated at 2%)

The maximum power output measured in live muscle fibres are 30W/kg for Oryctes and 60W/kg in Bombus (Machin & Pringle, 1959), and 76W/kg for Neoconocephalus (Josephson, 1985).

The large Q_{10} measured for the power output compared to the Q_{10}

for the optimum frequency means that the activation energy for the two processes is different (being greater for the steps that limit the power output of the muscle). This is consistent with the cross-bridge model presented in Chapters 3 and 4. The tension generating step, which governs the frequency response of the muscle, is faster than, and not controlled by, the rate-limiting step. The rate-limiting step controls the cross-bridge cycling rate and ATPase activity. The mechanical power output is coupled to the cross-bridge cycling rate.

Chemo-mechanical Efficiency :

The calculation of chemo-mechanical efficiency here is different form the chemo-mechanical coupling of Steiger & Ruegg (1969) and Pybus & Tregear (1975). They measured the difference in the ATPase rate between working and non-working fibres. This was then used to calculate the net chemo-mechanical efficiency (or coupling). Here the work done was divided by the total ATP hydrolysed to give the gross chemo-mechanical efficiency. It is this gross efficiency that is important to the live insect.

Ellington (1985) has estimated the overall efficiency of insect flight muscle. He has calculated the aerodynamic power requirements of a flying insect and compared this to the metabolic power input (the oxygen consumption rate).

A break-down of the power dissipation in insect flight muscle is given in Scheme 5.1. In order to compare the muscle efficiency measured here with Ellington's calculated values, an assumption about the efficiency of ATP production must be made. Wilkie (1968) found this to be around 55% efficient. This means that the maximum overall efficiency of Apis flight muscle would be 20%*55% = 11 %. This agrees well with Ellington's estimates for Apis when the storage of

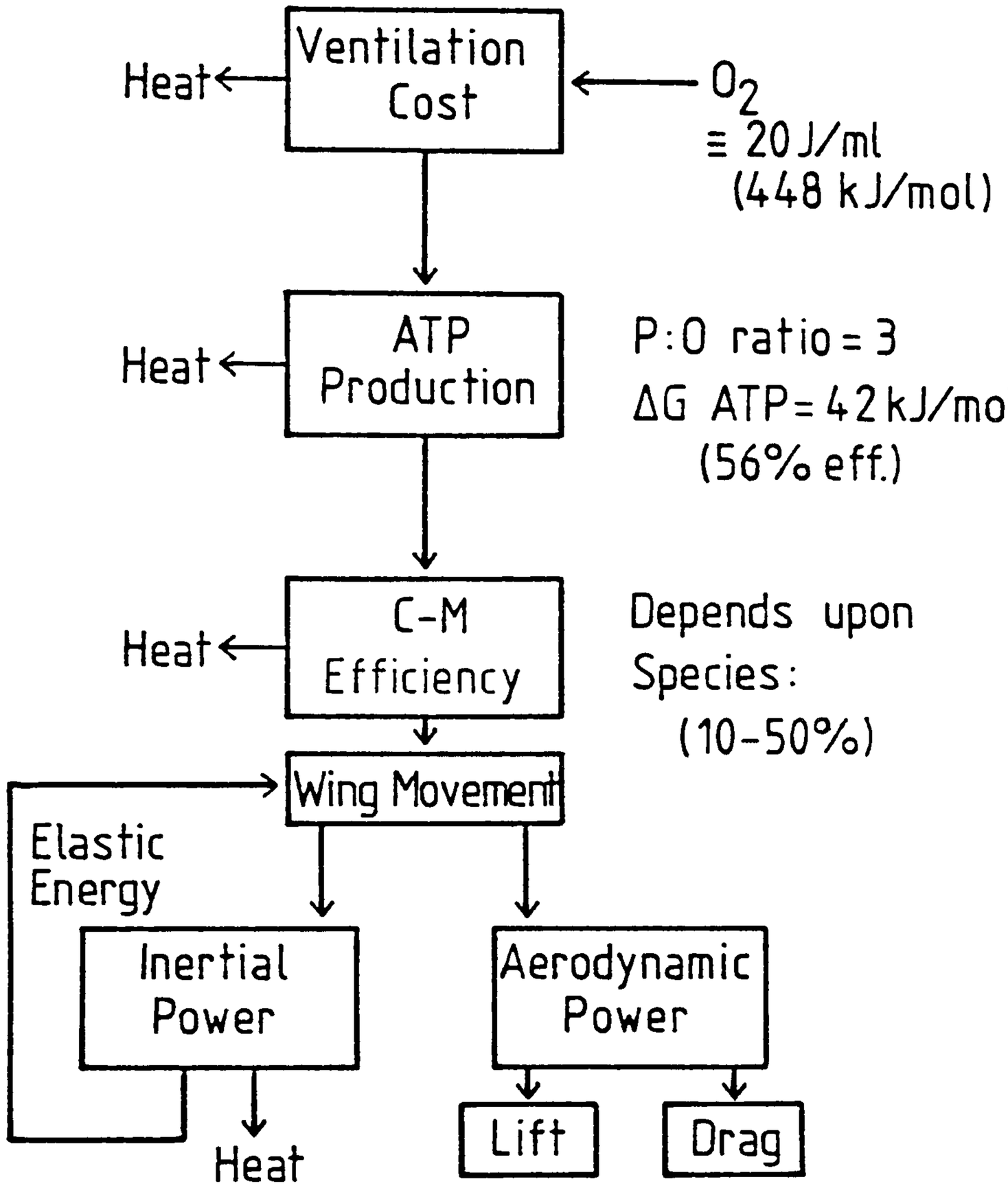

Energy Transduction in Insect Flight Muscle

SCHEME 5.1

Scheme to show how metabolic energy is converted into aerodynamic energy in insect flight muscle.

Inertial power, used to accelerate the wings can be stored as elastic energy. The chemo-mechanical efficiency measured in Apis, in this study, implies that the elastic energy storage is about 50% efficient (Ellington, 1985).

elastic energy in the cuticle is about 50% efficient.

5.3.4 The Effect of Sarcomere Length :

As Ruegg (1968) observed, short sarcomeres connected in series will have an increased shortening velocity and a reduced maximum force compared to long sarcomeres. The power output of the muscle with shorter sarcomeres will be slightly reduced because the 'bare zone', (the region in the centre of the thick filament with no cross-bridge projections) which generates no force, will be proportionately increased. There would seem to be some advantage in the evolution of shorter sarcomeres, with increased shortening velocity, and only slightly diminished power output, in insects with a high wingbeat frequency. However, the measured sarcomere length does not change in a systematic fashion with wingbeat frequency. Although the long sarcomere length found in Tipula is consistent with the unusually low wingbeat frequency found in this small dipteran insect.

According to Wray (1979), stretch activation in insect fibrillar flight muscle can be explained by the identity in helical repeat of the thick and thin filaments. A filament movement of 3% (37.5 nm/half sarcomere) in Lethocerus changes the thick and thin filament register from one of mismatch to match (or *vice versa*). The degree of muscle shortening required to move the wings of some insects could well be different from 3%. If the thick and thin filament repeats are the same in different insects, the only way to obtain the same degree of activation by this model would be to change the sarcomere length. The variation of sarcomere length found in different insects could be a means of tuning the activation mechanism to the degree of muscle shortening required to move the wings. Using the reverse argument for the specific case of Tipula, the long sarcomere length, 3.5μm,

predicts that the optimum shortening distance would be lower than for other insects. In fact the measured thoracic movement of 4% is larger than the 2% found for bumble bees (Boettiger & Furshpan, 1954).

5.3.5 Strategies to Cope with a Variable Environmental Temperature :

The maximum power output of insect flight muscle falls sharply as the temperature is reduced. Also the frequency at which the maximum power is obtained falls. The dramatic effect of temperature upon the mechanical performance of insect flight muscle presents a problem for these small animals. Many insects need to be able to fly in an environment whose temperature can change by 10-20°C. in a very short period of time.

Because of differences in surface area to volume ratio, the specific rate of heat loss from small insects is very much greater than from large insects. The very high metabolic rate of the flight muscles during flight means that the thoracic temperature of large insects necessarily rises above ambient. Many of these insects have regulatory mechanisms and maintain a thoracic 'endothermy' (Heinrich, 1974). The rapid rate of heat loss from small insects, means that the cost of endothermy is prohibitive. This means that the thoracic temperature of small, glabrous, insects remains near ambient. Clearly the strategies used by small and large insects, which allow them to fly over a range of ambient temperatures, must be different.

There appear to be two basic strategies:

1) Maintain a thoracic endothermy and have an obligatory pre-flight warm-up at low ambient temperatures.

2) Have a wingbeat frequency that can be varied to match the frequency of maximum power output of the flight muscles and also

carry extra flight muscle to yield sufficient power at low ambient temperatures.

The choice of strategy will be determined by the size of the insect.

Performance of the flight muscles :

Figure 5.6 shows how a small insect, with a variable thoracic temperature, can ameliorate the problem of power loss from the flight muscles at low ambient temperatures. The available power from the flight muscles will be optimised if the wingbeat frequency is tuned to match the frequency for maximum power (f_{PMAX}) of the flight muscles at different temperatures. In the example given (Figure 5.6) the available power is, approximately, doubled by reducing the wingbeat frequency at the lower muscle temperature (the curves of Figure 5.6 were derived from the power output obtained from a single Lethocerus griseus fibre measured at the three different temperatures). Figure 5.7 provides evidence that just such a mechanism operates in D. melanogaster. This very small, dipteran, insect (mass < 1mg) will have a thoracic, and therefore muscle, temperature that is very close to ambient. The measured wingbeat frequency in D melanogaster is well correlated to the ambient temperature (Williams & Chadwick 1953). One reason why small insects are able to fly over a wide range of environmental temperatures is because they can alter their wingbeat frequency and so maximise the power output of their muscles.

Cuticle stiffness :

In order for small insects to change their wingbeat frequency the natural resonance characteristics of the wing must be adjustable. The

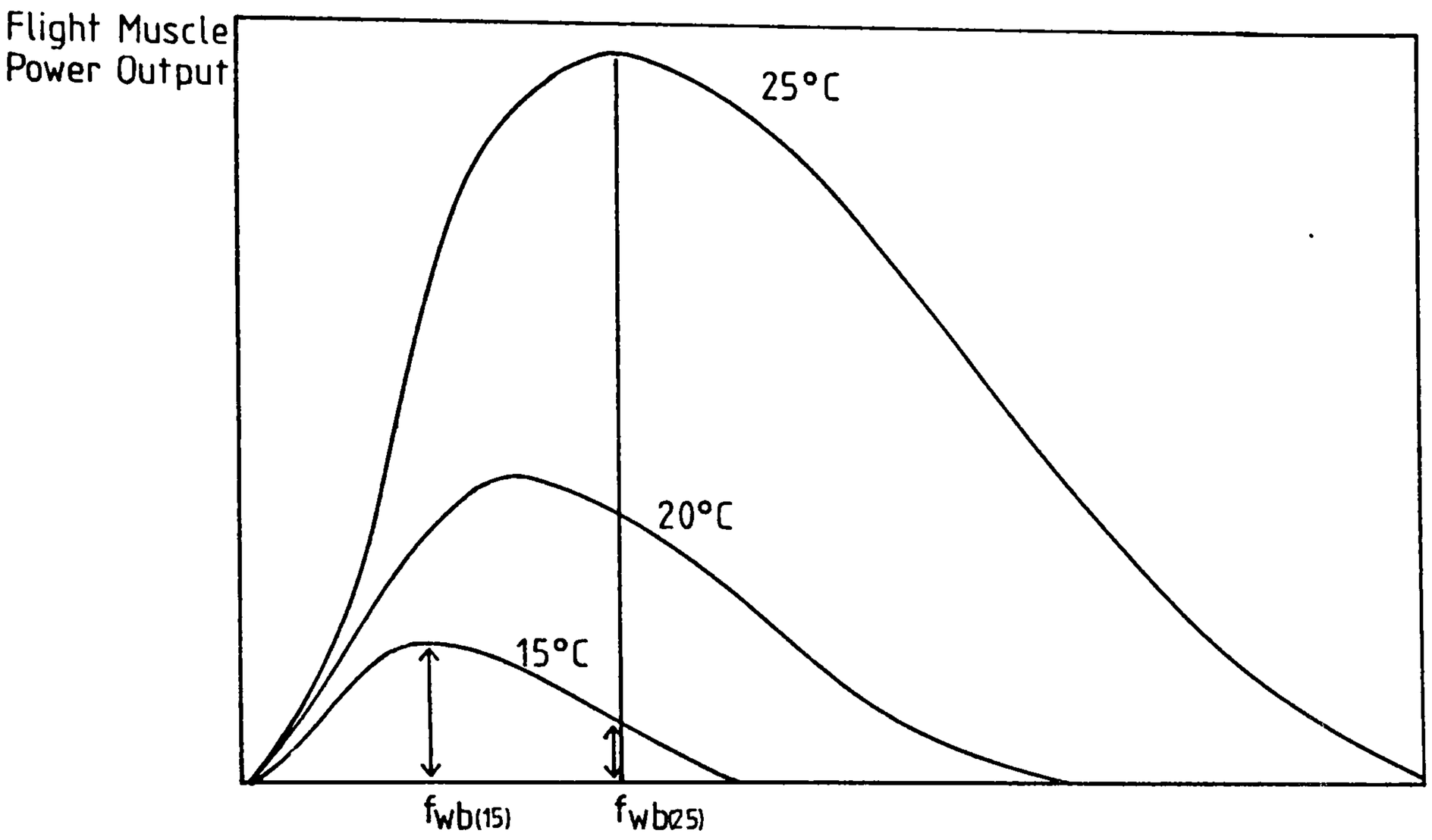

FIGURE 5.6

Family of curves to show how the power output from the flight muscles changes with thoracic (and in the case of small insects ambient) temperature, at different wingbeat frequencies.

The thoracic temperature of small insects remains very near to the ambient temperature. At low ambient temperatures the power ouptut of the muscles will be maximised if the wingbeat frequency is reduced.

The optimum wingbeat frequency at two environmental temperatures (15° and 25°C) is shown.

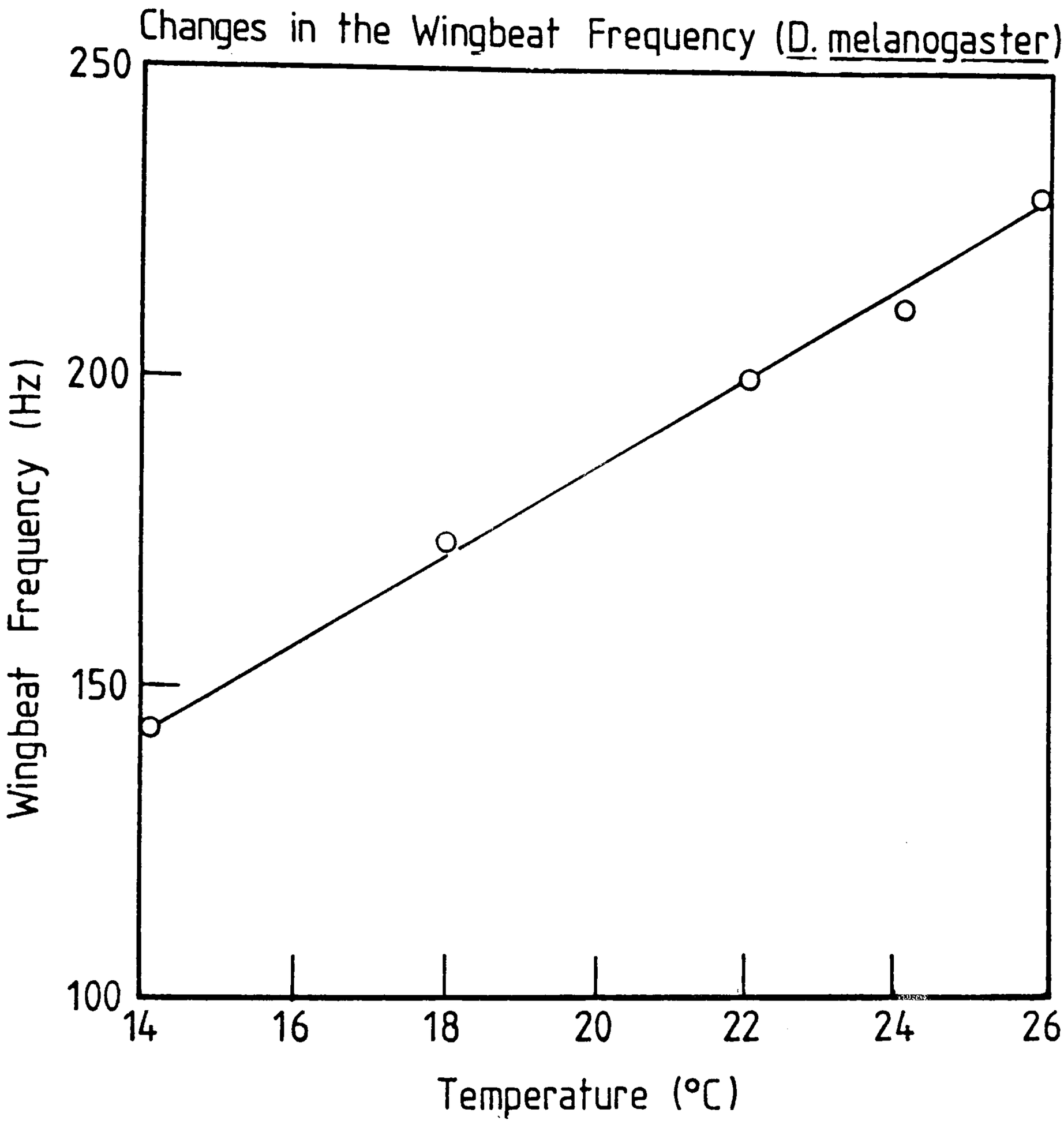

FIGURE 5.7

Drosophila melanogaster is able to tune its wingbeat frequency to the frequency of maximum power output of its flight muscles. In so doing it is able to obtain sufficient power for flight over a wide range of environmental (and therefore thoracic) temperatures.

Data from Chadwick, 1953.

natural resonance frequency is given by :

$$f_{RES} = 2\pi\sqrt{K/I} \qquad \ldots\ldots 5.1$$

f_{RES} = Resonant frequency
K = Stiffness of the wing mounting
I = Inertia of the wing

The thoracic cuticle of the small diptera is braced by (non-fibrillar) pleurosternal muscles. Nachtigall and Wilson (1967) showed that the function of these muscles is to adjust the resonant frequency of the thorax and so change the natural frequency of the wings.

A compliant thoracic cuticle, whose stiffness is governed by tension in the sternopleural muscles would allow the wingbeat frequency to be altered over a wide range.

The thoracic cuticle of Calliphora is noticebly more compliant than the cuticle of a similar sized pubescent honeybee, Apis. The hairy honeybee has opted to be endothermic (Heinrich, 1979), and requires a pre-flight warm-up on cold days. The significance of the stiff thoracic cuticle is that the main method for heat generation in this insect is by "shivering". Pre-flight contractions of the flight muscles (Kammer & Heinrich 1978) against a stiff cuticle will produce 'waste' heat faster than against a compliant cuticle, and there would be great advantage in being able to warm-up rapidly on cold days.

A prediction is that insects which have biochemical shunts enabling "non-shivering thermogenesis" (Newsholme et al., 1972) may also have evolved thoracic cuticles that are less stiff.

Proportion of flight muscle :

Figure 5.6 shows that even when the wingbeat frequency is tuned to f_{PMAX} of the flight muscle fibres there is still a reduction in power output with temperature. Small glabrous insects will therefore

require a proportionately larger mass of flight muscle if they are to fly over a wide range of temperatures. There will of course be exceptions when a diverse variety of insects are studied, but the high proportion of muscle in Calliphora is consistent with this idea. Casey et al. (1985) measured the thoracic mass in a closely related group of insects (euglossine bees) and found that the proportionate weight in the glabrous insects was 10% greater than in the pubescent ones. At present this is the best supporting evidence for the prediction of the strategy proposed here.

In Summary :

Large, pubescent, insects have evolved a stiff thoracic cuticle to allow a rapid pre-flight warm-up. The wingbeat frequency of these animals will be independent of the ambient temperature. At cool ambient temperatures longer pre-flight warm-ups are required.

Small, glabrous, insects have a flexible thoracic cuticle whose stiffness is dramatically affected by tension in the sterno-pleural muscles which brace the thoracic box. The wingbeat frequency may be adjusted to match the frequency of maximum power output of the myofibrils. These insects can fly over a wide range of temperatures with no pre-flight warm-up, but fly better at higher ambient temperatures. They require additional muscle to provide the necessary power for flight at low ambient temperatures.

CHAPTER 6 :
THE MECHANICAL PROPERTIES OF *DROSOPHILA MELANOGASTER* FIBRILLAR FLIGHT MUSCLE WITH MUTANT MUSCLE PROTEINS

THE MECHANICAL PROPERTIES OF *DROSOPHILA MELANOGASTER* FIBRILLAR FLIGHT MUSCLE WITH MUTANT MUSCLE PROTEINS.

6.1 INTRODUCTION :

One approach to the study of muscle contraction is to remove or modify a component of the contractile apparatus and measure the effect of this alteration on the muscle performance. Using chemical techniques it is often difficult to modify or remove a single protein throughout the muscle tissue without affecting the other proteins. By inducing genetic mutations in muscle protein genes, specific changes can be made throughout the tissue. This study investigates the mechanical properties of the indirect flight muscle from Drosophila melanogaster with mutant muscle proteins. The genetics of Drosophila are the best understood of any eukaryote and the flight muscle of this insect is large enough to be mounted on a mechanical test apparatus.

The dorsal-longitudinal muscle (DLM) of Drosophila is shown in Figure 6.1, it is one of the two indirect flight muscles (IFM) used to power the insect in flight. One advantage of using this fibrillar flight muscle for mechanical experiments is that it is one of the best studied muscle types. Also, flies with reduced function in this muscle are still able to survive and breed (the mutants are 'viable'). Altered muscle function caused by specific, conservative, changes to the muscle proteins were analysed under three different conditions; when the muscle was relaxed, active and in rigor. The results are compared to the wild-type response.

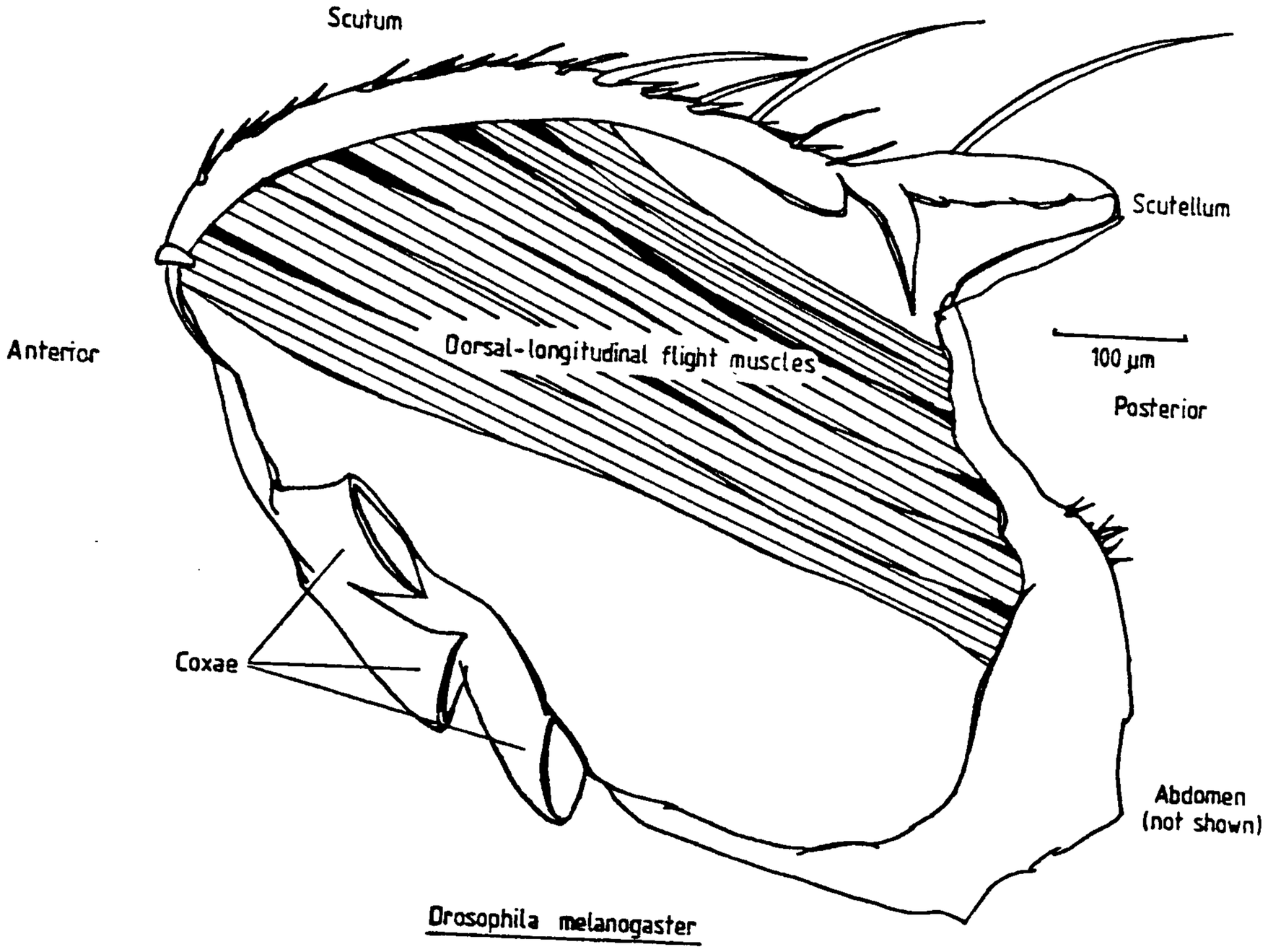

FIGURE 6.1

Diagram to show the position of the indirect, dorsal longitudinal muscles in a sagittally dissected D. melanogaster thorax.

The muscles were glycerol-extracted in situ and cut from the thorax prior to mechanical experiments with a pair of microdissection scissors.

Muscle fibres were pared down to a diameter of about 80µm and then carefully crimped in aluminium "T" clips. The fibre could then be mounted on the mechanical test apparatus.

6.2 LOCATION OF MUSCLE GENES IN THE DROSOPHILA GENOME :

The Drosophila genome is shown in Figure 6.2, the position of the loci coding for some of the muscle-specific proteins are labelled. The number and letter code given to each gene is based upon the physical location of that gene within the genome.

6.3 VIABILITY OF MUSCLE MUTANTS :

An important feature of Figure 6.2 is that there are several different genes coding for actin and these genes are randomly dispersed in the genome (Fyrberg et al., 1980). Of the six actin genes, only one codes for an IFM specific actin, *Act88F*. The remaining genes; *Act5C*, *Act42A*, *Act57A*, *Act87E* and *Act79B* code for actins found elsewhere in the fly (Fyrberg et al., 1983). Mutations in *Act88F* result in flies with altered IFM without affecting viability of the progeny.

It is also possible to produce viable flies with mutant IFM myosin. The single copy of the myosin heavy chain gene has developmentally regulated transcripts (Rozek & Davidson, 1983, Bernstein et al., 1986). Regions of the gene are specific to particular muscle myosins. This permits non-lethal mutations in parts of the gene which are only expressed in the indirect flight muscles. However, all the myosin heavy chain mutants available to date have grossly aberrant muscle structure.

All the mutants used in this study were actin mutants. The primary amino acid sequence of actin is highly conserved between different organisms (Pollard & Cooper, 1986) so, functional changes in the mutant Drosophila muscle can be related to other systems.

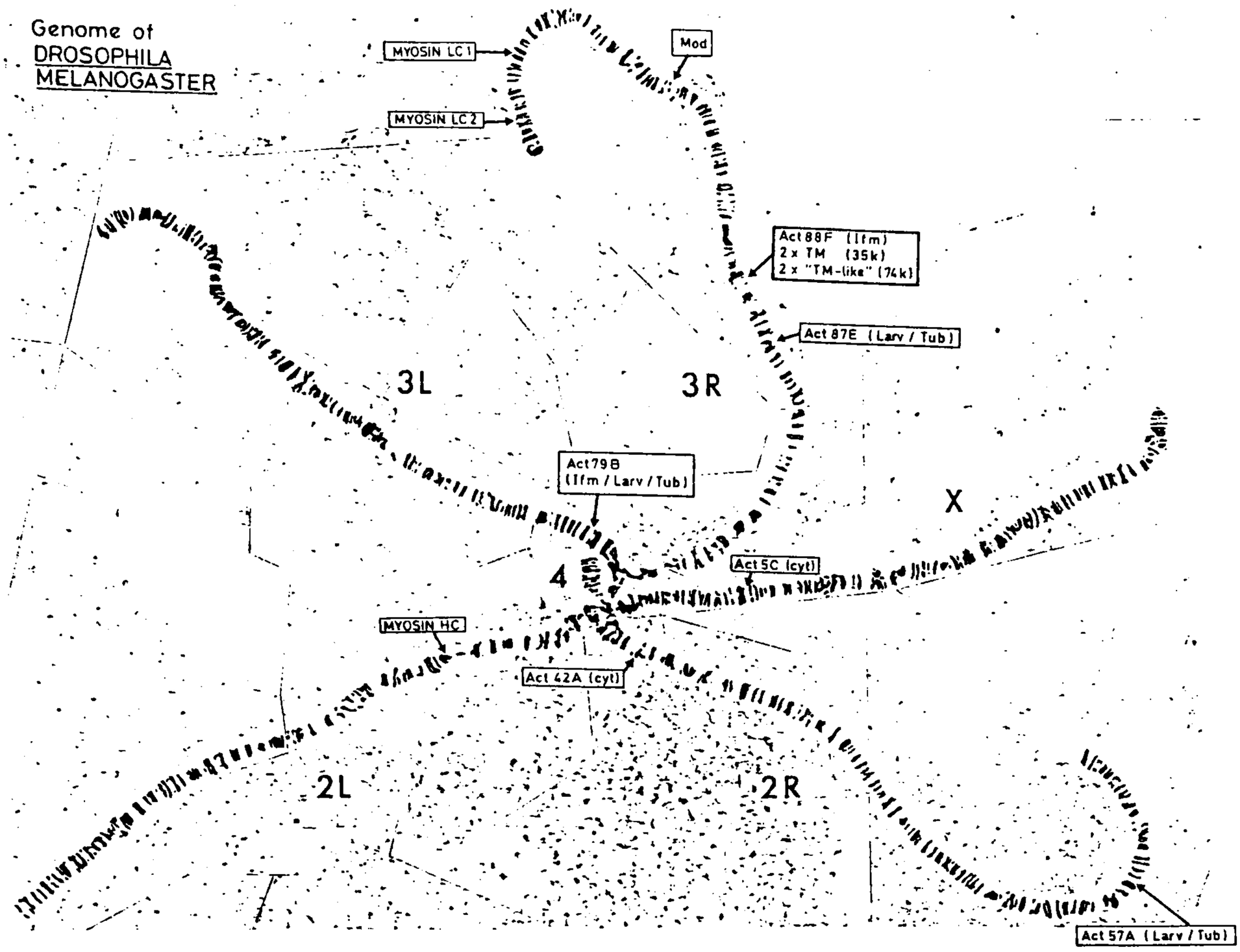

FIGURE 6.2

The genome of Drosophila melanogaster the position of the flight muscle protein genes that have so far been identified are shown labelled on the four chromosomes.
The number and letter code for each gene refers to its physical position within the genome.

	Chromosomal region	
Chromosome	Number	Letter (subdivision)
X	1 - 20	A - F
2L	21 - 40	"
2R	41 - 60	"
3L	61 - 80	"
3R	81 - 100	"
4	101 - 102	"

(i.e. Act88F is located in the most distal part of region 88, on chromosome 3R)

6.4 METHODS :

The production, isolation and identification of the Drosophila melanogaster mutants was performed at York by Drs. E. Ball & J.C. Sparrow.

6.4.1 Production of Flies with Mutant Flight Muscle :

Flies with IFM specific mutations were isolated by two genetic techniques.

a) Random chemical mutagenesis and selective breeding :

Drs. E. Ball and J.C. Sparrow, induced mutations with the chemical mutagen, ethyl-methane sulphonate (EMS). The level of mutagenesis, on average, induced a single base change per chromosome. The progeny of these flies were screened for flightlessness and analysed for changes in muscle structure and altered muscle proteins. The muscles were viewed by phase contrast microscopy and the proteins were analysed by two dimensional gel electrophoresis. These methods produced an interesting flightless actin mutant *Act88F*^{M342} (The mutant is hereafter designated *M342*) (Ball et al., 1987).

b) Germ-line transformation to make chimeric genes :

Mutants with chimeric actin genes were obtained from the laboratory of Dr. E.A. Fyrberg (Johns Hopkins University, Baltimore, U.S.A.). Chimeric genes were produced by using recombinant DNA techniques to splice lengths other actin genes into the *Act88F* gene. The altered genes were then introduced into flies lacking functional *Act88F* copies (*Act88F*^{km88}) by P-element transformation (Rubin & Spradling, 1982). Four chimeras were available, they all contained flanking regions of *Act88F* with inserts from other actin genes.

i) *Act88F/Act79B*
ii) *Act88F/Act57A*
iii) *Act88F/Act42A*
iv) *Act88F/Yact* (yeast actin)

Dr. Fyrberg's laboratory also provided another mutant *mod*$^{-}$. This fly was judged as having impaired flight ability (Fyrberg, E.A. Pers. comm.), but was not tested by the method described in Section 6.4.2. The mutants lack a protein associated with the post-translational modification of IFM actin.

A spontaneous flightless mutation *raised*, with a 'wings-up' phenotype, was isolated by Ives (1945). This mutant had grossly aberrant muscle structure. Mahaffey (1985), partially 'rescued' this phenotype by germline transfection with a copy of the wild-type *Act88F* gene. It transpired that the original *raised* strain contained two distinct mutations; one in a non-coding part of the *Act88F* gene, the other mapped to region 97B (see Figure 6.2). The exact nature of the 97B mutation is still not known (Mahaffey et al., 1985). The 97B mutation blocks the post-translational modification of actin isoform II (found in other muscle tissues) to actin isoform III (the isoform present in the IFMs). For this reason the mutant allele was given the abbreviated gene symbol *mod*$^{-}$ (The mutant is hereafter designated *mod*). The events leading to actin III formation are shown below (Scheme 6.1):

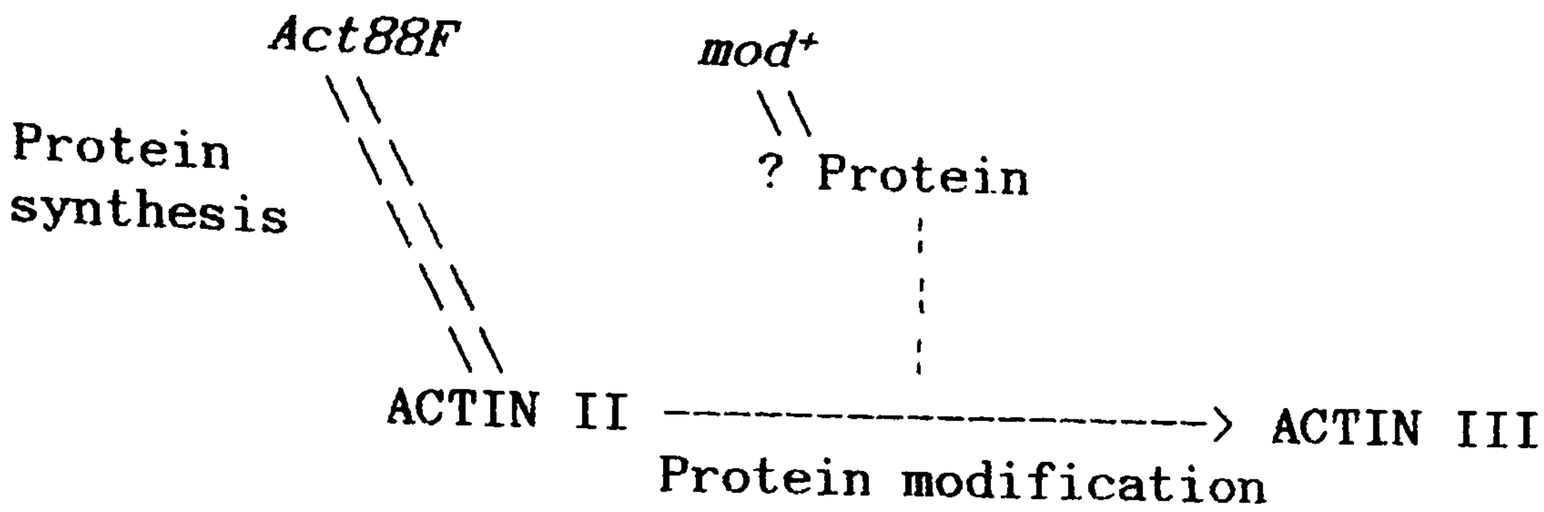

Scheme 6.1
Formation of two actin isoforms in the muscles of Drosophila melanogaster (Mahaffey et al., 1985).

With the exception of *mod*, changes in the amino acid sequence were determined by DNA sequencing of the coding region of the *Act88F* gene. The changes are summarised in Figure 6.3a and 6.3b.

6.4.2 A Test of *in vivo* Muscle Performance :

An immediate test of whether the genetic mutations are of functional importance consists of flight-testing the adult flies. Flight-testing was performed by Drs. E. Ball and J.C. Sparrow. The flies were thrown down a 10cm diameter glass cylinder, coated with a sticky lining. Flightless flies fall straight down (into a collecting jar) and the wild-type flies become stuck to the lining of the tube (Green et al., 1986).

6.4.3 Mechanical Testing of D. melanogaster Flight Muscle :

Skinned fibres from the DLM were used for the mechanical experiments. The flies were dissected, the muscles glycerol extracted and then mounted on the mechanical test apparatus, as described in Chapter 2. The muscle fibres were skinned for a minimum of 4 hours and were always used within 2 weeks of extraction.

Protocol :

The muscle fibres were first incubated in relaxing solution containing a creatine phosphate/creatine kinase ATP backup system

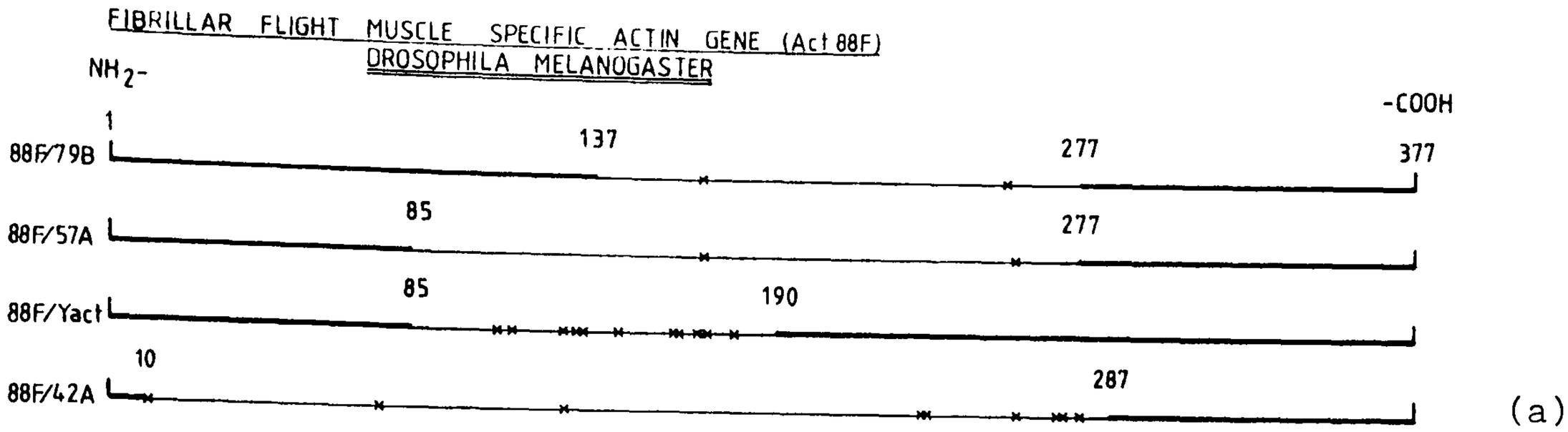

(b)

	10	76	93	110	114	129	132	135	144	166	162	167	169	170	178	232	234	257	260	271	274	278
88F/88F	Ile	Ile	Glu	Leu	Ala	Ser	Met	Ala	Ala	Ser	Thr	Glu	Phe	Ala	Leu	Ala	Thr	Cys	Ala	Ser	Ile	Val
88F/79B													Tyr					Thr				
88F/57A													Tyr						Ser			
88F/yact				Met	Ser	Val	Phe	Ser	Ser	Thr	Val	Ala		Ser	Ile							
88F/42A	Val	Val				Thr										Ser	Ser		Ser	Ala	Leu	Thr
M342			Lys																			

FIGURE 6.3

Changes to the amino acid sequence in the mutant: M342, 88F/79B, 88F/57A, 88F/Yact and 88F/42A.
Part a shows the position of the DNA insects (thin lines) and the position of amino acid changes within those inserts. Part b shows the nature of the amino acid substitutions. All the changes were determined by DNA sequencing of the coding region of ACT88F, performed in the laboratory of Dr. Fyrberg (Baltimore, USA).

(Table 2.2b). The muscle length was carefully adjusted, using the tension transducer micromanipulator, until the fibre was just taut (just at zero tension). A series of brief step length changes were performed on a fast time base (5ms/division) to establish that the muscle was truly at zero tension (by a step release of 1%) and that it was well connected (by a step stretch of 1%). The relaxing solution was then washed out of the bath with 250µl of activating solution. The tension change relative to zero tension was determined with a step release (of 1-2%). The fibre was then subjected to a series of length step stretches and the delayed tension response, if present, was recorded, usually on a time base of 5 or 10ms/division. Finally the activating solution was washed out of the bath with 4 mls of rigor solution and the fibre was left for 5-10 minutes. The tension change was determined by a step release and the stiffness by a brief stretch.

The sequence of length changes is summarised schematically in Figure 6.4.

6.4.4 *mod* :

mod was the first mutant to become available. The homozygous strain provided by Dr. Fyrberg's laboratory contained an additional mutation (as a genetic marker) called 'stubloid'. One unfortunate aspect of this mutation is that it causes many of the adult flies to have damaged wings. It was therefore not possible to flight test the adult flies using the method of Green et al. (1986). Muscle fibres from three individuals were tested mechanically. Because it was unknown whether the adult flies were able to fly this was a 'blind trial' of muscle function.

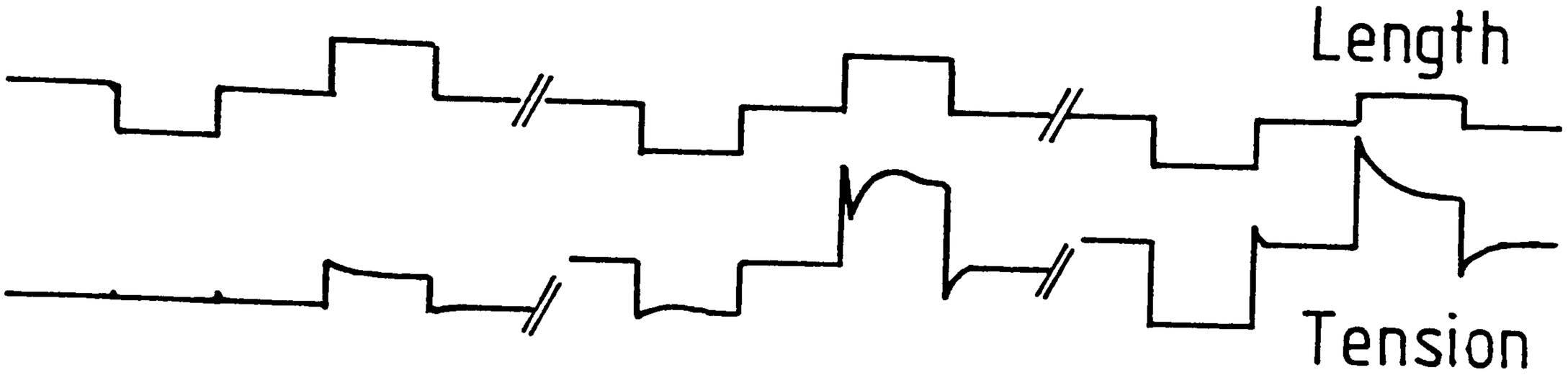

The Series of Length Changes Used to Test the Mechanical Properties of Flight Muscle from <u>D. melanogaster</u>
(Schematic)

FIGURE 6.4

Experiments were performed using the solutions of Table 2.2b. In order to measure the instantaneous stiffness of the muscle fibres, a fast oscilloscope time base was selected and the tension change was plotted against length over the course of the length step ramp.

The active response was monitored on a timebase of 5-10ms/div this allowed the rate constant of the delayed tension transient to be fit by the curve fitting program DISCRETE (Provencher, 1977).

6.4.5 The Chimeras and M342 :

In order to produce self-consistent results, all the chimeras were tested in a single series of experiments. A set routine of dissection, extraction and mechanical testing was adopted.

Six individuals of each mutant stock were dissected and the best half-thorax of each individual was glycerol-extracted overnight. Fibre preparations that did not produce reasonable tensions in relaxing solution were discarded. A fibre preparation was tested from each of the six individuals. Each preparation was scored by visual inspection of the oscilloscope traces obtained in relaxing, activating and rigor solutions. With the exception of *M342*, the mechanical measurements were made before the results from the flight testing were disclosed. The mechanical results were analysed, therefore, as a blind-trial of muscle function.

Initial experiments showed that the stiffness of *M342* muscle fibres was very nearly the same in all three test solutions. Mechanical experiments were performed on five *M342* and five wild type fibres, from separate individuals. The mechanical response of the fibres in each solution was tested in the usual way by applying small, rapid ("step"), changes of length and recording the resulting timecourse of the change in tension. The rise time of the applied length change was about 400 μs. The *instantaneous stiffness* of the fibre in any given solution was measured by plotting the tension versus the length during the step, and determining the slope at the steepest part of the curve. In order to normalise the data the number of thick filaments in the fibre cross-sections was estimated.

At the end of each mechanical experiment the muscle fibre was fixed with gluteraldehyde (3% in 100 mM sodium phosphate buffer, *p*H 7.0) while still attached to the apparatus. The fibre was then post-

fixed in 1% osmium tetroxide, dehydrated in a series of acetone solutions and embedded for microscopy in Araldite. Thin cross-sections were stained with lead citrate and uranyl acetate and electron micrographs were taken; from these the average number of thick filaments per myofibril was estimated. Thick cross-sections were stained with toluidine blue O (Sigma); from light photomicrographs the total number of myofibrils in each preparation was counted. The preparations used had between 400 and 1600 myofibrils. I am indebted to Mrs M. Stark (University of York) who performed all of the microscopy.

6.6 RESULTS :

6.6.1 *mod* :

The mechanical response of the muscle preparations from the three individuals tested was very similar to wild-type. The active response from one of the individuals is compared with wild-type in Figure 6.5. The measured rate constant for the delayed tension process was $254s^{-1}$. Table 6.1 compares the measured rate constants for delayed tension in wild type and *mod*, the significance of these results is discussed later.

Wild-Type	*mod*
$206\ s^{-1}$	$254s^{-1}$*
$192\ s^{-1}$	$272s^{-1}$*
$195\ s^{-1}$	$273s^{-1}$
	$169s^{-1}$
Mean ±S.E.M. $197\pm4s^{-1}$	$242\pm25s^{-1}$

*Same individual

Table 6.1
Measured rate constant for the delayed tension transient in activating solution (@15°C.) for the mutant *mod* compared with wild-type.

D.melanogaster Wild Type

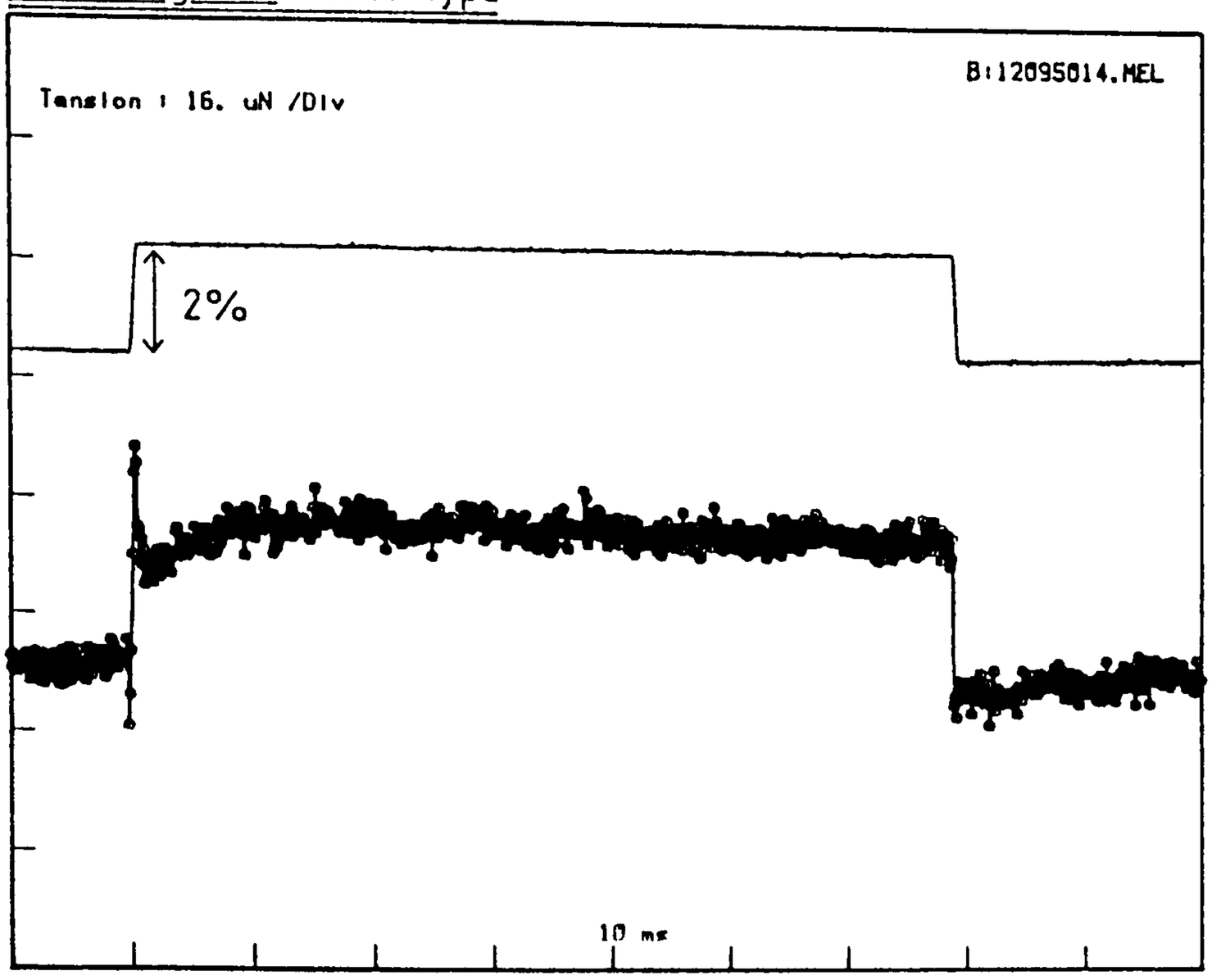

D.melanogaster MOD⁻

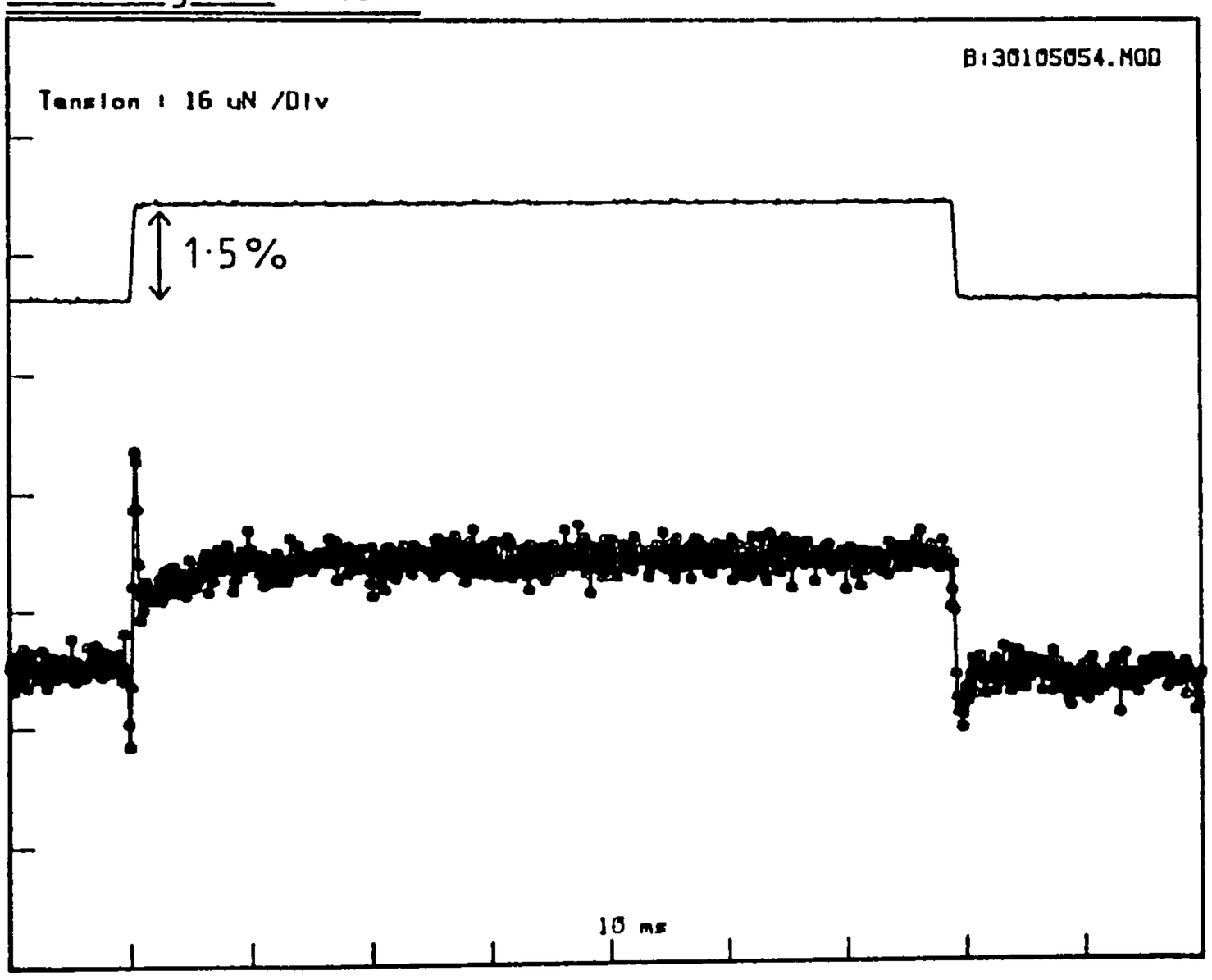

FIGURE 6.5

Active transient tension response to a step length change measured in wild type and the mutant mod. The fitted rate constants to the delayed tension transients were: Wild type : 192 s^{-1}

mod : 254 s^{-1}

6.6.2 *M342* :

Muscle fibres from *M342* behaved very differently upon dissection. They were easier to mount than the wild-type fibres because they did not fray into myofibrils to such a great extent. Electron micrographs of the fibre cross-sections showed that the myofibrils were less coherent than the wild type and on average contained fewer thick filaments (see Table 6.2).

The instantaneous stiffness of wild type fibres when relaxed, active and in rigor is significantly different (one way Analysis of Variance ; P < 1%) (data shown in Table 6.3). There was no significant difference in stiffness between *M342* fibres measured when relaxed and active however the stiffness of fibres when in rigor was significantly greater (P < 1%).

	WILD TYPE			*M342*		
	Mean	SEM	Highest	Mean	SEM	Highest
Relaxed	31.6	8.1	81	17.3	5.2	37
Active	47.8	14.6	149	18.1	5.6	37
Rigor	125.1	29.9	386	48.6	24.7	169

Table 6.3

Instantaneous stiffness of *Oregon* and *M342* fibres in the relaxed and rigor states.

Tension versus length plots used to calculate the instantaneous stiffness of the fibres are shown in Figure 6.6.

The full mechanical response of both *M342* and wild type fibres is shown in Figure 6.7, for each of the three test solutions. When these experiments were performed the quality of the data was the best that I

M342			Wild type		
MEAN	STDEV	N	MEAN	STDEV	N
480	124.4	(15)	946	34.3	(7)
427	134.9	(12)	994	65.8	(7)
425	166.3	(17)	864	53.2	(6)
509	180	(13)	744	84.3	(11)
756	210.3	(13)	771	20.04	(10)
			831	76.5	(8)
			831	35.2	(4)
			876	191.5	(4)
			1088	49.2	(4)
			1048	24.2	(5)
519	55	(5)	899	35	(10)

Table 6.2

Mean number of myofilaments per myofibril; counted in both *M342* and wild type fibre preparations used for mechanical experiments.

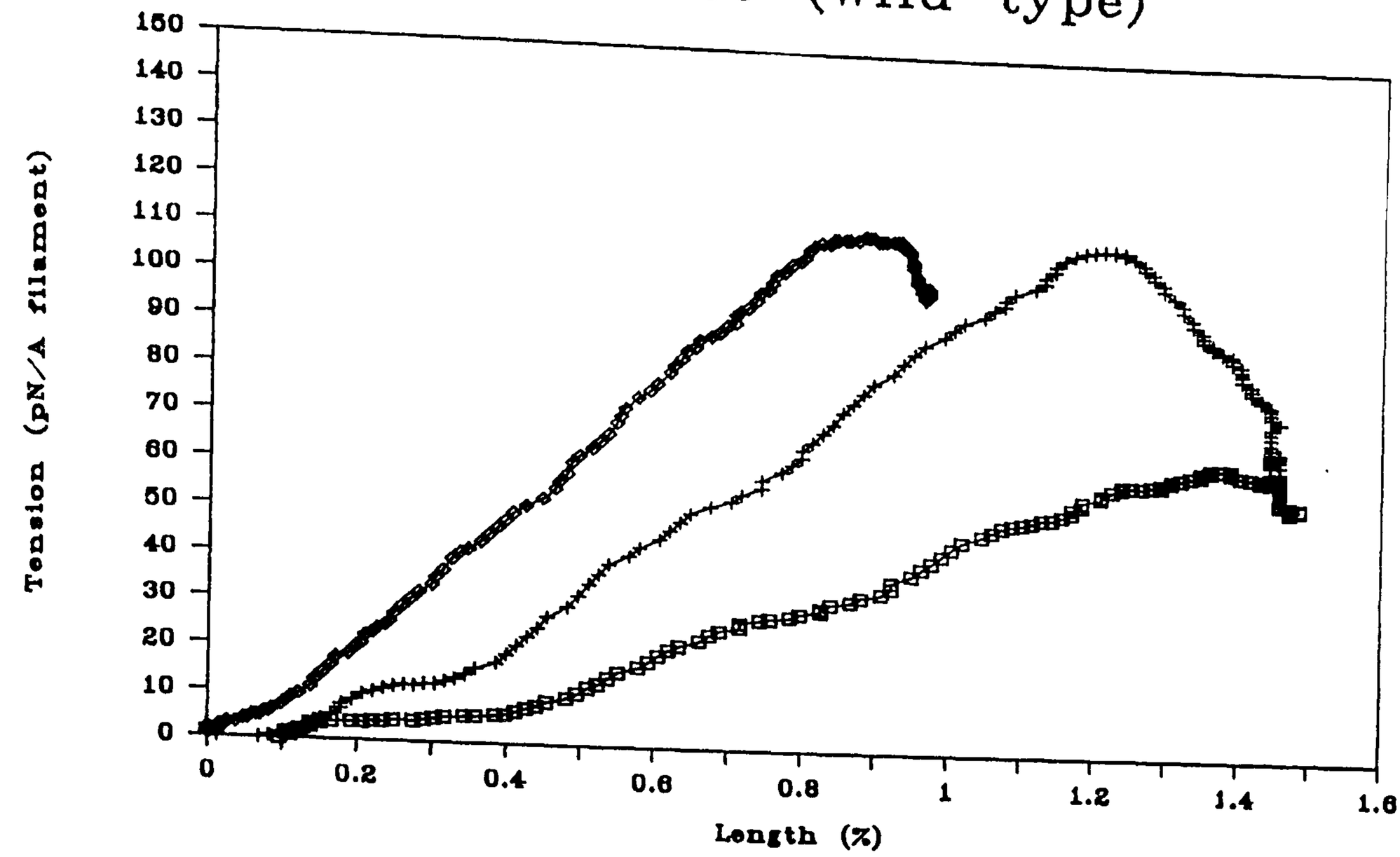

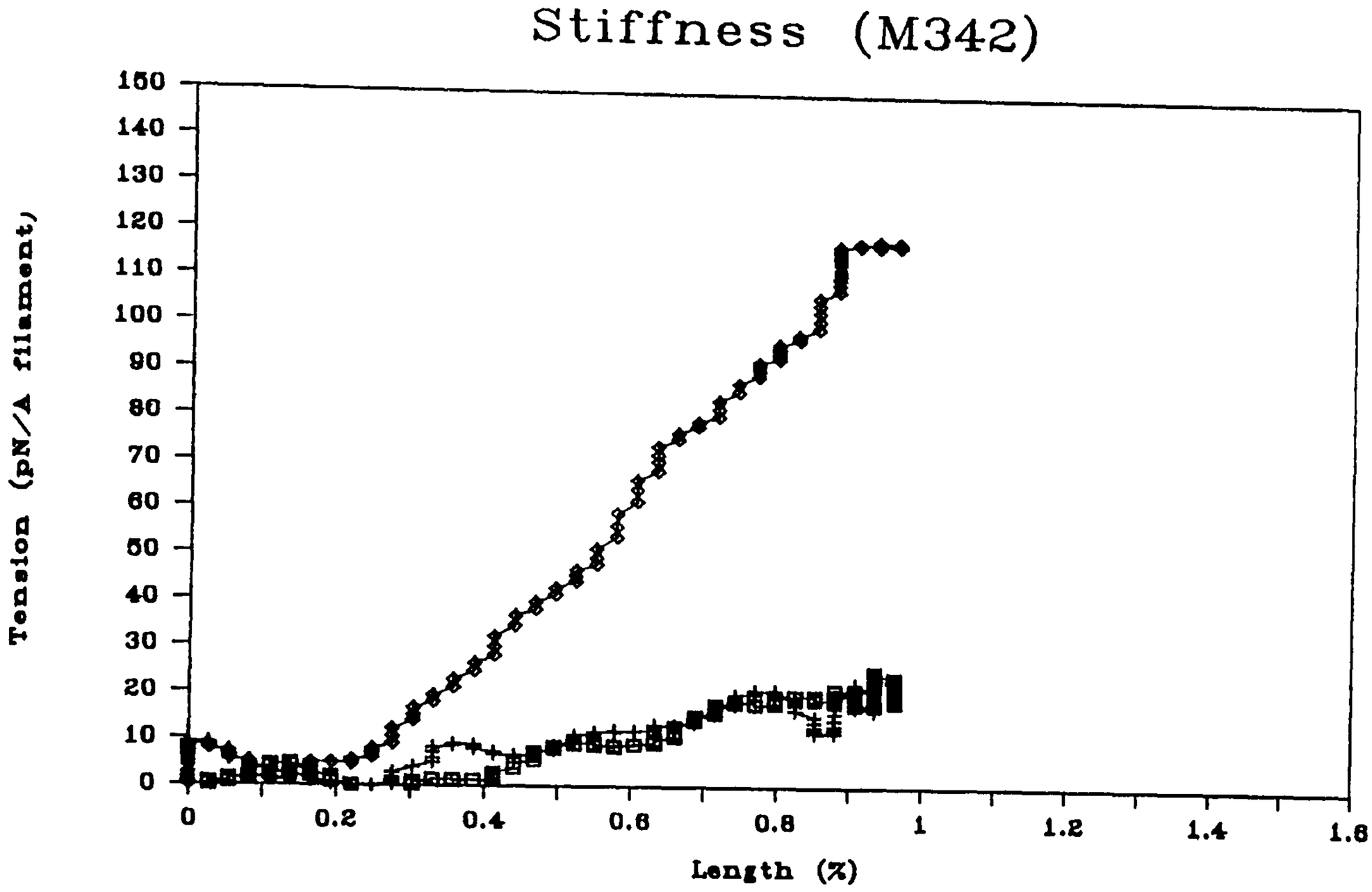

FIGURE 6.6

Tension-length diagrams for D. melanogaster wild type and mutant M342. The tension has been plotted during the course of the step length change (rise time = 400us). The gradient of the lines is equal to the instantaneous stiffness of the muscle fibres.

The stiffness of M342 muscle is the same in activating and relaxing solution, but increassed in rigor. The stiffness of wild type muscle increases from relaxed to active to rigor.

(□) = Relaxing solution

(+) = Activating solution

(◇) = Rigor solution

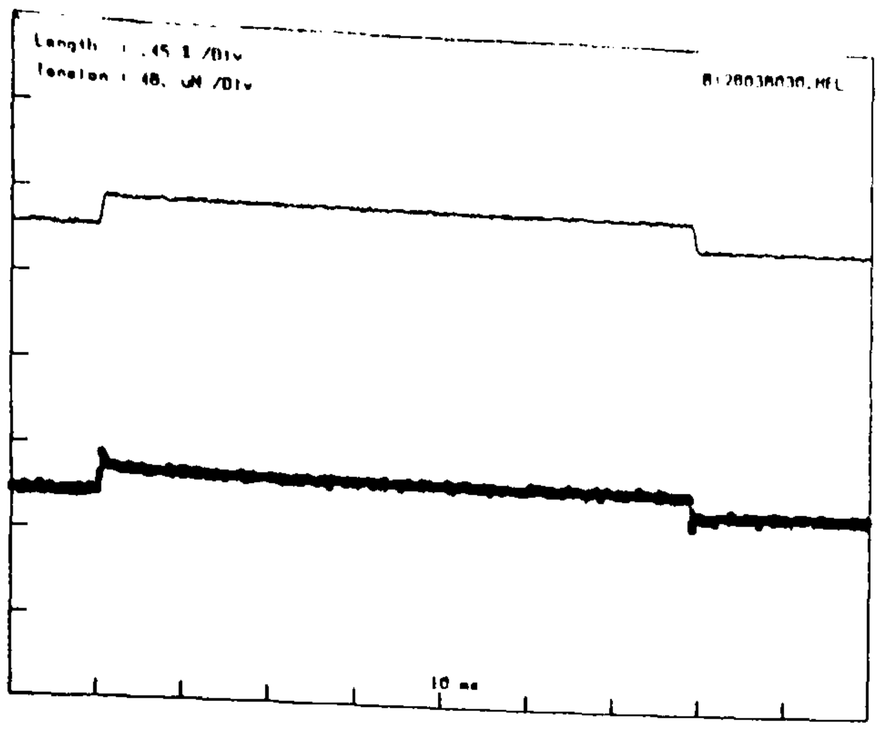

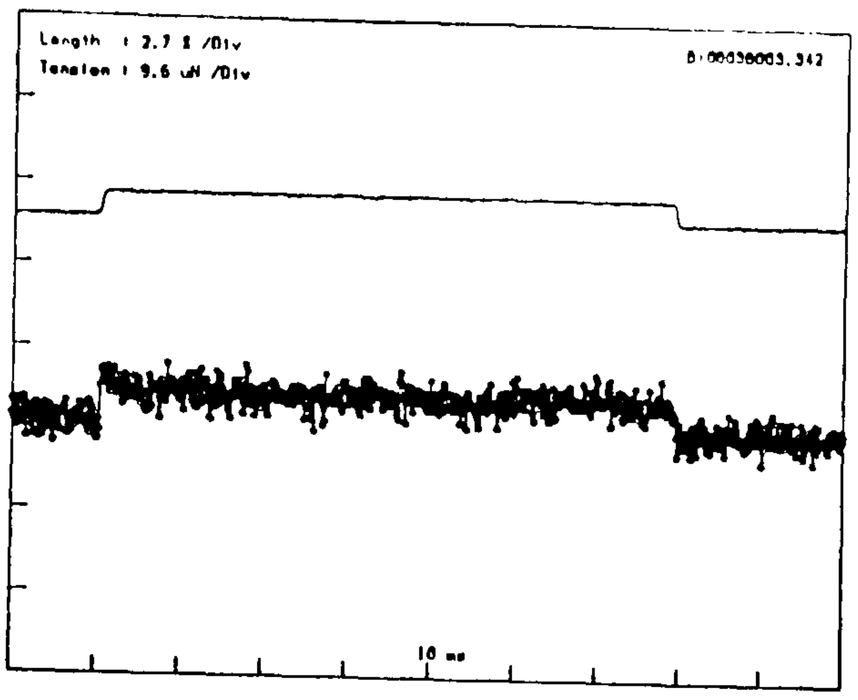

RELAXED

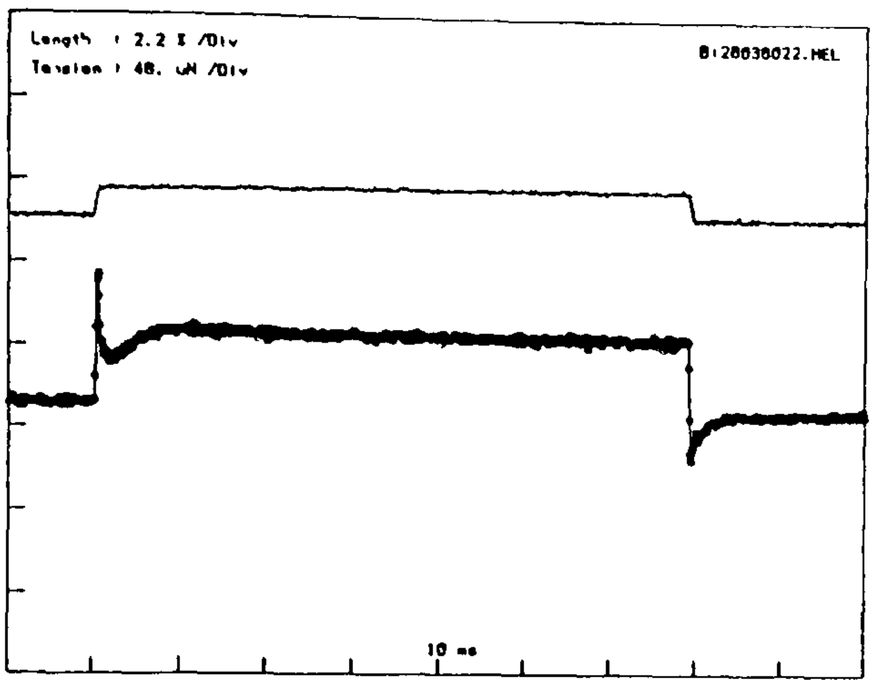

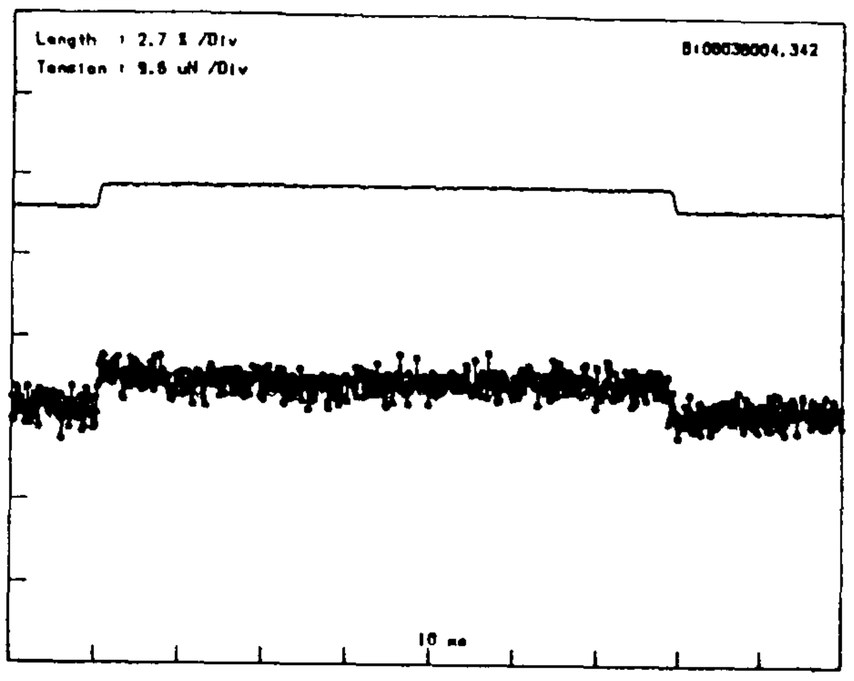

ACTIVE

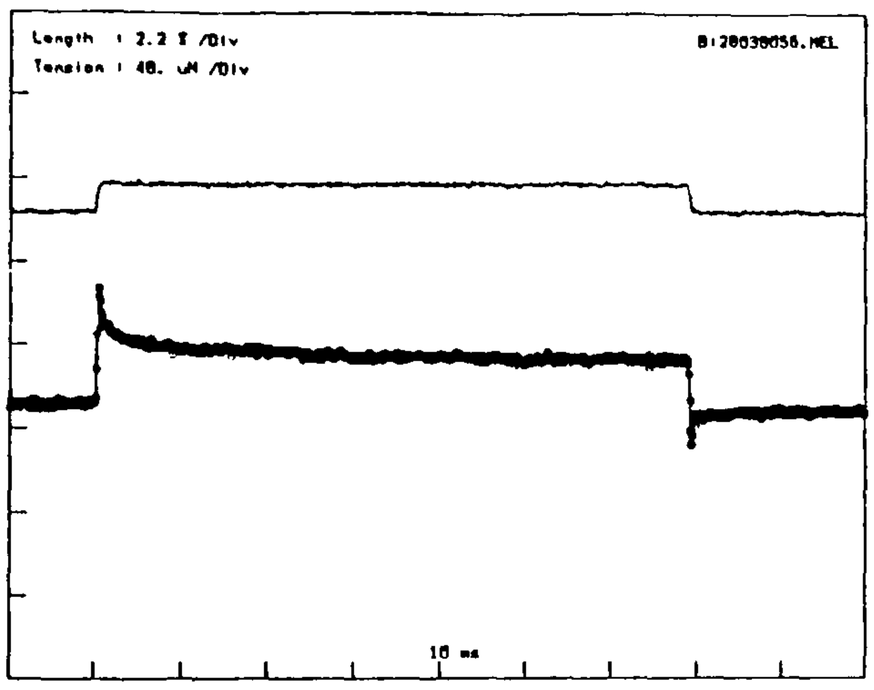

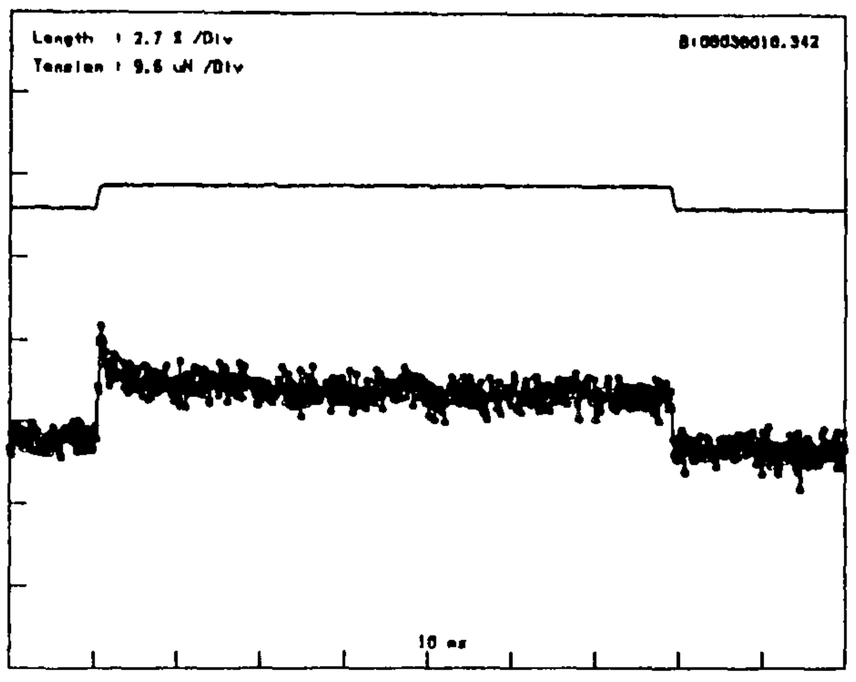

RIGOR

WILD TYPE

M342

FIGURE 6.7

Comparison of the relaxed, active and rigor tension transients measured in wild type and mutant M342 muscle.
The delayed tension response is absent in M342, however, there is an increase in stiffness in rigor solution in the mutant muscle.
The wild type response shown here is particularly good and should not be compared with series of experiments performed on other mutants.

have obtained and the wild type responses shown here should not be compared with mutants tested at other times (i.e. the following experiments).

6.6.3 The Chimeras :

Act88F/Act88F (wild-type)

The wild-type response, at the time that these tests were made, showed 70% of the preparations to be active (delayed tension). Also, 85% showed a good rigor response (at least a doubling of stiffness over the active level). The wild type, active delayed tension response, although not as impressive as for the *mod* and *M342* experimental series, is still clearly visible. A representative set of results is shown in Figure 6.8a.

Act88F/Act79B

The 79B actin sequence codes for muscle actin found in adult tubular muscle (found in the legs and head of the fruit fly (Fyrberg, 1983)). The chimeric actin sequence contains 2 amino acid substitutions (see Figure 6.3). The homozygous adults are flighted. Four out of the six fibres tested showed a delayed tension transient and five showed an increase in stiffness in rigor. A representative result from the mechanical testing is shown in Figure 6.8b.

Act88F/Act57A

The 57A actin gene codes for muscle actin found in the larval body wall muscle (Fyrberg, 1983). The chimeric actin sequence has two substitutions (one being the same as in *Act88F/Act79B*). Upon flight testing, half of these flies were able to fly. Four out of the six fibres tested showed delayed tension and five an increase in stiffness in rigor. Results from mechanical testing are shown in Figure 6.8c.

88F/88F

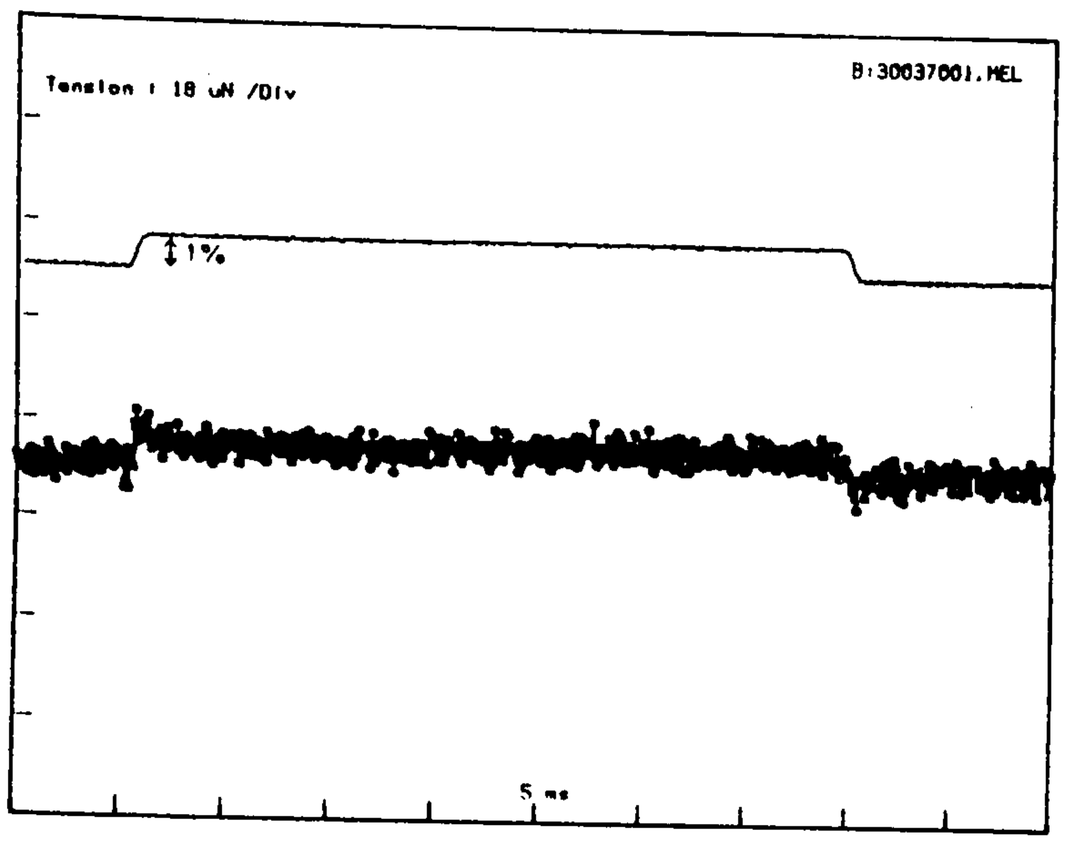

RELAXED

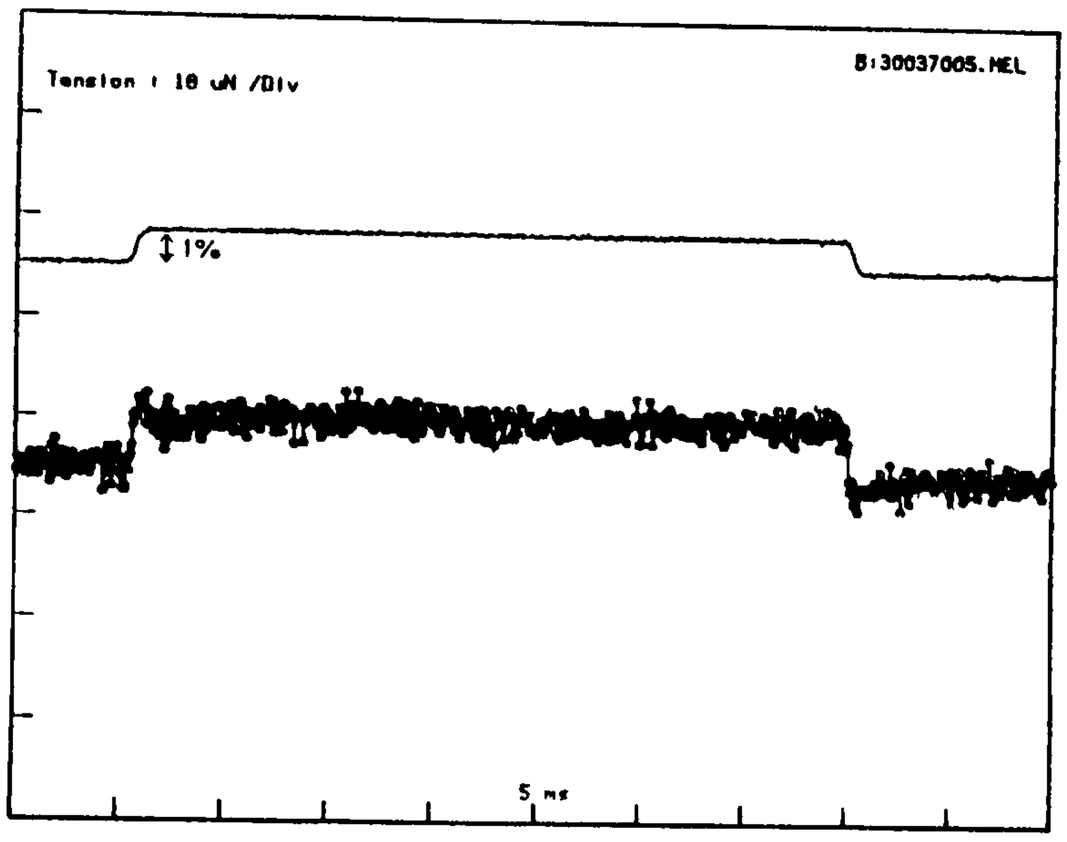

ACTIVE

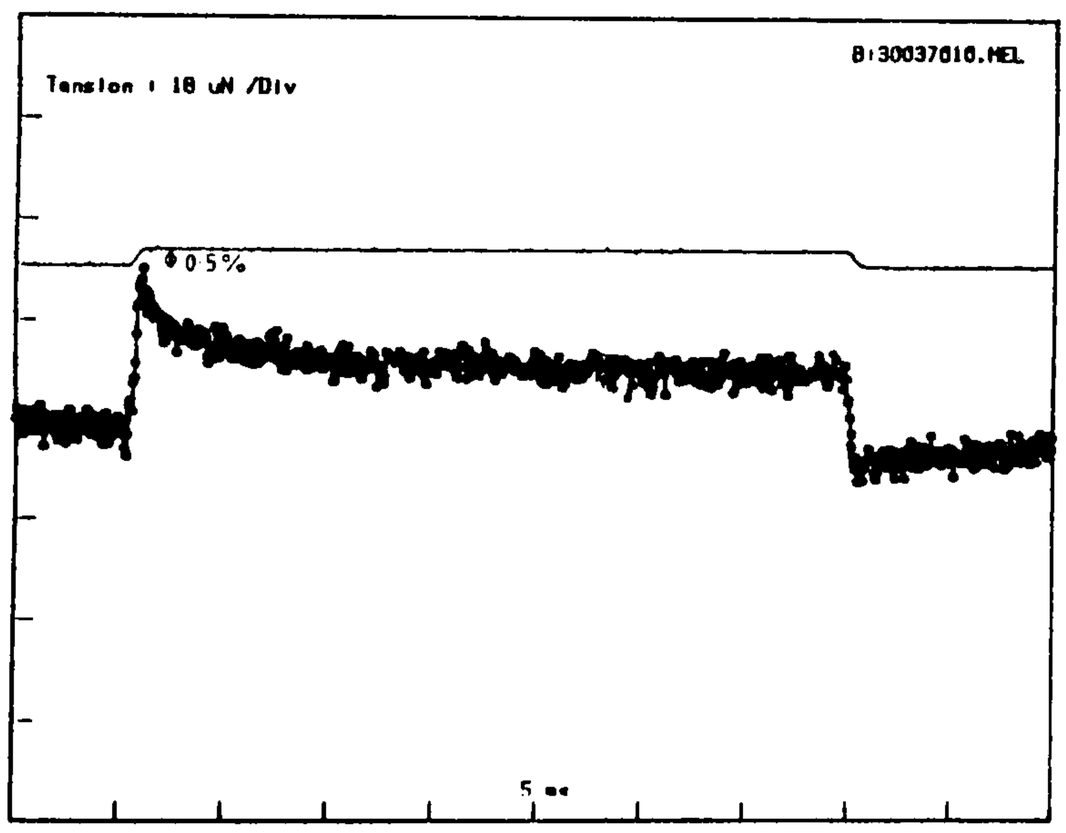

RIGOR

FIGURE 6.8 (a)

WILD TYPE response obtained at the time the chimeras were tested. Note that the delayed tension transient in activating solution is present (although of rather small amplitude). There is an increase in stiffness in rigor solution (note the smaller length change in that record).

88F/79B

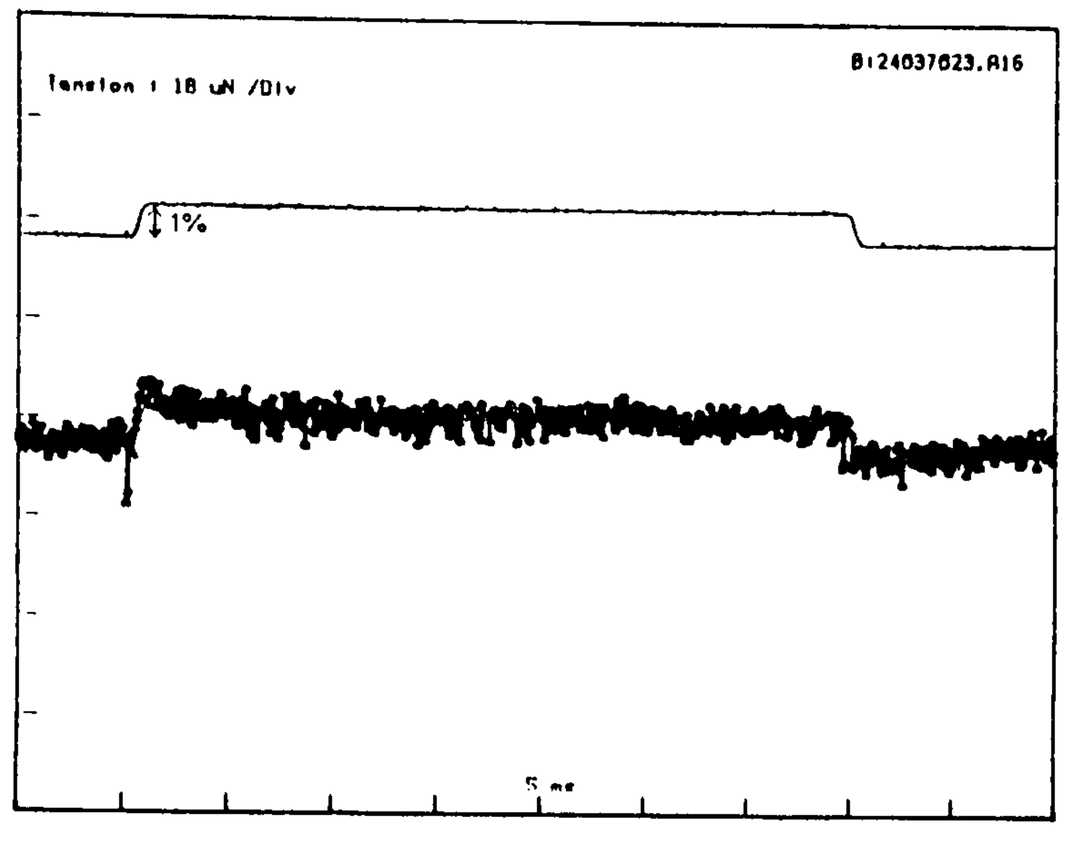

RELAXED

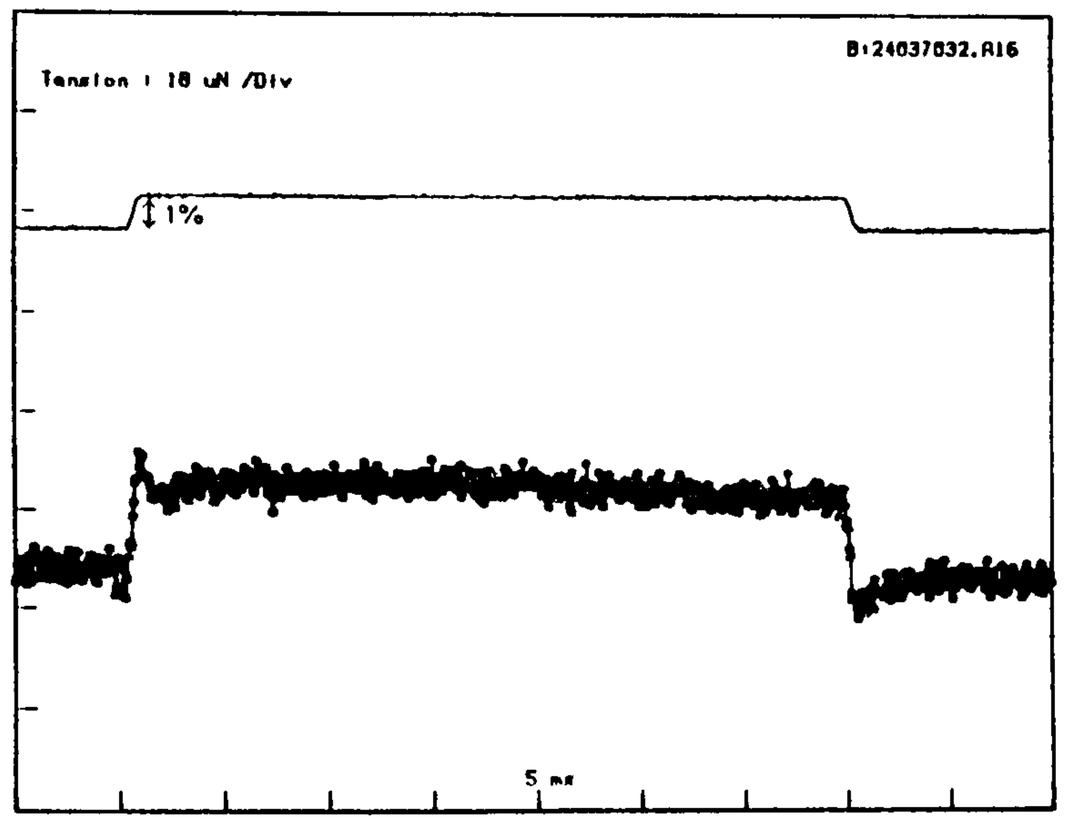

ACTIVE

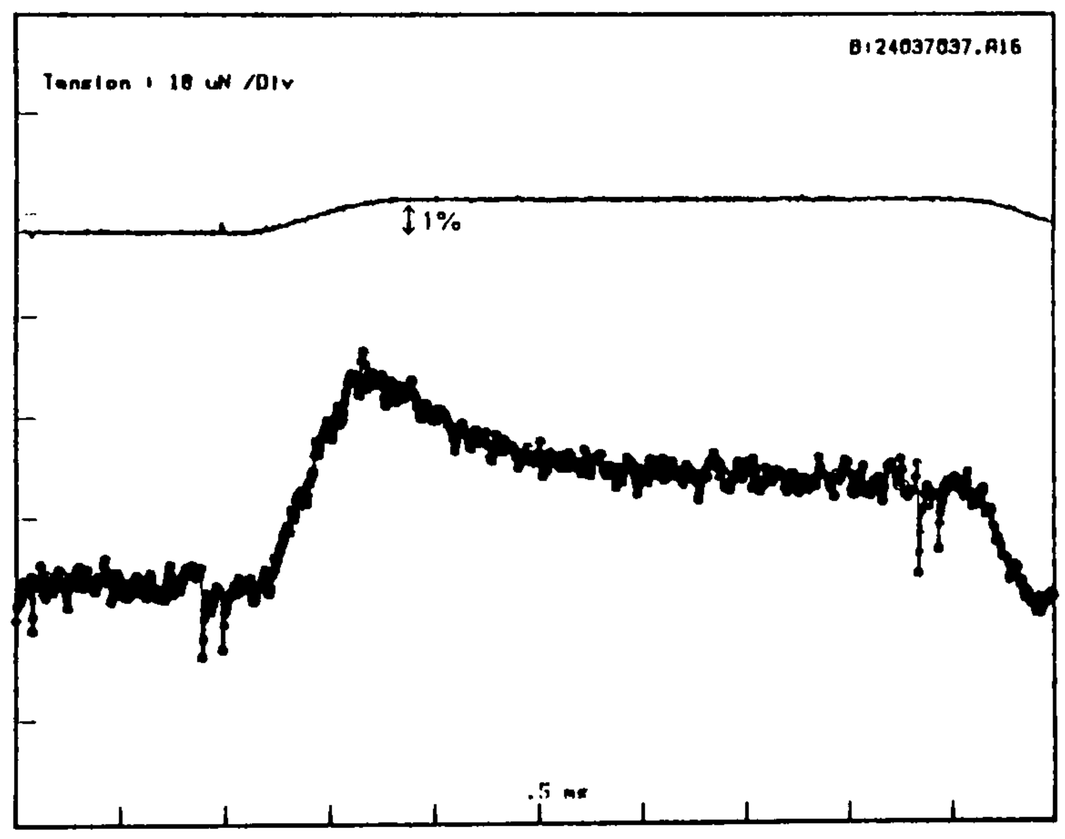

RIGOR

FIGURE 6.8 (b)

CHIMERA 88F/79B transient tension responses obtained in the three test solutions (compare with Figure 6.8(a))

88F/57A

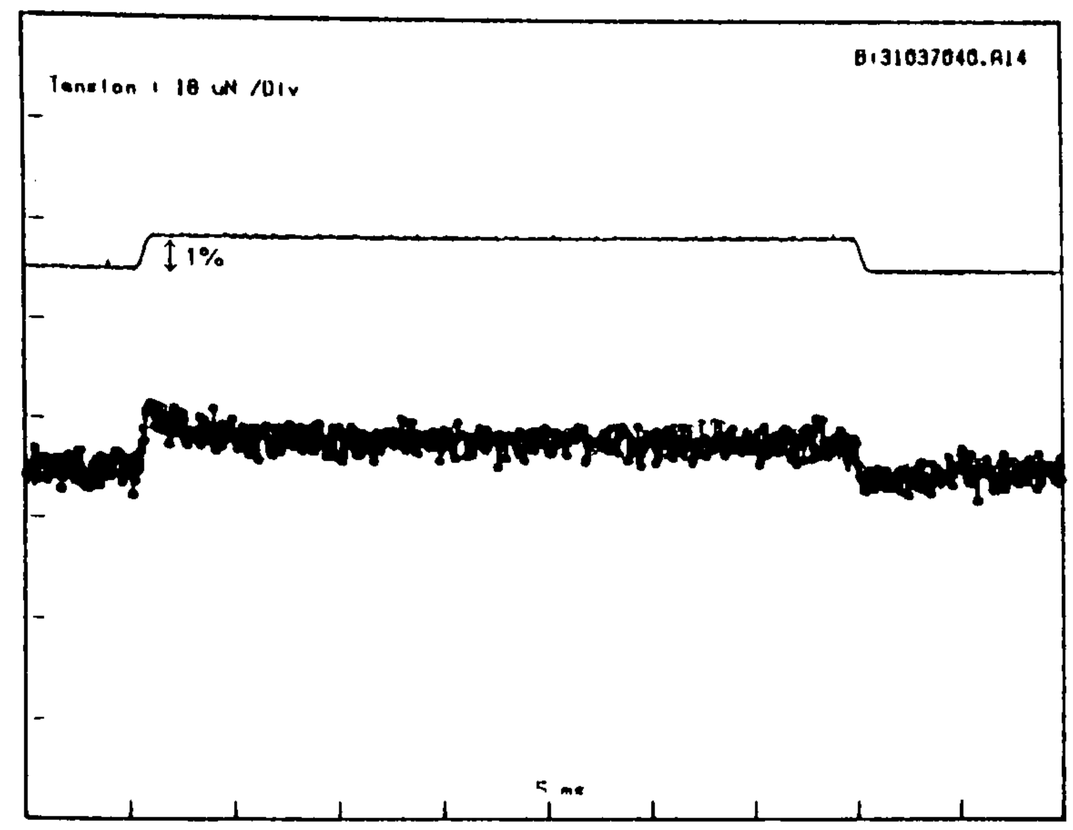

RELAXED

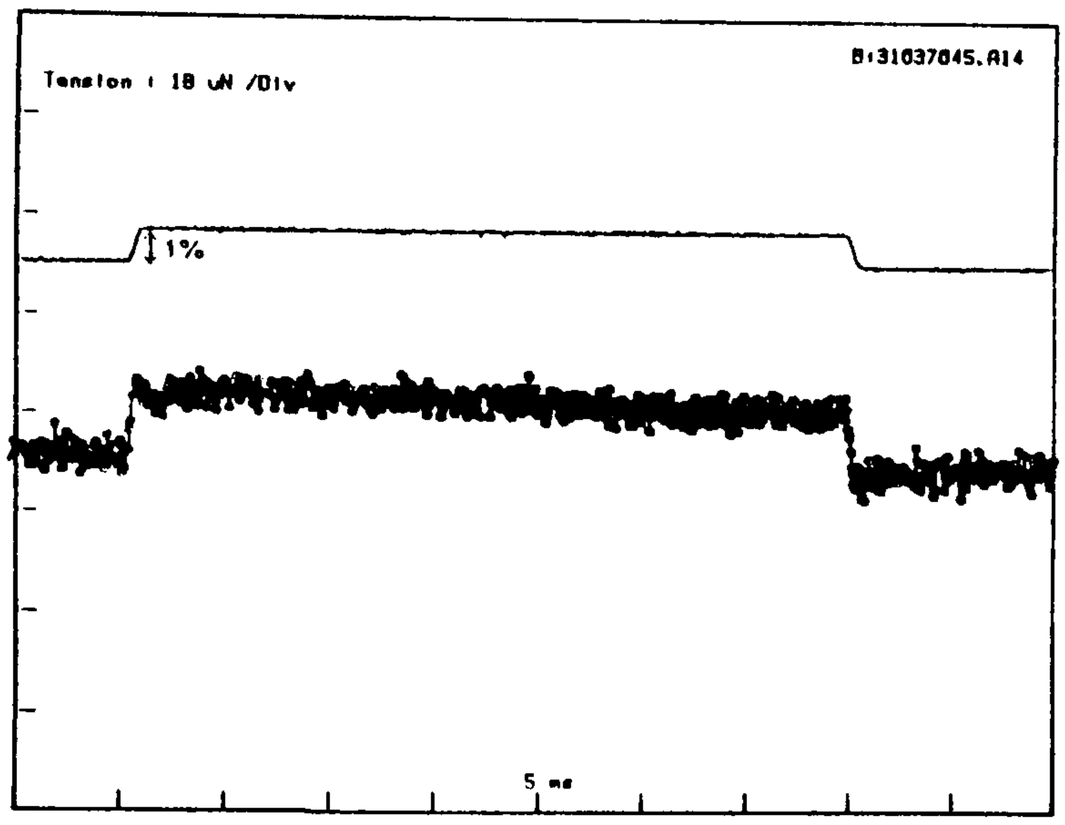

ACTIVE

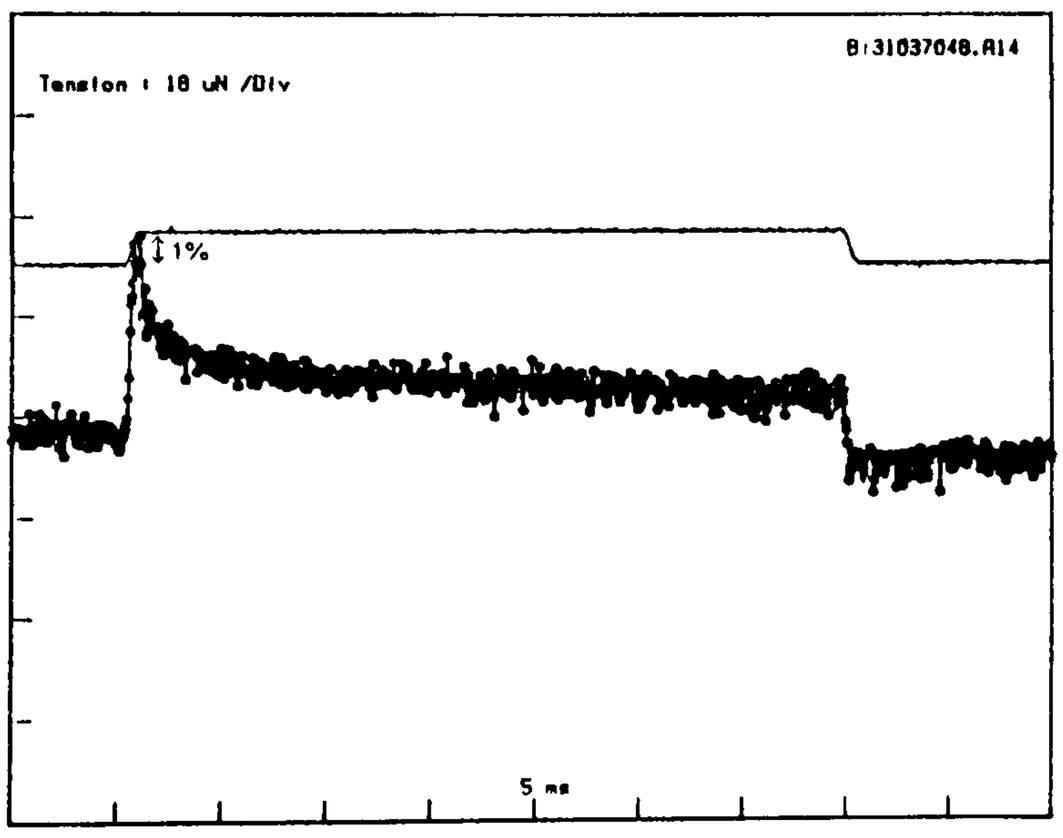

RIGOR

FIGURE 6.8(c)

CHIMERA 88F/57A transient tension responses obtained in the three test solutions (compare with Figure 6.8 (a)).

Act88F/Yact

The Yact actin gene is from yeast actin, which is a cytoplasmic actin. The chimera has a total of 11 substitutions and the adult flies are nearly all flightless. However, some of the small flies are able to fly. The muscle tissue teased more easily upon dissection, in a manner similar to *M342*. Two out of the six fibres showed delayed tension and five a rigor response. Results from mechanical testing are shown in Figure 6.8d.

88F/42A

The 42A actin gene codes for cytoplasmic actin in Drosophila (Fyrberg, 1983). There are 9 amino acid substitutions in this chimera. None of the fibres showed delayed tension, but four showed a rigor response. The adult flies are completely flightless, mechanical results are shown in Figure 6.8e.

The results from the mechanical and *in vivo* flight testing are summarised in Figure 6.9.

6.7 DISCUSSION :

There was a major problem in estimating the cross-sectional area of the muscle preparation between the 'T' clips. The very small fibre size made sectioning of the fibres very difficult and time consuming. For this reason all the measured tensions, except for those in the series of experiments performed on *M342*, were quoted as absolute values. The diameter of the fibre preparations was kept as near constant as possible (at about 80μm). A further difficulty arising from the short muscle length was the effect of 'end compliance'. Because of damage, the crimped ends of the fibre are more compliant than the rest of the preparation. The length change measured at the

88F/Yact

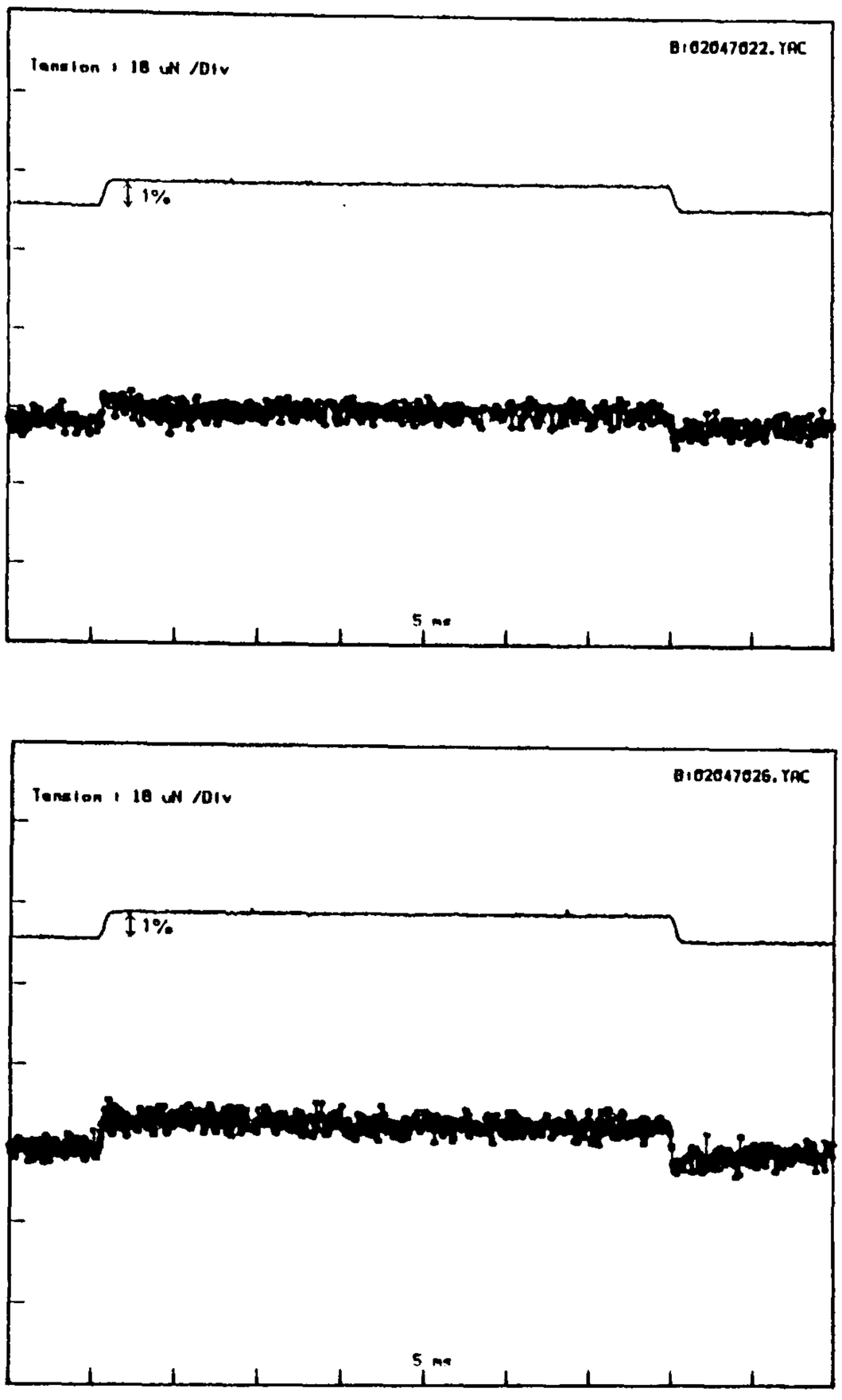

RELAXED

ACTIVE

RIGOR

FIGURE 6.8 (d)

CHIMERA 88F/Yact transient tension responses obtained in the three test solutions (compare with Figure 6.8 (a)).

88F/42A

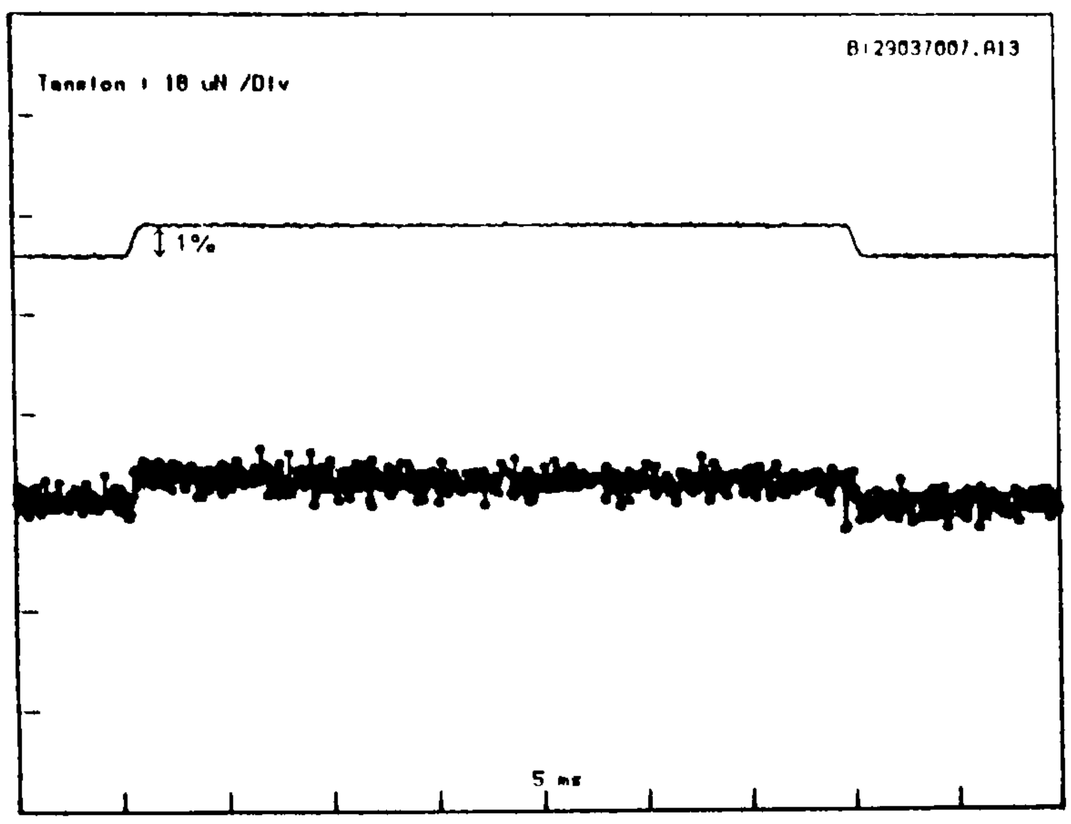

RELAXED

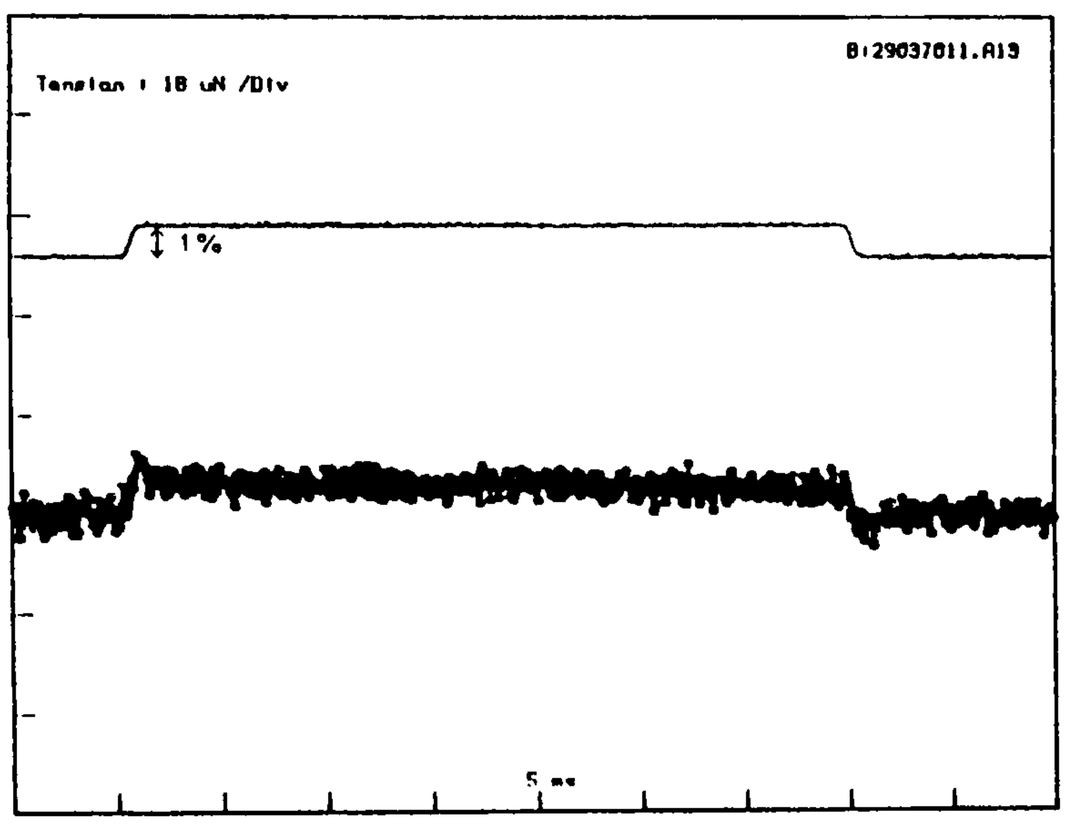

ACTIVE

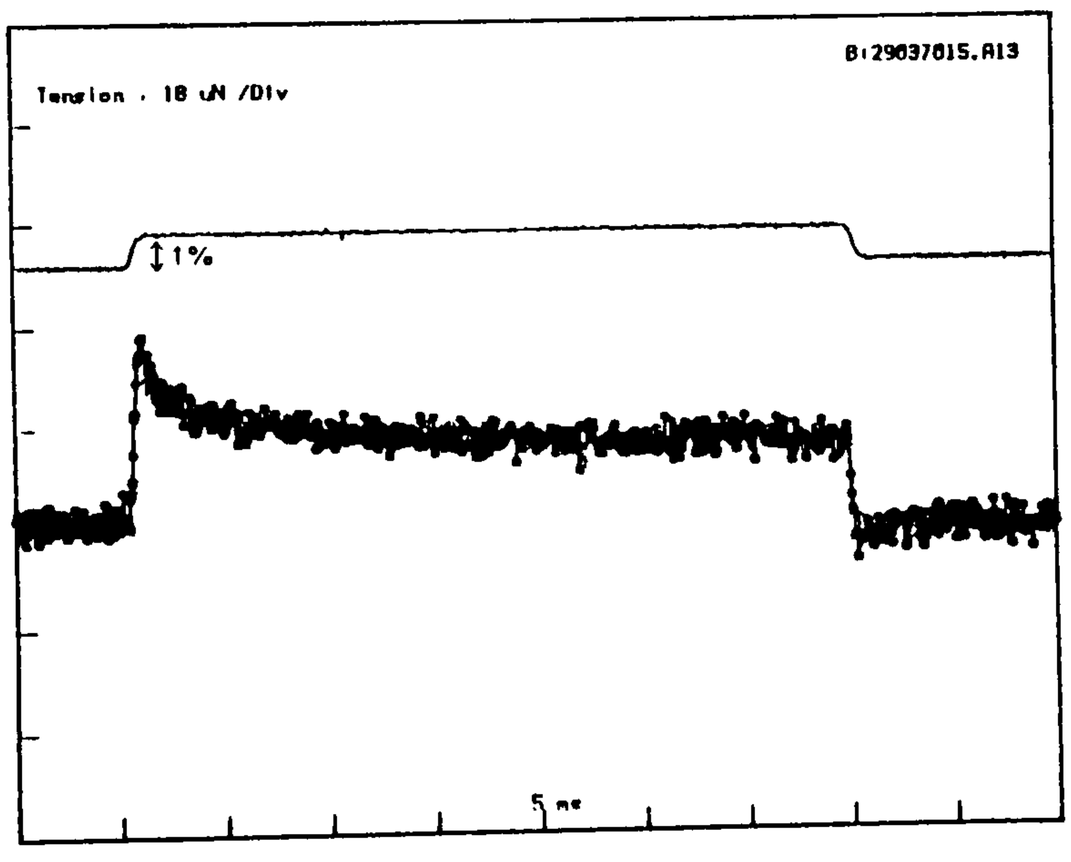

RIGOR

FIGURE 6.8 (e)

CHIMERA 88F/42A transient tension responses obtained in the three test solutions (compare with Figure 6.8 (a)).

Strain	Relaxed	Active	Rigor	Flight
W-T	+ +	+ +	+ +	+ +
Mod	+ +	+ +	+ +	?
79B	+ +	+ +	+ +	+ +
57A	+ +	+ +	+ +	+ -
Yact	+ +	+ -	+ +	- -(+)
42A	+ +	- -	+ +	- -
M342	+ +	- -	+ +	- -

(Small males fly)

FIGURE 6.9

Summary of results from the mechanical testing and flight testing.

(++) = Wild type response.

(--) = Wild type response absent.

(?) = Result unknown

(+-) = Intermediate response.

W-T, wild type;

Mutants :

MOD : mod

79B : 88F/79B

57A : 88F/57A

Yact: 88F/Yact

42A : 88F/42A

M342: M342

length hook will be an underestimate of the length change experienced in the active central region of the fibre. For this reason a laser diffraction, sarcomere length detector was constructed. Unfortunately there was insufficient time to incorporate this into the muscle test apparatus. The measured length changes in this study are therefore subject to error.

The mechanical measurements on D. melanogaster were not easy to perform and sometimes the wild-type muscle would not show an active response. The reason for this appeared to be skill in the dissection technique. The proportion of working, wild-type, preparations increased during the course of a series of experiments. For this reason the response of mutant fly muscle fibres was compared to the wild-type response at that time.

Hambly et al. (1986) have recently reviewed our present knowledge of the structural and functional domains of actin. A figure summarising functional significance in the actin amino acid sequence is reproduced in Figure 6.10.

The observation that the amino acid sequence of actin is highly conserved implies that most amino acids are of functional or structural importance. An interpretation of Figure 6.10 demonstrates just such an effect, nearly all of the amino acid sequence has been attributed a direct functional significance.

A criticism of the present study is that specific changes in the amino acid sequence may not be of immediate significance but may have a disruptive effect on the three dimensional conformation of some distant part of the actin sequence. The effects of a single amino acid substitution on the 3-dimensional structure of a protein are extremely difficult to predict. However, all of the amino acid

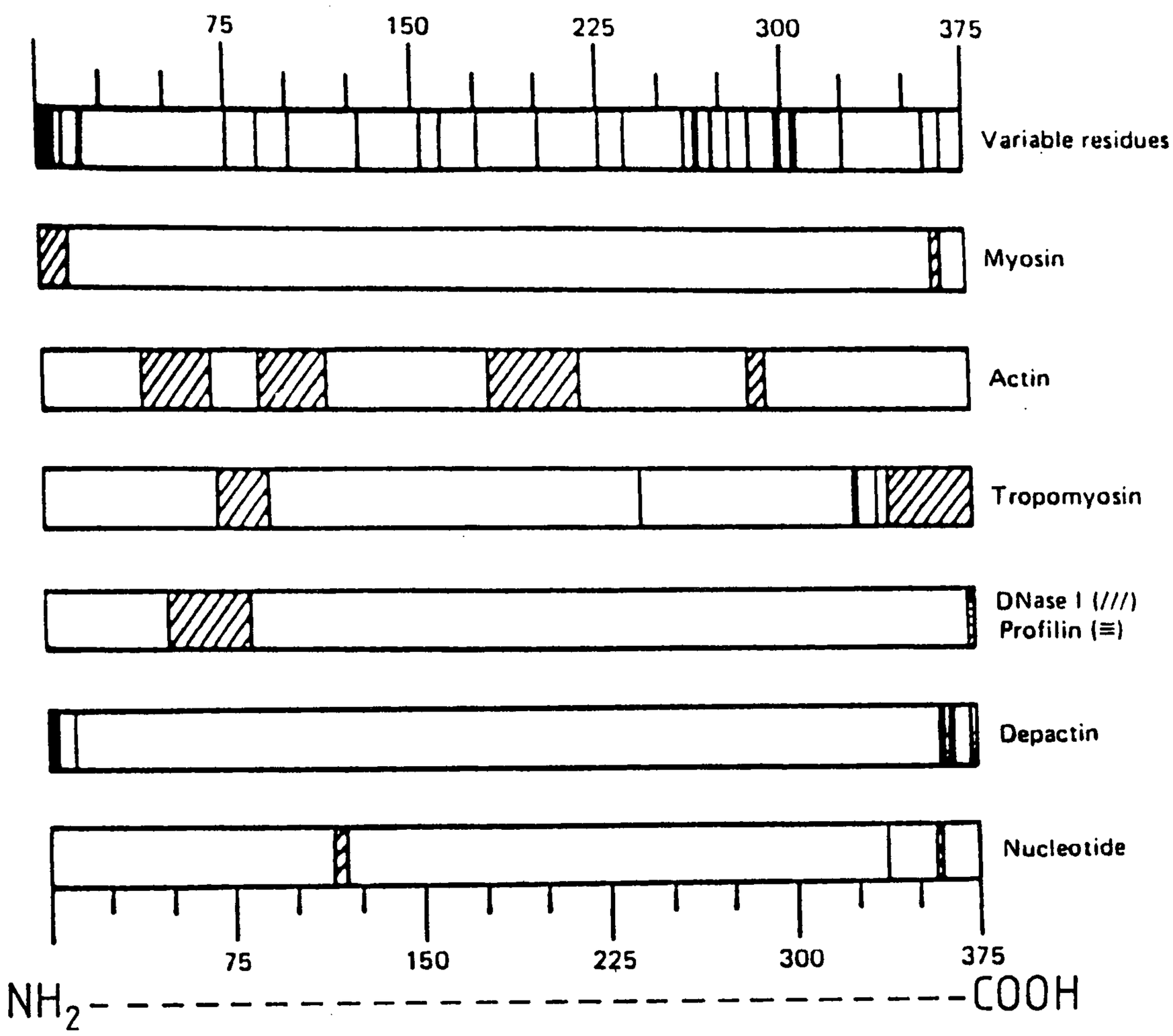

(Shaded areas designate proposed binding sites)

FIGURE 6.10

Structural and Functional Domains of Actin

Hambly et al. (1986)

substitutions in the mutants in this study can be classified as conservative by the criteria of Doolittle (1985).

Electron-micrographical (E.M.) studies made on the chimeras and *M342* (Reedy, M.K. pers. comm.) indicate that all the mutants have recognisable thick and thin filaments in the IFMs. The fact that the mutant actin can form filaments is good evidence that the 3-dimensional structure of the protein is near normal.

6.7.1 MOD :

The results from the mechanical testing of IFM from the D. melanogaster mutant *mod*, predict that the adult flies should have some flight ability when the stubloid mutation is removed. If 2-dimensional electrophoresis of the IFM's show that indeed only actin isoform II is present, the conclusion is that actin isoform III is not necessary for the formation of functional IFM thin filaments. The observed difference in the delayed tension mechanical rate constant from wild-type deserves further study. If this difference is genuine the delayed tension kinetics would no longer match the resonant frequency of the wings. The resulting reduced power output at the wingbeat frequency would explain the difference in flight ability reported by Dr. Fyrberg. The implications of this finding are extremely interesting because the mechanism of strain activation in insect flight muscle is still not fully understood. To have a mutation which affects the kinetics of this process would provide many experimental possibilities.

6.7.2 M342 :

Phase-contrast microscopy has shown that the sarcomere structure of *M342* is highly disrupted (Ball, 1987). E.M. investigations (Reedy, M.K. & Ball, E. pers. comm.) showed that the sarcomeres lacked 'Z'

discs and the structure was highly disordered, however both thick and thin filaments were present.

The finding that *M342* muscle shows an increase in stiffness upon entering rigor is consistent with the work of Kyrtatas (1987). He used the method of Lovell and Harrington (1981) to probe, indirectly, acto-myosin interaction in *M342*. One of the sites of tryptic digestion of the myosin S1 head is "hidden" when the head is bound to actin (i.e. in rigor). He found that, like wild-type muscle, the site of tryptic digestion was protected only when the *M342* myofibrils were digested in a rigor solution. His work together with the findings of this study imply that acto-myosin interaction in rigor occurs in *M342*. The intriguing property of *M342* flight muscle then, is although rigor cross-bridge formation occurs, that the active response is completely abolished.

There are two aspects to the active response; 1) activation by calcium leads to an increase in the number of attached cross-bridges in the isometric muscle (increase in the instantaneous stiffness), 2) activation by stretch, appearance of the delayed tension transient in response to a step length change.

The stiffness of *M342* flight muscle, in both relaxing and activating solutions, was comparable to the wild type relaxed stiffness. This implies that the muscle is not activated by calcium, because of this, stretch activation can then not occur. However, because of the gross disruptions to the muscle structure this is rather speculative.

The significance of the single glutamate to lysine substitution at position 93 in the amino acid sequence has been discussed by Ball et al. (1987). The co-migration of of the muscle protein, Arthrin

(Bullard, 1977) and actin III on 2-dimensional gels in *M342* is evidence that arthrin is a modified version of actin III. Residues 87-123 of actin have previously (Mimura & Asano, 1987) been implicated in αactinin binding. αActinin is thought to bind the end of the actin filaments to the Z-line (Goll et al., 1977). This is consistent with the finding that the Z-lines were highly diffuse, or non-existent, in the E.M..

The passive elasticity of relaxed insect flight muscle has been explained by the presence of connecting filaments (White, 1983) which link the thick filaments to the Z line. Relaxed stiffness in *M342* can be explained either by thick filament continuity (White, 1983; Trombitas & Tigyi-Sebes, 1979; Maruyama et al., 1978 and Horowits et al., 1986), or by the tangled thick and thin filaments forming a structural link.

6.7.3 The Chimeras :

The chimeras *Act88F/Act79B* and *Act88F/Act57A* have a very similar amino acid sequence. The finding that 50% of the *Act88F/Act57A* adults are flightless is most intriguing. This finding is inconsistent with the mechanical testing of the muscle which showed no difference in performance between wild-type, *Act88F/Act79B* and *Act88F/Act57A*. However, because the fibre diameters were not accurately determined the absolute amplitude of the delayed tensions cannot strictly be compared. Further mechanical experiments are required to resolve any differences in the magnitude of the delayed tension response.

The eleven changes in the *Act88F/yact* chimera fall mainly in a region of the actin sequence which has not yet been assigned a specific function (Hambly, et al 1986). The active response of the skinned fibres was either poor or absent. However, a good rigor

response was obtained. The observed difference in the muscle during dissection is consistent with E.M. studies (Reedy, M.K pers. comm.) where a disordered filament lattice was observed. The chimeric actin can still form filaments (Reedy, M.K. Pers. comm.) and crossbridge binding is dependent upon the ATP concentration (this study). However, some subtle change in the thin filament structure has caused a loss of order in the filament lattice and reduced the active response. The only amino acid substitutions that occur in a region that has previously been implicated in actin-actin binding (Johnson & Stockmal, 1982) are two rather conservative changes (Leu->Met and Ala->Ser) at positions 110 and 114 (see Figure 6.10).

The chimera *Act88F/Act42A* contains 9 rather conservative amino acid substitutions. The active response is completely abolished in this chimera but the rigor response persists. Once again the chimeric actin shows an ATP dependent myosin binding. Perhaps, as proposed for *Act88F/yact*, it is the disorganisation of the actin filaments which abolishes the active response. The most radical amino acid substitution (val->thr) is at position 278, very close to a region implicated in actin-actin contact (Figure 6.10).

The rigor results from the mutants with chimeric actin are consistent with the idea that the topography of the myosin binding site(s) is similar in the different actins. The rather conservative amino acid substitutions in these chimeras does not alter greatly the myosin binding site(s). A more quantitative acto-myosin binding study with purified actin would be the best approach to examine this effect in greater detail (White, 1986).

The two chimeras containing inserts from cytoplasmic actins have impaired active responses. The delayed tension in active insect fibrillar flight muscle is probably, dependent upon the organisation

of the thin filament lattice (Wray, 1979). The prediction is that X-ray diffraction will reveal a change in thin filament order in these mutants. The finding that actin and myosin can form tension bearing rigor cross-bridges in the mutant *Act88F/Act42A* and yet the delayed tension is completely abolished is evidence that strain activation in insect flight muscle is critically dependent upon thick and thin filament lattice order.

REFERENCES

REFERENCES

Abbott, R.H. (1972) An interpretation of the effects of fibre length and calcium on the mechanical properties of insect flight muscle. *Cold Spring Harbor Symp. Quant. Biol.*, 37, 647-654.

Abbott, R.H. & Cage, P.E. (1979) Periodicity in insect flight muscle stretch activation. *J. Physiol., (Lond).*, 289, 32-33p.

Armitage, P., Miller, A., Rodger, C.D. & Tregear, R.T. (1972) The structure and function of insect muscle. *Cold Spring Harbor Symp. Quant. Biol.*, 37, 379-387.

Ashurst, D.E. (1977) The Z-line : Its structure and evidence for the presence of connecting filaments. In Tregear, R.T. (ed): *Insect Flight Muscle.* pp. 57-74. Amsterdam: North Holland

Aubert, X., Roquet, M.L. & Van der Est, J. (1951) The tension-length diagram of frog's sartorius muscle. *Arch. Int. Physiol.*, 59, 239-241.

Ball, E., Karlik, C.C., Beall, C.J., Saville, C.L., Sparrow, J.C., Bullard, B. & Fryberg, E.A. (1987) Arthrin, a myofibrillar protein of insect flight muscle, is an actin-ubiquitin conjugate. *Cell*, 51, 221-228.

Barany, M. (1967) ATPase activity of myosin correlated with speed of muscle shortening. *J. Gen. Physiol.*, 50, 197-218.

Barber, S.B. & Pringle, J.W.S. (1966) Functional aspects of flight in belostomatid bugs (Heteroptera). *Proc. Roy. Soc. Lond. B. Biol. Sci.*, 164, 21-39.

Baron, E.S.G. & Tahmisian, T.N. (1948) Metabolism of cockroach muscle. I. *J. Cell Comp. Physiol.*, 32, 57-76

Bernstein, S., Mogami, K., Donady, J. & Emerson, C. (1983) Drosophila myosin heavy chain is encoded by a single gene located in a chromosomal region of other muscle genes. *Nature (Lond.)*, 302, 393-397.

Boettiger, E.G. (1957) The machinery of insect flight. In Scheer, B.T. (ed): *Recent Advances in Invertebrate Physiology.* pp. 117-142. Oregon: University of Oregon

Boettiger, E.G. & Furshpan, E. (1954) The response of fibrillar flight muscle to rapid release and stretch. *Biol. Bull., Woods Hole*, 107, 305.

Bullard, B. (1983) Contractile proteins of insect flight muscle. *Trends Biochem. Sci.*, 8, 68-70.

Bullard, B., Bell, J., Craig, R. & Leonard, K. (1985) Arthrin: a new actin-like protein in insect flight muscle. *J. Mol. Biol.*, 182, 443-454.

Carslaw, H.S. & Jaegar, J.C. (1959) *Conduction of heat in solids.* Oxford: Clarendon Press, pp. 510.

Casey, T.M., May, M.L. & Morgan, K.R. (1985) Flight energetics of euglossine bees in relation to morphology and wing stroke frequency. *J. Exp. Biol.*, 116, 271-289.

Chadwick, L.E. (1953) The motion of the wings. In Roeder, K. (ed): *Insect Physiology.* pp. 577-614. New York: John Wiley

Chan, S.K. & Margoliash, G. (1965) Properties and primary structure of the cytochrome c from flight muscles of the moth Samia cynthia. *J. Biol. Chem.*, 241, 335-348.

Chaplain, R.A. & Tregear, R.T. (1966) The mass of myosin per cross-bridge in insect fibrillar flight muscle. *J. Mol. Biol.*, 21, 275-280.

Chinery, M. (1976) *A field guide to the insects of Britain and Northern Europe.* London: Collins.

Cooke, R. & Pate, E. (1985) The effects of ADP and phosphate on the contraction of muscle fibers. *Biophys. J.*, 48, 789-798.

Cullen, M.J. (1974) The distribution of asynchronous muscle in insects with particular reference to the hemiptera: an electron microscope study. *J. Entomol. Ser. A : Gen. Ento*, 49, 17-41.

Doolittle, R.F. (1985) Proteins. *Sci. Am.*, 253, 74-83.

Dorsett, D.A. (1962) Preparation for flight by hawkmoths. *J. Exp. Biol.*, 39, 579-588.

Drabkin, D.L. (1950) The distribution of the chromoproteins, hemoglobin, myoglobin and cytochrome c, in the tissues of different species, and the relationship of the total content of each chromoprotein to body mass. *J. Biol. Chem.*,, 182, 317-333.

Drew, K.J. (1984) Control of muscle experiments using the IBM Personal Computer. *Msc. Thesis, York*, .

Eisenberg, E. & Hill, T.L. (1985) Muscle contraction and free energy transduction in biological systems. *Science (Wash. D.C.)*, 227, 999-1006.

Ellington, C.P. (1984) The aerodynamics of hovering insect flight. *Phil. Trans. Roy. Soc. B.*, 305, 1-181.

Ellington, C.P. (1985) Power and efficiency of insect flight muscle. *J. Exp. Biol.*, 115, 293-304.

Estabrook, R.W. & Pullman, M.E. (1967) *Methods in Enzymology.* New York: Academic Press, pp. 339-352.

Ford, L.E., Huxley, A.F. & Simmons, R.M. (1977) Tension response to sudden length change in stimulated frog muscles near slack length. *J.Physiol.*, 269, 441-515.

Ford, L.E., Huxley, A.F. & Simmons, R.M. (1985) Tension transients during steady shortening of frog muscle fibres. *J. Physiol., (Lond).*, 361, 131-150.

Ford, L.E., Huxley, A.F. & Simmons, R.M. (1986) Tension transients during the rise of tetanic tension in frog muscle fibres. *J. Physiol., (Lond).*, 372, 595-609.

Fyrberg, E.A., Kindle, K.L., Davidson, N. & Sodja, A. (1980) The actin genes of Drosophila : a dispersed multigene family. *Cell*, 19, 365-378.

Fyrberg, E.A., Mahaffey, J.W., Bond, B.J. & Davidson, N. (1983) Transcripts of the six Drosophila actin genes accumulate in stage and tissue specific manner. *Cell*, 33, 115-123.

Gabriel, J.M., Ellington, C.P. & Casey, T.M. (1988) Scaling of muscle ultrastructure, mechanics and energetics in Euglossine bees. (Submitted for publication to *American Zoologist*).

Geeves, M.A., Goody, R.S. & Gutfreund, H. (1984) Kinetics of acto-S1 interaction as a guide to a model for the cross-bridge cycle. *J. Muscle Res. Cell Motil.*, 5, 351-362.

Glyn, H. & Sleep, J. (1985) Dependence of adenosine triphosphatase activity of rabbit psoas muscle fibres and myofibrils on substrate concentration. *J. Physiol., (Lond).*, 365, 259-276.

Goldman, Y.E., Hibberd, M.G., McCray, J.A. & Trentham, D.R. (1982) Relaxation of muscle fibres by photolysis of caged ATP. *Nature (Lond.)*, 300, 701-705.

Goldman, Y.E., Hibberd, M.G. & Trentham, D.R. (1984a) Initiation of active contraction by photogeneration of ATP in rabbit psoas muscle fibres. *J. Physiol., (Lond).*, 354, 605-624.

Goldman, Y.E. & Simmons, R.M. (1984b) Control of sarcomere length in skinned muscle fibres of Rana temporaria during mechanical transients. *J. Physiol., (Lond).*, 350, 497-518.

Goll, D.E., Stromer, M.H., Robson, R.M., Luke, B.M. & Hammond, K.S. (1977) Extraction, purification and localization of α-actinin from asynchronous insect flight muscle. In Tregear, R.T. (ed): *Insect Flight Muscle.* pp. 15-40. Amsterdam: North Holland

Gordon, A.M., Huxley, A.F. & Julian, F.J. (1966) The variation in isometric tension with sarcomere length in vertebrate muscle fibres. *J. Physiol., (Lond).*, 184, 170-192.

Green, C.C., Sparrow, J.C. & Ball, E. (1986) Flight testing column. *Drosophila Information Service*, 63, 141.

Greenewalt, C.H. (1962) Dimensional relationships for flying animals. *Smithson. Misc. Collect.*, 144(2), 1-46.

Hambly, B.D., Barden, J.A., Miki, M. & dos Remedios, C. (1986) Structural and functional domains on actin. *Bioessays*, 4, 124-128.

Hanson, J. & Huxley, H.E. (1953) The structural basis of the cross striations in muscle. *Nature (Lond.)*, 171, 530-532.

Heinrich, B. (1974) Thermoregulation in endothermic insects. *Science (Wash. D.C.)*, 185, 747-756.

Heinrich, B. (1979) Thermoregulation of African and European honeybees during foraging, attack and hive exits and returns. *J. Exp. Biol.*, 80, 217-229.

Heinrich, B. (1987) Thermoregulation by winter-flying endothermic moths. *J. Exp. Biol.*, 127, 313-332.

Herzig, J.W. (1977) A model of stretch activation based on stiffness measurements in glycerol-extracted insect fibrillar flight muscle. In Tregear, R.T. (ed): *Insect Flight Muscle*. pp. 209-219. Amsterdam: North Holland Publishing Co.

Hibberd, M.G. & Trentham, D.R. (1986) Relationships between chemical and mechanical events during muscular contraction. *Annu. Rev. Biophys. Biophys. Chem.*, 15, 119-161.

Hibberd, M.G., Webb, M.R., Goldman, Y.E. & Trentham, D.R. (1985) Oxygen exchange between phosphate and water accompanies calcium-regulated ATPase activity of skinned fibers from rabbit skeletal muscle. *J. Biol. Chem.*, 260, 3496-3500.

Hill, A.V. (1938) The heat of shortening and the dynamic constants of muscle. *Proc. Roy. Soc. Lond. B. Biol. Sci.*, 126, 136-195.

Hill, T.L. (1974) Theoretical formalism for the sliding filament model of contraction of striated muscle: Part I. *Prog. Biophys. Molec. Biol.*, 28, 267-340.

Horowits, R., Kempner, E.S., Bisher, M.E. & Podolsky, R.J. (1986) A physiological role for titin and nebulin in skeletal muscle. *Nature (Lond.)*, 323, 160-164.

Huxley, A.F. (1957) Muscle structure and theories of contraction. *Prog. Biophys. Molec. Biol.*, 7, 255-318.

Huxley, A.F. & Niedergerke, R. (1954) Interference microscopy of living muscle fibres. *Nature (Lond.)*, 173, 971-973.

Huxley, A.F. & Simmons, R.M. (1968) A capacitance gauge tension transducer. *J. Physiol., (Lond).*, 197, 12p.

Huxley, A.F. & Simmons, R.M. (1971) Proposed mechanism of force generation in muscle. *Nature (Lond.)*, 233, 533-538.

Huxley, A.F. & Simmons, R.M. (1971b) Mechanical properties of the cross-bridges of frog and striated muscle. *J. Physiol., (Lond.)*, 218, 59-60P.

Hibberd, M.G., Dantzig, J.A., Trentham, D.R. & Goldman, Y.E. (1985b) Phosphate release and force generation in skeletal muscle fibres. Science (Wash. D.C.), 228, 1317-1319.

Huxley, H.E. (1953) Electron microscope studies of the organisation of the filaments in striated muscle. *Biochim. Biophys. Acta*, 12, 387-394.

Huxley, H.E. (1969) The mechanism of muscular contraction. *Science (Wash. D.C.)*, 164, 1356-1366.

Huxley, H.E. & Kress, M. (1985) Cross-bridge behaviour during muscle contraction. *J. Muscle Res. Cell Motil.*, 6, 153-162.

Ives, P.T. (1945) Melanogaster new mutants. *Drosophila Information Service*, 19, 46.

Jewell, B.R. & Ruegg, J.C. (1966) Oscillatory contraction of insect fibrillar flight muscle after glycerol extraction. *Proc. Roy. Soc. Lond. B. Biol. Sci.*, 164, 428-459.

Johnson, P. & Stockmal, V.B. (1982) Studies on actin fragments obtained by digestion with thrombin, BNPS-Skatole and nitrothiocyanobenzoic acid. *Int. J. Biol. Macromol.*, 4, 252-255.

Josephson, R.K. (1985) The mechanical power output of a tettigoniid wing muscle during singing and flight. *J. Exp. Biol.*, 117, 357-368.

Josephson, R.K. & Young, D. (1985) A synchronous insect muscle with an operating frequency greater than 500 Hz. *J. Exp. Biol.*, 118, 185-208.

Julian, F.J. (1969) Activation in a skeletal muscle contraction model with a modification for insect fibrillar muscle. *Biophys. J.*, 9, 547-570.

Kammer, A.E. & Heinrich, B. (1978) Insect flight metabolism. *Adv. Insect. Physiol.*, 13, 133-228.

Keilin, D. (1925) On cytochrome, a respiratory pigment common to animals, yeast and higher plants. *Proc. Roy. Soc. Lond. B. Biol. Sci.*, 98, 312-339.

Kushmeric, M.J. (1983) Energetics of muscle contraction. In Peachey, L.D., Adrian, R.H. & Geiger, S.R. (eds): *Handbook of Physiology (section 10 : Skeletal Muscle)*. pp. 189-236. Bethesda: American Physiological Society

Kushmeric, M.J. & Davies, R.E. (1969) The chemical energetics of muscle contraction. II. The chemistry, efficiency and power of maximally working sartorius muscles. *Proc. Roy. Soc. Lond. B. Biol. Sci.*, 174, 293-313.

Kyrtatas (1987) Cross-bridge structure and kinetics of insect fibrillar flight muscle. *D.Phil. Thesis, York.*, .

Laemmli, U.K. (1970) Cleavage of structural proteins during the assembly of the head of bacteriophage T4. *Nature (Lond.)*, 227, 680-.

Laurie-Ahlberg, C.C., Barnes, P.T., Curtsinger, J.W., Emigh, T.H., Karlin, B., Morris, R., Norman, R.A. & Wilton, A.N. (1985) Genetic variability of flight metabolism in Drosophila melanogaster II. Relationship between power output and enzyme activity levels. *Genetics*, 111, 845-868.

Lehninger, A.L. (1975) *Biochemistry*. New York: Worth Publishers.

Leston, D., Pringle, J.W.S. & White, D.C.S. (1965) Muscular activity during preparation for flight in a beetle. *J. Exp. Biol.*, 42, 409-414.

Levenbook, L. & Williams, C.M. (1956) Mitochondria in the flight muscles of insects III. Mitochondrial cytochrome c in relation to the aging and wing beat frequency of flies. *J. Gen. Physiol.*, 39, 497-512.

Lovell, S.J., Knight, P.J. & Harrington, W.F. (1981) Fraction of myosin heads bound to thin filaments in rigor fibrils from insect flight and vertebrate muscles. *Nature (Lond.)*, 293, 664-666.

Lund, J., Webb, M.R. & White, D.C.S. (1987) Changes in the ATPase activity of insect fibrillar flight muscle during calcium and strain activation probed by phosphate-water oxygen exchange. *J. Biol. Chem.*, 262, 8584-8590.

Lund, J., Webb, M.R. & White, D.C.S. (1988) Changes in the ATPase activity of insect fibrillar flight muscle during sinusoidal length oscillation probed by phosphate-water oxygen exchange. *J. Biol. Chem.*, 263, March.

Lymn, R.W. & Taylor, E.W. (1971) Mechanism of adenosine triphosphate hydrolysis by actomyosin. *Biochemistry*, 10, 4617-4624.

Machin, K.E. & Pringle, J.W.S. (1959) The physiology of insect fibrillar muscle. II. Mechanical properties of a beetle flight muscle. *Proc. Roy. Soc. Lond. B. Biol. Sci.*, 151, 204-255.

Mahaffey, J.W., Coutu, M.D., Fyrberg, E.A. & Inwood, W. (1985) The flightless Drosophila mutant *raised* has two distinct genetic lesions affecting accumulation of myofibrillar proteins in flight muscle. *Cell*, 40, 101-110.

Margossian, S.S. & Lowey, S. (1982) Preparation of myosin and its subfragments from rabbit skeletal muscle. In Frederiksen, D.W. & Cunningham, L.W. (eds): *Methods Enzymol. Structural and Contractile Proteins.* pp. 55-71. New York: Academic Press

Martell, A.E. & Smith, R.M. (1974-6;82) *Critical Stability Constants.* New York: Plenum Press.

Maruyama, K., Cage, P.E. & Bell, J.L. (1978) The role of connectin in elastic properties of insect flight muscle. *Comp. Biochem. Physiol.*, 61A, 623-627.

Mendelson, R.A., Morales, M.F. & Botts, J. (1973) Segmental flexibility of the S-1 moiety of myosin. *Biochem.*, 12, 2250-2255

Mimura, N. & Asano, A. (1987) Further characterization of a conserved actin-binding 27-kDa fragment of actinogelin and α-actinins and mapping of their binding sites on the actin molecule by chemical cross-linking. *J. Biol. Chem.*, 262, 4717-4723.

Miyan, J.A. & Ewing, A.W. (1985) How diptera move their wings. A re-examination of the wingbase articulation and muscle systems concerned with flight. *Phil. Trans. Roy. Soc. B.*, 311, 271-302.

Molloy, J.E., Kyrtatas, V.K., Sparrow, J.C. & White, D.C.S. (1987) Kinetics of flight muscles from insects with different wingbeat frequencies. *Nature*, 328, 449-451.

Mueller, H. & Perry, S.V. (1962) The degradation of heavy meromyosin by trypsin. *Biochem. J*, 85, 431-435.

Nachtigall, W. & Wilson, D.M. (1967) Neuromuscular control of dipteran flight. *J. Exp. Biol.*, 47, 77-97.

Newsholme, E.A., Crabtree, B., Higgins, S.J., Thronton, S.D. & Start, C. (1972) The activities of fructose diphosphatase in flight muscles from the bumble-bee and the role of this enzyme in heat generation. *Biochem. J.*, 128, 89-97.

Offer, G. & Elliott, A. (1978) Can a myosin molecule bind to two actin filaments ? *Nature (Lond.)*, 271, 325-329.

Pennycuik, C.J. & Rezende, M.A. (1984) The specific power output of aerobic muscle, related to the power density of the mitochondria. *J. Exp. Biol.*, 108, 377-392.

Perrin, D.D. & Sayce, I.G. (1967) Computer calculation of equilibrium concentrations in mixtures of metal ions and complexing species. *Talanta*, 14, 833-842.

Podolsky, R.J. (1960) Kinetics of muscular contraction: the approach to the steady state. *Nature*, 188, 666-668

Podolsky, R.J., Nolan, A.C. & Zaveler, S.A. (1969) Cross-bridge properties derived from muscle isotonic velocity transients. *Proc. Natl. Acad. Sci. U.S.A.*, 64, 504-511.

Pollard, T.D. & Cooper, J.A. (1986) Actin and actin-binding proteins. A critical evaluation of mechanisms and functions. *Annu. Rev. Biochem.*, 55, 987-1035.

Poole, K.J.V. (1984) Mechanical measurements of cross-bridge activity in insect fibrillar flight muscle. *D.Phil. Thesis, York.*, .

Portzehl, H., Caldwell, P.C. & Ruegg, J.C. (1964) The dependence of contraction and relaxation of mucle fibres from the crab, Maia squinado, on the internal concentration of free calcium ions. *Biochim. Biophys. Acta*, 79, 581-591.

Pringle, J.W.S. (1949) The excitation and contraction of the flight muscles of insects. *J. Physiol., (Lond).*, 108, 226-232.

Pringle, J.W.S. (1957) *Insect Flight*. Cambridge: Cambridge University Press, p. 133.

Pringle, J.W.S. (1967) The contractile mechanism of insect fibrillar muscle. *Prog. Biophys. Molec. Biol.*, 17, 1-60.

Pringle, J.W.S. (1978) Stretch activation of muscle: function and mechanism. *Proc. Roy. Soc. Lond. B. Biol. Sci.*, 201, 107-130.

Pringle, J.W.S. & Tregear, R.T. (1969) Mechanical properties of insect fibrillar muscle at large amplitudes of oscillation. *Proc. Roy. Soc. Lond. B. Biol. Sci.*, 174, 33-50.

Provencher, S.W. (1976) A Fourier method for the analysis of exponential decay curves. *Biophys. J.*, 16, 27-41.

Pybus, J. & Tregear, R.T. (1972) Estimates of force and time of interaction in an active muscle and of the number interacting at any one time. *Cold Spring Harbor Symp. Quant. Biol.*, 37, 655-660.

Pybus, J. & Tregear, R.T. (1975) The relationship of adenosine triphosphatase activity to tension and power output of insect flight muscle. *J. Physiol., (Lond).*, 247, 71-89.

Reedy, M.K., Holmes, K.C. & Tregear, R.T. (1965) Induced changes in orientation of the cross-bridges of glycerinated insect flight muscle. *Nature (Lond.)*, 207, 1276-1280.

Reedy, M.K., Leonard, K.R., Freeman, R. & Arad, T. (1981) Thick myofilament mass determination by electron scattering measurements with the scanning transmission electron microscope. *J. Muscle Res. Cell Motil.*, 2, 45-64.

Rosenfeld, S.S. & Taylor, E.W. (1984) The ATPase mechanism of skeletal and smooth muscle acto-subfragment 1. *J. Biol. Chem.*, 259, 11908-11919.

Rozek, C.E. & Davidson, N. (1983) Drosophila has one myosin heavy chain gene with three developmentally regulated transcripts. *Cell*, 32, 23-34.

Rubin, G.M. & Spradling, A.C. (1982) Genetic transformation of Drosophila with transposable element vectors. *Science (Wash. D.C.)*, 218, 348-353.

Rudel, R. & Zite-Ferenczy, F. (1979) Interpretation of light diffraction by cross-striated muscle as Bragg reflection of light by the lattice contractile proteins. *J. Physiol., (Lond).*, 290, 317-330.

Schoenberg, M., Brenner, B., Chalovich, J.M., Greene, L.E. & Eisenberg, E. (1984) Cross-bridge attachment in relaxed muscle. In Pollack, G.H. & Sugi, H. (eds): *Contractile mechanisms in muscle.* pp. 269-284. New York: Plenum

Sheetz, M.P. & Spudich, J.A. (1983) Movement of myosin-coated fluorescent beads on actin cables in vitro. *Nature (Lond.)*, 303, 31-35.

Sleep, J.A., Hackney, D.D. & Boyer, P.D. (1980) The equivalence of phosphate oxygens for exchange and the hydrolysis characteristics revealed by the distribution of [^{18}O]Pi species formed by myosin and actomyosin ATPase. *J. Biol. Chem.*, 255, 4094-4099.

Smith, D.S. (1966) The organisation and function of the sarcoplasmic reticulum and T-system of muscle cells. *Progr. Biophys. Molec. Biol.*, 16, 107-142.

Sotavalta, O. (1947) The flight tone (wing stroke frequency) of insects. *Acta Entomol. Fenn.*, 4, 1-117.

Steiger, G.J. & Ruegg, J.C. (1969) Energetics and "Efficiency" in the isolated contractile machinery of an insect fibrillar muscle at various frequencies of oscillation. *Pflugers Arch.*, 307, 1-21.

Stubbs, A.E. & Falk, S.J. (1983) *British hoverflies. An illustrated identification guide.* London: British Entomol. & Nat. Hist. Soc.

Sutoh, K. (1982) Identification of myosin-binding sites on the actin sequence. *Biochemistry*, 21, 3654-3661.

Szent-Gyorgyi, A.E. (1949) Free energy relations and contraction of actomyosin. *Biol. Bull., Woods Hole*, 96, 140-161.

Thorson, J.W. & White, D.C.S. (1969) Distributed representations for actin-myosin interaction in the oscillatory contraction of muscle. *Biophys. J.*, 9, 360-390.

Thorson, J.W. & White, D.C.S. (1983) Role of cross-bridge distortion in the small-signal mechanical dynamics of insect and rabbit striated muscle. *J. Physiol., (Lond).*, 343, 59-84.

Tiegs, O.W. (1955) The flight muscle of insects - their anatomy and histology, with some observations on the structure of striated muscle in general. *Phil. Trans. Roy. Soc. B.*, 238, 221-359.

Tregear, R.T. (1967) The oscillation of insect flight muscle. *Curr. Top. Bioenerg.*, 2, 269-286.

Tregear, R.T. (1977) (ed) : *Insect Flight Muscle.* Amsterdam: North Holland, pp. 367.

Trombitas, K. & Tigyi-Sebes, A. (1979) The continuity of thick filaments between sarcomeres in honey bee flight muscle. *Nature (Lond.)*, 281, 319-320.

Webb, M.R., Hibberd, M.G., Goldman, Y.E. & Trentham, D.R. (1986) Oxygen exchange between Pi in the medium and water during ATP hydrolysis mediated by skinned fibers from rabbit skeletal muscle: evidence for Pi binding to a force generating state. *J. Biol. Chem.*, 261, 15557-15564.

Webb, M.R. & Trentham, D.R. (1981) The mechanism of ATP hydrolysis catalysed by myosin and actomyosin, using rapid reaction techniques to study oxygen exchange. *J. Biol. Chem.*, 256, 10910-10916.

Weeds, A.G. & Pope, B. (1977) Studies on the chymotryptic digestion of myosin. Effects of divalent cations on proteolytic susceptibility. *J. Mol. Biol.*, 111, 129-157.

Weis-Fogh, T. & Alexander, R.M. (1977) The sustained power output from striated muscle. In Pedley, T.J. (ed): *Scale effects in animal locomotion.* pp. 511-525. London: Academic Press

White, D.C.S. (1973) Links between mechanical and biochemical kinetics of muscle. *Cold Spring Harbor Symp. Quant. Biol.*, 37, 201-213.

White, D.C.S. (1974) *Biological Physics.* London: Chapman and Hall, p. 293.

White, D.C.S. (1983) The elasticity of relaxed insect fibrillar flight muscle. *J. Physiol., (Lond).*, 343, 31-57.

White, D.C.S. (1987) Muscle Mechanics. In McLennan, H., Ledsome, J.R., McIntosh, C.H.S. & Jones, D.R. (eds): *Advances in Physiological Research.* pp. 271-293. New York & London: Plenum

White, D.C.S., Donaldson, M.M.K., Pearce, G.E. & Wilson, M.G.A. (1977) The resting elasticity of insect fibrillar flight muscle and properties of the cross-bridge cycle. In Tregear, R.T. (ed): *Insect Flight Muscle.* pp. 197-208. London: North Holland

White, D.C.S., Lund, J. & Webb, M.R. (1988) Cross-bridge kinetics in asynchronous insect flight muscle. In Sugi, H. & Pollack, G.H. (eds): *Molecular mechanism of muscle contraction*: City Publishers

White, D.C.S., Ricigliano, J.W. & Webb, M.R. (1987) Analysis of the ATPase mechanism of myosin subfragment 1 from insect fibrillar flight muscle in the presence and absence of actin, using phosphate-water oxygen exchange measurements. *J. Muscle Res. Cell Motil.*, 8, 537-540.

White, D.C.S. & Thorson, J.W. (1972) Phosphate starvation and the nonlinear dynamics of insect fibrillar flight muscle. *J. Gen. Physiol.*, 60, 307-336.

White, D.C.S. & Thorson, J.W. (1974) *The kinetics of muscle contraction.* Oxford: Pergamon Press, pp. 85.

Wilkie, D.R. (1968) Heat, work and phosphorylcreatine break-down in muscle. *J. Physiol., (Lond).*, 195, 157-183.

Wray, J. (1979) Filament geometry and the activation of insect flight muscles. *Nature (Lond.)*, 280, 325-326.

Zebe, E., Meinrenken, W. & Ruegg, J.C. (1968) Superkontraktion glycerinextrahierter asynchroner insektenmuskeln in gegenwart von ITP. *Z. Zellforschung*, 87, 603-621.